

University of Dundee

DOCTOR OF PHILOSOPHY

Epigenetic dysregulation of novel candidate genes in melanoma

Wang, Hexiao

Award date:
2013

Awarding institution:
University of Dundee

[Link to publication](#)

General rights

Copyright and moral rights for the publications made accessible in the public portal are retained by the authors and/or other copyright owners and it is a condition of accessing publications that users recognise and abide by the legal requirements associated with these rights.

- Users may download and print one copy of any publication from the public portal for the purpose of private study or research.
- You may not further distribute the material or use it for any profit-making activity or commercial gain
- You may freely distribute the URL identifying the publication in the public portal

Take down policy

If you believe that this document breaches copyright please contact us providing details, and we will remove access to the work immediately and investigate your claim.

DOCTOR OF PHILOSOPHY

Epigenetic dysregulation of novel
candidate genes in melanoma

Hexiao Wang

2013

University of Dundee

Conditions for Use and Duplication

Copyright of this work belongs to the author unless otherwise identified in the body of the thesis. It is permitted to use and duplicate this work only for personal and non-commercial research, study or criticism/review. You must obtain prior written consent from the author for any other use. Any quotation from this thesis must be acknowledged using the normal academic conventions. It is not permitted to supply the whole or part of this thesis to any other person or to post the same on any website or other online location without the prior written consent of the author. Contact the Discovery team (discovery@dundee.ac.uk) with any queries about the use or acknowledgement of this work.



Epigenetic dysregulation of novel candidate genes in melanoma

Hexiao Wang

BSc, MSc

**Submitted in fulfilment of the requirements for
the degree of Doctor of Philosophy**

**Supervisors:
Professor Charlotte Proby,
Dr Tim Crook,
Dr Gareth Inman.**

August 2013

Table of Contents

Table of Contents.....	I
List of Figures	IV
List of Tables.....	VII
Abbreviations.....	VIII
Declaration	XI
Acknowledgements	XII
Abstract	XIV
Aims.....	XVI
Chapter 1 Introduction	1
1.1 Cutaneous Melanoma (CM).....	2
1.1.1 Epidemiology of melanoma.....	3
1.1.2 Histological progression of melanoma.....	4
1.1.3 Subtypes of CM.....	7
1.1.4 Staging system of melanoma.....	7
1.1.5 Risk factors for melanoma	13
1.2 Genetic and epigenetic aberrations of melanoma.....	19
1.2.1 Genetic dysregulation of melanoma.....	19
1.2.2 Targeted therapies for melanoma.....	26
1.2.3 Epigenetic dysregulation of melanoma	28
Chapter 2 Materials and Methods	39
2.1 Cell lines and culture conditions.....	40
2.1.1 Human melanocyte and melanoma cell culture	40
2.1.2 Human melanoma cell line culture for microarray.....	42
2.1.3 Disassociation, freezing and recovery of cells	43
2.2 Tissue and serum samples	44
2.3 Molecular biology methods	45
2.3.1 DNA and RNA Purification.....	45
2.3.2 Reverse transcription of mRNA to cDNA	49
2.3.3 Quantitative real-time polymerase chain reaction (qPCR)	50

2.3.4 DNA Methylation analysis	53
2.4 Protein procedures.....	61
2.4.1 Western blotting.....	61
2.4.2 Immunofluorescence	66
2.5 Cell biology assays	67
2.5.1 Transient transfection of short interfering RNA (siRNA).....	67
2.5.2 Methylation reversal assay.....	70
2.5.3 Hypoxia treatment.....	70
2.5.4 Cell counting	71
2.6 Microarray analysis	71
2.6.1 Methylation reversal assay with expression microarray	71
2.6.2 Expression microarray	72
2.6.3 Methylation microarray.....	72
2.7 Statistics	73
Chapter 3 Identification of candidate biomarkers by systematic approaches	74
3.1 Introduction	75
3.1.1 Tissue factor pathway inhibitor 2 (TFPI2).....	77
3.1.2 Early growth response gene 2 (EGR2)	79
3.1.3 Dickkopf homolog 1 (DKK1).....	80
3.1.4 SMAD family member 3 (SMAD3).....	81
3.1.5 TSC22 domain family, member 1 (TSC22D1)	82
3.2 Results	82
3.2.1 Identification of candidate genes by methylation reversal assay combined with gene expression profiling	82
3.2.2 Identification of candidate genes by systematic methylation profiling and gene expression profiling in paired melanoma cell lines.....	111
3.3 Discussion	117
Chapter 4 Methylation investigation of candidate genes <i>NT5E</i> , <i>DUSP2</i> , and <i>Dab2</i> ..	123
4.1 Introduction	124
4.1.1 NT5E (ecto-5'-nucleotidase, CD73)	124
4.1.2 DUSP2 (Dual-specificity phosphatase 2).....	126
4.1.3 Dab2 (Disabled-2).....	128
4.2 Results	129
4.2.1 <i>NT5E</i> methylation in melanoma	129
4.2.2 <i>DUSP2</i> methylation in melanoma.....	138
4.2.3 <i>Dab2</i> methylation in melanoma.....	146

4.3 Discussion	150
Chapter 5 CpG island methylation dependent transcriptional silencing of prolyl hydroxylases in melanoma	155
5.1 Introduction	156
5.1.1 Collagen prolyl hydroxylases (C-PHs).....	156
5.1.2 HIF prolyl hydroxylases (HIF-PHs).....	159
5.2 Results	162
5.2.1 Analysis of the biomarker utility for <i>C-P3H</i> and <i>C-P4H</i> CpG island methylation in melanoma	162
5.2.2 Identification of <i>EGLN3</i> methylation and mechanistic study of <i>EGLN3</i> in melanoma	176
5.3 Discussion	188
5.3.1 Specific C-PHs are transcriptionally silenced by methylation in melanoma	188
5.3.2 <i>EGLN3</i> methylation and involvement of <i>EGLN3</i> in HIF1- α independent pathway in melanoma.....	191
Chapter 6 Conclusions and Future Perspectives.....	196
6.1 Conclusions.....	197
6.2 Future perspectives.....	202
6.2.1 Serum epigenetic biomarkers for detection of metastatic disease	202
6.2.2 Epigenetic biomarkers in melanoma tissues	205
6.2.3 Epigenetic candidates as new therapeutic targets.....	207
6.2.4 Summary.....	208
7 References	209

List of Figures

Figure 1-1: Incidence of melanoma diagnosed in Scotland from 1991 to 2011, including all age groups and both sexes.	4
Figure 1-2: Melanoma progression from benign naevus to melanoma based on the Clark model. (Miller and Mihm 2006)	6
Figure 1-3: Histopathological subtypes of primary melanoma.....	6
Figure 1-4: Staging system of melanoma based on 2008 AJCC staging system.	10
Figure 1- 5: Schematic of MAPK signalling pathway.....	21
Figure 1-6: Schematic of DNA methylation and regulation of gene expression by DNA methylation.....	31
Figure 2-1: Morphology of WM239A (A, C) and WM115 (B, D) cell lines under different culture media.....	43
Figure 2-2: Visualisation of ribosomal RNA 18S and 28S in five RNA samples by 1% of denaturing agarose gel eletrophoresis with ethidium bromide staining.	47
Figure 2-3: An RNA sample prepared for gene expression microarray showed full integrity with a RIN of 10.	48
Figure 2-4: Visualisation of qPCR amplification plot by Rotor-Gene Q 2.0.2 (build 4) software.	52
Figure 2-5: Comparison of the efficiency of four transfection reagents in COLO829 melanoma cell line: Oligofectamine™ reagent, Lipofectamine™ 2000, HiPerFect transfection reagent and Lipofectamine™ RNAiMAX.....	69
Figure 3-1: Analysis of methylation reversal screen in cell line C81-61.	84
Figure 3-2: Pathway analysis by David bioinformatics (National Institute of Allergy and Infectious Diseases (NIAID)).	85
Figure 3-3: Genomic structure of human <i>TFPI2</i> gene.	86
Figure 3-4: Identification of <i>TFPI2</i> methylation in melanoma cell lines by MSP (A) and pyrosequencing (B).	88
Figure 3-5: Inverse correlation of <i>TFPI2</i> methylation and gene expression.	90
Figure 3-6: Reactivation of <i>TFPI2</i> expression by pharmacological demethylation.	92
Figure 3-7: <i>TFPI2</i> CpG island methylation and expression in paired melanoma cell lines.	93

Figure 3-8: Pyrosequencing profiles of <i>TFPI2</i> CpG island methylation in benign naevi, primary and metastatic melanomas.	95
Figure 3-9: Mann Whitney <i>U</i> analysis of <i>TFPI2</i> CpG island methylation in benign naevi, primary and metastatic melanomas.	96
Figure 3-10: <i>TFPI2</i> CpG island methylation increases in metastatic melanoma relative to matched primary melanoma.	97
Figure 3-11: Quantitative <i>TFPI2</i> CpG island methylation profiles from serum of healthy volunteers (Normals), patients with no metastases and patients with metastases.	98
Figure 3-12: Detection of methylated <i>TFPI2</i> CpG island genomic DNA in serum is associated with metastatic melanoma.	101
Figure 3-13: Expression of <i>DKK1</i> and <i>EGR2</i> in melanoma cell lines with methylation reversal treatment.	102
Figure 3-14: Methylation and expression of <i>EGR2</i> , as well as methylation of <i>DKK1</i>	104
Figure 3-15: Expression (A) and methylation (B) of <i>SMAD3</i> in melanoma cell lines and melanocyte HEMA and keratinocyte NHK.	106
Figure 3-16: Reactivation of <i>TSC22D1.1</i> and <i>TSC22D1.2</i> expression by pharmacological demethylation (A, B) and the genomic structure of the human <i>TSC22D1</i> gene (C).	109
Figure 3-17: Methylation and expression of <i>TSC22D1.2</i> in melanoma cell lines.	110
Figure 3-18: Heat map visualization of 60 genes that are significantly downregulated in all three lymph node metastatic or 4/5 metastatic melanoma cell lines.	113
Figure 3-19: Data mining work flow for the identification of differentially epigenetically regulated candidate genes in 3 paired melanoma cell lines.	115
Figure 4-1: <i>NT5E</i> was methylated in the less aggressive melanoma cell line C81-61 but not in the more aggressive derivative, C8161.	131
Figure 4-2: Analysis of <i>NT5E</i> expression and methylation in melanoma cell line panel.	132
Figure 4-3: <i>NT5E</i> methylation in two sets of paired melanoma with both primary melanoma and lymph node metastasis were both available.	133
Figure 4-4: <i>NT5E</i> methylation in 27 well characterised primary melanomas.	135
Figure 4-5: Detection of <i>NT5E</i> methylation in 23 melanoma metastasis.	137
Figure 4-6: Identification of <i>DUSP2</i> methylation and mRNA expression in melanoma cell lines.	139
Figure 4-7: Expression and methylation of <i>DUSP2</i> in paired melanoma cell lines.	141
Figure 4-8: <i>DUSP2</i> methylation in melanoma tissues.	143
Figure 4-9: <i>DUSP2</i> methylation in paired melanoma tissues.	145
Figure 4-10: <i>Dab2</i> was not methylated in melanoma cell lines.	147

Figure 4-11: <i>Dab2</i> methylation in melanoma tissues and benign naevi.....	149
Figure 5-1: Invasion and intravasation of melanoma cells.	158
Figure 5-2: Scheme representing the classical hypoxia pathway.	160
Figure 5-3: CpG island methylation and expression of <i>C-P3H</i> and <i>C-P4H</i> in melanoma cell line panel.	164
Figure 5-4: Pyrosequencing analysis of <i>LEPREL1</i> , <i>P4HA1</i> , <i>P4HA2</i> and <i>P4HA3</i> in 3 sets of paired primary melanoma and metastatic cell lines.....	166
Figure 5-5: Methylation of <i>P4HA3</i> in melanoma clinical samples and benign naevi. (A): Methylation percentage of 10 cases of benign naevi and 50 cases of melanoma. (B): Mann-Whitney <i>U</i> test of methylation level between benign naevi and melanomas. ($p < 0.01$).....	168
Figure 5-6: <i>P4HA3</i> CpG island methylation in 8 pairs of clinical samples comprising primary melanomas and their matched lymph node metastasis derived from the same patient.....	170
Figure 5-7: Quantitative <i>LEPREL1</i> CpG island methylation profiles in melanoma clinical samples (tissue and serum) and benign naevi.	172
Figure 5-8: <i>P4HA3</i> CpG island methylation in melanoma serum samples.....	175
Figure 5-9: <i>EGLN3</i> methylation in melanoma cell lines.....	177
Figure 5-10: Western blots of <i>EGLN3</i> and HIF1- α protein in 8 melanoma cell lines...	178
Figure 5-11: Subcellular localisation of HIF1- α , <i>EGLN1</i> , <i>EGLN2</i> and <i>EGLN3</i>	180
Figure 5-12: Measurement of hypoxic response of WM266.4 cells.	183
Figure 5-13: <i>EGLN3</i> knock down in WM266.4 and LM2 by siRNA.	184
Figure 5 -14: <i>EGLN3</i> knock down does not interfere the HIF1- α pathway.	185
Figure 5-15: Cell counting in WM266.4 and LM2 cell lines.....	187

List of Tables

Table 1-1: Melanoma TNM classification based on 2008 AJCC staging system (Nading et al. 2010).	12
Table 1-2: Hypermethylated genes identified in melanoma tissues.....	33
Table 2-1: Description, source and culture media of the cell lines used in this study. 41	
Table 2-2: Description of clinical cases.....	44
Table 2-3: Composition of reverse transcription reaction	49
Table 2-4: Reverse transcription thermal programme cycling conditions.....	49
Table 2-5: Three-step cycling programme for qPCR	50
Table 2-6: Symbol, description and ID of TaqMan [®] gene expression assays.....	51
Table 2-7: Reaction Composition using Hot Star Taq DNA polymerase	55
Table 2-8: Cycling protocol for MSP	56
Table 2-9: MSP Primers and annealing temperature of candidate genes	57
Table 2-10: Primers and annealing temperatures of target genes for Pyrosequencing	59
Table 2-11: Name, description, supplier and dilution of primary antibodies	64
Table 2-12: Name, description, supplier and dilution of secondary antibodies	65
Table 2-13: Name, company and target sequence of siRNAs	68
Table 3-1: Investigation of <i>TFPI2</i> CpG island methylation in human cancers	78
Table 3-2: Candidate genes identified by Methylation reversal screen.....	85
Table 3-3: Mean methylation (%) and methylation status of <i>TFPI2</i> in melanoma cell lines, melanocytes and keratinocytes by pyrosequencing and MSP, respectively.....	89
Table 3-4: <i>TFPI2</i> methylation at individual CpG site of promoter region in 6 paired primary and metastatic melanomas from the same patients	97
Table 3-5: Paired melanoma cell lines used for microarray analysis	111
Table 3- 6: Differential expression results of candidate genes in RIKER, HAQQ TALANTOV, XU tissue studies and their CpG island status	116
Table 5-1: Mean % methylation level of <i>C-PHs</i> in paired melanoma cell lines	166
Table 5-2: <i>LEPREL1</i> methylation level in paired melanomas	173
Table 5-3: Risk analysis of association between <i>P4HA3</i> methylation and melanoma metastasis	174

Abbreviations

5' AZA	5'-azacytidine
5hmc	5-hydroxymethyl cytosine
5mc	5' methylcytosine
6-4 PPs	6-4 photoproducts
AJCC	American Joint Committee on Cancer
ALM	Acral lentiginous melanoma
AMP	Adenosine 5' monophosphate
ANOVA	Analysis of Variances
ARNT	Aryl hydrocarbon receptor nuclear translocator
ASIP	Agouti stimulating protein
ATCC	American Type Culture Collection
ATP	Adenosine triphosphate
AUC	Area under the curve
B2M	β 2-microglobulin
Bl	Bladder
Bo	Bone
Br	Brain
BRAF	V-raf murine sarcoma viral oncogene homolog B1
BSA	Bovine serum albumin
BT	Breslow thickness
CDK4	Cyclin-dependent kinase 4
CDKN2A	Cyclin-dependent kinase inhibitor 2A
cDNA	Complementary DNA
CM	Cutaneous melanoma
C-P3Hs	Collagen prolyl 3 hydroxylases
C-P4Hs	Collagen prolyl 4 hydroxylases
CPD	Cyclobutane pyrimidine dimers
C-PHs	Collagen prolyl hydroxylases
CRTAP	Cartilage-related protein
CRUK	Cancer research UK
C _T	Cycle threshold
CTLA4	Cytotoxic T-Lymphocyte Antigen 4
Cu	Cutaneous
Dab2	Disabled-2
DAPI	4', 6-diamidino-2-phenylindole
DEJ	Dermo-epidermal junction
DKK1	Dickkopf homolog 1

DMSO	Dimethyl Sulphoxide
DNMT	DNA methyltransferase
DUSP2	Dual-specificity phosphatase 2
ECM	Extracellular matrix
EDTA	Ethylenediaminetetraacetic Acid
EGR2	Early growth response gene 2
FBS	Fetal bovine serum
FDA	U.S. Food and Drug Administration
FDR	False discovery rate
FFPE	Formalin-fixed, paraffin-embedded
gp	Glycoprotein
HDAC	Histone deacetylase
HIF	Hypoxia-inducible factor
HIF-PH	HIF prolyl hydroxylase
HMGS2	Human melanocyte growth supplement-2
HNSCC	Head and neck squamous cell carcinoma
HRP	Horseradish peroxidase
ISD	Information services division
KEGG	Kyoto Encyclopedia of Genes and Genomes
LDH	Lactate dehydrogenase
LEPRE1	Leucineproline-enriched proteoglycan 1, leprecan
LEPREL1	Leprecan-like 1
LEPREL2	Leprecan-like 2
LEPREL4	Leprecan-like 4
Li	Liver
Limma	Linear models for microarray
LMM	Lentigo maligna melanoma
LN	Lymph node
Lu	Lung
MAP	Mitogen-activated protein
MC1R	Melanocortin-1 receptor
MDT	Multi Disciplinary Team
MITF	Microphthalmia-associated transcription
MMPs	Matrix metalloproteases
MSP	Methylation-specific PCR
MSREs	Methylation-Sensitive Restriction Enzymes
MVPs	Methylation variable positions
NC1	Noncollagenous 1
NIAID	National Institute of Allergy and Infectious Diseases
NM	Nodular melanoma
NT5E	Ecto-5'-nucleotidase, CD73
OS	Overall survival
P4HA1	Collagen prolyl 4 hydroxylase isoform 1
P4HA2	Collagen prolyl 4 hydroxylase isoform 2

P4HA3	Collagen prolyl 4 hydroxylase isoform 3
PBS	Phosphate buffered saline
PCA	Principle component analysis
PCR	Polymerase chain reaction
PFS	Progression-free survival
PHD	Prolyl hydroxylase domain-containing protein
PP5	Placental protein 5
PTEN	Phosphatase and tensin homolog
PVDF	Polyvinylidene fluoride
qPCR	Quantitative real-time polymerase chain reaction
RRBS	Reduced representation bisulfite sequencing
RGP	Radial growth phase
RIPA	Radio-immune Precipitation
ROC	Receiver operating characteristic
ROS	Reactive oxygen species
SAM	Significance analysis of microarrays
SDS-PAGE	Sodium dodecyl sulphate polyacrylamide gel electrophoresis
siRNA	Short interfering RNA
SLNB	Sentinel lymph node biopsy
SMAD3	SMAD family Member 3
SLNB	Sentinel lymph node biopsy
Sp	Spleen
SSM	Superficial spreading melanoma
ST	Soft tissue
SWAN	Subset-quantile within array normalization
TBS-T	Tris buffered saline-Tween
TFPI2	Tissue factor pathway inhibitor 2
TME	Tumour microenvironment
TNM	Tumour Node Metastasis
TSA	Trichostatin A
TSC22D1	TSC22 Domain Family, Member 1
TSS	Transcription start site
TYR	Tyrosinase
UVR	Ultraviolet radiation
VGP	Vertical growth phase

Declaration

I, Hexiao Wang, declare that this thesis entitled 'Epigenetic dysregulation of novel candidate genes in melanoma' and the work presented in this thesis are my own. This work was done under the guidance of Professor Charlotte Proby and Dr Tim Crook at the University of Dundee. Any contributions of others including references cited and acknowledgement of collaborative research are clearly stated. This thesis has not been previously submitted for the award of any degree.

Date:

Signature:

I confirm that Hexiao Wang has spent the equivalent of 3 years in research in the Division of Cancer Research, Medical Research Institute, University of Dundee, Ninewells Hospital & Medical School. She has fulfilled the conditions in accordance with the University of Dundee's regulations, thereby qualifying her to submit this thesis in application for the degree of Doctor of Philosophy.

Date:

Signature:

Acknowledgements

First of all, I wish to acknowledge Leng Charitable Trust and Tayside Dermatology for their financial support.

My deepest gratitude goes to my supervisors Professor Charlotte Proby, Dr Tim Crook and Dr Gareth Inman for giving me the opportunity to work on this fascinating project, and also for their support, motivation, encouragement, and immense knowledge. I am sincerely grateful for all I have learnt from them, not only academically, but also in particular, their enthusiasm in medical contribution. They will be my leading examples for my entire life.

I am also grateful for the generous help from all my other supervisors Dr Colin Fleming, Professor Irene Leigh, Dr Alan Evans, and Professor Catherine Harwood.

I would like to express my appreciation to Dr Cristiana Lo Nigro and Miss Laura Lattanzio for pyrosequencing service, to Dr Rubeta Martin who collected all the melanoma tissues and blood samples in the Barts and London collection, and Dr Karin Purdie for assistance with this, to Dr Runxuan Zhang and Dr Helena Carén for their support with microarray analysis, to Dr Mathieu Boniol for his statistical advice, and to Tayside Tissue Bank for providing the service for processing tumour tissue samples.

Special thanks go to Dr Lynda Weir, Miss Angela McHugh and Dr Bhavya Rao for their family-like friendship, help, and caring. I would also like to thank all the colleagues in skin tumour laboratory for all their help and encouragement and the excellent and friendly atmosphere in our laboratory created by them.

Finally, I would like to thank my parents and my husband for their endless love. They are always there supporting me and cheering me up.

Abstract

Cutaneous melanoma (CM) is an aggressive neoplastic disorder of melanocytes accounting for 4% of skin cancers, but over 75% of skin cancer-related deaths. The outlook for advanced melanoma is typically poor, particularly for patients with distant and/or visceral metastatic disease. Although new melanoma therapies including vemurafenib and ipilimumab confer significant clinical benefit, accumulating evidence suggests that they are less effective when tumour load is high and patient performance status poor, as is often the case in advanced disease. New strategies for the early detection of sub-clinical relapsed and/or metastatic disease are therefore urgently required. Development of such biomarkers, combining sensitivity and specificity, would allow the deployment of these treatments when tumour volume is low thereby maximising anti-melanoma efficacy. Cancer-associated gene promoter methylation is recognized as an important mechanism in tumour initiation and progression. Exploring the epigenetic profiles of melanoma will lead to the generation of new strategies for molecular subtyping, discovery of diagnostic and prognostic biomarkers and development of novel therapeutic targets.

In the present study, I have identified a panel of promising epigenetic melanoma biomarkers by exploiting both a systematic approach and candidate gene approach. Biomarkers *TFPI2* and *P4HA3* showed a high frequency and high level of methylation in melanoma cell lines. Significantly increased methylation in melanoma suggests a role for *TFPI2* and *P4HA3* as epigenetic biomarkers that can potentially predict poor prognosis of melanoma. Furthermore, in my work a highly significant correlation has been established between detection of methylated genomic DNA of

TFPI2 and *P4HA3* in melanoma patients' sera and metastatic disease. This implies potential clinical utility for *TFPI2* and *P4HA3* as serum biomarkers for the detection of metastatic melanoma. In contrast, the presence of *NT5E* and *DUSP2* methylation is likely to be a good prognostic biomarker for both primary melanoma and metastatic disease. *NT5E* methylation was associated with early stage melanoma but became undetectable when melanoma metastasis progressed to visceral sites. Similarly, the significantly higher methylation level of *DUSP2* in primary melanomas than in metastatic disease implies that *DUSP2* methylation may also be a biomarker of good prognosis in melanoma.

In summary, my study proposes that epigenetic dysregulation by CpG island methylation of tumour-related genes *TFPI2*, *P4HA3*, *NT5E* and *DUSP2* is important in melanoma development and progression and that detection of methylated DNA from these genes may provide novel biomarkers for predicting tumour progression and patient outcome. Molecular functions of these biomarkers in melanoma should be investigated in future work for the purpose of better understanding the biology of this highly aggressive tumour. Such studies may also lead to new therapeutic strategies for advanced melanoma. For example, antibodies to *NT5E* show efficacy in animal models of metastatic breast cancer and merit assessment in melanoma. Moreover, detection of circulating methylated genomic DNA from *TFPI2* and *P4HA3* in patient sera may be useful for predicting prognosis and for the early diagnosis of metastatic disease. Given the emerging evidence that new melanoma therapeutics, particularly ipilimumab, are most effective when used in low volume metastatic disease, such epigenetic biomarkers are likely to be of value in informing the clinical deployment of such agents.

Aims

The major aim of this project is to build up a portfolio of novel candidate biomarkers that are epigenetically dysregulated in melanoma. A systematic approach and candidate gene approach will be performed for identification and investigation of potential melanoma biomarkers. For selected genes, the following investigation will be performed:

- (1) Analysis of CpG island methylation status for selected genes in human melanoma cell lines and normal melanocytes.
- (2) Methylation profiling of selected genes in melanoma clinical samples and benign melanocytic naevi to examine the association between DNA methylation and melanoma progression.
- (3) Analysis of circulating methylated DNA in melanoma patients' sera to determine the potential utility of detection of methylated genes in detection of metastatic melanoma.
- (4) Investigation of molecular function for candidate genes in the initiation and progression of melanoma.

Chapter 1 Introduction

1.1 Cutaneous Melanoma (CM)

Cutaneous melanoma (CM) is an aggressive neoplastic disorder of melanocytes accounting for 4% of skin cancers, but over 75% of skin cancer-related deaths (Miller and Mihm 2006). Melanoma was probably first described in the fifth century B.C. by Hippocrates. The term of melanoma was first adopted in 1838 by Robert Carswell (Urteaga and Pack 1966). In 1840, Samuel Cooper stated melanoma is untreatable without early removal (Cooper 1840). This remains true today, with early diagnosis and surgical excision the cornerstone of treatment. Melanoma has a high propensity to disseminate and form metastasis at which point surgery is not curative. The outlook for metastatic melanoma is poor, particularly for patients with distant organ involvement, including liver, lung, brain and bones, with a median survival time of less than 12 months (Balch et al. 2009). This poor outcome is in large part because metastatic melanoma is intrinsically resistant to conventional cytotoxic agents which are the mainstay of the medical management of other solid tumours. The recent clinical launch of targeted anti-melanoma agents, including Vemurafenib that targets a subset of patients harboring *BRAF* mutation and the anti-CTLA4 (Cytotoxic T-Lymphocyte Antigen 4) antibody, ipilimumab, has improved the management of unresectable or metastatic melanomas (Hodi et al. 2010; Chapman et al. 2011; Robert et al. 2011). However, despite a response rate to Vemurafenib of > 50%, the great majority of patients develop resistant disease within a few months and die rapidly. Development of new strategies for early diagnosis and more effective therapies

for metastatic melanomas are therefore urgently needed and are priorities in melanoma research.

1.1.1 Epidemiology of melanoma

It is estimated that the incidence of CM has doubled in the past 20 years, and the highest incidence is reported in Queensland, Australia (Lens and Dawes 2004; MacKie et al. 2009). The incidence of CM is increasing rapidly in Caucasian populations with approximately 13,000 new diagnoses in the UK each year (CRUK 2013). It was the 6th most common cancer in British males and females in 2010 (CRUK 2013). In Scotland, the overall incidence of CM has significantly increased in the last two decade, from 491 cases in 1991 to 1,202 cases in 2011 (ISD 2011) (Figure 1-1). A disproportionately high incidence of CM is seen in young adults and it is now the 5th commonest cancer in persons aged 15-24 years in the UK (North West Cancer Intelligence Service 2011). A predictive model has forecast that the CM rate will continue to rise to 2-3 times the current incidence over the next 30 years (Diffey 2004). Despite most melanoma patients having a favourable prognosis, those with metastatic disease especially to visceral sites have a poor prognosis (Balch et al. 2009). More than 2,000 patients died from melanoma annually in the UK between 2008 to 2010, of which 5% were under 40 years and more than half were less than 70 years (CRUK 2013). In Scotland, the mortality rate has nearly doubled in the last two decades (ISD 2011).

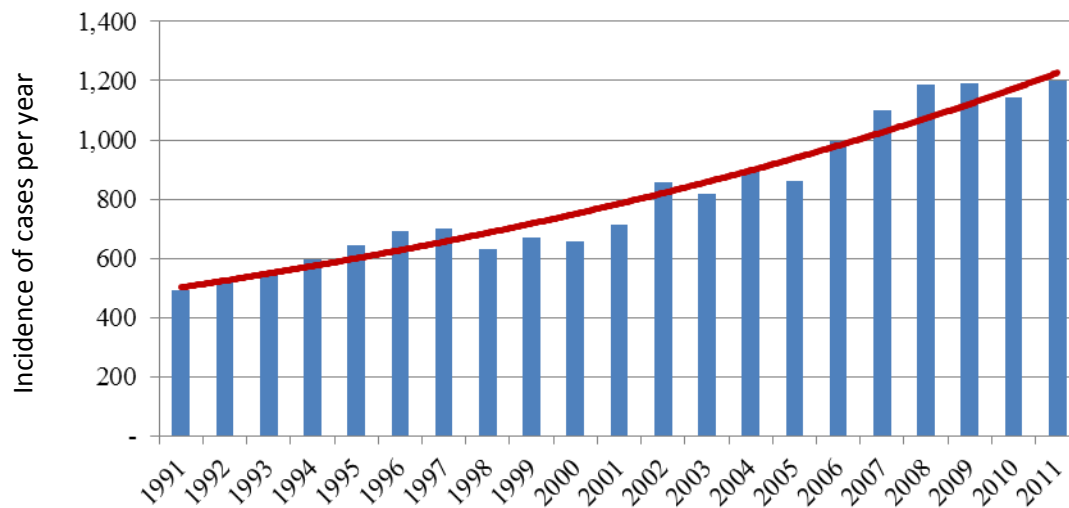


Figure 1-1: Incidence of melanoma diagnosed in Scotland from 1991 to 2011, including all age groups and both sexes.

Based on database from ISD Scotland cancer statistics (ISD 2011).

1.1.2 Histological progression of melanoma

Melanocytes are dendritic cells derived from neural crest and mostly located in the basal layer of epidermis, accounting for 1-2% of the total epidermal cell population (Jhappan et al. 2003). Being capable of producing melanin pigment, melanocytes influence skin and hair colour and interact with neighbouring keratinocytes via dendritic processes (Elder 1992). A cluster of normal melanocytes is called a benign naevus. Some melanocyte naevi may transform to the potential precursor of melanoma, the dysplastic naevi. These naevi show a

phenotype of irregular shape, increased horizontal size and multiple colours with premalignant histological features (Pacheco et al. 2011). Melanomas can be simply categorized into radial growth phase (RGP) or vertical growth phase (VGP) according to their growth pattern (Rigel 2005). RGP melanoma is characterized by the presence of scattered melanoma cells within the epidermis (MacKie 2000). Inexorable proliferation discriminates RGP melanoma from benign naevi, although melanoma cells at this phase still show a low proliferation rate (Elder 1992). The simultaneous presence of melanoma cells in the epidermis and dermis indicates VGP melanoma. During this stage, melanoma cells grow and invade vertically downwards to within the dermis, and have greater potential to disseminate to other areas of the skin or to distant organs (Miller and Mihm 2006). Thus, mortality rates increase significantly as melanomas progress from RGP to VGP. The last step of the malignant process is metastasis. Metastatic melanomas have a generally very poor prognosis. Melanoma with local and resectable disease, particular for lymph node only disease, may have an extended survival rate. Metastatic melanoma disseminated to distant visceral organs has the worst prognosis (Balch et al. 2009).

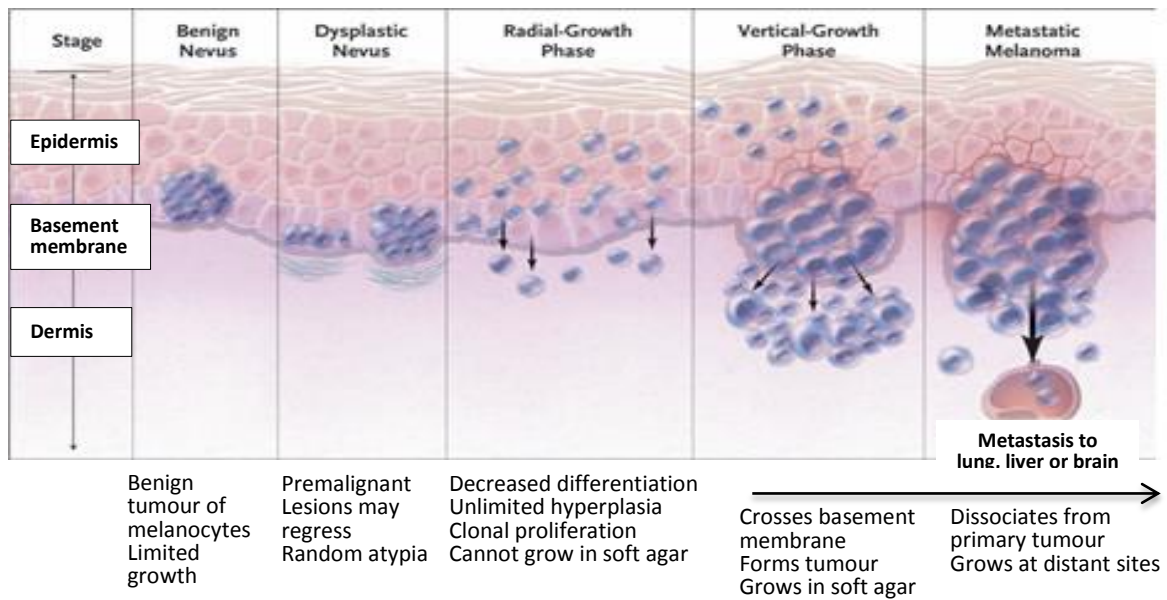


Figure 1-2: Melanoma progression from benign naevus to melanoma based on the Clark model. (Miller and Mihm 2006)

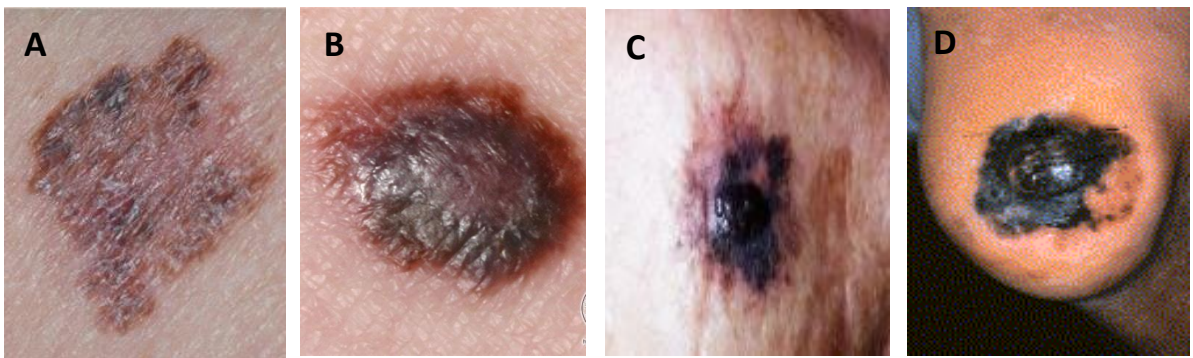


Figure 1-3: Histopathological subtypes of primary melanoma.

(A): Superficial spreading melanoma (SSM) (Dermatology information system).
 (B): Nodular melanoma (NM) (Dermatology information system). (C): Lentigo maligna melanoma (LMM) (NZ). (D) Acral lentiginous melanoma (ALM) (JANCIN 2009).

1.1.3 Subtypes of CM

There are four major histopathological types of cutaneous melanoma. These are superficial spreading melanoma, nodular melanoma, lentigo maligna melanoma and acral lentiginous melanoma (MacKie 2000) (Figure 1-3). Superficial spreading melanoma accounts for approximately 70% of melanoma incidence in white race melanoma populations and correlates with the number and size of pre-existing melanocytic naevi. Nodular melanoma and lentigo maligna melanoma occur preferentially in middle and old age, respectively. The peak incidence of acral lentiginous melanoma is seen in dark-skinned populations (Lens 2008), and the predominant sites for this type of melanoma are on toes and fingers.

1.1.4 Staging system of melanoma

Current melanoma staging is based on the American Joint Committee on Cancer (AJCC) staging system which uses the TNM (Tumour Node Metastasis) classification. The AJCC melanoma staging system, revised in 2008, includes a number of clinico-pathological parameters for melanoma classification: Breslow thickness (tumour depth), presence of ulceration, mitotic rate, lymph node metastasis, and the site of distant metastases (Balch et al. 2004) (Figure 1-4 and Table 1-1). The revised AJCC database was based on an expansion of the patient sample size to 50,000 from 17 major melanoma centres on three continents (Soong et al. 2010).

Breslow thickness, ulceration and the mitotic rate are the dominant determinants of risk of metastasis for localized melanomas. Breslow thickness refers to the absolute depth of melanoma from the uppermost layer of epidermis to the deepest adjacent melanoma cells at the base of the tumour (Breslow 1979). Whilst thin lesions (Breslow thickness <1mm, T1) are almost always cured by surgical excision (5-year survival of over 95%), thicker tumours (Breslow >4mm, T4) have a significant risk of metastatic spread and a 5-year survival of less than 50% (Balch et al. 2009). Most invasive melanomas presenting in the UK are less than 2mm and can be excised completely without further treatment. Ulceration describes a histological situation where there is an absence of intact dermis overlying the primary melanoma, and is associated with a worse prognosis for melanomas of an equivalent thickness without ulceration (Dickson and Gershenwald 2011). It is mostly present in thick melanomas, despite being an independent predictor of melanoma patient outcome. Interestingly, T3 non-ulcerated melanomas and T2 ulcerated melanomas have shown a similar 5 year survival, suggesting that the presence of ulceration upgrades the melanoma prognosis to a more advanced stage. Mitotic rate was intensively studied before being incorporated into the latest version of AJCC as a new independent prognostic factor for primary melanoma (Balch et al. 2009). Mitotic rate is a measure of proliferation, and is particularly useful for predicting outcome of vertical growth phase melanomas (Elder et al. 2005). Being equally useful as Breslow thickness and ulceration in predicting melanoma patient survival and clinical outcome, the mitotic rate has replaced Clark's level of invasion in the new

staging system. In fact, it is one of the most reliable prognostic predictors of melanoma, and its assessment can be easily performed during routine histopathological examination (Mervic 2012). Two cohort studies involving 3,661 and 1,284 melanoma patients carried out in Australia and UK, respectively, have shown evidence for the higher prognostic significance of the mitotic rate over many other variables (Retsas et al. 2002; Azzola et al. 2003).

Approximately 20% of patients will develop spread of melanoma beyond the skin (metastasis). For melanomas with a higher potential to metastasize, sentinel lymph node biopsy (SLNB) is undertaken to investigate whether there is dissemination of melanoma into lymph nodes. SLNB safely and reliably stages regional lymph nodes with minimal invasiveness (Sondak et al. 2013). Five year survival rates decrease from 70% to 39% when the number of lymph node metastases increases to three. SLNB is an important prognostic tool in melanoma staging, but its therapeutic value remains controversial (Thompson and Shaw 2007).

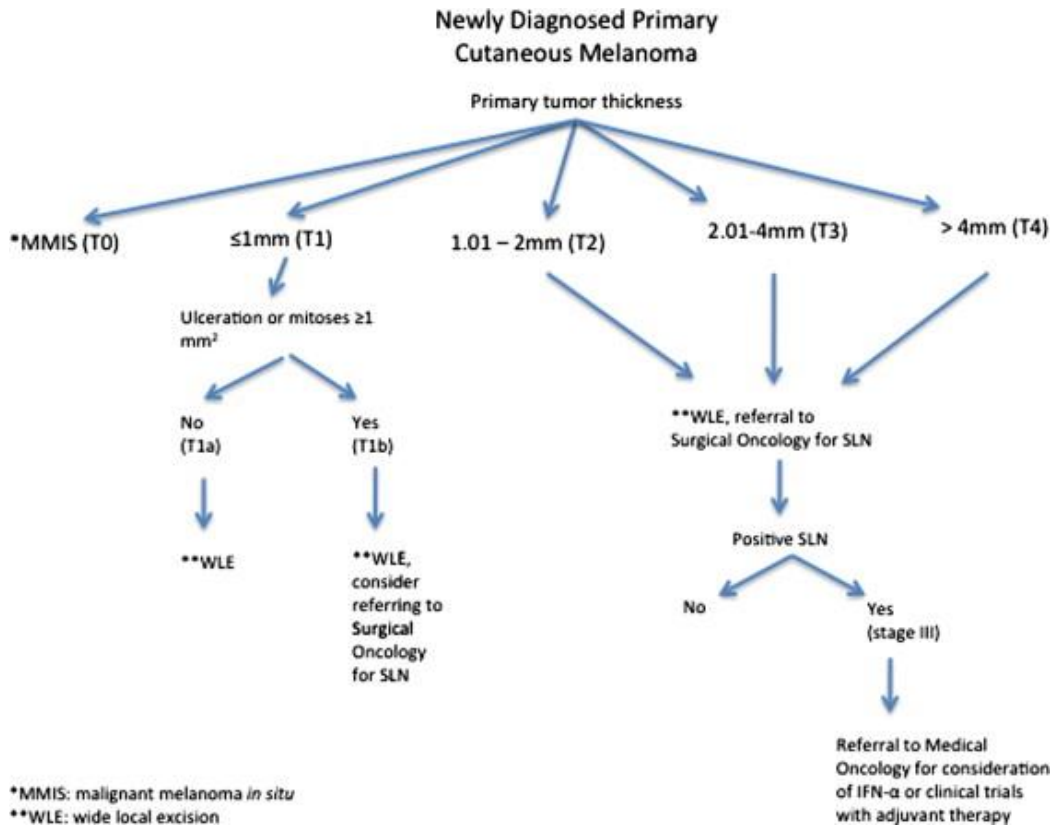


Figure 1-4: Staging system of melanoma based on 2008 AJCC staging system.

(Nading et al. 2010)

Patients with disseminated melanoma have poor survival and outcome. Anatomical site and number of metastases are the most informative prognostic factors for this patient population. For those with stage IV melanoma, non-pulmonary visceral metastasis has the poorest one year survival of 33%, whereas distant skin, subcutaneous and lymph node metastasis has a relatively better one year survival of 62% (Dickson and Gershenwald 2011). In addition to metastasis, elevated serum lactate dehydrogenase (LDH) also acts as a most unfavourable prognostic parameter that predicts poor patient outcome. It is an independent indicator for patients at Stage IV when their serum LDH level rises above the upper limits of normal, regardless of the sites and the numbers of distant metastases (Neuman et al. 2008). The mechanism of increased LDH levels in serum is still unclear. The hypoxic environment of tumour cells may be a cause, as melanoma cell necrosis and LDH release occur when insufficient blood is supplied to the tumour (Agarwala et al. 2009).

**Table 1-1: Melanoma TNM classification based on 2008 AJCC staging system
(Nading et al. 2010).**

Regional Lymph Nodes (N)	No. of Metastatic Nodes	Nodal Metastatic Mass
N classification		
N1	1	a. Micrometastasis b. Macrometastasis
N2	2-3	a. Micrometastasis b. Macrometastasis c. In transit met(s)/ satellite(s) without metastatic nodes
N3	4 or more metastatic nodes, or matted nodes, or in transit met(s)/satellite(s) with metastatic node(s)	
NX	Patients in whom the regional nodes cannot be assessed (eg, previously removed for another reason)	
N0	No regional metastases detected	
Distant Metastasis (M)	Site	Serum LDH
M classification		
M1a	Distant skin, subcutaneous, or nodal metastasis	Normal
M1b	Lung metastases	Normal
M1c	All other visceral metastases	Normal
	Any distant metastases	Elevated
M0	No detectable evidence of distant metastases	

1.1.5 Risk factors for melanoma

The carcinogenesis of cancers is multifactorial, with a contribution from both environmental and intrinsic factors. Likewise, cutaneous melanoma in Caucasians is predominantly caused by environmental factors, particularly ultraviolet radiation (UVR) exposure causing genetic and epigenetic changes, and familial predisposition (Jhappan et al. 2003).

1.1.5.1 Environmental risk factor

It is widely accepted that UV radiation is the leading environmental factor for melanomagenesis, and is responsible for 80% of melanoma cases arising on skin areas with intermittent sun exposure (Garbe and Leiter 2009). A meta-analysis of 57 epidemiological studies has identified intermittent exposure and sunburn history as essential risk factors for melanoma, despite the heterogeneity across the studies. Chronic sun exposure, on the other hand, is associated with the elderly patient population who developed lentigo maligna melanomas on the head and neck (Whiteman et al. 2006). Additionally, the most common mutation in melanoma, BRAFV600E mutation, is correlated with intermittent sun exposure history (Davies et al. 2002; Maldonado et al. 2003). Chronic sun exposure, in contrast, has not shown a significant correlation with melanoma incidence, or the most common melanoma mutation of BRAFV600E (Curtin et al. 2005). The other forms of UV radiation, such as artificial sunbeds, may also contribute to the

melanomagenesis (Swerdlow and Weinstock 1998; MacKie et al. 2009). A significant contribution of cosmetic sunbeds to melanoma risk has been confirmed by the International Agency for Research on Cancer (IARC) in a meta-analysis of 19 studies involving 7,355 melanoma patients (Erratum 2007).

Based on wavelength, UVR is comprised of three bands: UVA (315-400nm), UVB (280-315nm), and UVC (100-280nm) (Hockberger 2002). As the ozone layer in the atmosphere absorbs wavelengths shorter than 310nm, 90% of UVA and only 5-10% of UVB will reach the surface of the earth, with UVC and most of the UVB being absorbed (Kanavy and Gerstenblith 2011). UVA and UVB have been shown to induce melanomas in different animal models, respectively (Setlow et al. 1993; Ley 1997; Bennett 2008). However, the contribution of UVA and UVB in melanoma development is difficult to quantify, and their individual molecular contributions to melanoma progression are still not fully understood.

UVA was initially considered harmless because it is poorly absorbed by DNA. However, accumulating evidence suggests that UVA may indirectly cause DNA changes through oxidative damage. One piece of evidence is that use of artificial sunbeds, which predominantly emit UVA, results in increased risk of developing melanoma (Erratum 2007). Epidemiological studies have also revealed an association with UVA exposure and melanoma mortality rates (Garland et al. 2003). Larger wavelength UVA can penetrate deep into the dermis interacting

with melanocytes within naevi and influencing the tumour microenvironment (Swalwell et al. 2012). High UVA doses cause intracellular oxidative stress by producing excessive reactive oxygen species (ROS) which generate highly mutagenic substances. The production of these mutagenic reactions will subsequently induce DNA damage through a variety of mechanisms, including base substitutions of G–T and G-C, DNA single-strand break, and carcinogenic events in epidermal keratinocytes (Ravanat et al. 2001; Costin and Hearing 2007; Wischermann et al. 2008). The association between UVA radiation and *BRAF* mutation V600E is still awaiting to be defined, although there is evidence suggesting UVA may activate the BRAF-MAKP pathway (Sekulic et al. 2010).

Despite limited penetration beyond the epidermis (Hoffmann et al. 2000), UVB can directly damage DNA via production of pre-mutagenic lesions of cyclobutane pyrimidine dimers (CPD) and 6-4 photoproducts (6-4 PPs), and consequently cause C to T, or CC to TT transversion mutations (Besaratina and Pfeifer 2008). These ‘UVB signature’ mutations are involved in multiple genetic processes, such as cell cycle dysregulation, apoptosis, and DNA repair, as well as epigenetic change, however, they are not related to BRAF mutation V600E in melanomas (Tommasi et al. 1997; Sarasin 1999). UVB-induced immunosuppression may be an additional mechanism in melanomagenesis (Schwarz 2008).

The mechanisms by which UVA and UVB drive tumourigenesis are still incompletely understood. In addition to genetic changes, oxidative stress may play a role in modulating DNA methylation in human cancers, including melanoma (Campos et al. 2007; Franco et al. 2008; Ziech et al. 2011). Other extrinsic risk factors, such as exposure to phototoxic drugs or cosmetic products which contain carcinogens, may also impact on the initiation and progression of melanomas (Volkovova et al. 2012).

Melanocytes protect skin from extrinsic stress through skin pigmentation. They synthesize and transfer melanin pigments to keratinocytes, their partner in the 'epidermal melanin unit' through dendritic processes. Melanin is a redox biopolymeric pigment synthesized in organelles called melanosomes and composed of eumelanin (black/brown) or phaeomelanin (red/yellow) (Hearing 1999). The amount and composition of eumelanin and phaeomelanin (red/yellow) pigments is variable across different population ethnicity, and their skin colour is determined accordingly (Sulaimon and Kitchell 2003). Melanin works as a photo-protective barrier by scattering and reducing the penetration of UV radiation through epidermis (Kaidbey et al. 1979). Phaeomelanin is less functional than eumelanin in terms of capability of shielding UVR (Hill and Hill 2000). Therefore, dark-skinned people with more eumelanin pigment generally have lower risk of CM than fair-skinned people (Gloster and Neal 2006; Brenner and Hearing 2008). Comparatively, populations that produce phaeomelanin with the phenotype of pale skin, red hair, freckles, are much more prone to melanomagenesis. In

addition to poor UV reflection, phaeomelanin could act as a photosensitizer to UVR due to ROS induction, thereby increasing tumourigenesis (Korytowski et al. 1987; Mitra et al. 2012).

1.1.5.2 Genetic risk factors

Family history is a significant genetic risk factor for melanoma. It is estimated that 5% to 12% of melanoma incidence has a hereditary history of melanoma in multiple (≥ 3) first-degree relatives and as much as a 70 fold increased risk of developing a melanoma (Goldstein and Tucker 2001). This type of melanoma is often diagnosed at an early age and is often thinner than non-familial melanomas. Linkage between familial melanomas and germline mutations of melanoma predisposition genes has been well addressed. There are both high penetrance melanoma susceptibility genes, such as tumour suppressor gene *CDKN2A* (cyclin-dependent kinase inhibitor 2A) and *CDK4* (cyclin-dependent kinase 4), and low penetrance melanoma susceptibility alleles, such as melanocortin-1 receptor (*MC1R*), agouti stimulating protein (*ASIP*) and tyrosinase (*TYR*) (Hayward 2003; Gudbjartsson et al. 2008; Raimondi et al. 2008). Genetic alterations of *CDKN2A* have been identified in approximately 40% of melanoma-prone families (Goldstein et al. 2006). There is evidence that such mutations in *CDKN2A* are influenced by UVR and contribute to the production of ROS (Jenkins et al. 2011). Germline mutations of *CDK4* are relatively less common and only present in 2-3% of melanoma families (Goldstein et al. 2006). Low

penetrance melanoma susceptibility genes *MC1R*, *ASIP* and *TYR* are involved in the pigmentation pathway. Variants of these genes show a significantly increased melanoma risk (Gudbjartsson et al. 2008; Raimondi et al. 2008), and associate with melanoma risk factors including fair skin, poor tanning response, red or blonde hair and freckles (Bliss et al. 1995). The co-existence of germline variants of *MC1R* with *CDKN2A* or *BRAF* mutations have also been reported to increase melanoma risk (Landi et al. 2006; Fargnoli et al. 2008; Pastorino et al. 2008). Establishment of the significance for these melanoma susceptibility genes should enable genetic testing in populations with strong family history of melanoma (Kasparian et al. 2007).

1.2 Genetic and epigenetic aberrations of melanoma

Progression from normal melanocyte to benign and dysplastic melanocytic naevus, to horizontal and vertical growth phase primary CM and, ultimately, to metastatic CM, reflects the accumulation of genetic and epigenetic changes in critical genes and pathways that control functions such as proliferation, differentiation, motility and apoptosis. These critical genes function as oncogenes (typically amplified or upregulated in cancer), or as tumour suppressor genes (deleted, mutated or downregulated in cancer). Exploring the genetic and epigenetic profiles of melanoma will help us to better understand the molecular mechanisms underlying the initiation and progression of this lethal malignant disease, in turn leading to the generation of new strategies for molecular subtyping, discovery of diagnostic and prognostic biomarkers and development of novel therapeutic targets.

1.2.1 Genetic dysregulation of melanoma

Multiple genetic events including gene mutation, chromosomal deletion, amplifications and translocations, may contribute to the molecular pathogenesis of melanoma (van Doorn et al. 2005). Dysregulation of several major signalling pathways has been shown to be of particular significance in the development and progression of melanoma: RAS-RAF-MEK-ERK-MAP, MITF signalling, CDKN2A

signalling, PTEN/AKT pathway, and p53 signalling (Miller and Mihm 2006; Dahl and Guldborg 2007; Palmieri et al. 2009).

1.2.1.1 RAS-RAF-MEK-ERK-MAP Kinase Pathway

Somatic mutations harboured by the components of RAS-RAF-MEK-ERK-Mitogen-activated protein (MAP) kinase pathway occur frequently in human cancer. Activating mutation in the gene encoding the serine/threonine protein kinase *BRAF* (v-raf murine sarcoma viral oncogene homolog B1) was carried by a high percentage of melanomas (40-60%), including a predominant form of a substitution of valine by glutamic at amino acid position of 599 (V600E), which accounts for approximately 90% of *BRAF* mutation (Davies et al. 2002; Dahl and Guldborg 2007; Flaherty et al. 2010). Interestingly, *BRAFV600E* mutation also occurs at a high frequency in benign naevi, with induction of senescence and triggers the activation of MAPK (Pollock et al. 2003). Additional molecular alterations are therefore necessarily required for the malignant switch from melanocyte to melanoma. For example, combination of *BRAFV600E* mutation and inactivation of tumour suppressor gene *p53* or *p16INK4a* triggers melanomagenesis *in vivo* (Patton et al. 2005; Dankort et al. 2007). Another frequently mutated member of this pathway is *NRAS*, accounting for approximately 10-20% melanomas that are not *BRAF* mutated (Albino et al. 1989; Davies et al. 2002; Curtin et al. 2005). This high frequency of *NRAS* and *BRAF* mutations underscores the importance of activation of the MAPK pathway for

melanomagenesis and reveals their potential clinical utility as therapeutic targets for melanoma. The significance of treatments targeting the MAPK pathway will be discussed.

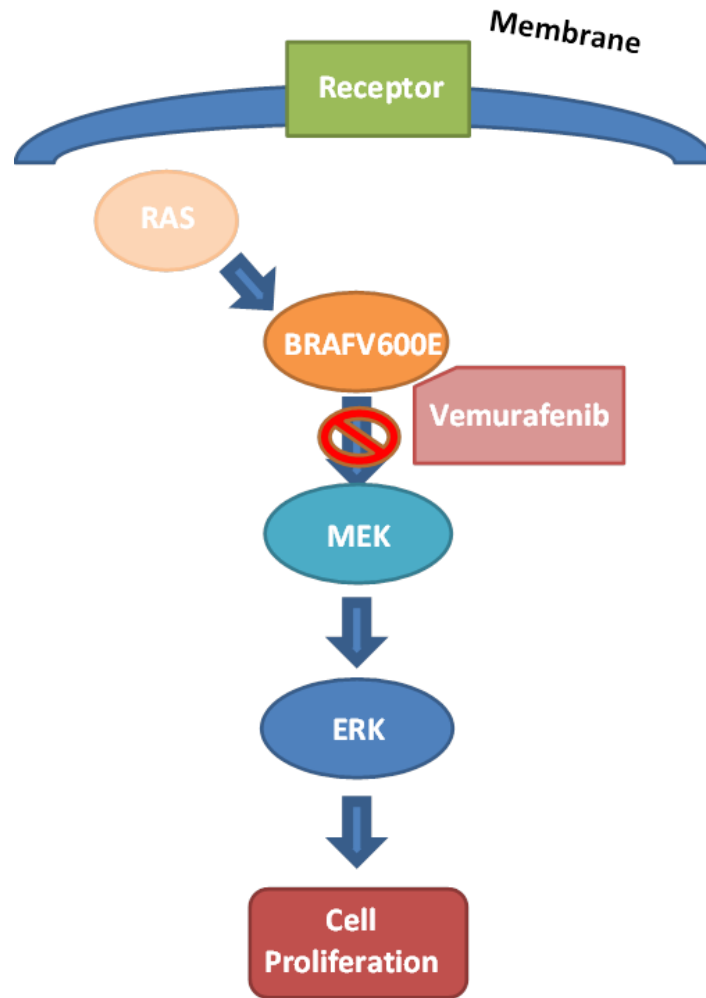


Figure 1- 5: Schematic of MAPK signalling pathway.

BRAF600E mutation activates the cell proliferation via increasing activity of MAPK pathway. BRAF mutation inhibitor Vemurafenib blocks the signal transduction of MAPK pathway.

1.2.1.2 MITF

Microphthalmia-associated transcription (MITF) is known as a 'master regulator' of melanocytic activities, including development, differentiation, cell survival and proliferation. Increased level of amplified MITF from melanocytes to primary melanomas and again to metastases identified by a microarray analysis has characterised MITF to be an oncogene (Hemesath et al. 1994; McGill et al. 2002; Du et al. 2004; Carreira et al. 2005; Loercher et al. 2005). A novel germline mutation of MITF recently identified in two independent studies suggested the association of MITF with familial melanoma (Bertolotto et al. 2011; Yokoyama et al. 2011). However, MITF acts as both a promoter and suppressor of cell proliferation when crosstalking with different pathways. It can drive cell proliferation by interacting with cell cycle regulator CDK2 (Du et al. 2004) or cause cell growth arrest by activating *p14ARF* (Loercher et al. 2005) or p21 (Carreira et al. 2005). MITF also associates with the apoptosis pathway by regulating apoptosis inhibitor BCL2 (McGill et al. 2002). MITF is a potential clinical target for assessing chemoresistance because reduced MITF activity increase the sensitivity of melanoma cells to chemotherapy (Garraway et al. 2005).

1.2.1.3 CDKN2A signalling

The *CDKN2A* locus, which encodes two tumour suppressor genes *p16INK4A* and *p14ARF* on chromosome 9p21 (Quelle et al. 1995) is frequently inactivated in melanoma (Curtin et al. 2005; Hodis et al. 2012). *p16INK4A* regulates the cell cycle transition at G1-S checkpoints by inhibiting activity of cyclin-dependent kinase 4 (CDK4) (Serrano et al. 1996). Dysregulation of *p16INK4A* by genetic alteration including somatic mutations (Hayward 2003) and epigenetic alteration of aberrant methylation have been reported in melanoma (Jonsson et al. 2010). Inactivation of *p16INK4A* by these alterations causes genetic instability of melanocytes (Fung et al. 2013) and leads to susceptibility of melanocytes to cellular oxidative stress (Jenkins et al. 2011), implying a critical role for *p16INK4A* in the initiation of melanomagenesis. Inactivation of *p16INK4A* will potentially abrogate senescence in cancer (Bennett 2008) and increased telomerase activity induced by inactive *p16INK4A*. Telomere shortening is a crucial mechanism for induction of replicative senescence. Being present in tumours, the enzyme telomerase catalyses the extension of telomeres and prevents cellular senescence. Telomerase activity increases with tumour progression from early stage primary melanoma to metastatic melanomas (Ramirez et al. 1999). *p14ARF* facilitates the stabilization of p53 by interacting with MDM2. Inactive *p14ARF* in melanoma therefore may be a mechanism that indirectly downregulates p53 (Freedberg et al. 2008).

1.2.1.4 PTEN/AKT signalling

PTEN (phosphatase and tensin homolog) is a putative tumour suppressor gene dysregulated in human cancers. In melanoma, expression of *PTEN* is often reduced or lost due to genetic deletions or mutations (Tsao et al. 1998; Celebi et al. 2000; Reifemberger et al. 2000; Goel et al. 2006). More than 100 genetic alterations of *PTEN* have been identified in melanomas, including three genetic changes discovered in both melanoma cell lines and melanoma tissues (Aguissa-Toure and Li 2012). Along with these genetic changes, other molecular mechanisms such as DNA methylation also contribute to the inactivation of *PTEN* in melanoma (Mirmohammadsadegh et al. 2006; Lahtz et al. 2010). Increased expression of *AKT*, the negative downstream mediator of *PTEN* has also been reported in melanoma (Dai et al. 2005). *PTEN/AKT* pathway together with downstream targets such as *BAD* (Li et al. 2003) and *NFKB* (Dhawan et al. 2002) regulates a number of critical cancerous activities including cell proliferation, apoptosis, migration, and metastasis in melanoma (Madhunapantula and Robertson 2009). Moreover, *PTEN* in the context of *MAPK* pathway upregulation clearly makes a contribution to the development and progression of melanoma, as well as drug sensitivity and efficacy of *MAPK* pathway components inhibitors (Tsao et al. 2004; Nogueira et al. 2010; Byron et al. 2012; Vredeveld et al. 2012; Nathanson et al. 2013).

1.2.1.5 p53 signalling

p53 has been described as the 'guardian of the genome' that regulates multiple tumour-related signalling pathways in response to stress, including apoptosis, DNA repair and cell cycle arrest (Vousden 2006). It is frequently mutated in human cancers, and has been pivotal to our understanding of the mechanisms of tumorigenesis. It is also an attractive target for new anticancer strategies. However, *p53* is rarely mutated in melanoma and most melanomas sustain a high expression level of the wild-type form (Bartek et al. 1991; Albino et al. 1994; Sparrow et al. 1995; Gwosdz et al. 2006). Nonetheless, accumulating evidence suggests an important role for *p53* and the p53 pathway in melanomagenesis. For example, co-existence of inactive *p53* and *RAS* or *RAF* mutations in animal models can trigger melanoma formation (Bardeesy et al. 2001; Dovey et al. 2009; Goel et al. 2009). Diverse mechanisms of *p53* pathway disruption in melanomas have also been reported, including overexpression of MDM2 (Muthusamy et al. 2006) and MDM4 (Gembarska et al. 2012) which degrades p53 via ubiquitination, as well as dysregulation of p53 responsive targets in apoptosis and cell cycle pathways (Avery-Kiejda et al. 2011), such as PTEN (Karst et al. 2005) and APARF-1 (Soengas et al. 2001). Additionally, two antagonistic isoforms of p53 and p53 regulated microRNA may also contribute to the regulation of the whole pathway, respectively (Hermeking 2007; Avery-Kiejda et al. 2008).

1.2.2 Targeted therapies for melanoma

Minimal improvement in the medical management of advanced melanoma has been made until very recently, with only the U.S. Food and Drug Administration (FDA) approved dacarbazine and interleukin 2 (IL-2) available as conventional therapy, both of which have unsatisfactory efficacy, with low patient response rates (Jang and Atkins 2013). However, this situation has changed remarkably with the introduction of targeted treatments in the last few years (Flaherty et al. 2010; Chapman et al. 2011; Flaherty et al. 2012; Hauschild et al. 2012; Long et al. 2012; administration 2013). Vemurafenib (PLX-4032), an inhibitor targeting the most common mutant form of BRAF in melanoma (V600E) (Figure 1-5), has significantly improved the management of stage 3C and stage 4 melanomas that harbour BRAFV600E mutation (Flaherty et al. 2010; Chapman et al. 2011). BRAFV600E alters the orientation of the α C helix and this enables vemurafenib to bind to V600E mutation, but not to wild type *BRAF* (Tsai et al. 2008). In a phase III BRIM (BRAF inhibitor in Melanoma) study (Chapman et al. 2011), Vemurafenib-treated patients with disseminated melanoma showed significantly improved 6-month overall survival (84%) compared with those treated with standard chemotherapy dacarbazine (64%). However, this new treatment only increased progression-free survival (PFS) by a few months (median PFS 5.3 months for vemurafenib versus 1.6 months for dacarbazine). Notwithstanding this evidence of clinical efficacy, it is clear that the majority of patients develop relapsed disease after a few months of therapy and the prognosis for patients with a large tumour burden remains poor (Flaherty et al. 2010). Relapsed

disease is probably because melanoma cells bypass inhibition of BRAF mutation and pursue proliferation through other associated pathways such as PI3K/AKT pathway and mTOR pathway (Britten 2013). Therefore, vemurafenib may show superior efficacy if metastatic disease could be detected earlier and therapy initiated with lower tumour volumes, because smaller volume tumours have less genetic and epigenetic diversity and is therefore less able to evolve drug resistance. In attempts to improve the efficacy of targeted therapy, dual therapy with the second generation BRAFV600E inhibitor, dabrafenib (Hauschild et al. 2012; Long et al. 2012) and the MEK inhibitor, trametinib (Flaherty et al. 2012) (both agents have recently been approved by FDA in 2013 for metastatic and unresectable melanoma) has been trialled and the combination shows markedly increased efficacy compared to dabrafenib alone (Ballantyne and Garnock-Jones 2013).

Ipilimumab is an immune-modulatory treatment for advanced melanoma that was approved by the FDA in 2011. It is a monoclonal antibody (Britten 2013) that specifically inhibits the activity of a negative regulator of T cells, cytotoxic T-lymphocyte-associated antigen 4 (CTLA-4) (Pardoll 2012). Ipilimumab significantly improved overall survival (OS) in comparison to the cancer vaccine glycoprotein (gp) 100 and when combined with dacarbazine compared to dacarbazine alone (Hodi et al. 2010; Robert et al. 2011). Autoimmune toxicities of ipilimumab remain a major concern, but these can be managed medically to allow maintenance of dose density and dose intensity.

1.2.3 Epigenetic dysregulation of melanoma

'Epigenetics' refers to heritable changes in gene expression without alterations in the primary DNA sequence, providing an additional layer of gene regulation through transcriptional control (Holliday 1987). Epigenetic regulation is functionally pivotal for numerous biological processes, including embryonic development, cell growth, chromosome stability maintenance and human diseases, including cancer (Lopez-Serra and Esteller 2008). The pathogenic effects of abnormal epigenetic changes have been extensively investigated, particularly in neoplasia. These come about by biochemical modifications such as methylation and acetylation, either of the DNA itself, or of the associated histone proteins (Gal-Yam et al. 2008). DNA methylation is the best-characterized epigenetic signature and has been extensively studied in human cancer.

1.2.3.1 DNA methylation

DNA methylation occurs exclusively on cytosine residues within cytosine-guanine dinucleotides (CpG dinucleotides) (Lopez et al. 2009). This biological process is catalysed by a family of methyltransferases which transfer a methyl group from S-adenosyl-methionine (SAM) to the 5-carbon of the cytosine ring (Herman and Baylin 2003; Foulks et al. 2012) (Figure 1-5). CpG dinucleotides are concentrated in short CpG rich regions, named CpG islands, which are preferentially located at the 5' end of genes and occupy 50%-70% of human

gene promoters (Bird 1986). Whilst most CpG sites outside of CpG islands in the genome are methylated, the majority of CpGs in CpG islands usually remain unmethylated during development and in normal human tissues (Eckhardt et al. 2006). CpG island methylation in normal cells is the main mechanism for gene silencing on the inactive X chromosome and for a process called genomic imprinting (Wong et al. 1999). Genomic imprinting can involve either DNA methylation or histone modulation with resultant monoallelic inheritance in a parent-of-origin-specific manner (Reik and Walter 2001). These methylation phenomena in normal tissues are essential for normal development and reprogramming of embryogenesis (Reik et al. 2001; Kim et al. 2009). Genomic imprinting may also ensure transposable elements remain epigenetically silenced to maintain genome integrity and one hypothesis for the origin of imprinting centres on the need to silence genes inserted into the genome by viruses (Barlow 1993). Aberrant DNA methylation is frequently detected in human cancers, particularly for those cancer-associated genes that are ubiquitously genetically altered in cancers, implying that DNA methylation is a hallmark of cancer, equally as important as genetic modifications of DNA (Esteller 2007). Human cancers undergo two major mechanisms of aberrant DNA methylation: hypermethylation and hypomethylation. Hypermethylation is a process to gain methylation which usually takes place within the promoter region of tumour suppressor genes leading to gene inactivation and promotion of tumourigenesis. Two suggested mechanisms explaining gene silencing by DNA methylation are inhibition of transcription factor binding to its recognised cognate sequence, and

recruitment of co-suppressors after methyl-binding proteins anchor to methylated DNA (Klose and Bird 2006). Methylation-dependent gene silencing is a major event in the onset of many cancers interacting with the cell cycle, apoptosis, cell adhesion, and angiogenesis (Herman and Baylin 2003). The contribution of DNA hypermethylation to metastasis is not fully understood, but a possible correlation has been suggested by increasing DNA methylation in parallel with tumour progression to metastasis (Rodenhiser 2009). DNA hypermethylation is not restricted to gene promoters, but can also occur in other areas including the gene body or the CpG shore (Maunakea et al. 2010; Hansen et al. 2011). Besides protein coding genes, tumour suppressors like non-coding RNA (micro-RNA) are also influenced by expression-associated DNA methylation in cancers with functional significance (Lujambio et al. 2008; Berdasco and Esteller 2010). On the other hand, the presence of global hypomethylation (loss of methylation) in DNA repetitive sequences may contribute to the re-expression of normally silent harmful viral genes and oncogenes, with loss of methylation promoting hyperproliferation and chromosomal instability (Esteller 2008). Consequently, hyper- or hypomethylation of DNA, or both are likely to drive tumour development (Lopez et al. 2009). Recent discovery of a new modified form of methylation, 5-hydroxymethyl cytosine (5hmc), has added further complexity. However, despite its presence in embryonic stem cells (Kriaucionis and Heintz 2009), 5hmc is likely to be absent in several human cancers (Haffner et al. 2011; Yang et al. 2013), including melanoma (Lian et al. 2012), suggesting in this investigation it is not necessary to distinguish the two forms of 5' methylcytosine (5mc) and 5hmc.

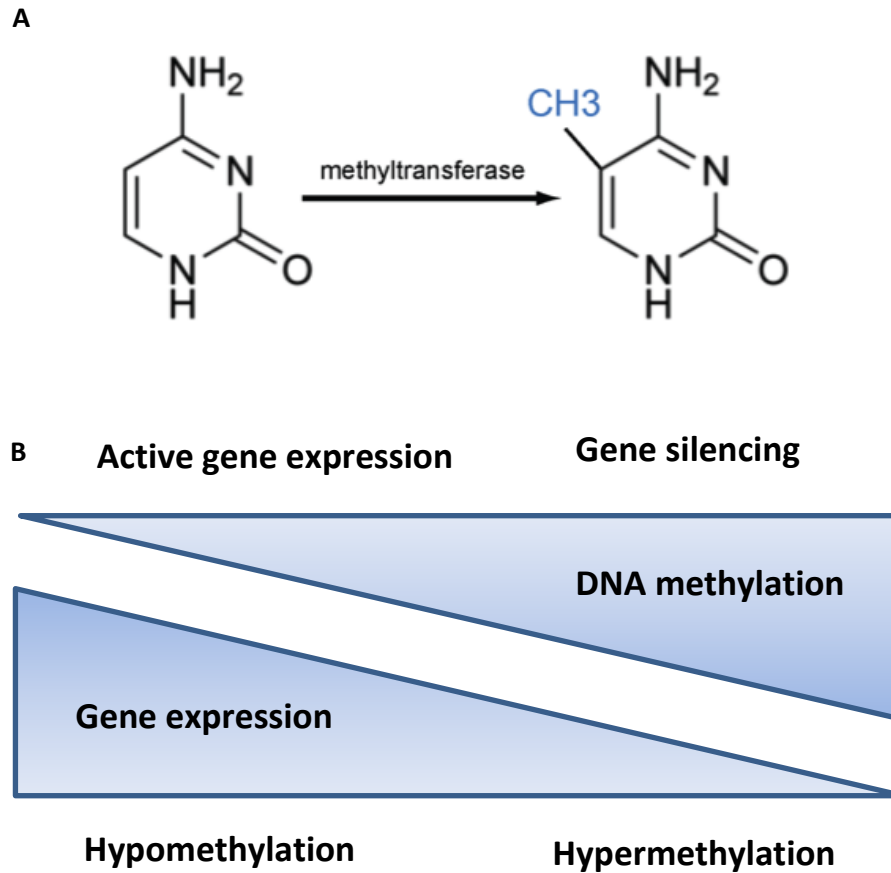


Figure 1-6: Schematic of DNA methylation and regulation of gene expression by DNA methylation.

(A): Biological conversion of cytosine to 5mC by methyltransferase. (B): DNA methylation transcriptionally regulates gene expression. Hypermethylation (gain of methylation) should correlate with reduced gene expression whilst hypomethylation (loss of methylation) correlates with increased gene expression.

1.2.3.2 DNA methylation in melanoma

Similar to most other human cancers, melanoma is subject to considerable epigenetic dysregulation, with a large number of genes being transcriptionally downregulated by DNA hypermethylation. Approximately 100 such genes have been found to be hypermethylated in melanoma (listed in Table 1-2) (Rothhammer and Bosserhoff 2007; Liu et al. 2008; Howell et al. 2009; Liu et al. 2009; van den Hurk et al. 2012), including putative tumour suppressors that are also genetically modified in melanoma, such as *p16INK4*, *p14ARF* and *PTEN*, suggesting that DNA methylation can cooperate with genetic changes, such as gene mutations, and further promote tumourigenicity. In addition, genes such as *MGMT*, *RASSF1A* and *E-cadherin* which have a high frequency of methylation in other human cancers are also methylated in melanoma (Esteller 2008). Importantly, many hypermethylated genes in melanoma are components of critical cancer-related pathways, with representative examples being *APC* in the WNT pathway, *DAPK* and *APAF1* in the apoptosis pathway and *TFPI2* in tumour invasion and metastasis (Soengas et al. 2001; van den Hurk et al. 2012), illustrating the indispensable role played by epigenetic dysregulation in concert with genetic changes during tumour development and progression. However, due to the unique biology of melanoma, a large number of additional epigenetically regulated genes undoubtedly still await identification and characterization.

Table 1-2: Hypermethylated genes identified in melanoma tissues.

(Rothhammer and Bosserhoff 2007; Liu et al. 2008; Howell et al. 2009; Liu et al. 2009; van den Hurk et al. 2012)

Functions	Gene symbols
Apoptosis	APAF1, ASC, DAPK, CASP8, HSPB1, p73, PIRIN, PYCARD, RARB (Haugen et al. 2004), SFN, TIMP3, TRAIL
Cell proliferation	CDH1, CDKN1B, CDKN1C, CDKN2A, CSK, DDIT4L, DNAJC15, EBP1, ER α , ET2, GDF15, IGFBP7, p14 ^{ARF} , p16 ^{INK4} , p73, PCNA, PI5, PRDX2, RARB (Haugen et al. 2004), RASSF1A, S100A1, SFN, TIMP1, TSP1
Migration and invasion	BST2, CDH1, CSK, PI5, PIRIN
Cell adhesion	CDH8, IGFBP7, ITGAE, ITGB8, THBS1, TIMP1, TIMP3
Immune response	CASP8, CCR7, CD10/MME, DPPIV, CSK, GDF15, IFIT1, LXN, MT2A, MX1, PTGS2, PYCARD, QPCT, SFN, SOCS1, SOCS2, SOCS3, SYK, TIMP1
Angiogenesis	TFPI2, TIMP1, TIMP3, WFDC1(McAlhany et al. 2003)
Senescence	BST2, p16 ^{INK4}
Metastasis	CDH1, HSPB1, PI5, PTGS2, TCF21(Arab et al. 2011), TM
Metabolism	CASP8, CYBA, LDHB, MTAP, PRDX2, 3-OST-2
Wnt pathway	APC, FRZB, WIF1
TGF-beta pathway	CSNK1G2, GDF15, RUNX3, THBS1, WFDC1(McAlhany et al. 2003)
MAPK pathway	ISGF3G, RGS3, TSP1
p53 signalling	MGMT, THBS1, TRAIL
PTEN/AKT pathway	PTEN
Unknown in cancers	HOXB13, KR18, LRRC1, NPM2, RARRES1, PDLIM4, RPL37A, TM, TRP1

Gene function was searched from Gene Cards Website (Database)

1.2.3.3 Methodologies for DNA methylation analysis

Accompanying the fast moving field of DNA methylation, with ever expanding complexities involving isoforms, transcription-specific CpG sites within promoter regions and other areas, and methylation in microRNA, the development and improvement of DNA methylation investigative methodologies has also rapidly evolved (Laird 2010). Methylation analysis is mainly based on three strategies: sodium bisulfite conversion, affinity enrichment and methylation-Sensitive Restriction Enzymes (MSREs) digestion (Ndlovu et al. 2011). Bisulfite conversion is a particularly useful technique enabling 5mc to be distinguished from cytosine by converting unmethylated cytosine to uracil whilst methylated cytosine remains unchanged. This provides a platform for many other techniques, including PCR-based, methylation-specific PCR (MSP), bisulfite sequencing and pyrosequencing, and large-scale, extensive coverage methods like deep sequencing, Illumina methylation microarray and genome-wide bisulfite sequencing (Laird 2010).

Simpler techniques such as MSP and pyrosequencing are relatively more practical in terms of time, cost and analysis. Pyrosequencing quantitatively measures DNA methylation at single CpG dinucleotide resolution with high accuracy, sensitivity and reproducibility (Dupont et al. 2004). The basic principle of this protocol is detection of the release of pyrophosphate generated during the synthesis of double stranded DNA when using single stranded DNA as template

(Ronaghi 2001). This sequencing technique has shown promising results in the detection of multiple methylated CpG islands in some tumour types, including melanoma and head and neck cancer (Gal-Yam et al. 2008; Shaw et al. 2008; Ugurel et al. 2009). MSP is based on gel electrophoresis by which methylated cytosines in a defined DNA fragment are directly displayed (Hamilton 2011). For the purpose of easy performance, analysis and interpretation, pyrosequencing and MSP will be explored in this thesis, with the aim of identifying potential epigenetically silenced biomarkers of melanoma. However, both these two protocols only allow evaluation of methylation within a limited length of DNA sequence, suggesting they are more applicable for methylation validation than for primary identification of methylated candidates. For unbiased analysis, a large-scale methylation analysis such as genome-wide methylation microarray is required. Currently, the widely used Illumina methylation microarray provides high-throughout, high-resolution, and more comprehensive methylation profiles, but simultaneously requires good quality starting materials, and significant bioinformatics expertise for the analysis (Bibikova et al. 2011).

Affinity enrichment and MSRE are also currently adapted for many downstream DNA methylation analyses (Laird 2010). The fundamental principles underpinning these two methods are enrichment of methyl-DNA by immunoprecipitation using a 5mc specific antibody and enzymatic digestion of methylated or unmethylated DNA sections by methylation-sensitive restriction enzyme, respectively (Acevedo et al. 2011). An important strength of these two

methods over bisulfite conversion based methods is the capability for discriminating 5mc from 5hmc (Gupta et al. 2010).

1.2.3.4 Clinical applications of DNA methylation in cancer

Identification of methylation-dependent silencing of tumour-related genes has extended our understanding of the initiation and progression of cancer and suggests a number of potential translational applications for aberrant DNA methylation, with particular interest in discovery of epigenetic biomarkers and development of epigenetic therapeutic strategies.

1.2.3.4.1 DNA methylation as a biomarker

Cancer related genes are likely to be epigenetically altered at a higher frequency than genetical mutations (Baylin and Jones 2011). Therefore, use of epigenetic biomarkers may be particularly helpful for early detection of metastatic disease. Identification of methylated DNA could also be useful for early diagnosis, molecular profiling of tumour progression, predicting treatment response and allowing selection of patients for specific targeted therapies (Hegi et al. 2005; Conway et al. 2011; Fukushige and Horii 2013). Promising example is the use of methylated *GSTP1* for early diagnosis and prognosis of prostate cancer. Van Van Neste et al. have reported an overall sensitivity of 82% and specificity of 95% of *GSTP1* methylation to discriminate prostate cancer from non-neoplastic

prostate tissue based on 35 studies (Van Neste et al. 2012). Another potential use for epigenetic biomarkers is for predicting the primary tumour in those patients diagnosed with metastatic disease of unknown primary origin (Fernandez et al. 2012). Methylated DNA is also attractive as a serum biomarker for tumour progression and prognosis. Recent studies have reported the application of serum epigenetic biomarkers for detecting metastases in human cancers (Li et al. 2012). In fact, measurement of biomarkers in patients' circulating blood is increasingly recommended because of its simplicity and minimal invasiveness (Tandler et al. 2012).

Metastatic melanoma is accompanied by increased serum levels of biochemical biomarkers. Currently available melanoma serum biomarkers LDH (as described in 1.1.4) and melanocyte lineage/differentiation antigens S100-beta are very insensitive and only detect disseminated melanoma when there is significant tumour burden with little chance of curative treatment (Ugurel et al. 2009). Therefore, serum biomarkers for early detection of metastases with high sensitivity are urgently required. Investigation of aberrantly hypermethylated tumour related genomic DNA circulating in the peripheral blood of cancer patients could allow pre-symptomatic detection of metastases with higher sensitivity and specificity, since tumour DNA is likely to be released from the circulating tumour cells, from lysis of necrotic tumour cells or from tumour cell-free DNA (Board et al. 2008; Heyn and Esteller 2012). The presence of detectable free tumour DNA is known to be correlated with a poor prognosis

(Silva et al. 1999; Dominguez et al. 2002; Lecomte et al. 2002). Thus, detection of circulating methylated DNA holds promise for improving the accuracy and early diagnosis of melanoma, including subclinical relapse and metastasis. Correlations of methylated *ER-α* (Mori et al. 2006) and *RASFF1A* (Mbulaiteye et al. 2006) in melanoma patients' blood with melanoma progression have been previously reported. However, the sample size for these studies was rather small and clinical validation of these serum biomarkers in bigger patient cohorts plus investigation of more promising epigenetic serum biomarkers are clearly needed.

1.2.3.4.2 Therapeutic strategy targeting DNA methylation

The methylation process is pharmacologically reversible and this may be exploitable to develop new therapeutic strategies for cancer. Demethylating agents, such as 5'-azacytidine and 5'-aza-2-deoxycytidine have shown efficacy in reactivating and up-regulating previously silenced tumour suppressor genes (Esteller 2006). 5'-azacytidine and 5'-aza-2-deoxycytidine have also been approved by FDA for the treatment of haematopoietic malignancies, particularly for patients with myelodysplastic syndrome (Kantarjian et al. 2007). By preferentially targeting replicating cells these demethylating agents trigger re-expression of tumour suppressor genes in tumour cells (Lopez et al. 2009). They could also be combined with chemotherapy to improve the clinical response, as chemotherapy resistance is often induced by transcriptionally silenced tumour-related genes.

Chapter 2 Materials and Methods

2.1 Cell lines and culture conditions

2.1.1 Human melanocyte and melanoma cell culture

Two benign immortalised melanocytes and 23 human melanoma cell lines have been collected for this study. These cell lines were purchased from Invitrogen, American Type Culture Collection (ATCC), or kindly provided by Dr Gareth Inman (Jacqui Wood Cancer Centre, Ninewells Hospital & Medical School, University of Dundee), Dr. Daniele Bergamaschi (Barts and London, School of Medicine and Dentistry, Queen Mary, University of London) and Dr Monica Rodolfo (Department of Experimental Oncology, Istituto Nazionale Tumori, Italy). Primary melanoma cell lines are categorized into radial growth phase, RGP, and vertical growth phase, VGP. Table 2-1 shows the name, disease stage, source and culture media of each cell line. All cell lines were grown at 37 °C and 5% CO₂, with regular mycoplasma contamination testing.

Table 2-1: Description, source and culture media of the cell lines used in this study.

Cell line	Source	Medium	Supplements
Normal Human Melanocytes			
HEMa-LP	Dr Daniele Bergamaschi	254 ^I	HMGS2 ^{II}
HEMn-LP	Invitrogen	254	HMGS2
Primary Melanoma, Radial Growth Phase (RGP)			
SBCL2	Dr Gareth Inman	RPMI ^{III}	10% FBS
PMWK	Dr Gareth Inman	DMEM ^{IV}	10% FBS
WM35	Dr Gareth Inman	RPMI	10% FBS
Primary Melanoma, Vertical Growth Phase (VGP)			
WM983A	ATCC	DMEM	5% FBS
WM115	ATCC	DMEM	5% FBS
LM2	Dr Monica Rodolfo	DMEM	5% FBS
WM902B	Dr Gareth Inman	RPMI	10% FBS
MEL224	Dr Daniele Bergamaschi	RPMI	10% FBS
MEL505	Dr Daniele Bergamaschi	RPMI	10% FBS
Metastatic Melanoma			
SKMEL2	Dr Gareth Inman	DMEM	10% FBS
SKMEL23	Dr Gareth Inman	DMEM	10% FBS
SKMEL147	Dr Gareth Inman	DMEM	10% FBS
SKMEL173	Dr Gareth Inman	DMEM	10% FBS
SKMEL30	Dr Gareth Inman	RPMI	10% FBS
MEL501	Dr Daniele Bergamaschi	RPMI	10% FBS
A375M	Dr Daniele Bergamaschi	RPMI	10% FBS
C8161	Dr Daniele Bergamaschi	RPMI	10% FBS
COLO829	Dr Gareth Inman	RPMI	10% FBS
WM266-4	Dr Gareth Inman	DMEM	5% FBS
WM239A	Dr Daniele Bergamaschi	DMEM	5% FBS
WM983B	ATCC	DMEM	5% FBS
LM9	Dr Monica Rodolfo	DMEM	5% FBS
LM29	Dr Monica Rodolfo	DMEM	5% FBS

^I254 Medium is purchased from Invitrogen, ^{II}RPMI and ^{IV}DMEM are purchased from Gibco. ^{II} Human melanocyte growth supplement-2 (HMGS2) contains bovine pituitary extract, fetal bovine serum (FBS), bovine insulin, bovine transferrin, basic fibroblast growth factor, hydrocortisone, heparin, and endothelin-1 (Invitrogen).

2.1.2 Human melanoma cell line culture for microarray

The following 3 sets of paired cell lines that are derived from the same patients were selected for gene HumanHT12 expression microarray and HumanMethylation450 microarray:

Set 1: WM983A and WM983B

Set 2: WM115, WM266.4 and WM239A

Set 3: LM2, LM9 and LM29

In order to minimize the variation cross the panel, the culture conditions, including the culture medium and the percentage (%) of FBS have been optimized. DMEM medium with additional 5% FBS was selected to culture all 8 cell lines, due to the maintenance of similar phenotypes and proliferation rates with the original medium on demand. Figure 2-1 shows the morphology of two representative cell lines grown in the original medium and optimized culture medium.

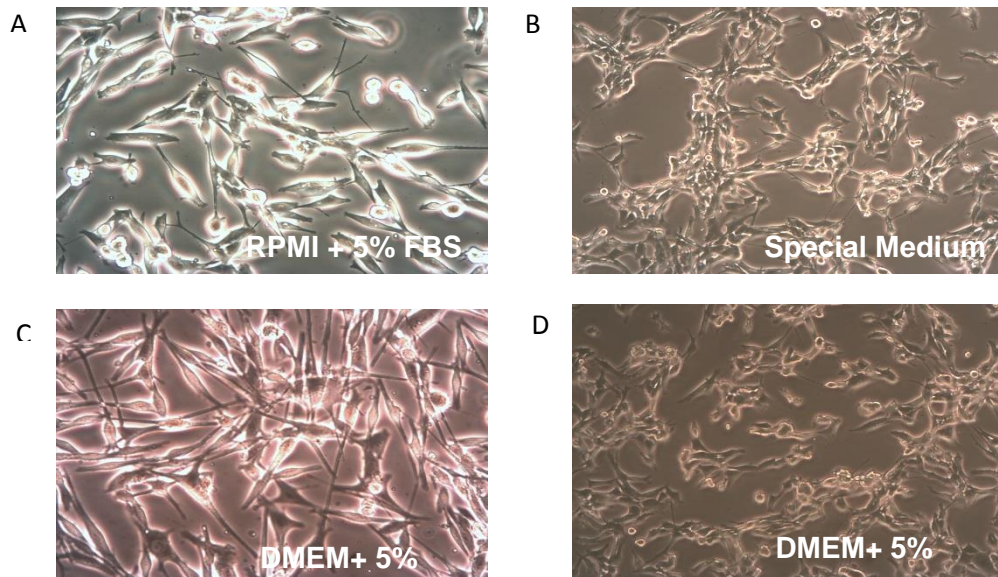


Figure 2-1: Morphology of WM239A (A, C) and WM115 (B, D) cell lines under different culture media.

(A): WM239A cell grown in RPMI and 5% FBS after one week; (B): WM115 cell lines grown in the special medium (MCDB153:L15 4:1, 2%FBS, CaCl₂ 1.68Mm, Insulin 5ug/ml and Collagen IV) recommended by ATCC; (C, D): WM239A (C) and WM115 (D) cell lines show similarly cellular phenotype and proliferation rate with A and B after being maintained in a solution of DMEM+5% FBS in one week.

2.1.3 Disassociation, freezing and recovery of cells

Cells were washed in phosphate buffered saline (PBS) before disassociation in 0.05% Trypsin-EDTA (Ethylendiaminetetraacetic Acid) (Gibco). Harvested cells were pelleted by centrifugation and resuspended in growth medium for passaging, or in a solution of 90% FBS and 10% dimethyl Sulphoxide (DMSO) for freezing. For recovery of frozen cells, cryovials containing the frozen cells that have been stored in liquid nitrogen were quickly thawed in water bath (37°C), and resuspended in culture media for recovery.

2.2 Tissue and serum samples

This project was approved by both the East London & City Health Authority Local Research Ethics Committee and by the Tayside Medical Research Ethics Committee. Formalin-fixed, paraffin-embedded (FFPE) tissue and serum samples from melanoma patients collected through Barts and The London were kindly provided by Dr Catherine Harwood^I. FFPE tissues from Dundee were selected and provided by Dr Alan Evans^{II}. Serum samples from melanoma patients for prospective study (Dundee) were collected by Amanda Degabriele^{III} and Leaca Crawford^{III}. Clinical information of melanoma patients was obtained from detailed inspection of clinical records including histopathology reports and Multi Disciplinary Team (MDT) entries. 39 samples were chosen for microdissection by histopathological examination under supervision by Dr Catherine Harwood.

^IBarts and The London, School of Medicine and Dentistry, Queen Mary, University of London.

^{II}Department of Pathology, Ninewells Hospital & Medical School, University of Dundee.

^{III}NHS Tayside, Ninewells Hospital & Medical School, University of Dundee.

Table 2-2: Description of clinical cases.

Clinical samples	Description	Number	Source
FFPE	stick cores of melanomas	~100	Barts and The London
	microdissected melanomas	39	
Frozen	benign naevi	10	
Serum	melanoma patients	85	
FFPE	paired melanoma samples	16	University of Dundee

2.3 Molecular biology methods

2.3.1 DNA and RNA Purification

2.3.1.1 DNA extraction from cultured cells and patient serum

The cell monolayer was washed by PBS, trypsinized, pelleted by centrifugation, and resuspended in 200µl PBS before DNA digestion. Cells in PBS were homogenised by vortexing. Genomic DNA was subsequently extracted using the QIAamp DNA Blood Mini Kit (Qiagen, Hilden, Germany) according to the manufacturer's instructions. Serum DNA was also extracted using the QIAamp DNA Blood Mini Kit.

2.3.1.2 RNA extraction from cultured cells

Cells were lysed in RLT buffer (supplied with the RNeasy mini kit, Qiagen) after washing in PBS and collected by cell scraper. The cell lysate in the RLT buffer was then processed for RNA extraction using the RNeasy Mini Kit following the manufacturer's protocol, including the on-column DNase digestion step.

2.3.1.3 DNA purification from paraffin embedded tissues

Xylene and ethanol was used for deparaffinization. DNA lysis buffer (x1 TNE= 100 mM NaCl, 10 mM Tris.Cl (pH8), 1 mM EDTA, 0.5%SDS (sodium dodecyl sulfate) containing 20 microlitres of proteinase K (Qiagen) was added to the samples with a following incubation at 55 °C. After the tissue was thoroughly digested, DNA was purified with phenol at room temperature and finally precipitated from the aqueous layer by addition of 2.5 volumes of 100% ethanol and storage at -80 °C for one hour. The DNA pellet was dried and dissolved in Tris EDTA buffer solution (TE, pH8).

2.3.1.4 RNA purification from paraffin embedded tissues

Sections were deparaffinized by xylene and 100% ethanol. The dried pellet was re-suspended in RNA lysis buffer (10 mM Tris/HCL (pH 8.0), 0.1 mM EDTA, 2% SDS) supplemented with 60 µl proteinase K, and incubated at 55°C until the tissue was completely solubilized. RNA was purified with phenol at room temperature and precipitated with isopropanol in the presence of 0.1 volume of 3 M sodium acetate (pH 5.2), and carrier glycogen at -20°C for 2 hours. The RNA pellet was washed once in 75% ethanol, and resuspended in RNase-free water.

2.3.1.5 Quantification and quality examination of DNA and RNA

DNA and RNA concentration were measured spectrophotometrically by Thermo Scientific NanoDrop 2000 (Labtech). The absorbance ratio at 260nm/280nm of 1.7-1.9 and 1.9-2.1 assured good quality of DNA and RNA, respectively. Integrity of RNA was checked by 1% denaturing agarose gel electrophoresis and ethidium bromide staining. As shown in Figure 2-2, the 28S and 18S ribosomal RNA bands in the 5 RNA samples are clearly visible, with an approximate ratio of 2:1, and indicated good integrity of these RNA samples.

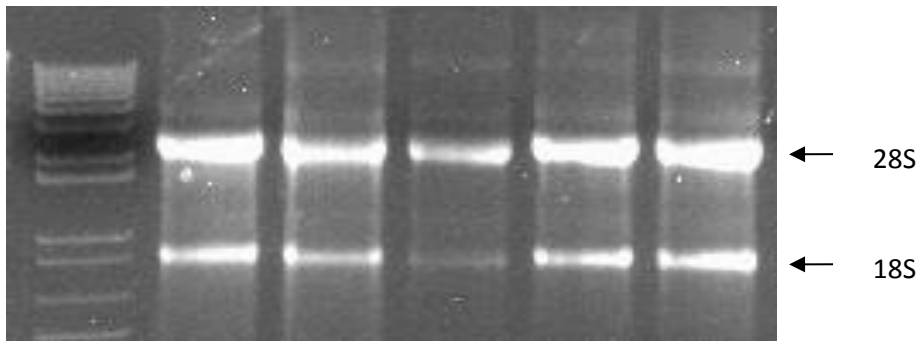
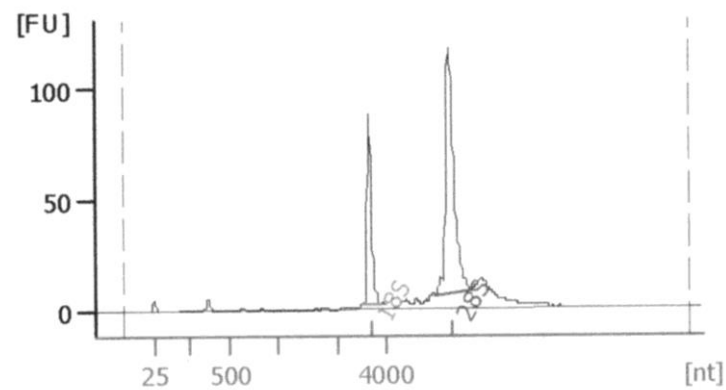


Figure 2-2: Visualisation of ribosomal RNA 18S and 28S in five RNA samples by 1% of denaturing agarose gel electrophoresis with ethidium bromide staining.

28S and 18S are approximate 5kb and 2kb in size. The presence of 28S and 18S bands at a ratio of 2:1 indicated good integrity of RNA samples.

RNA samples prepared for gene expression microarrays were sent to Tayside Tissue Bank (University of Dundee) to examine the RNA Integrity Number (RIN) algorithm. RIN is a more rigorous parameter in examining RNA integrity than denaturing agarose gel electrophoresis, particularly for the downstream application of gene expression microarrays. This technique indicates the presence or absence of degradation products and automatically interprets the results. A RIN score of 10 Indicating full integrity of an RNA sample is shown in Figure 2-3.



Overall Results for sample 3 :	<u>B-3</u>
RNA Area:	489.6
RNA Concentration:	364 ng/ μ l
rRNA Ratio [28s / 18s]:	2.1
RNA Integrity Number (RIN):	10.0 (B.02.03)

Figure 2-3: An RNA sample prepared for gene expression microarray showed full integrity with a RIN of 10.

The RIN detects RNA integrity, based on a range from 1 to 10, with 10 being the best integrity and 1 being the most degraded.

2.3.2 Reverse transcription of mRNA to cDNA

Complementary DNA (cDNA) synthesis was performed using the High Capacity cDNA Reverse Transcription Kit (Applied Biosystems), with 1 µg of total RNA. The reaction was performed in a Tetrad 2 Peltier Thermal Cycler (BioRad). The cycling conditions for cDNA synthesis are shown in Table 2-4. Synthesized cDNA was diluted in nuclease-free water to a final concentration of 100ng/ µl.

Table 2-3: Composition of reverse transcription reaction

Components	Volume (µl)	Final concentration
10x RT Buffer	2.0	1 x
25x dNTP Mix (100mM)	0.8	1 x
10x RT Random Primers	2.0	1 x
MultiScribe Reverse Transcriptase (50 Units/µl)	1.0	2.5 Units/µl
RNase Inhibitor (20 Units/µl)	1.0	1.0 Units/µl
Nuclease-free water	variable	
Template RNA	variable	1 µg/reaction
Total volume	20	

Table 2-4: Reverse transcription thermal programme cycling conditions

	Step 1	Step 2	Step 3	Step 4
Temperature	25°C	37°C	85°C	4°C
Duration	10 mins	2 hours	5 mins	Hold

2.3.3 Quantitative real-time polymerase chain reaction (qPCR)

2.3.3.1 qPCR Reaction

TaqMan[®] gene expression assays on demand (Table 2-6) were designed for each gene by Applied Biosystems. All the assays in this study were labeled with a 5' fluorescent reporter dye 6-carboxyfluorescein (FAM). TaqMan is a probe-based qPCR approach that quantifies the PCR products by detecting the fluorescence emission during the PCR reaction. The fluorescent signal is emitted when the probe is cleaved by Taq polymerase as the hybridization progresses, which prevents the quencher from suppressing the reporter fluorescence. This repetitive process in every cycle does not interfere with the accumulation of PCR product (Bustin 2000; Arya et al. 2005).

Table 2-5: Three-step cycling programme for qPCR

Step	Hold 1	Hold 2	Cycling	
Cycles	1	1	40-45	
Temperature	50°C	95°C	95°C	60°C
Time	2 mins	10 mins	15 s	1 min

The qPCR reaction was pipetted by QIAgility robot (Qiagen) into Rotor-Gene strip tubes (Qiagen), and PCR was performed by a Rotor-Gene Q instrument (Qiagen). Each reaction mixture is composed of 5µl of TaqMan[®] Gene Expression Master Mix (contains AmpliTaq Gold[®] DNA Polymerase UP (Ultra

Pure), Uracil-DNA Glycosylase, dNTPs with dUTP), cDNA template and additional Nuclease-free water to a final volume of 20 μ l. RNA expression levels were normalized against the endogenous control β 2-microglobulin (B2M). DNA contamination was ruled out by running no-template controls. Each sample was analyzed in at least duplicates.

Table 2-6: Symbol, description and ID of TaqMan[®] gene expression assays

Gene Symbol	Gene Description	Probe Assay ID
B2M	Beta-2-microglobulin	Hs99999907_m1
DAB2	Disabled homolog 2, mitogen-responsive phosphoprotein	Hs01120080_m1
DKK1	Dickkopf 1 homolog	Hs00931312_g1
DUSP2	Dual specificity phosphatase 2	Hs00358879_m1
EGLN1	Egl nine homolog 1	Hs00254392_m1
EGLN2	Egl nine homolog 2	Hs01086086_g1
EGLN3	Egl nine homolog 3	Hs00222966_m1
EGR2	Early growth response 2	Hs00166165_m1
NT5E	5'-Nucleotidase, ecto (CD73)	Hs01554888_m1
SMAD3	SMAD family member 3	Hs00969210_m1
TFPI2	Tissue factor pathway inhibitor 2	Hs00197918_m1
TSC22D1	TSC22 domain family, member 1	Hs00394659_m1

2.3.3.2 qPCR Normalisation and Analysis

The relative expression of target genes was calculated using the formula $2^{-\Delta C_T}$. Cycle threshold (C_T) value is the cycle number at the point where the amplification curve passes the threshold line, whilst the threshold was manually set above the baseline of no-template control to avoid the background noise (Figure 2-4). ΔC_T was equal to the average C_T for target gene minus the average C_T of endogenous B2M control in each sample.

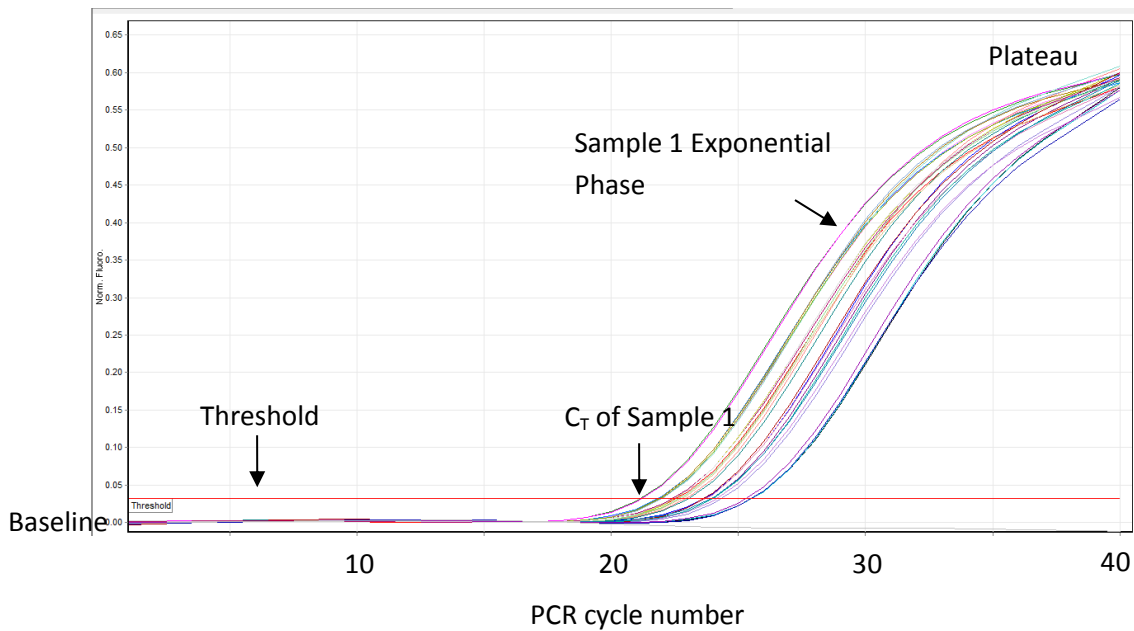


Figure 2-4: Visualisation of qPCR amplification plot by Rotor-Gene Q 2.0.2 (build 4) software.

2.3.4 DNA Methylation analysis

2.3.4.1 Bisulfite Modification of genomic DNA

500ng-1µg genomic DNA from cell lines, FFPE samples or 45µl serum DNA was subjected to bisulfite modification using the EZ DNA Methylation™ Kit (Zymo, California) following the manufacturer's instructions. The basic principle of this protocol is to treat methylated DNA with sodium bisulfite, which converts unmethylated cytosine residues to uracil whilst methylated cytosines remain unchanged. The methylation profile of modified DNA samples is then examined in downstream applications, including MSP (methylation-specific polymerase chain reaction (PCR), pyrosequencing, and bisulfite sequencing.

2.3.4.2 Primer Design

Genome CpG island sequence was obtained from the UCSC Genome Browser (Browser). Primers for MSP and bisulfite sequencing were designed using MethPrimer (MethPrimer). The primers were selected in a CpG-rich region with close proximity to the transcription start site. Primers for bisulfite sequencing and pyrosequencing were designed to avoid CpGs within the primer sequence. Conversely, MSP primers were required to include at least 3 CpGs.

2.3.4.3 Reconstitution of lyophilized PCR primers

PCR primers were supplied from MWG lyophilized at ambient temperature. The vials were briefly centrifuged before dissolving in TE buffer (pH 8.0) to make a concentration of 100 μ M for stock. Once completely dissolved after vortexing and incubation at room temperature, the PCR primers were diluted to a final concentration of 10 μ M in small aliquots to avoid repeated freezing and thawing cycles, and stored at -20°C. The optimal annealing temperature for each primer set was determined by gradient PCR.

2.3.4.4 Agarose-gel electrophoresis

2% agarose gels were prepared in 1 × Tris-Acetic Acid-EDTA (TAE) buffer (50 ×, Bio-Rad) in a microwave, with additional SYBR[®] Safe DNA gel stain (10,000 ×, Invitrogen) added after cooling down. Samples were mixed with Sample Loading Dye (Bioline), along with DNA ladder (Bioline) and loaded onto the gels in 1 × TAE buffer and resolved by electrophoresis at 120 V for 60 minutes. DNA fragments were visualised by UV illumination or VersaDoc imaging system (Bio-Rad).

2.3.4.5 Methylation specific PCR (MSP)

MSP is a non-quantitative technique that measures DNA methylation based on a gel-electrophoresis method. Bisulfite modified genomic DNA was amplified with either a methylated-specific (M) or unmethylated-specific (U) primer set using Hot Star Taq DNA Polymerase kit (Taqman) in a Tetrad 2 Peltier Thermal Cycler (BioRad). Bisulfite modified methylated and unmethylated DNA samples (Qiagen) were included in each amplification as methylated and unmethylated controls respectively.

Table 2-7: Reaction Composition using Hot Star Taq DNA polymerase

Component	Volume/Reaction	Final concentration
10x PCR Buffer	2.5µl	1X
dNTP mix (10mM) each	0.5µl	0.2mM
Forward primer (10µM)	1µl	0.4µM
Reverse primer (10µM)	1µl	0.4µM
HotStar Taq polymerase	0.125µl	
DNA template	Variable	
Nuclease-free water	Variable	
Total	25 µl	

Primers and annealing temperatures of candidate genes are listed in Table 2-9. DNA products were loaded onto 2% denaturing agarose gel electrophoresis as described in 2.3.4.4, and visualized under VersaDoc imaging system.

Table 2-8: Cycling protocol for MSP

Step	Duration	Temperature
3 step cycling x8		
Initial activation	2min	95°C
	30sec	60°C
	30sec	72°C
3 step cycling x35		
Denaturation	30sec	95°C
Annealing	30sec	variable
Extension	30sec	72°C
Final extension	5 min	72°C

Table 2-9: MSP Primers and annealing temperature of candidate genes

Gene	Primer Forward 5'	Primer Reverse 3'	Primer Type	Annealing Temperature
Dab2	GACCGAAAACCTTCGAAACCGCGCGA	GGGGTTTTTTGCGTCGTTGTAGCGC	Methylated	61°C
	ACCAACCAAAAACCTTCAAACCCACACAA	GTGGGGTTTTTTGTGTTGTTGTAGTGT	Unmethylated	54°C
SMAD3	CGTCGGTTAAGGGTTTTGAC	GAACGACTCGATTAAAATTACGAA	Methylated	57°C
	GTGTTGGTTAAGGGTTTTGATG	CAAACAACCTCAATTAATAATTACAAA	Unmethylated	55°C
TFPI2	GTTCGTTGGGTAAGGCGTTC	AACGACGAAATAACAATCCCCGTA	Methylated	55°C
	GGTTTGTTGGGTAAGGTGTTTGA	AAAACAACAAAATAACAATCCCCAT	Unmethylated	55°C
EGR2	TTTTTTTCGATAGTCGCGCGTTTTTC	GACGACGCCGATTTTCCTTAACGAT	Methylated	55°C
	TTTTTGATAGTTGTGTGTTTTTGT	AACAACACCAATTTTCCTTAACAAT	Unmethylated	55°C

2.3.4.6 Pyrosequencing

Pyrosequencing quantitatively measures methylation of an individual CpG site at high sensitivity. This technique is frequently used to indicate the frequency and level of methylation for candidate genes. All pyrosequencing analysis referred to in this study was performed in collaboration with Miss Laura Lattanzio (Santa Croce e Carle Hospital, Cuneo, Italy). Bisulfite modified DNA was amplified for subsequent pyrosequencing using a Hot Star Taq DNA Polymerase kit. The composition of PCR reactions and cycling conditions are shown in 2.3.4.5. PCR products were detected by agarose gel electrophoresis as described in 2.3.4.4, in order to ensure adequate PCR product of appropriate size without the presence of contamination. Pyrosequencing was performed in the PyroMark ID System (Biotage, Sweden). CpGenome Universal Methylated DNA (Millipore) and placental sexed male DNA (Sigma) were used as methylation positive and negative controls, respectively.

Table 2-10: Primers and annealing temperatures of target genes for Pyrosequencing

Gene	Primer Forward 5'	Primer Reverse 3'	Annealing Temperature °C	Sequencing Primer
Dab2	ATGGAGTTAGAGGGAAGAAGGGT	AAAATCCTCAACTACCAACATCT	55	F
TFPI2	GGGTTTATGGTGTAGGGGG	CAACCACCCCTCAAACCTCC	57	F
SMAD3	GAGAATAAAAATAGTTTAGGGG	AATACACCCTAAAAAAAACCC	57	F
AGTR1	GTTAGGATTTTAGGTAGTAG	CTCCAACCACTCCCAT	53	R
LEPREL 1	GGGGTTGTTTTATAGTGG	AAATACCCCAAACCCCTC	52	F
LEPREL 2	GTAGATTGTTTGATTTAGTG	CCACCTAATAATAAACCCCTC	53	F
P4H A1	GGTTGTTGTGGTAATTTGGG	AACTAAAACCACTAAACAACC	55	R
P4H A2	GTTTTTTTTGTTTAGTTTTTGGG	CTCTCCCTACAACCCC	54	F
P4H A3	GGTATAGTGTATTTTATTGAG	ACTACTAAAACCTACTAAAAC	49	F
DUSP2	GTAGATAGGAGTTTTGGAGT	CTCTTCCCCTCCTTACAAA	55	F
TSC22D1_ SET 1	GGGTTATAAATAGGAAGTTTT	ACTATAAAAACCCCCACAC-	52	F
TSC22D1_ SET 2	TAATGGTTTAGTGTTTTGAGG	CCCCATTCTCCAAATCC	55	F
TSC22D1_ SET 3	GTGGGGGTGGGGGGAGG	CAACTCTAAACCAAACTCCC	57	F
TSC22D1_ SET 4	GGTTTAGAGTTGAGTGGAGTT	CAACTTCTAAAACCTTAATAATCC	56	F

2.3.4.7 Bisulfite sequencing

Bisulfite sequencing data was provided by Dr Tim Crook. Briefly, bisulfite modified DNA was subject to amplification, and PCR products were detected by agarose gel electrophoresis as described in 2.3.4.4. A gel slice containing the appropriately sized DNA fragment of interest was excised under UV illumination, and extracted for purification. The purified DNA fragment was end-extended, cloned, used to transform TOP10 electrocompetent cells (Invitrogen), and plated on agar plates containing Kanamycin (1ml/100ml). Selected colonies were added to 5ml of liquid broth containing Kanamycin. Plasmid DNA was purified and sequenced.

2.4 Protein procedures

2.4.1 Western blotting

2.4.1.1 Preparation of protein lysates

Adherent cells seeded in 10mm dishes were washed three times in ice-cold PBS before harvest. Protein lysis buffer including Radio-immune Precipitation (RIPA) Buffer (1x, Thermo Scientific), Halt™ Protease Inhibitor Cocktail (100x, Pierce®, Thermo Scientific), Halt™ Protease and phosphatase Inhibitor Cocktail (100x, Pierce®, Thermo Scientific), and 0.5M EDTA (100x, Thermo Scientific) was added to the cells. The cells were scraped off and transferred into 1.5ml Eppendorf® microcentrifuges tube, followed by 15 minutes of incubation on ice and centrifugation at full speed in a cold centrifuge for 10 minutes to pellet insoluble cell debris. Supernatant containing the protein was then transferred to a 1.5ml eppendorf and stored at -80°C.

2.4.1.2 Protein concentration

Protein concentration was analysed by the Bio-Rad *DC*™ protein assay. Protein extract was thawed on ice, and diluted 1 in 10 in a 96 well plate. Reagents were added to the plate according to the manufacturer's protocol. Plate containing mixtures of reagents and either standard protein Bovine serum albumin (BSA), or

protein samples was incubated at room temperature for 15 minutes and read by Modulus™ II microplate multimode reader at a wavelength of 750nm.

2.4.1.3 Sodium dodecyl sulphate polyacrylamide gel electrophoresis (SDS-PAGE)

20-50 µg of each protein sample was mixed with NuPAGE® LDS Loading Buffer (4x, Invitrogen) and denatured by heating at 70°C for 10 minutes prior to loading. Prepared samples, along with a mixture of SeeBlue® Plus 2 pre-stained standard (Invitrogen) and Precision Plus Protein™ unstained standards (Bio-Rad), were loaded into wells of NuPAGE® Novet 4-12% Bis-Tris Mini Gels (Invitrogen) in XCell SureLock™ Mini-Cell (Invitrogen) containing 1x NuPAGE® MOPS SDS running buffer (50 mM MOPS, 50 mM Tris Base, 0.1% SDS, 1 mM EDTA, pH 7.7, Invitrogen). Electrophoresis was performed at 150V for 90 minutes before being transferred to a solid support for further analysis.

2.4.1.4 Transfer of proteins to solid support

Trans-Blot[®] Turbo[™] Mini PVDF (polyvinylidene fluoride) Transfer Packs (Bio-Rad) containing pre-cut PVDF membrane, filter paper and transfer buffer was used for transfer of proteins. An assembled sandwich with the gel placed between top and bottom stacks was placed on the cassette base, after ensuring air bubbles were excluded by rolling out between the layers. Transfer was carried out by Trans-Blot[®] Turbo[™] Transfer System (Bio-Rad) for 30 minutes. The success of transfer was evaluated by Ponceau S staining.

2.4.1.5 Immunodetection

The successfully transferred membrane was blocked in 1× TBS-T (Tris buffered saline-Tween, 2 mM Tris, 15 mM NaCl and 0.05% Tween (v/v), pH 7.6) with 1% non-fat dried milk (w/v, Marvel) for 1 hour at room temperature to block non-specific binding of antibody, and incubated in primary antibody (listed in Table 2-11) that was appropriately diluted in block solution overnight at 4°C.

Table 2-11: Name, description, supplier and dilution of primary antibodies

Protein	Primary antibody	Supplier	Dilution	Size (kDa)
PHD2, EGLN1	Rabbit polyclonal	Abcam	1/1000	46
PHD1, EGLN2	Rabbit polyclonal	Abcam	1/1000	44
PHD3, EGLN3	Rabbit polyclonal	NOVUS	1/1000	27
HIF-1 α	Rabbit polyclonal	GeneTex	1/500	115
Actin	Mouse monoclonal	Santa Cruz	1/2000	43
Ku80	Mouse monoclonal	Abcam	1/2000	86

On the following day, the membrane was washed three times for 10 minutes in TBS-T solution and incubated with block solution containing species specific horseradish peroxidase (HRP) - conjugated secondary antibody (Table 2-12) for 1 hour at room temperature. Precision Protein™ StrepTactin-HRP Conjugate was also added for detection of Precision Plus Protein unstained standards. Three times of 10 minutes washes by TBS-T buffer were subsequently required. Equal volume of Luminol and Peroxide solution (Immobilon Western Chemiluminescent HRP Substrate kit, Millipore) were applied to the membrane before visualization by VersaDoc imaging system.

Table 2-12: Name, description, supplier and dilution of secondary antibodies

Conjugated	Target	Secondary antibody	Supplier	Dilution
HRP	Mouse IgG	Goat polyclonal	Dako	1:10, 000
HRP	Rabbit IgG	Swine polyclonal	Dako	1:10, 000

2.4.1.6 Normalization with loading control

To evaluate the loading equivalence, levels of loading controls (Ku80 and Actin) were measured either by separating the blot with target protein and control protein, or re-probing the loading controls after stripping (7% Trichloroacetic acid (w/v), Sigma) the membrane. Following a series of washes, stripped membranes were blocked, re-probed with loading control and visualised as described in 2.4.1.4.

2.4.2 Immunofluorescence

Cells were grown as monolayer in Nunc[®] Lab-Tek[®] Chamber Slide[™] (0.8 m²/well, Sigma-Aldrich) to reach 50% of confluence (approximate 0.1 million cells/well). By the time of harvest, cells were washed by PBS before fixed with 300 µl 4% (w/v) paraformaldehyde for 20 minutes. To stop the fixation, paraformaldehyde was washed off by PBS three times, followed by permeabilization of cells with 300 µl of 0.1% Triton for 5 minutes and subsequent three times of PBS washes. Cells were sequentially incubated in blocking buffer (0.3% BSA in PBS) for 1 hour, primary antibody (1:100 dilution) for 1 hour, and fluorescent conjugated secondary antibody (1:800 dilution) in dark for 1 hour, with each step followed by 3 times of washes by PBS. After the chamber was removed, the slides containing the cells were mounted with ProLong[®] Gold antifade reagent with DAPI (4', 6-diamidino-2-phenylindole) (Invitrogen), sealed with coverslip on top and nail polish along the edges to prevent drying and contamination, and movement under microscope. All steps were carried out at room temperature. Results were examined by Zeiss Axioskop2 microscope with fluorescence.

2.5 Cell biology assays

2.5.1 Transient transfection of short interfering RNA (siRNA)

2.5.1.1 Resuspension of siRNA

Pelleted siRNA was briefly centrifuged and dissolved in a mixture of 1 volume 5x siRNA buffer (Dharmacon) and 4 volumes of RNase-free water to make a stock at final concentration of 20 μ M. Once dissolved by gently pipetting and mixing on an orbital shaker for 30 minutes at room temperature, siRNA solution was aliquoted and stored at -20°C. siRNAs used in this project were listed in Table 2-13.

2.5.1.2 Optimisation of transfection reagents

The transfection efficiency of Oligofectamine[™] reagent (Invitrogen), Lipofectamine[™] 2000 (Invitrogen), HiPerFect transfection reagent (Qiagen) and Lipofectamine[™] RNAiMAX (Invitrogen) was compared in the melanoma cell line COLO829 treated by SMAD4 ON-TARGET plus SMARTpool siRNA (detailed in Table 2-13) at a final concentration of 100nM. Control cells were treated with 100nM of AllStars negative control siRNA. Lipofectamine[™] RNAiMAX showed the best efficiency of silencing SMAD4 protein expression (Figure 2-5). It is difficult to judge the efficiency of Lipofectamine[™] 2000 due to its severe toxicity.

Comparatively, COLO829 cells were more tolerant to the other three transfection reagents. Therefore, Lipofectamine™ RNAiMAX was selected to transfect the siRNAs in this study.

Table 2-13: Name, company and target sequence of siRNAs

Gene target	Company	Target sequence
SMAD4	Thermo Scientific	GUACAGAGUUACUACUUAG
		GAAUCCAUAUCACUACGAA
		CCACAACCUUUAGACUGA
		GCAAUUGAAAGUUUGGUAA
EGLN3	Thermo Scientific	GGAGCCGGCUGGGCAAUA
		CAAGCUACAUGGUGGGAUC
		GAUAUGCUAUGACUGUCUG
		UCUACUAUCUGAACAAGAA

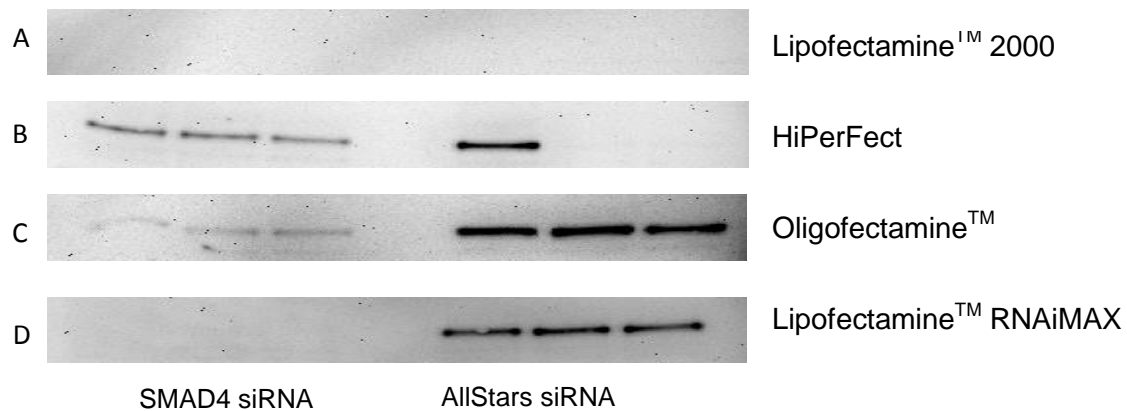


Figure 2-5: Comparison of the efficiency of four transfection reagents in COLO829 melanoma cell line: Oligofectamine™ reagent, Lipofectamine™ 2000, HiPerFect transfection reagent and Lipofectamine™ RNAiMAX.

Both SMAD4 and AllStars siRNA were used at a final concentration of 100Nm. A: No SMAD4 expression was detected in SMAD4 siRNA or negative control probably due to the severe toxicity of Lipofectamine™ 2000. B, C: Degrees of SMAD4 protein silencing compared to the negative controls when transfected by HiperFect or Oligofectamine™. D: Total silencing of SMAD4 protein expression when transfected with Lipofectamine™ RNAiMAX.

2.5.1.3 siRNA transfection procedure

Cells were seeded the day before transfection in medium without antibiotics. Appropriate volumes of RNAi and Lipofectamine™ RNAiMAX were mixed with Opti-MEM® I Reduced Serum Medium by gently mixing, respectively. Two mixtures were combined, mixed gently and incubated for 20 minutes at room temperature before drop-wise adding to the cells. The final concentration of RNAi and the duration of the treatment were optimized for each individual siRNA.

2.5.2 Methylation reversal assay

Cells were grown to confluence and split into 10cm dishes before 5 days of methylation reversal treatment with or without the demethylating reagent 5'-azacytidine (5' AZA, dissolved in DMSO to a final concentration of 5µM, Sigma). DMSO, the dissolving solution of 5' AZA, was added to the control cells. Replacement of fresh medium supplemented with either 5' AZA or DMSO was carried out every 2 days. During the last 24 hours, additional trichostatin A (TSA, dissolved in DMSO to a final concentration of 500nM, Sigma) was added to cells treated with 5' AZA. Each treatment was performed in triplicate. RNA was extracted from both treated and control cell lines as described in 2.3.1.2.

2.5.3 Hypoxia treatment

Cells were seeded at 50% confluence in T25 flasks. On the following day, flasks containing cells for each time point were placed into the In Vivo 500 hypoxia workstation (Ruskin Technologies, Bridgend, UK) (37°C, 1% O²). At the time point of harvest, cells for RNA or protein were lysed by the corresponding lysis buffer and scraped into eppendorfs as described in 2.3.1.2 and 2.4.1.1, respectively.

2.5.4 Cell counting

Cells were seeded at a density of 0.1×10^6 cells/well in 12-well plates before the day the appropriate treatment was added to the cells. At each time point, cells were disassociated with 400 μ l of trypsin, neutralised with 600 μ l of culture medium and counted by CASY[®] cell counter (Innovatis).

2.6 Microarray analysis

2.6.1 Methylation reversal assay with expression microarray

Methylation reversal assay was performed on cell lines MEL224, MEL501, MEL505, C8161 and C81-61 as described in 2.5.2. RNA samples were harvested and sent to the Institute of Cancer Research (London) for in house cDNA arrays, which included two colour hybridizations. The data was generated by GenePix software, and analysed by Dr Alan MacKay (The Breakthrough Breast Cancer Research Centre, Institute of Cancer Research) using Significance Analysis of Microarrays (SAM) statistical software.

2.6.2 Expression microarray

RNA samples prepared as described in 2.1.2 were analysed on HumanHT12 v4 expression microarrays by Cambridge Genomic services (University of Cambridge). RNA samples were amplified using Ambion[®] TotalPrep™ RNA Amplification Kit and hybridized on the HumanHT12 v4 BeadChip following Direct Hybridisation Assay (Illumina). The data was scanned by the Bead Array Reader. Quality control and analysis were performed by Dr Runxuan Zhang (The James Hutton Institute, Dundee). Briefly, the raw data was loaded to R (version 2.13.0) for density plot before and after normalization. Normalized data were tested by Hierarchical Clustering, Principle Component Analysis (PCA). Analysis of Variances (ANOVA) was used to detect differentially expressed genes according to the experimental design. The p values were corrected for multiple testing using Benjamini & Hochberg method and a FDR (adjusted p value, also known as false discovery rate) of 0.01 was used as threshold to select the significantly differentially expressed genes.

2.6.3 Methylation microarray

DNA samples prepared as described in 2.1.2 were analysed on Infinium[®] HumanMethylation450 microarrays by Cambridge Genomic services (University of Cambridge). The methylation profiling consists of a bisulfite modification (EZ DNA Methylation™ Kit, Zymo), Illumina's Infinium methylation procedure, and

loading samples on the Infinium[®] HumanMethylation450 BeadChip. Slides were scanned on the iScan for analysis. Normalisation and analysis were undertaken by Dr Helena Carén (Sahlgrenska Cancer Center, Gothenburg, Sweden). Raw data was normalised with Illumina's Subset-quantile Within Array Normalization (SWAN) and analysed by Limma (Linear Models for Microarray) package for the pairwise comparisons and p value correction. The output files from the Limma analysis contain methylation variable positions (MVPs) with an adjusted p-value of <0.01 and a change in the beta-value (methylation frequency) of more than 20%.

2.7 Statistics

Statistical analysis, including t-test, Mann-Whitney U test, Receiver operator characteristic (ROC) and one way ANOVA were all performed by GraphPad Prism[®] software. Statistical analysis of the significance of P4HA3 methylation as a melanoma serum biomarker was kindly performed by Dr Mathieu Boniol (International Prevention Research Institute, Lyon, France) using SAS version 9.2 software. In his analysis, Kernel density analysis was used to examine the distribution of all tested CpG sites within a target gene. Multivariate regression analysis was used to compute the various odd ratios.

Chapter 3 Identification of candidate biomarkers by systematic approaches

3.1 Introduction

DNA methylation is a biologically crucial mechanism that transcriptionally silences gene expression. One research and therapeutic opportunity presented by DNA methylation is that the modification to DNA induced by methylation is potentially reversible with demethylating agents, such as 5' azacytidine (5' AZA), which inhibits DNA methylation by binding to DNA methyltransferase (DNMT) I (Kaminskas et al. 2005). 5' AZA has been frequently used to investigate genes that are dysregulated by DNA methylation in human cancers and, importantly, a low dose of 5' AZA will not interfere with DNA replication. The histone deacetylase (HDAC) inhibitor, trichostatin A (TSA), is often used in conjunction with 5' AZA in methylation reversal experiments. TSA removes acetyl residue groups to make chromatin less condensed and more transcriptionally active allowing better interaction between 5' AZA and DNMT. Combining methylation reversal treatment with gene expression profiling has proven to be a powerful tool for *de novo* identification of genes silenced by DNA methylation and this approach has been widely explored in epigenetic biomarker discovery studies (Arai et al. 2006; Mikata et al. 2006; Wong et al. 2007; Nojima et al. 2009; He et al. 2011).

DNA methylation analytical methodology has undergone rapid evolution development lately (section 1.2.3.3). The recent introduction of Infinium Methylation 450K microarray provided a powerful method for genome-wide methylation profiling. It is a robust technique comprehensively and proportionally

investigates methylated DNA at single-base resolution (Kilaru et al. 2012). Approximately 480,000 CpG sites are assayed by this microarray, with a coverage of 96% of CpG islands as well as regions outside CpG islands, such as island shores and the regions flanking them (Dedeurwaerder et al. 2011). Infinium Methylation 450K microarray has shown promising results for the investigation of aberrant methylated genes in several human cancers (Devaney et al. 2013; Heyn et al. 2013; Shen et al. 2013), and this technique also exhibits good consistency with other methodologies such as reduced representation bisulfite sequencing (RRBS) (Pan et al. 2012).

In this section of work my aim was to investigate epigenetically dysregulated genes by several systematic approaches including methylation reversal screening, gene expression profiling and methylation profiling. I proposed to investigate the methylation status of candidate genes identified using systematic approaches in melanoma cell lines and patient materials, and to determine whether they have potential clinical utility as diagnostic and/or prognostic biomarkers that predict tumour progression and patient outcome. Importantly, the candidacy of these genes as serum epigenetic biomarkers will also be assessed, in particular evaluating the significance of detection of methylated DNA in patient sera as a predictor of metastatic disease.

By performing a methylation reversal screen, Dr Tim Crook has identified a number of candidate genes (shown in Table 3-2). I have selected 5 (*TFPI2*,

DKK1, *EGR2*, *SMAD3* and *TSC22D1*) for further validation and investigation. The background for these candidate biomarkers is now introduced:

3.1.1 Tissue factor pathway inhibitor 2 (TFPI2)

TFPI2, also known as placental protein 5 (PP5), was named and characterised based on its TFPI-like features (Kisiel et al. 1994). As a member of the matrix-associated Kunitz-type serine proteinase inhibitor family and being capable of inhibiting serine proteinases such as factor VIIa-tissue factor, trypsin and plasmin (Petersen et al. 1996), TFPI2 functions in the regulation of a number of biological processes, including extracellular matrix (ECM) digestion, tissue remodeling and blood coagulation. Its role in ECM remodeling makes it a good candidate as a 'metastasis' gene.

DNA methylation of *TFPI2* has been reported in a variety of human cancers in the last few years (summarised in Table 3-1). Detection of methylated genomic DNA in circulating blood has been described in both gastric cancer (Hibi et al. 2011) and hepatocellular carcinoma (Sun et al. 2013). Interestingly, methylated genomic DNA in serum from gastric cancer patients becomes undetectable after curative surgery (Hibi et al. 2012). Investigation of *TFPI2* methylation in melanoma has revealed a low frequency in one study ((Liu et al. 2008) and methylation exclusively in metastases (Nobeyama et al. 2007). Investigation of

TFPI2 methylation in human cancers has suggested an important potential role for *TFPI2* as an epigenetic biomarker for human cancers.

Table 3-1: Investigation of *TFPI2* CpG island methylation in human cancers

Cancer	Methylation frequency in human cancers	Reference
Gastric carcinoma	80.9% (123/152) primary gastric cancers	(Jee et al. 2009)
Gastric cancer	83% (15/18) primary gastric cancers	(Takada et al.)
Pancreatic ductal adenocarcinoma	73%(102/140) pancreatic cancer xenografts and primary pancreatic adenocarcinomas	(Sato et al. 2005)
Colorectal cancer	97%(55/56) adenomas (pre-malignant lesions) and 99%(114/115) colorectal cancers	(Glockner et al. 2009)
Hepatocellular carcinoma	47% (16/34) primary hepatocellular carcinomas	(Wong et al. 2007)
Cervical carcinoma	82% (18/22) invasive cervical cancer	(Sova et al. 2006)
Non-small-cell lung cancer	30% (12/40) cases of non-small-cell lung cancer, with more frequent methylation in late stage and metastases	(Rollin et al. 2005)
Melanoma	29% (5/17) metastatic melanomas, 0% (0/20) primary melanomas	(Nobeyama et al. 2007)
	12.5%(5/40) freshly procured melanoma samples	(Liu et al. 2008)
	21.7%(overall 122) melanomas	(Tanemura et al. 2009)

Together with its characterisation as a promising epigenetic biomarker for cancers, the molecular function of TFPI2 in tumourigenesis and progression has also been extensively studied. *In vitro* and *in vivo* studies have provided evidence of its negative regulatory function in tumour proliferation, invasion, metastasis and angiogenesis, which is probably associated with its broad spectrum inhibitory action on serine proteinases and matrix metalloproteases (MMPs) (Rao et al. 1999; Izumi et al. 2000; Konduri et al. 2001; Chand et al. 2004; Yanamandra et al. 2005; Gessler et al. 2011). There is also likely to be cross-talk between TFPI2 and cancer-related pathways, such as the apoptotic pathway (George et al. 2007), TGF- β pathway (Fuchshofer et al. 2009), and MKK7/JNK pathway (Chand et al. 2005).

3.1.2 Early growth response gene 2 (EGR2)

EGR2 protein, encoded by the *EGR2* gene, is a transcription factor with zinc-finger DNA binding motifs (Joseph et al. 1988). The zinc-finger DNA binding structure of EGR2 allows its interaction with multiple signaling pathways. EGR2 has also been reported to cause human disease such as Charcot-Marie-Tooth syndrome (Warner et al. 1998). The mechanism of EGR2 action in terms of its molecular function in regulating tumour behaviour is not well understood. EGR2 has been previously reported to be a tumour suppressor acting to induce apoptosis (Unoki and Nakamura 2003; Yokota et al. 2010) and positively mediating PTEN growth-suppressive signaling in human cancers (Unoki and

Nakamura 2001). Conversely, EGR2 is also reported to act in an oncogenic manner by inhibiting T cell activation to cause anergy wherein it acts in concert with its family member EGR3 (Safford et al. 2005), and increasing expression of ErbB2, a poor prognostic factor for breast cancer (Dillon et al. 2007).

3.1.3 Dickkopf homolog 1 (DKK1)

DKK1 encodes a member of the dickkopf family that inhibits the canonical Wnt/ β -catenin pathway. The Wnt pathway modulates cellular activities including cell proliferation, migration, senescence and apoptosis. The function of DKK1 in human cancers remains controversial (Menezes et al. 2012). Evidence has shown both increased and decreased DKK1 expression in cancers in a context-dependent pattern. DKK1 is more likely to be a tumour suppressor in melanoma. Expression of DKK1 is inducible by UVB in melanocytes (Yang et al. 2006), but, conversely, is reduced in melanoma (Kuphal et al. 2006). Promoter methylation appears to be a mechanism that silences DKK1 expression in some cancers (Kocemba et al. 2012; Na et al. 2012; Wang et al. 2013), but no direct evidence for methylation has been previously reported in melanoma. Another possible explanation for the reduction of DKK1 expression in melanoma is the cross-talk between MAPK signaling and Wnt/ β -catenin signaling (Parisi et al. 2012). Melanoma cells with a BRAFV600E mutation are able to inhibit the activity of DKK1 and prevent induction of senescence.

3.1.4 SMAD family member 3 (SMAD3)

SMAD3 is an intracellular mediator of the TGF- β pathway that transduces signals and activates transcription after activation of the TGF- β receptor by TGF- β ligand. The most well-established signalling effector pathway activated after TGF- β signalling is through a cell-surface complex of the TGF- β receptors known as the SMAD signalling pathway (Feng and Derynck 2005). TGF β receptor phosphorylates and drives Smad2 and Smad3 to form a complex with Smad4. This complex then translocates to the nucleus and activates the transcription of TGF- β target genes (Derynck et al. 2001; Millet and Zhang 2007). TGF- β is a pleiotropic cytokine acting as a potent tumour suppressor in many early stage cancers, but switching to become a potent tumour promoter in advanced malignancy (Ikushima and Miyazono 2010). The switch to a pro-proliferative TGF- β response may be controlled epigenetically and may be a crucial biomarker for high risk head and neck squamous cell carcinoma (Hannigan et al. 2011). TGF- β pathway impairment has not previously been reported in melanoma, but identification of *SMAD3* by our methylation reversal screen suggests the possibility that *SMAD3* may be silenced by DNA methylation in some melanomas which may indirectly impact on TGF- β signalling.

3.1.5 TSC22 domain family, member 1 (TSC22D1)

TSC22D1 is a TGF- β responsive transcription factor, composed of a long isoform TSC22D1.1 and a short isoform TSC22D1.2 (Shibanuma et al. 1992; Fiol et al. 2007). Reduced TSC22D1 expression in human cancers implicates it as a tumour suppressor (Shostak et al. 2003; Shostak et al. 2005; Rentsch et al. 2006). For the short isoform, functions such as inhibiting cell proliferation, inducing apoptosis and senescence and inhibition of degradation of p53 have been identified in human cancers (Nakashiro et al. 1998; Hino et al. 2000; Homig-Holzel et al. 2011; Yoon et al. 2012). Reduced gene expression due to DNA methylation of *TSC22D1.2* has been reported in leukaemic transformation (Yu et al. 2009).

3.2 Results

3.2.1 Identification of candidate genes by methylation reversal assay combined with gene expression profiling

Dr Tim Crook provided preliminary data from a methylation reversal screen on 5 melanoma cell lines MEL224, MEL501, MEL505, C81-61 and C8161. Briefly, these melanoma cell lines were treated with the methylation reversal agents 5' AZA, with or without additional TSA. DMSO which is the diluent reagent for 5' AZA and TSA was used as the negative control. This data has been analysed by Dr Alan MacKay (The Breakthrough Breast Cancer Research Centre, Institute of

Cancer Research). To confirm the reproducibility of the analysis, we sent data from one cell line, C81-61, to Dr Runxuan Zhang (The James Hutton Institute, Dundee) for repeat analysis. Principle component analysis performed by Dr Runxuan Zhang revealed all 4 treatments as different clusters with tight clustering of replicates, suggesting good reproducibility of the replicates in each group (Figure 3-A). Notably, 5' AZA and 5' AZA+TSA treatment groups are clustering closely and are widely separated from the DMSO control, illustrating more similar gene expression profiling between the 5' AZA and 5' AZA+TSA treatments than the negative control. ANOVA carried out using treatment as a single factor showed genes significantly differentially expressed (Fold change >1.5 or <-1.5, FDR<0.05) due to different treatments (Figure 3-B). In cell line C81-61, a total of 54 genes were similarly influenced by treatments of 5' AZA and 5' AZA+TSA.

A large number of candidate genes potentially subject to methylation-dependent transcriptional silencing have been identified. 78 genes were significantly upregulated following methylation reversal in at least 2 of 5 melanoma cell lines (Fold change > 1.5, Listed in Table 3-2), including 2 genes *TIMP1* and *DKK1* that were up-regulated in all 5 cell lines, and 7 genes *PPM2C*, *SERPINI1*, *GLRX*, *EGR2*, *KDELR3*, *FN1* and *TMEM158* that were up-regulated in 3 cell lines. We selected two genes *DKK1* and *EGR2* for further investigation due to their large CpG islands. *TFPI2* was also chosen for additional study because it showed the highest fold change in two cell lines.

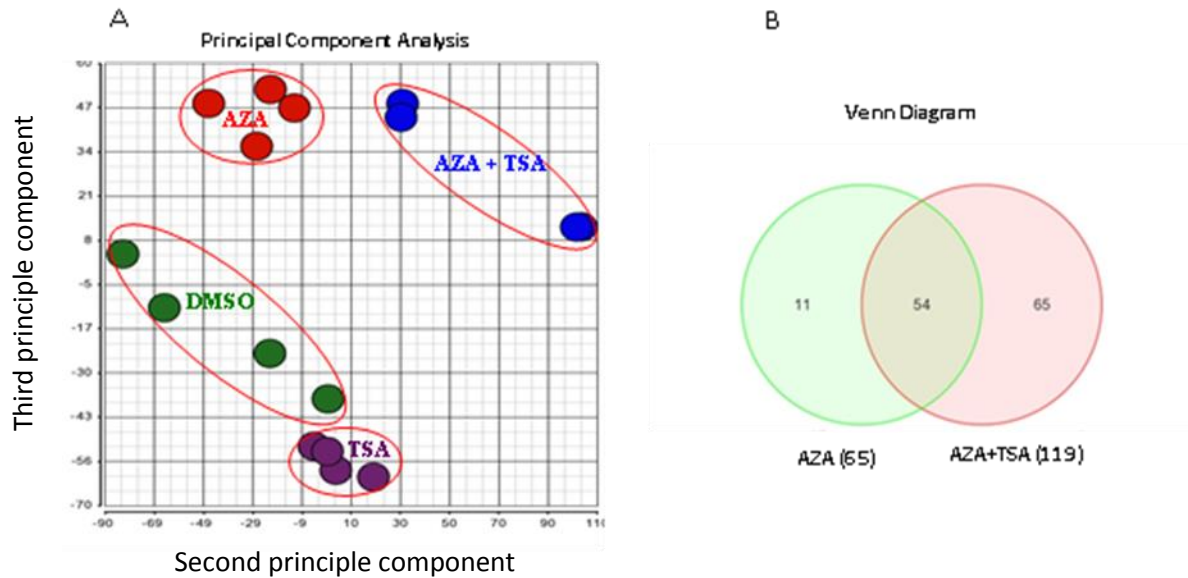


Figure 3-1: Analysis of methylation reversal screen in cell line C81-61.

(A): Principle component analysis investigating the effects of distinct treatments during methylation reversal assay. The figure shows that the effects of AZA are mainly captured on the second principle component while on the third principle component clearly shows the effects of TSA. There is clear clustering of gene expression according to treatment with AZA or with AZA plus TSA compared with DMSO control. (B): Venn Diagram showing the gene profiles in 5' AZA treated group and 5' AZA+TSA treated group.

To gain insight into the biological function of these candidate genes, pathway analysis was carried out using the DAVID (the database for Annotation, Visualization and Integrated discovery) bioinformatics tool. Candidate genes involved in pathways such as TGF- β signalling, antigen presentation and processing signalling and cancer related pathways (Figure 3-2) were visualized on Kyoto Encyclopedia of Genes and Genomes (KEGG) pathway database. TGF- β signalling plays a critical role in the regulation of multiple cancer associated biological events in a context dependent manner (Hannigan et al.). It

has both pro-oncogenic and tumour suppressive functions in human cancers. Hence, I selected two TGF- β signalling components *SMAD3* and *TSC22D1* identified in our screen, and have investigated their impact on TGF- β signalling in the context of transcriptional silencing by DNA methylation.

Table 3-2: Candidate genes identified by Methylation reversal screen

PPM2C	DUSP1	ODC1	ARNTL	TncRNA	DUSP6	LOC151534	SERPINE2
SERPINI1	HIST1H2BK	CCL20	BIRC3	ZNF135	ENC1	KLF4	LEP
GLRX	RBM15	GCH1	C21orf2	CYR61	APLP2	ERRFI1	SMAD3
EGR2	FUCA1	ACVRL1	FLNB	DDR1	CDKN2B	CXADR	HIST2H2BE
KDELR3	PBEF1	CD36	GADD45A	IL8	TFPI2	FAT	LPL
FN1	TCEB3	DCBLD2	GJB1	LYRM7	LGMN	MGST3	PDE6G
TMEM158	HIST1H1C	VIM	GJB2	SLC7A8	LOC729408	KDM1A	SULT1C1
TSC22D1	NFE2L3	C4orf18	SOD2	HLA-A	MYO15B	ADFP	MYO5A
ID1	HSPA2	MMP1	IER3	HLA-B	TMSB4X	ARFGAP3	
ANXA1	CTGF	HPRT1	GLIPR1	THBS2	DKK1	TIMP1	

Sublist	Category	Term	RT	Genes	Count	%	P-Value	Benjamini
<input type="checkbox"/>	KEGG_PATHWAY	TGF-beta signaling pathway	RT		5	0.7	2.5E-3	1.2E-1
<input type="checkbox"/>	KEGG_PATHWAY	Antigen processing and presentation	RT		4	0.5	1.7E-2	3.7E-1
<input type="checkbox"/>	KEGG_PATHWAY	Pathways in cancer	RT		6	0.8	6.5E-2	6.9E-1
<input type="checkbox"/>	KEGG_PATHWAY	PPAR signaling pathway	RT		3	0.4	7.7E-2	6.5E-1

Figure 3-2: Pathway analysis by David bioinformatics (National Institute of Allergy and Infectious Diseases (NIAID)).

<http://david.abcc.ncifcrf.gov/>

3.2.1.1 Investigation of *TFPI2* methylation in melanoma

3.2.1.1.1 Genomic structure of *TFPI2*

TFPI2 is located on the reverse strand of chromosome 7q22, and consists of five exons and four introns, with its CpG island overlapping the promoter region, Exon 1 and Exon 2 (Figure 3-3 A). In this study, I have explored two analytic techniques, MSP and pyrosequencing to examine the methylation status of *TFPI2* in melanomas. Pyrosequencing analysis was performed in collaboration with Dr Cristiana Lo Nigro (Cuneo, Italy). Figure 3-3 B shows the positions of the primers for two protocols that were designed with proximity to the transcription start site (TSS).

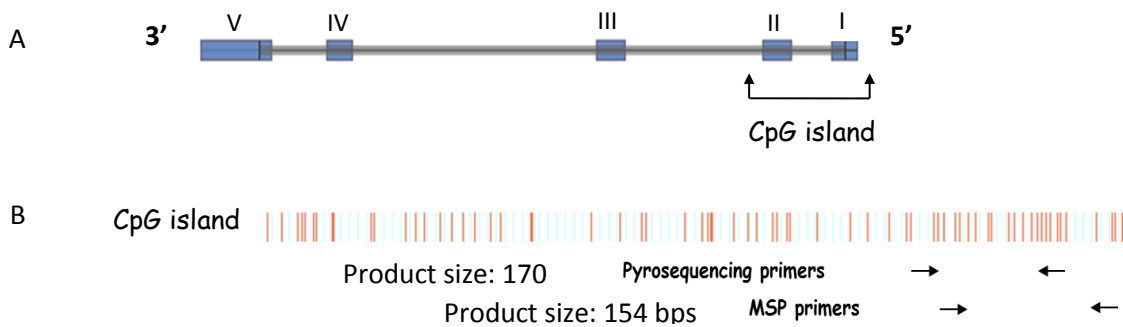


Figure 3-3: Genomic structure of human *TFPI2* gene.

(A): Schematic diagram of *TFPI2* gene including 5' and 3' UTRs, exon-intron boundaries and the location of the CpG island; (B): CpG dinucleotides of CpG island and the location of MSP and pyrosequencing primers. Red bars represent the individual CpG dinucleotides.

3.2.1.1.2 Identification of *TFPI2* methylation in melanoma cell lines

I initially tested the reproducibility of the two methylation-investigative techniques in a subset of cell lines. MSP analysis showed that *TFPI2* was methylated in 3 of 6 melanoma cell lines, and unmethylated in 2 independent preparations of normal human epidermal melanocytes, HEMA-LP and HEMN-LP (Figure 3-4 A). Consistent methylation status of the same cell lines was shown by pyrosequencing (Table 3-3), indicating good reproducibility for the two assays. In total, I have observed *TFPI2* DNA methylation in 11/17 of the melanoma cell lines in our panel and complete absence of methylation in the melanocytes (and normal keratinocyte) controls.

The mean methylation level and methylation status of *TFPI2* is shown in Table 3-2. Representative pyrograms of *TFPI2* unmethylated cell line WM266.4 and methylated cell line SKMEL-23 are shown in Figure 3-4 B.

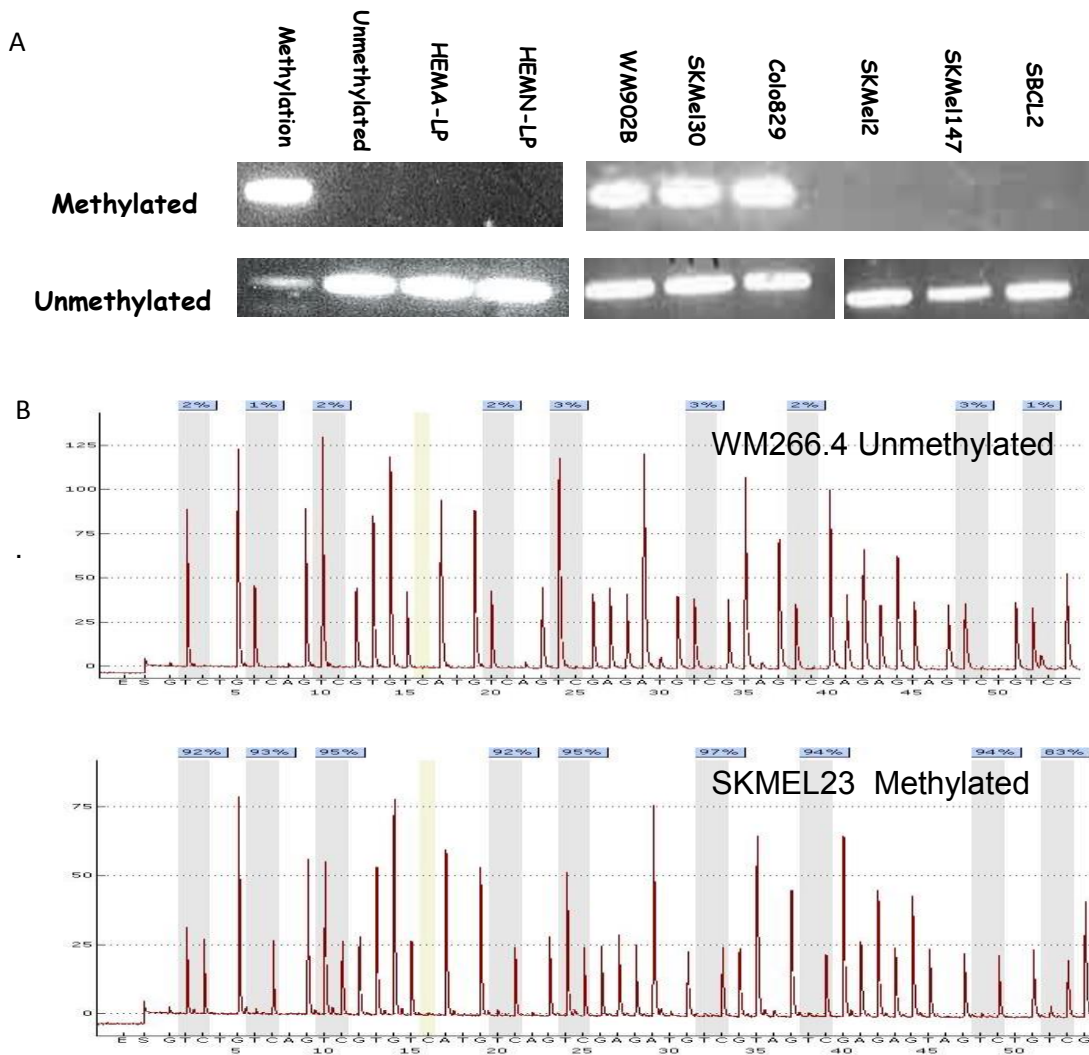


Figure 3-4: Identification of *TFPI2* methylation in melanoma cell lines by MSP (A) and pyrosequencing (B).

(A): MSP analysis of *TFPI2* methylation. The presence of visible bands in the methylated or unmethylated lanes indicates the methylation status of *TFPI2*. Methylated and unmethylated control DNA samples, processed in parallel with test samples, were included in the MSP reactions. (B): Pyrograms of *TFPI2* methylation in WM266.4 and SKMEL23 cell lines. The digital numbers (%) represent the methylation percentage of individual CG dinucleotides.

Table 3-3: Mean methylation (%) and methylation status of *TFPI2* in melanoma cell lines, melanocytes and keratinocytes by pyrosequencing and MSP, respectively.

	HEMA-LP	HEMN-LP	MeI501	MeI505	MeI224	C8161	A375M	WM239A	WM902B	SKMeI30	SKMeI173	Colo829	SkmeI23	PMWK	WM266-4	SKMeI2	SKMeI147	SBCL2	WM35	Keratinocyte
Pyro	2	5	90	90	2	1	20	20	32	81	38	50	93	67	2	2	2	2	42	2
MSP	U	U	M	M	U	U	M	M	M	M	M	M	M	M	U	U	U	U	M	U

*The digital numbers represent the methylation percentage (%) of candidate genes in melanoma cell lines. (M and U represent the methylation status of candidate genes).

3.2.1.1.3 *TFPI2* mRNA expression is transcriptionally regulated by promoter methylation

I subsequently analysed expression of *TFPI2* by qPCR in the same cell line panel and observed a significant inverse correlation between methylation and gene expression ($p < 0.05$, Figure 3-5 A). For example (Figure 3-5 B, C), *TFPI2* was almost fully methylated in Mel501 and Mel505 cell lines with no associated gene expression. In contrast, methylation was undetectable in cell line C8161 which showed abundant *TFPI2* expression. Mean methylation of 20% in A375M and WM239A cell lines correlated with low *TFPI2* expression, suggesting that modest levels of DNA methylation may be sufficient to reduce expression.

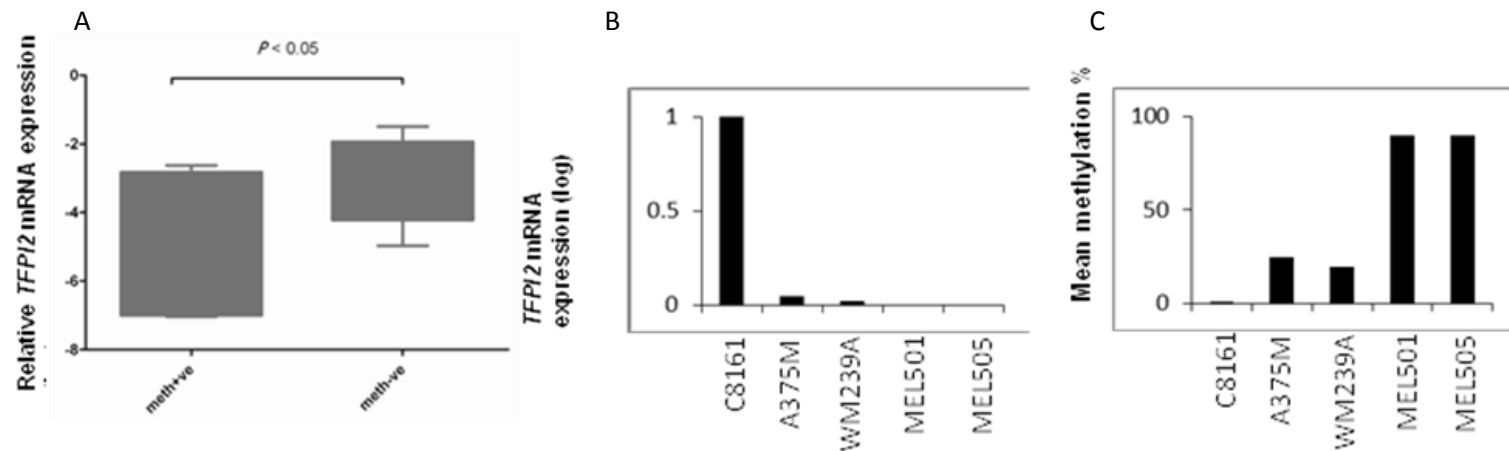


Figure 3-5: Inverse correlation of *TFPI2* methylation and gene expression.

(A): Mann Whitney test (one-tailed, $p < 0.05$) showing that expression of *TFPI2* in cases positive for CpG island methylation was significantly lower than in cases negative. (B, C): Gene expression and methylation of *TFPI2* in five representative melanoma cell lines, showing inverse correlation between expression (B) and CpG island methylation (C).

To seek further evidence that *TFPI2* CPG island methylation transcriptionally silences gene expression, I treated melanoma cell lines with the demethylating agent 5' AZA, with or without additional TSA. Cell lines COLO829 (50% *TFPI2* methylation) and MEL501 (90% *TFPI2* methylation) do not normally express *TFPI2* mRNA, however, treatment with 5' AZA and TSA dramatically restored expression (Figure 3-6). Interestingly, methylation reversal treatment also produced a small increase in *TFPI2* expression in cell line SKMEL2, a cell line with no detectable methylation. In comparison, COLO819 and MEL501 showed a >1700 fold change increase in mRNA but only a five-fold increase was seen in SKMEL2. Moreover, restored *TFPI2* expression in SKMEL2 remained lower than in the other two cell lines. Modest upregulation of *TFPI2* gene expression in SKMEL2 may be due to an indirect effect of upstream targets, as methylation reversal treatment causes a global hypomethylation, and is not restricted to specific targets. Another explanation for this observation is that expression associated DNA methylation at alternative CpG sites has not been sampled by our methodology.

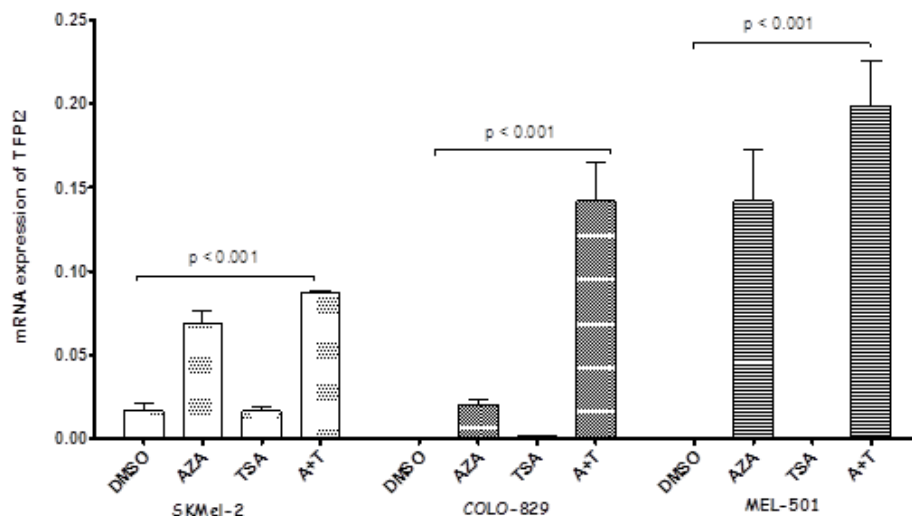


Figure 3-6: Reactivation of *TFPI2* expression by pharmacological demethylation.

The indicated cell lines were grown in the presence of 5' AZA, TSA, both agents (A + T) or drug vehicle only (DMSO). Expression of *TFPI2* was determined by qPCR. Data shown are mean +/- 1SD from 3 independent experiments.

3.2.1.1.3 *TFPI2* CpG island methylation and expression in paired melanoma cell lines

Next I extended my cell line investigations to examine *TFPI2* in poorly metastatic parental cell lines and matched highly metastatic daughter cell lines. A significant decrease in *TFPI2* expression was detected in the highly metastatic derivatives WM266.4 and WM293A, LM9 and LM29 in comparison to their parental lines WM115 and LM2, respectively (Figure 3-7 A). An inverse pattern of *TFPI2* methylation was also shown (Figure 3-7 B). However, I noticed that the level of methylation in the paired metastatic derivatives was quantitatively different (Figure 3-7 B) with rather less methylation and less suppression of mRNA in LM9

than LM29. Thus, absolute silencing of *TFPI2* is not a prerequisite for metastasis. Notably, increased *TFPI2* methylation was not exactly proportional to the decrease in gene expression, suggesting other genetic or epigenetic mechanisms may regulate *TFPI2* mRNA expression co-ordinately with DNA methylation. Alternatively, methylation of other CpG dinucleotides within the CpG island may contribute to transcriptional downregulation of gene expression.

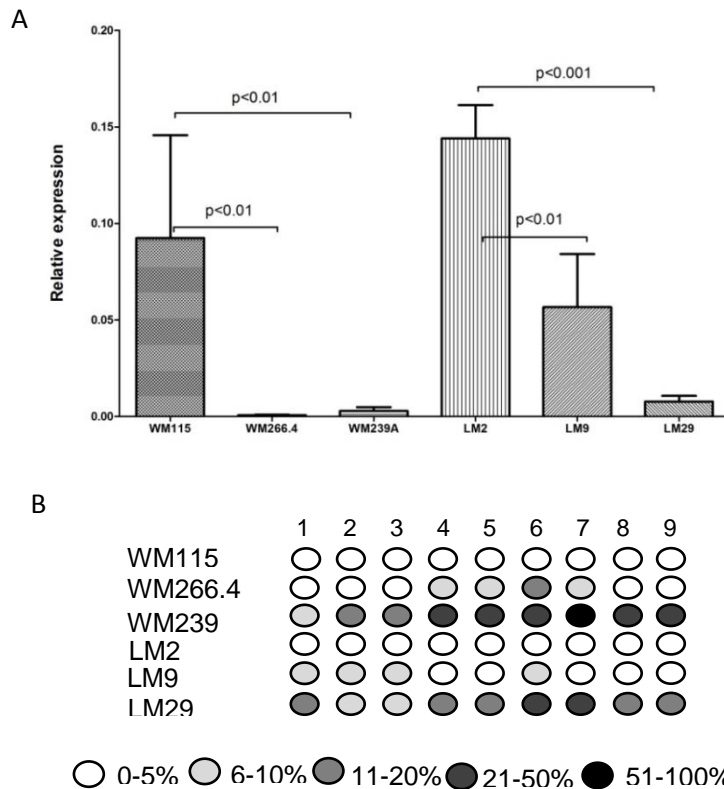


Figure 3-7: *TFPI2* CpG island methylation and expression in paired melanoma cell lines.

(A): qPCR analysis of *TFPI2* in paired (non-metastatic / weakly metastatic) parental cell lines and highly metastatic daughter cell lines. Data shown are mean +/- 1SD from 3 independent experiments. B: Pyrograms of *TFPI2* CpG island in the same cell lines. Methylation was quantified by the intensity of shading in the circles, each of which represents an individual CG dinucleotide. 5 levels of shading are used as indicated in the figure. In all cases, methylation increased in the highly metastatic cell lines relative to the respective parental cell line.

3.2.1.1.4 TFPI2 CpG island methylation may correlate with melanoma progression

Identification of *TFPI2* methylation in melanoma cell lines and the likely association with metastasis, prompted me to investigate the methylation status of *TFPI2* in clinical melanoma samples. Accordingly, pyrosequencing was performed on 122 clinical samples from melanoma patients at different stages of disease. The study population included 53 primary melanomas, 59 metastases and 9 benign pigmented naevi which served as negative controls. Less than 5 % mean methylation is usually considered as background noise. Pyrosequencing analysis showed that *TFPI2* was methylated at higher than 5% in 0/9 of benign naevi, 35/44 (80%) of primary melanomas and 56/64 (88%) of metastatic melanomas. The complete absence of *TFPI2* methylation in all 9 benign naevi and the high frequency of *TFPI2* methylation in both primary and metastatic melanomas (Figure 3-8 and 3-9) suggests that *TFPI2* methylation is an appropriate cancer biomarker being specifically detectable in cancer but not in the benign control.

The level of methylation in the *TFPI2* CpG island increased as a function of melanoma progression with the highest methylation level found in the metastatic cases (Figure 3-9). By performing the Mann-Whitney *U* test, I observed a significantly higher level of *TFPI2* CpG island methylation in metastases compared to primary tumours ($p < 0.05$), and both groups showed a much higher methylation level than benign controls ($p < 0.01$ and $p < 0.001$, Figure 3-9). It

appears that *TFPI2* methylation does correlate with melanoma progression. This now requires validation in a larger data set.

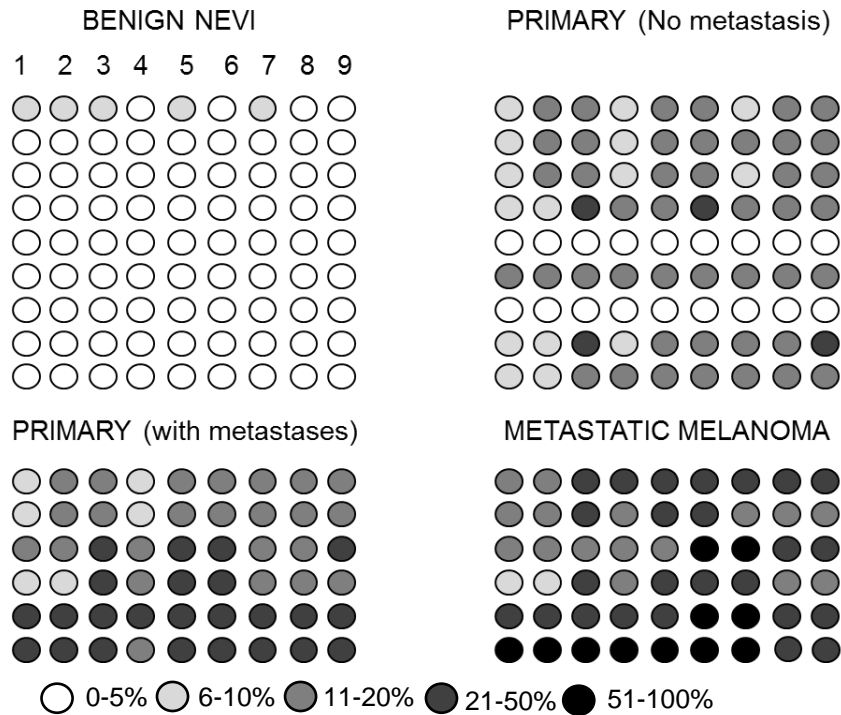


Figure 3-8: Pyrosequencing profiles of *TFPI2* CpG island methylation in benign naevi, primary and metastatic melanomas.

Methylation is quantified by the intensity of shading in the circles, each of which represents an individual CpG dinucleotide. 5 levels of shading are used as indicated in the figure.

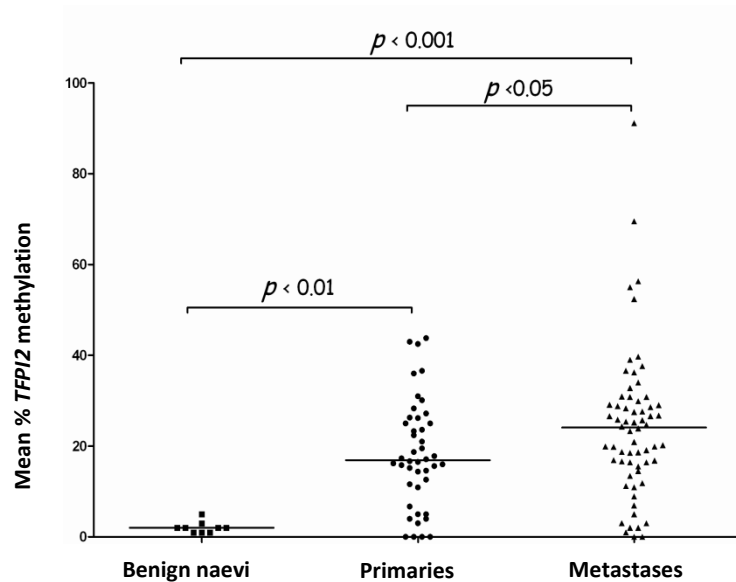


Figure 3-9: Mann Whitney *U* analysis of *TFPI2* CpG island methylation in benign naevi, primary and metastatic melanomas.

Mean % methylation was determined by pyrosequencing. Methylation is strongly associated with melanoma and specifically with metastatic melanoma.

Having observed a correlation between *TFPI2* methylation and melanoma progression, I proceeded to investigate *TFPI2* methylation in paired primary melanoma and metastases collected from the same patients. I performed crude micro-dissection on these specimens after histopathological examination to obtain high tumour cell representation without contamination from normal tissue and/or inflammatory cells. This will allow us to make a relatively more accurate assessment of the difference between primary melanomas and metastatic disease. However, only limited numbers of melanoma tissues are suitable for crude micro-dissection, because of technical difficulties posed by high pigment levels inside tumours or high levels of tumour-associated inflammatory cells, or extensive infiltration of tumour cells into the stroma.

Table 3-4: *TFPI2* methylation at individual CpG site of promoter region in 6 paired primary and metastatic melanomas from the same patients

Patient	CpG 1	CpG 2	CpG 3	CpG 4	CpG 5	CpG 6	CpG 7	CpG 8	CpG 9	Sum
1 P	8	15	31	20	25	36	21	23	21	200
M	19	29	34	36	36	48	49	31	34	316
2 P	4	39	59	32	43	22	1	4	1	205
M	14	17	65	44	44	52	65	16	15	332
3 P	0	0	10	0	3	7	0	0	0	20
M	0	0	14	2	5	8	0	2	2	31
4 P	0	0	13	0	2	7	0	1	2	23
M	0	0	23	0	11	15	0	2	1	51
5 P	0	0	10	0	8	13	0	0	0	31
M	0	0	21	6	11	16	0	4	7	58
6 P	0	0	21	1	9	12	0	3	4	50
M	0	0	19	1	7	11	0	4	4	46

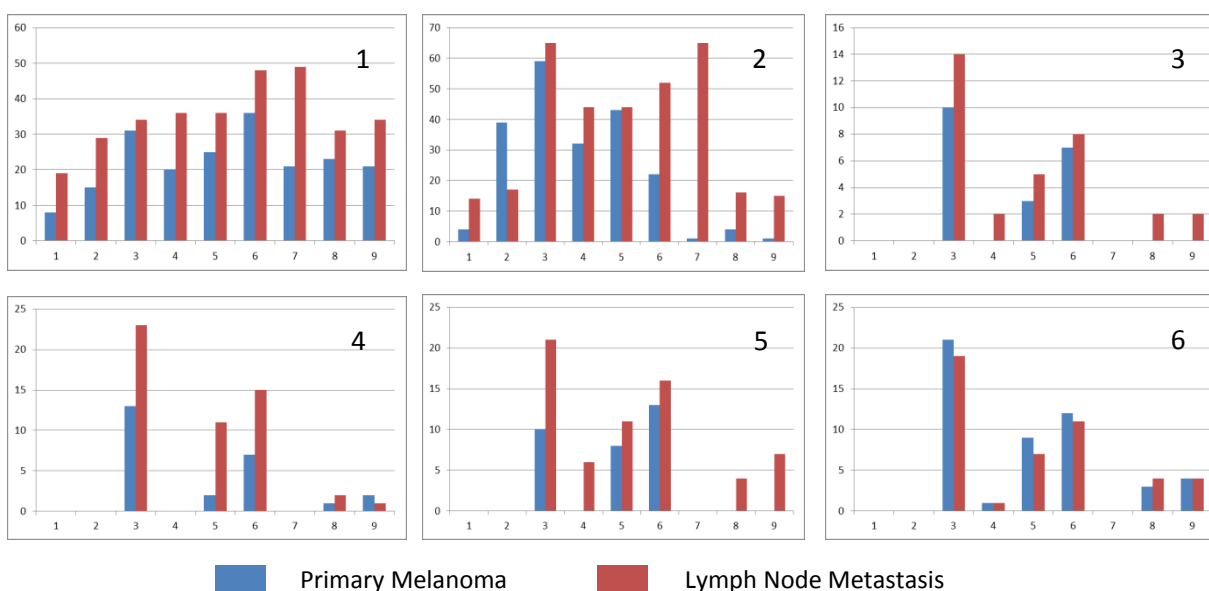


Figure 3-10: *TFPI2* CpG island methylation increases in metastatic melanoma relative to matched primary melanoma.

Eight paired primary and metastatic melanomas from the same patients were analysed by pyrosequencing for *TFPI2* methylation. The figure shows % methylation at each of 9 individual CpG dinucleotides. Primary melanomas are shown in blue and metastatic melanomas in red. The metastases were lymph node in all cases. Tissues were subject to microdissection to enrich for malignant cells prior to DNA isolation.

Of 8 paired melanomas that I examined, 5 pairs (patients 1, 2, 3, 4, and 5) showed increased *TFPI2* methylation in the metastasis compared to the matched primary melanomas at each CG dinucleotide, one pair (patient 6) showed similar methylation levels, and 2 pairs did not show clear differences with higher methylation in some CpGs in metastases but lower methylation in the others (Table 3-4 and Figure 3-10). These results clearly support a potential role for *TFPI2* CpG island methylation in predicting tumour progression.

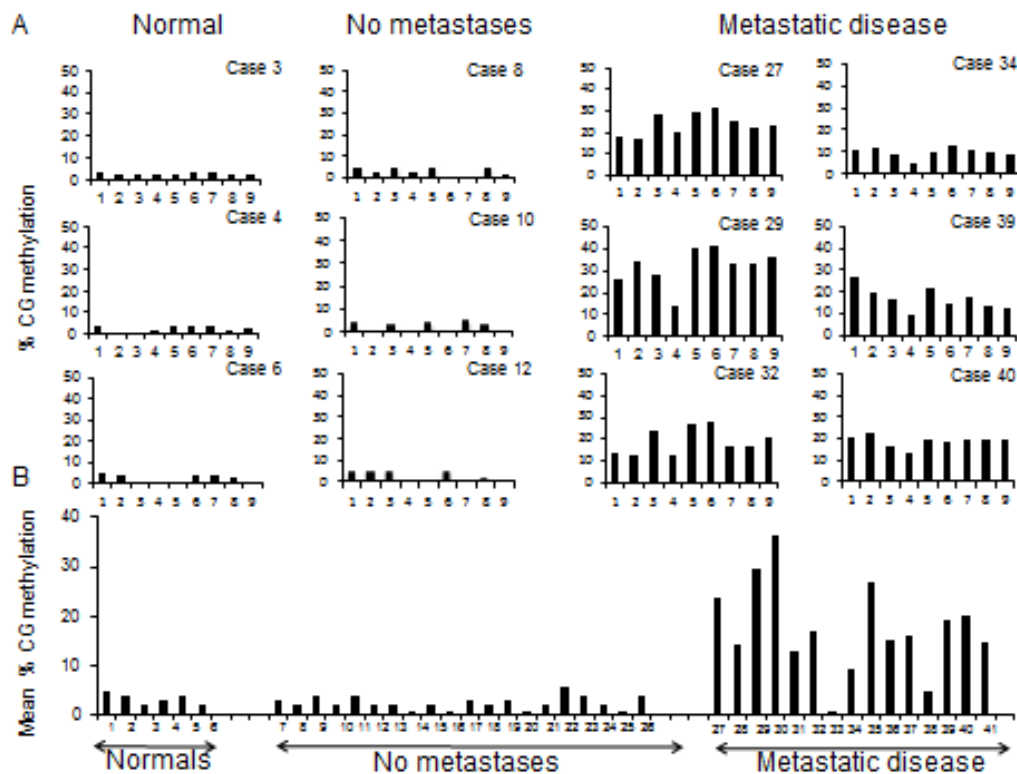


Figure 3-11: Quantitative *TFPI2* CpG island methylation profiles from serum of healthy volunteers (Normals), patients with no metastases and patients with metastases.

(A): Representative profiles. (B): Summarised analysis of all sera. Mean % methylation was determined by pyrosequencing as described in Methods.

3.2.1.1.5 *TFPI2* CpG island methylation in melanoma patient sera

The presence in serum of circulating DNA released from tumour cells has provided us with a novel approach to detect DNA methylation in cancer patients' peripheral blood. Theoretically, therefore, increased methylated DNA will be detected in patients who develop metastatic disease, particularly those patients with visceral metastases. To address this hypothesis, we used pyrosequencing to determine *TFPI2* CpG island methylation levels in a series of 41 serum samples from 6 healthy volunteers and 35 melanoma patients. An advantage of pyrosequencing over many other methylation detection techniques is the high sensitivity and resolution (at the level of individual CG dinucleotides). DNA in circulating blood released from tumour cells is typically present at low levels and is difficult to quantify by conventional methods. However, a number of studies have illustrated the utility of pyrosequencing in detecting circulating DNA methylation in cancer patients' peripheral blood (Korshunova et al. 2008; Sturgeon et al. 2012; van Bommel et al. 2012; Yoon et al. 2012; Tahara et al. 2013; Zmetakova et al. 2013).

In my study, I successfully detected *TFPI2* methylation in circulating blood from melanoma patients, and *TFPI2* methylation increased according to the degree of tumour progression as shown in Figure 3-9. Unsurprisingly, *TFPI2* methylation was detectable but at lower levels in serum from 6 healthy volunteers and from melanoma patients with no metastases.

I next compared *TFPI2* methylation in 20 cases where both tissue and serum samples were available, and observed an overall correlation between the two groups. Importantly, patients with *TFPI2* methylation in serum also showed detectable methylated DNA in their tissues (Figure 3-12 A), although the methylation level of *TFPI2* in serum samples did not correlate with Breslow thickness (Figure 3-12 B). However, I discovered that the level of *TFPI2* methylation was statistically significantly higher ($p < 0.01$, Figure 3-12 C) in cases where metastatic involvement was known compared to cases in which metastasis was not suspected, regardless of the Breslow thickness of the primary tumour. To assess the significance of *TFPI2* methylation in specifically detecting metastatic disease, a receiver operator characteristic (ROC) curve was generated by GraphPad Prism Software to compare *TFPI2* methylation levels between individuals with and without metastases. This analysis demonstrated a diagnostic sensitivity of 74% and specificity of 91% for metastatic disease when a mean methylation cut-off value of *TFPI2* methylation of 4.5% in serum is applied. The area (0.9015) under the curve (AUC) measurement illustrated that 86% of melanoma patients with metastases have significantly higher *TFPI2* methylation level than individuals without metastases ($p < 0.0001$, Figure 3-12 D).

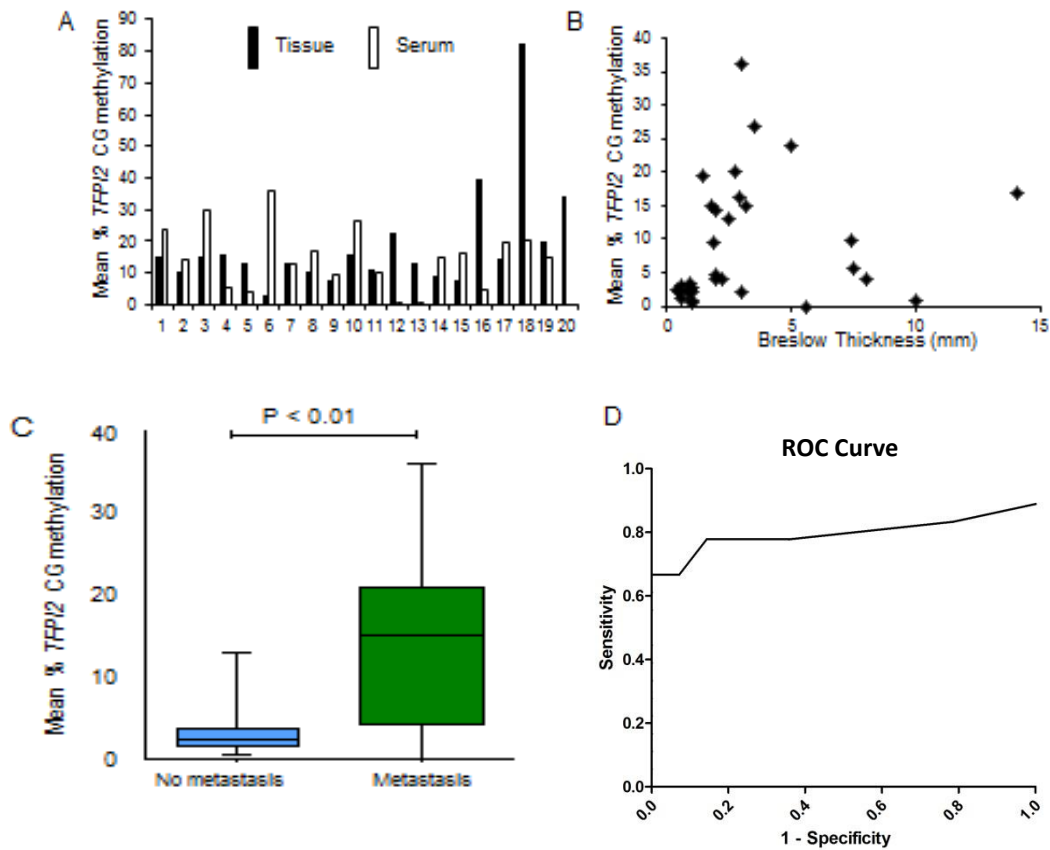


Figure 3-12: Detection of methylated *TFPI2* CpG island genomic DNA in serum is associated with metastatic melanoma.

(A): Concordance of tissue and serum pyrosequencing of *TFPI2* CpG island in melanoma patients. Pyrosequencing of genomic DNA from tissue and serum was done as described in Methods. The figure shows the 20 paired cases for which tissue and serum was available. In each case, mean % *TFPI2* CpG island methylation in melanoma tissue is shown in the black box and mean % *TFPI2* CpG island methylation in corresponding serum is shown in the white box. (B): Scatter plot of serum *TFPI2* CpG island methylation vs Breslow thickness. CpG island methylation is independent of Breslow thickness. (C): Mann-Whitney analysis of mean % CG methylation in patients without metastatic disease (No metastasis) and known metastatic disease (Metastasis). Detection of *TFPI2* CpG island methylated DNA in serum is strongly associated with the presence of metastatic disease ($p < 0.01$). (D): Receiver Operator Characteristic curve showing predictive utility of detection of *TFPI2* CpG island methylated DNA in serum of patients with melanoma in the diagnosis of metastatic disease. The ROC curve was constructed as described in Materials and Methods.

3.2.1.2 DNA methylation of *DKK1* and *EGR2*

I initially validated methylation reversal data in cell lines MEL501, MEL505 and MEL224 that showed up-regulated expression of *DKK1* and *EGR2* upon methylation reversal treatment. Consistent with the microarray data, these three cell lines all showed significant restored *DKK1* and *EGR2* gene expression (Figure 3-13).

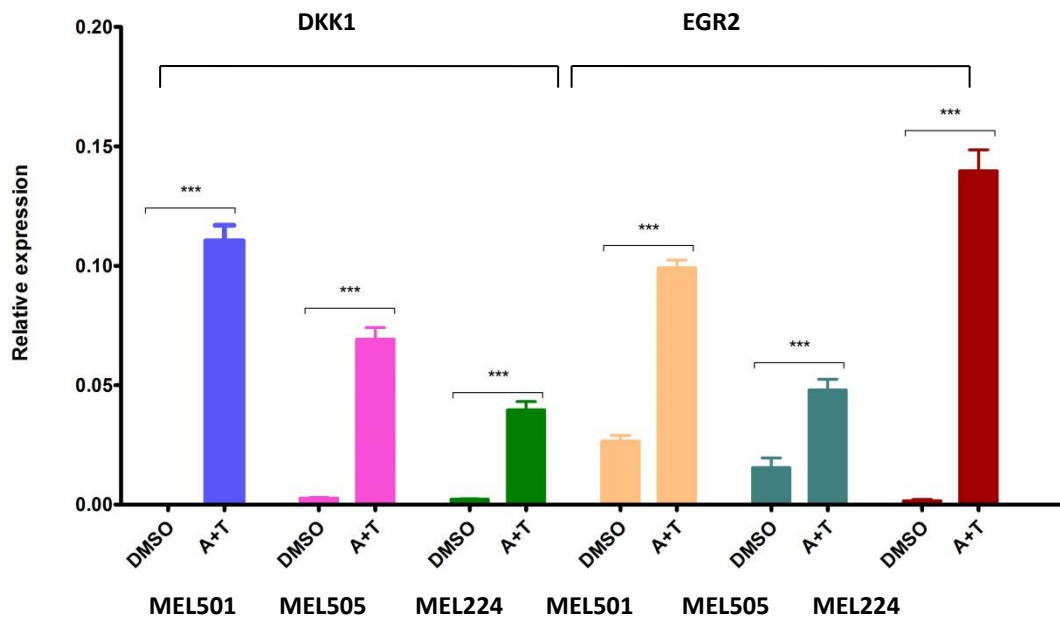


Figure 3-13: Expression of *DKK1* and *EGR2* in melanoma cell lines with methylation reversal treatment.

All cell lines were either treated with DMSO as the negative control or treated with demethylating agents 5' AZA and TSA. Each treatment condition was performed in biological triplicates. Gene expression was measured by qPCR. T test was used to compare the significant difference between DMSO control and 5'AZA+TSA treatment. *** is p value < 0.001.

MSP was then performed to identify the methylation status of these two candidates in our melanoma cell line panel and in normal melanocytes and both genes have shown a high frequency of methylation.

EGR2 was methylated in 12/17 (71%, Figure 3-14 B) of the melanoma cell lines, but not in normal melanocytes, (HEMA). Disappointingly, I did not observe a correlation between DNA methylation and mRNA expression (Figure 3-14 C). For example, in MEL501 and SKMEL2 cell lines, ie those with the highest expression, *EGR2* was found to be methylated, and in contrast cell lines that were unmethylated showed generally a low level of mRNA expression. *EGR2* methylation has been reported to act like an enhancer that induces gene expression (Unoki and Nakamura 2003), but I did not detect this correlation in our methylation positive cell lines. Lack of correlation between *EGR2* methylation and gene expression suggested *EGR2* methylation is not a gene expression regulatory mechanism in melanoma cell lines.

EGR2 was not methylated in cell line MEL505, a line in which gene expression was induced by methylation reversal treatment (Figure 3-13). Upregulation of *EGR2* expression in MEL505 cells after methylation reversal treatment may represent an indirect effect of demethylating an upstream gene. Another possibility is that failure to detect methylation of *EGR2* by MSP may be a false negative result.

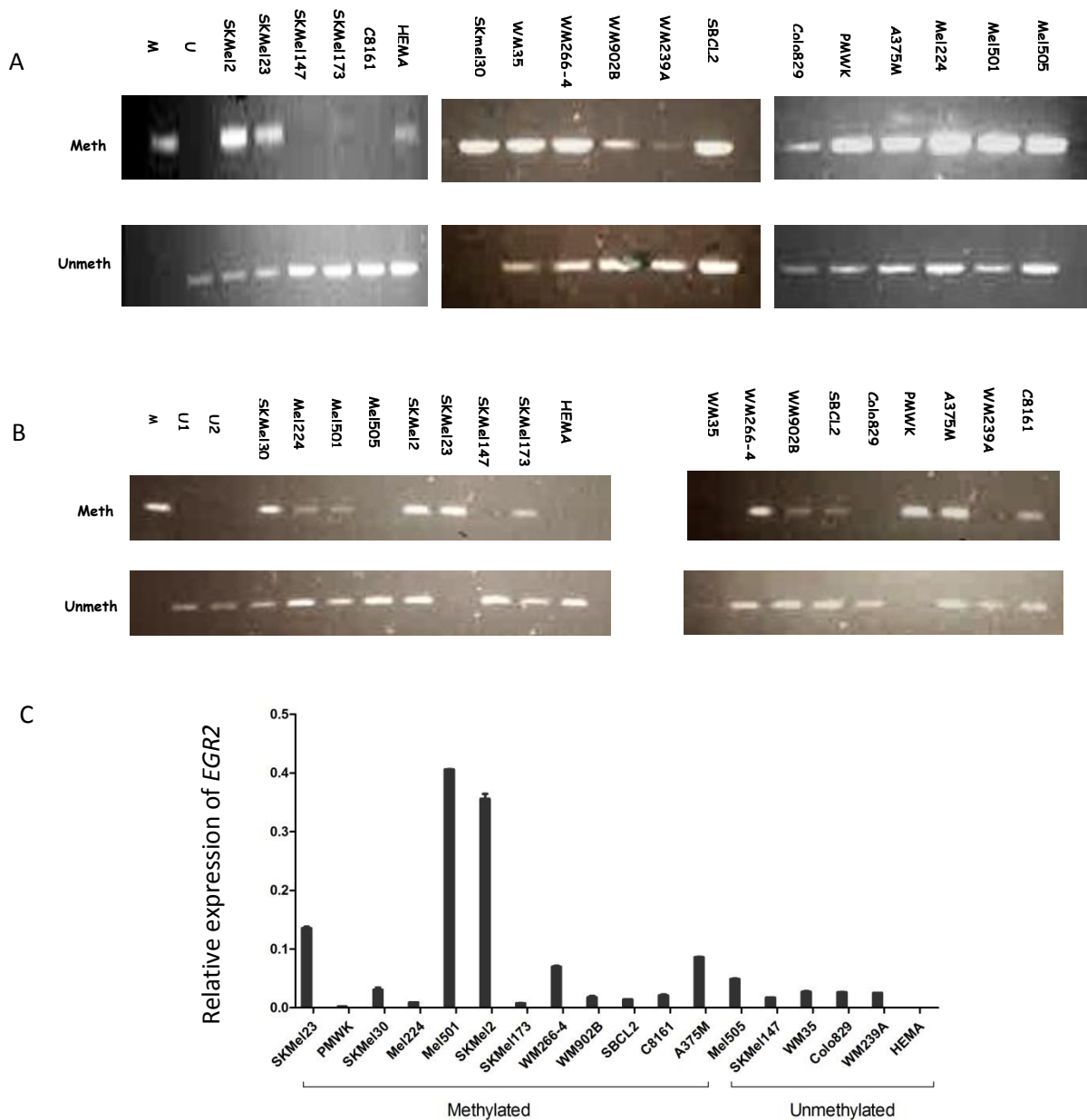


Figure 3-14: Methylation and expression of *EGR2*, as well as methylation of *DKK1*.

(A), (B): Methylation of *DKK1* and *EGR2* in 17 melanoma cell lines and melanocyte HEMA by MSP, respectively. (C): Relative expression of *EGR2* mRNA (qPCR) in 12 methylated and 5 unmethylated cell lines and unmethylated melanocytes (HMEMA).

Despite the high frequency of methylation seen in melanoma cell lines (14/17, 77%, Figure 3-14 A), *DKK1* was also methylated in normal human melanocytes (HEMA), indicating that *DKK1* is not exclusively differentially dysregulated in melanomas. As such, *DKK1* does not meet the criteria for a melanoma biomarker.

Taken together, these results imply that despite being frequently methylated in melanoma cell lines, *EGR2* and *DKK1* are not suitable melanoma biomarkers for further development.

3.2.1.3 CpG island methylation of TGF- β signalling components *SMAD3* and *TSC22D1*

3.2.1.3.1 *SMAD3*

I have identified *SMAD3* methylation in melanoma by pyrosequencing. To our knowledge, *SMAD3* methylation has not been reported previously in human cancers. In my study, *SMAD3* showed a high frequency of methylation in the melanoma cell line panel (14/17, 82%), but a low frequency in melanoma tissues (24/94, 22%). *SMAD3* methylation was also detected at only a low level in normal human keratinocytes (NHK, 7%) and melanocytes (HEMA, 10%). However, promoter methylation of *SMAD3* is unlikely to be a mechanism to regulate gene expression, because I was unable to show any correlation between *SMAD3* mRNA expression (Figure 3-15 A) and methylation (Figure 3-15 B).

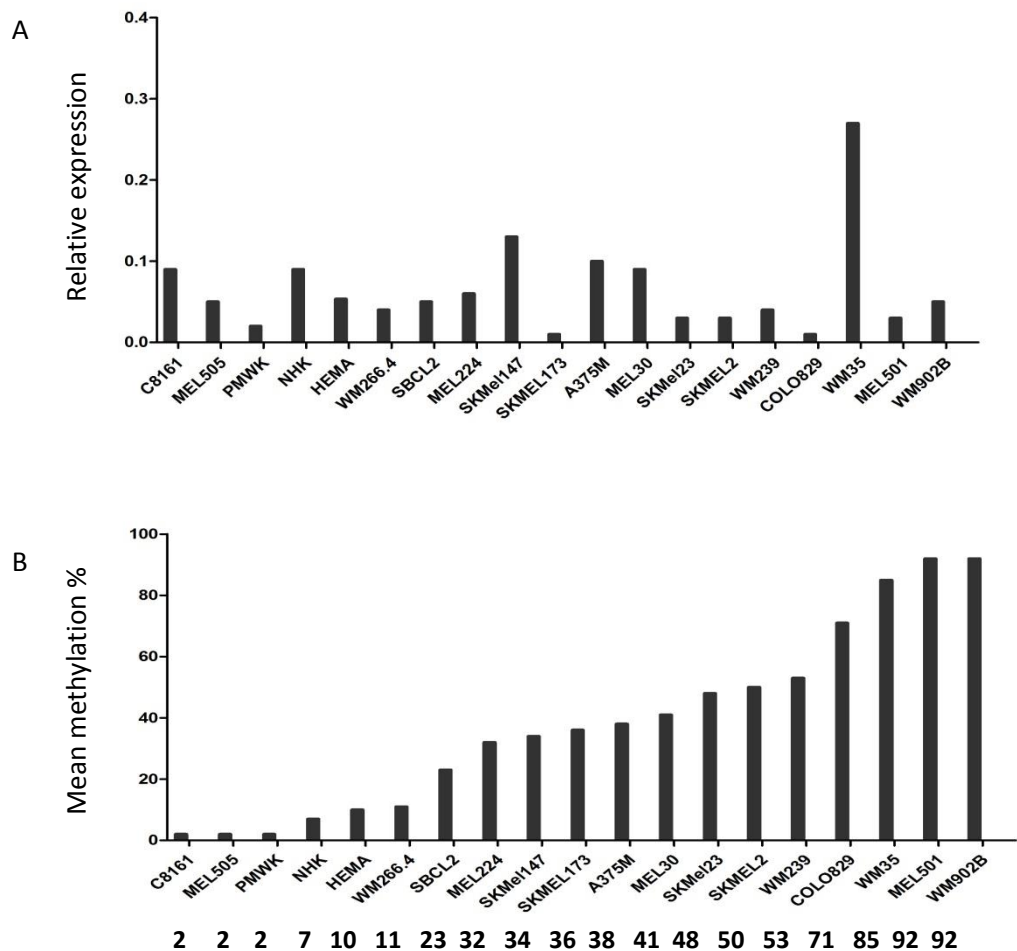


Figure 3-15: Expression (A) and methylation (B) of *SMAD3* in melanoma cell lines and melanocyte HEMA and keratinocyte NHK.

(A): Relative expression of *SMAD3* mRNA (qPCR) in 17 melanoma cell lines, a melanocyte line (HEMA) and normal human keratinocytes (NHK). (B): Average methylation (%) of CpG dinucleotides within *SMAD3* gene promoter determined by pyrosequencing in 17 melanoma cell lines, HEMA and NHK.”

3.2.1.3.2 TSC22D1

There are two isoforms of *TSC22D1*, a short isoform *TSC22D1.1* and a long isoform *TSC22D1.2* (Figure 3-16 C). Homig-Holzel et al. have reported their antagonistic roles in regulating senescence in human keratinocytes and melanocytes (Homig-Holzel et al. 2011). Our methylation reversal screen suggested that *TSC22D1* was potentially methylated in melanoma, so I hypothesized that methylation-related *TSC22D1* gene silencing may be a mechanism that attenuates the senescence pathway in melanoma.

To test this hypothesis, I first needed to determine the methylation status of *TSC22D1* gene in melanoma cell lines. The antagonistic function of the two isoforms in senescence prompted me to study the two isoforms separately. I performed qPCR on methylation reversal agent-treated cell lines including MEL501, MEL505, as well as cell line MEL224 which showed upregulated *TSC22D1* expression in microarray data. Demethylating agents 5' AZA and TSA failed to restore gene expression of *TSC22D1.1* in all three cell lines (Figure 3-16 A), suggesting that expression of *TSC22D1.1* is not controlled by methylation. Conversely 5' AZA and TSA treatment upregulated *TSC22D1.2* expression in MEL501 and MEL224 (Figure 3-16 B), although not significantly, suggesting *TSC22D1* isoform 2 may be methylated in melanoma.

I next used pyrosequencing to verify *TSC22D1.2* methylation in 10 melanoma cell lines. *TSC22D1.2* has a short CpG island of 244 base pairs, and I designed 4 sets of pyrosequencing primers whose products cover the whole CpG island. The PCR product of the fourth set of primers was near the TSS. As shown in Figure 3-17 A and B, cell line PMWK is heavily methylated through the whole CpG island, and this is associated with absent gene expression. Methylation was also detected in cell lines C8161 and SKMEL23, albeit at different locations. Low mRNA expression in SKMEL23 cell line and high mRNA expression in C8161 cell line implies that methylation near TSS has more influence on regulation of gene expression. In the remaining 7 melanoma cell lines I did not detect methylation of *TSC22D1.2* by pyrosequencing. In a subset of 30 melanoma tissue samples, *TSC22D1.2* was only methylated in 2 cases. The low frequency of methylation in *TSC22D1.2* in melanoma cell lines and tissues suggested that *TSC22D1.2* methylation is only detectable in a small subset of melanoma and is not, therefore, likely to have utility as a melanoma biomarker.

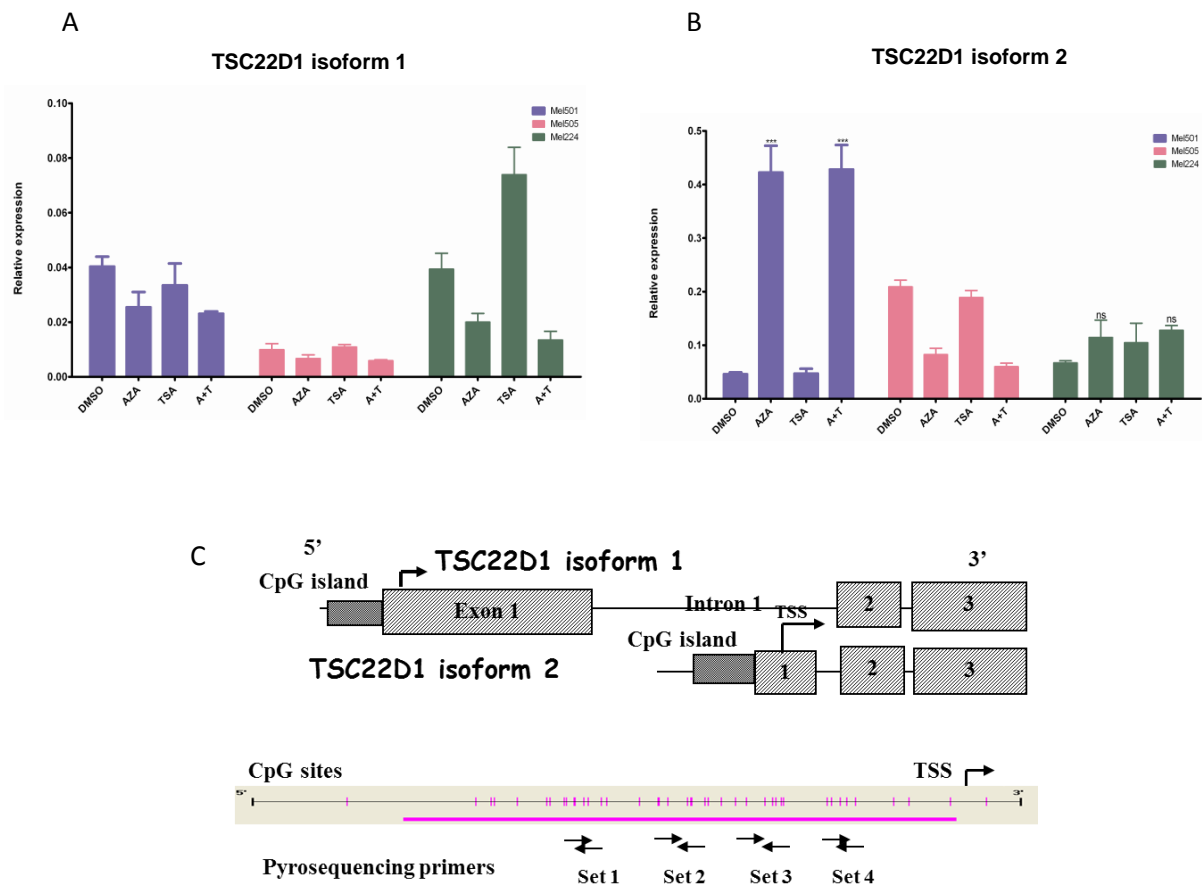
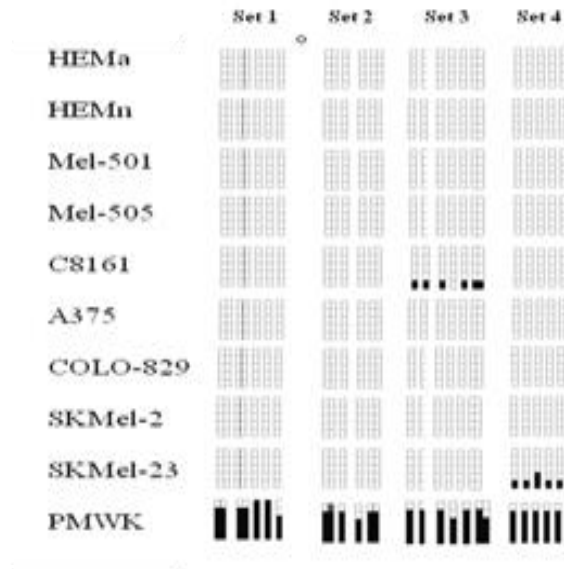


Figure 3-16: Reactivation of *TSC22D1.1* and *TSC22D1.2* expression by pharmacological demethylation (A, B) and the genomic structure of the human *TSC22D1* gene (C).

(A, B): The indicated cell lines were grown in the presence of 5' AZA, TSA, both agents (A + T) or drug vehicle only (DMSO). Expression of *TSC22D1.1* and *TSC22D1.2* was determined by qPCR. Data shown is mean \pm 1SD from 3 independent experiments. (C): Schematic diagram of *TSC22D1* gene including 5' and 3' UTRs, exon-intron boundaries, CpG island, and the location of pyrosequencing primers.

A



B

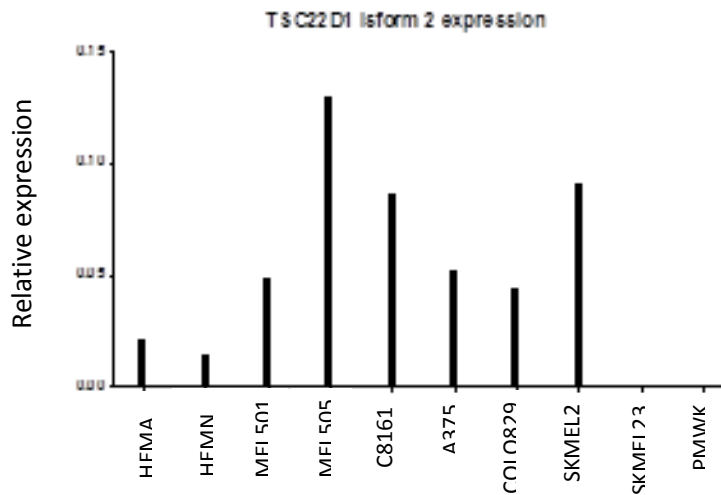


Figure 3-17: Methylation and expression of *TSC22D1.2* in melanoma cell lines.

(A): Detection of *TSC22D1.2* CpG island methylation by 4 sets of pyrosequencing primers. (B): mRNA expression of *TSC22D1.2* by qPCR.

3.2.2 Identification of candidate genes by systematic methylation profiling and gene expression profiling in paired melanoma cell lines

Gene expression profiling and methylation profiling for identification of genes that are differentially epigenetically regulated between primary and metastatic melanoma cell lines were performed on the following 3 sets of melanoma cell lines which were derived from 3 patients:

Table 3-5: Paired melanoma cell lines used for microarray analysis

	Primary	Metastasis Lymph node	Metastasis Skin
Set 1	WM115	WM239A	WM266.4
Set 2	LM2	LM9	LM29
Set 3	WM983A	WM983B	

For initial data analysis (work flow shown in Figure 3-19), gene expression from a microarray experiment was analysed by Dr Runxuan Zhang (The James Hutton Institute, Dundee) (analysis protocol shown in section 2.6.2). This generated a list of 60 genes that were either downregulated in three lymph node metastatic cell lines (WM239A, LM9, and WM983B) or in any 4 out of the 5 metastatic cell lines. A filter criteria of at least a 1.5-fold change with adjusted $p < 0.01$ (Figure 3-18) was applied to this analysis. To investigate whether downregulation of these 60 candidates was dependent upon DNA methylation, Dr Helena Carén (Sahlgrenska Cancer Centre, Gothenburg, Sweden) compared methylation levels

between primary and metastases within each set of cell lines This study identified 30 genes (*A2M, ACOX2, BCAT1, CA9, CBFA2T3, CYP1B1, GOLGA8B, HRH2, KIF26B, MAOA, MAP1B, MAP1LC3A, PCSK1, PDK4, PRDM16, RAB31, SEZ6L2, TCEA2, TUBB2B, ZNF788, EFNB2, FAM-134B, HLA-DPA1, IFITM1, LIMCH1, MT1E, MX1, RASAL1, TCEA3, TFPI2*) which showed methylation changes at more than 5 methylation variable positions (MVPs); selected through a filter criteria of an adjusted p-value of <0.01 and with a change in the beta-value (methylation frequency) of more than 20%.

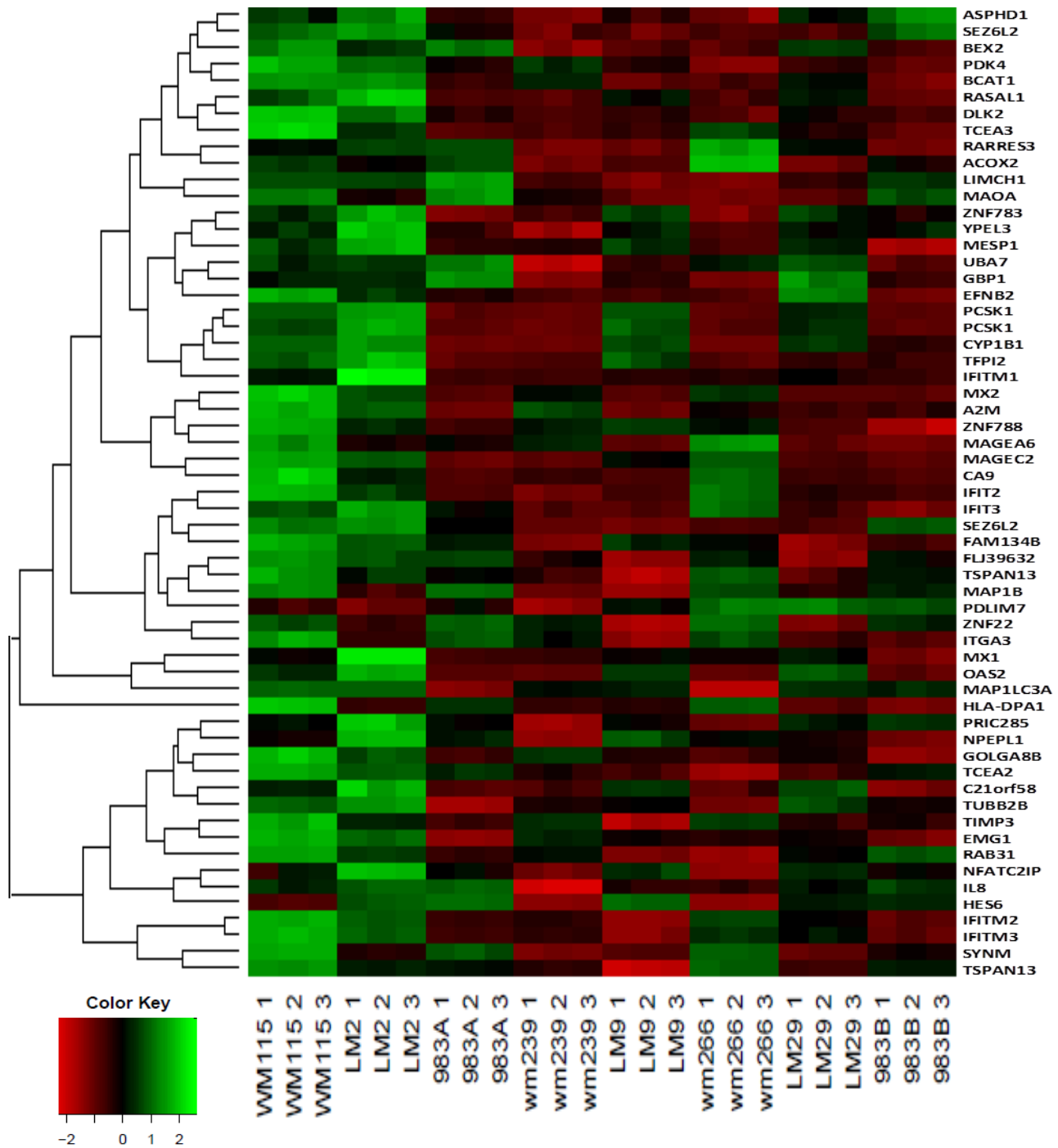


Figure 3-18: Heat map visualization of 60 genes that are significantly downregulated in all three lymph node metastatic or 4/5 metastatic melanoma cell lines.

Columns: samples; rows: genes; colour key indicates gene expression (mRNA) where red is significantly downregulated compared with green. Primary melanoma cell lines WM115, LM2 and WM983A were clustered at left of figure whereas metastatic cell lines WM239, LM9, WM266, LM9 and WM983B were clustered to the right.

A further data mining process investigated whether these 31 genes are differentially regulated in other gene expression studies by searching a cancer microarray database platform, Oncomine (Rhodes et al. 2004). Three separate studies, the Riker study, the Haqq study, and the Talantov study, detailed in Oncomine website, have systematically compared gene expression between melanoma tissues and normal tissues. From this process only 7 of 30 from the original gene panel remained (Table 3-6). These 7 genes were also significantly downregulated in the metastasis compared to primary melanomas in three studies Riker, Xu, and Haqq. Of these 7 genes all had a well-defined CpG island and so all 7 genes passed the selection criteria for suitable candidate methylated genes for melanoma. Summary of the data mining results for these 7 genes:

A: significantly downregulated in metastasis of all 3 paired primary and metastatic melanoma cell lines.

B: methylated at significantly higher levels in metastasis in all 3 sets.

C: significantly downregulated in melanoma tissue samples compared to benign neavus

D: have a well-defined CpG island

Therefore, further investigation of gene expression and methylation of these 7 genes (*LIMCH1*, *HLA-DPA1*, *EFNB2*, *RASAL1*, *TCEA3*, *MT1E*, *FAM134B*) will be undertaken in our collection of melanoma cell lines, melanoma tissues and serum samples. This will be a future continuation of my work and is beyond the scope of this thesis.

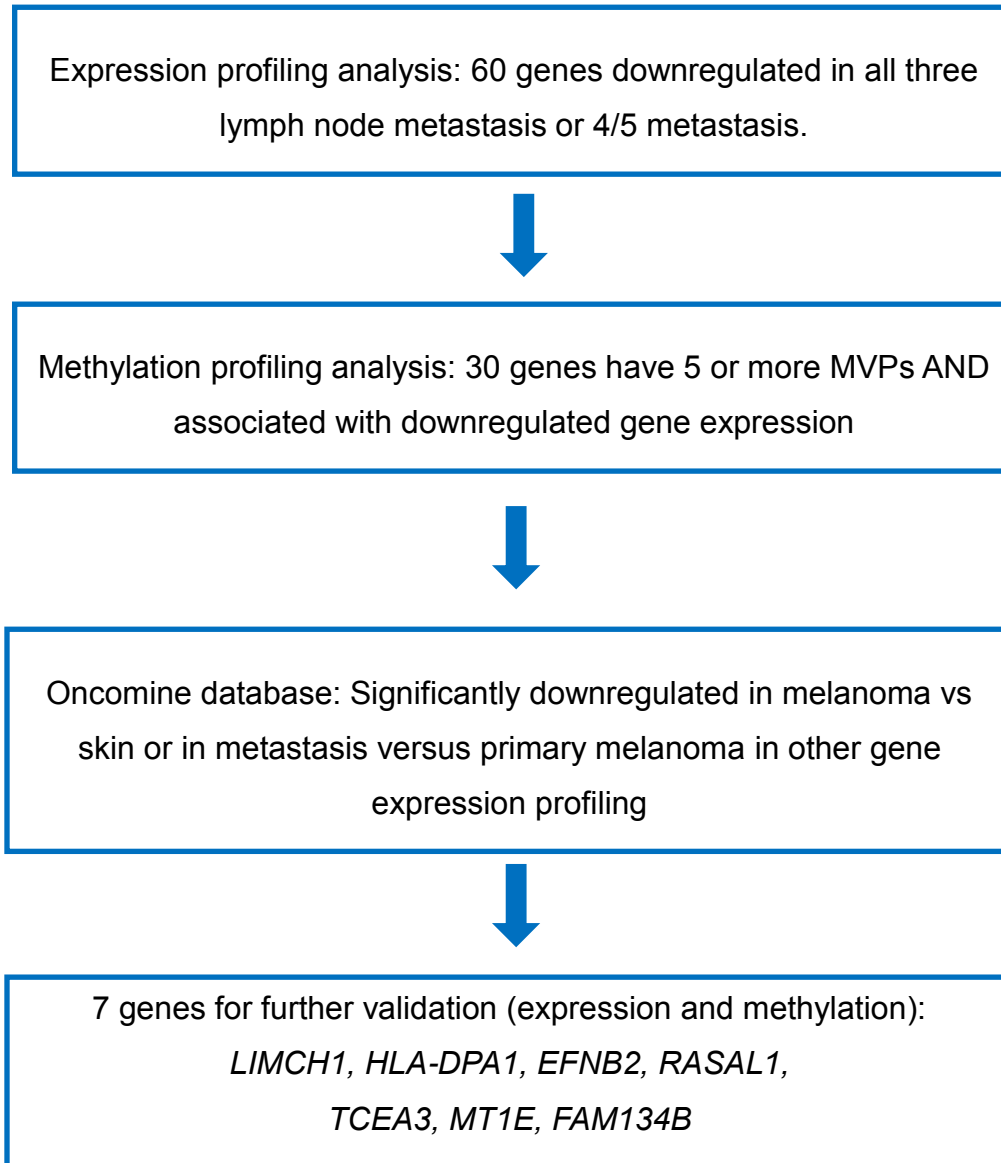


Figure 3-19: Data mining work flow for the identification of differentially epigenetically regulated candidate genes in 3 paired melanoma cell lines.

Table 3- 6: Differential expression results of candidate genes in RIKER, HAQQ TALANTOV, XU tissue studies and their CpG island status

Melanoma versus skin (√: Significantly downregulated in melanoma versus benign naevus other skin)				
	RIKER	HAQQ	TALANTOV	CpG island
LIMCH1	√	√	√	√
HLA-DPA1	NO	NO	√	√
EFNB2	√	√	√	√
RASAL1	NO	N.D.	√	√
TCEA3	√	√	N.D.	√
MT1E	√	NO	NO	√
FAM134B	√	NO	NO	√
Metastasis versus primary melanomas (√: Significantly downregulated in metastatic melanoma versus primary melanomas.)				
	RIKER	XU	Haqq	CpG island
LIMCH1	√	√	NO	√
HLA-DPA1	NO	√	NO	√
EFNB2	NO	√	√	√
RASAL1	√	√	N.D.	√
TCEA3	√	NO	UP	√
MT1E	NO	√	NO	√
FAM134B	NO	√	√	√

NO: No statistical significance. N.D.: Not done. UP: upregulated

RIKER, HAQQ, TALANTOV analysis results were obtained from Oncomine website (<https://www.oncomine.com>).

CpG island status was obtained from UCSC genome browser (genome.ucsc.edu/).

3.3 Discussion

The use of pharmacological demethylation to identify epigenetically silenced genes is a recent technique building upon the basis that DNA methylation is a reversible phenomenon. It has been successfully used to study methylation events in tumours, particularly when accompanied by gene expression profiling to identify candidate genes that are transcriptionally silenced by DNA methylation whose expression is reactivated by demethylation. This approach has established useful protocols for DNA methylation studies, and these are especially applicable for methylation biomarker investigation.

However, the results of methylation reversal experiments must be interpreted with some caution. Methylation reversal only informs as to whether a particular gene is potentially methylated, but it does not provide information about the exact gene sequence where methylation occurs. Many genes have extensive CpG islands containing hundreds of CpG sites, within which only a small part of the CpG island, such as the part near the TSS is likely to be critical for transcriptional regulation. Techniques such as MSP or sequencing based techniques such as pyrosequencing or bisulfite sequencing can be used to narrow down the methylation status to a specific region in the gene sequence. In the case of pyrosequencing, multiple sets of primers may be required to cover as much of the entire CpG island as possible, as the optimal size of pyrosequencing product is only approximately 100 base pairs, and can be even smaller when testing

patient materials. This potentially limits the utility of this technique in gene discovery given the cost of pyrosequencing.

Global demethylation can also result in inappropriate upregulation of some genes. Many genes can be spuriously or indirectly upregulated by global demethylation. For example, expression of a particular gene can be altered due to methylation of an upstream regulator of this particular gene. Therefore, upregulation of a particular gene may be a consequence of restored gene expression of its methylated upstream regulator by the demethylating treatment. We have seen this in our methylation reversal screen, where a large number of genes were upregulated, yet, many of these candidates don't have CpG islands. I saw this with *TIMP1*, *HLA-A* and *IL8*. However, we must bear in mind that methylation of areas other than the CpG island may also regulate gene expression (Jones 2012). Inconsistent results between methylation reversal screens and downstream investigations have been reported for some genes. In my study for example, *EGR2* was upregulated in cell line MEL505 in our methylation reversal screen, but its methylation was undetectable by MSP.

Another technique often used in place of methylation reversal is a methylation microarray. This methodology has the advantage of being applicable to a wider range of starting materials, including cell line material, frozen tissue and paraffin-embedded tissue whereas methylation reversal analysis clearly requires living cell line starting material. Methylation microarray is also more powerful than

methylation reversal analysis because it can inform the methylation level of a particular gene and of the exact sequence that is methylated. It should be noted, however, that methylation of candidate genes identified by methylation microarrays may not correlate with gene expression. Many genes that undergo methylation are very likely to be related to non-tumourigenic events, such as maintained cell type specific lineage commitment which was already established in embryogenesis (Sproul et al. 2011), or *de novo* (new) methylation which occurs in normal tissues later than embryogenesis, such as *de novo* methylation on inactive X-chromosome (Keshet et al. 2006). This disadvantage can be overcome by integrating methylation data with gene expression data to validate methylation reversal assay results. Indeed I have attempted to do this here in my work. Integration of gene expression profiling and methylation profiling has rigorously selected the candidate genes whose regulation is dependent upon methylation. Data mining has ultimately provided us with 8 candidate genes for further investigation. Of particular note is *TFPI2* which was also identified by both methylation reversal analysis and integrative analysis, suggesting consistency between methylation reversal screen results and methylation profiling candidate approaches.

Identification of *TFPI2* by our methylation reversal screen has provided us with an encouraging and promising methylation biomarker for melanoma. An eligible epigenetic biomarker for melanoma must meet certain criteria: (i) exclusively and frequently dysregulated by DNA methylation in melanoma, but not in the benign

tissue equivalent; (ii) clinically useful for predicting tumour progression and patient outcome; (iii) correlation of methylation with gene expression, with functional significance for the initiation and progression of melanoma. An additional necessary requirement for a serum epigenetic biomarker is that methylation should be detectable in serum from melanoma patients with metastasis, and that this level of methylation should be significantly higher than that detected in serum from patients with non-metastatic melanomas. This would lead to the possibility of early detection of metastasis by a simple and minimally invasive blood test.

The data presented in this chapter shows that *TFPI2* has met these requirements. First, I have observed a high frequency and high level of *TFPI2* methylation in melanoma cell lines and patient specimens. In patient samples, including a clinical series of approximately equal numbers of non-metastatic and metastatic melanomas, and paired primary and metastatic melanomas from the same patients, a significantly increased level of *TFPI2* CpG island methylation has been detected in aggressive metastatic disease. Importantly, methylation in the control benign naevi was uniformly low. These results support a role for *TFPI2* as an epigenetic biomarker that can potentially predict the advanced stages of melanoma. The association between *TFPI2* methylation and reduced gene expression in melanoma cell lines further supports the importance of *TFPI2* silencing in driving the tumour progression.

TFPI2 methylation frequencies of 10-20% have been reported in three previous melanoma studies (Nobeyama et al. 2007; Liu et al. 2008; Tanemura et al. 2009). Comparatively, *TFPI2* showed a much higher methylation frequency in our melanoma clinical cases. This could be because less sensitive methods for detecting methylation were used by these groups. All three studies (Nobeyama et al. 2007; Liu et al. 2008; Tanemura et al. 2009) used MSP to assess *TFPI2* methylation in their melanoma patients which is somewhat less sensitive a method than the pyrosequencing technique employed in my study. Pyrosequencing quantitatively measures the level of cytosine methylation at each individual CG site whereas MSP provides a more global assessment of methylation. Detection of methylation in patients' sera requires a very sensitive method that can detect the extremely low concentration of free DNA circulating in patients' blood. Additionally, these other studies (Nobeyama et al. 2007; Liu et al. 2008; Tanemura et al. 2009) have used patient cohorts from Japan and USA. Our patients are UK-based, and there may be distinct population variations in melanomagenesis associated with different geographical locations. In this study, I successfully detected methylated DNA in the serum samples, and most importantly, the presence of *TFPI2* methylation is associated with metastatic disease, regardless of the Breslow thickness of the primary melanoma. A high sensitivity of 74% and specificity of 91% of *TFPI2* methylation in metastasis implies utility as a serum biomarker to detect metastatic disease. I would now like to take this forward to determine if *TFPI2* is a robust serum biomarker in a multi centre prospective study.

The other candidate genes highlighted in my investigation have not fully met the requirements for an appropriate biomarker. I detected a high frequency of *DKK1* and *SMAD3* methylation in our melanoma cell lines, however, both genes were also methylated in benign melanocytes, suggesting that the DNA methylation of these candidates was not a specific event in melanomagenesis. *EGR2* was also an unsuitable biomarker because of the lack of association between DNA methylation and dysregulated gene expression. The low frequency of *TSC22D1* methylation in melanoma cell lines and melanoma tissue samples illustrated its lack of utility as a melanoma biomarker.

In future work confirmation of *TFPI2* as a melanoma progression biomarker and a melanoma serum biomarker will be undertaken in a larger scale study of melanoma tissues and a prospective study, respectively. The molecular function of *TFPI2* in driving the initiation and progression of melanoma should also be investigated. In addition, other candidate genes identified by the integrative genome-wide methylation profiling and expression profiling will be evaluated for their potential as epigenetic biomarkers in melanoma.

Chapter 4 Methylation
investigation of candidate genes
NT5E, DUSP2, and Dab2.

4.1 Introduction

Hundreds of genes have been found to be hypermethylated in human cancers (Baylin and Jones 2011). These include those that are ubiquitously methylated in a broad range of cancers and those whose methylation is more cancer type specific. For example, a mediator of alkylating chemotherapeutic agents' sensitivity (Christmann et al. 2011), O6-methylguanine-DNA methyltransferase (*MGMT*) is methylated in colon cancer, lung cancer, prostate cancer and lymphoma etc (Heyn and Esteller 2012), and *TFPI2* is methylated in more than ten human cancers, as introduced in Chapter 3.1.1. Loss of expression of these genes by promoter methylation is therefore likely to be important for the initiation and progression of multiple cancer types. It is also very likely that methylation of some tumour-related genes is a cancer type specific event (Esteller et al. 2001). I therefore wished to determine the methylation status of specific genes in melanoma to expand our knowledge of the methylome of this disease. The methylation study of *NT5E*, *DUSP2* and *Dab2* will be described in this chapter, including the background of these three candidates.

4.1.1 *NT5E* (ecto-5'-nucleotidase, CD73)

NT5E encodes an enzyme located at the plasma membrane that hydrolyses extracellular nucleotides into membrane permeable nucleosides (Klemens et al. 1990). The most recognised signalling pathway involving the catalytic function of

NT5E is the phosphohydrolytic conversion from extracellular adenosine triphosphate (ATP) to adenosine. The last step of this conversion, generation of adenosine from adenosine 5' monophosphate (AMP) requires NT5E to stimulate an adenosine cascade (Zimmermann 1992). Along with its catalytic function, NT5E also acts as an adhesive protein that mediates endothelium-binding (Airas et al. 1995; Arvilommi et al. 1997) and activation and proliferation of lymphocytes (Airas et al. 1997). NT5E activity or expression is elevated in breast carcinoma (Canbolat et al. 1996), cutaneous T cell lymphoma (Fukunaga et al. 1989), gastric cancer (Durak et al. 1994), and melanoma (Sadej et al. 2006). The well-established immunosuppressive role of NT5E involving adenosine combined with the lymphocyte mediating function of NT5E implies that NT5E will have important regulatory functions in the host immune response to human cancers. Improved efficacy of T cell immunotherapy and increased in vivo survival rate in an ovarian mouse model with NT5E knock down has been observed (Jin et al. 2010). Further, Stagg et al. have shown that melanoma mice with deficient NT5E escaped from immunosuppression and development of metastasis (Stagg et al. 2011). More recently Forte et al. introduced the concept of a tumour immunity inhibitory role of NT5E by revealing improved anti-tumour immunity when inducing B cells in mouse melanoma treated with an NT5E inhibitor (Forte et al. 2012). These recent studies have provided evidence that NT5E alters tumour immunity and tumour progression.

It appears that adenosine drives tumour progression via promotion of cell proliferation, angiogenesis and drug resistance (Spsychala 2000), implying a possible involvement of NT5E in these cancer promoting processes. A positive correlation between NT5E expression and breast cancer cell growth, invasion, migration and adhesion has been described using in vitro knockdown (Zhi et al. 2007) and over-expression experiments (Zhou et al. 2007; Wang et al. 2008) and in in vivo studies (Zhou et al. 2007). However, different studies have reported that NT5E may be associated with good or poor prognosis in two breast cancer cohorts (Leth-Larsen et al. 2009; Supernat et al. 2012). A reverse impact on cell migration of NT5E has been demonstrated in hepatic cells, suggesting its potential as a tumour suppressor (Andrade et al. 2011). NT5E has been shown to be induced by TGF- β (Regateiro et al. 2013) and in hypoxia (Synnestvedt et al. 2002; Li et al. 2006). The controversial roles of NT5E shown in different studies and regulation of NT5E by microenvironmental elements suggest that NT5E may be expressed in a context-dependent and cell specific manner and suggest further study of NT5E may yield valuable data.

4.1.2 DUSP2 (Dual-specificity phosphatase 2)

DUSP2 encodes a protein belonging to a subfamily of dual-specificity phosphatases which negatively regulate members of the mitogen-activated protein (MAP) kinase pathway, i.e. ERK, JNK and p38 by dephosphorylation (Yi et al. 1995). The high frequency of aberrant regulation of the MAPK pathway in

melanoma suggested the potential involvement of DUSP family members in this tumour. Being first cloned in human T cells (Rohan et al. 1993), DUSP2 has been identified as involved with immune regulation since it is highly induced by activated immune cells and it positively mediates immune cell function and the immune response through JNK and ERK kinase (Jeffrey et al. 2006). DUSP2 has higher binding affinity to ERK than to p38 and JNK (Zhang et al. 2005) and decreased DUSP2 expression has been identified in a variety of human cancer cells. By using knockdown and re-expression techniques a role for DUSP2 in negatively regulating hypoxia-induced chemoresistance, apoptosis, angiogenesis and cell survival has been illustrated (Lin et al. 2011). Yin et al. found that DUSP2 is a transcriptional target for p53 that mediates p53-induced apoptosis and growth suppression (Yin et al. 2003). Wu et al. further proved the engagement of DUSP2 in apoptosis by showing that ectopic DUSP2 expression induces apoptosis and suppresses ERK in an E2F-1 dependent manner (Wu et al. 2007). Taken together, these studies are consistent with a tumour suppressive role for DUSP2. The molecular mechanism facilitating downregulation of *DUSP2* have not been established, but identification of *DUSP2* methylation in breast cancer cells (Demircan et al. 2009), implies that promoter methylation of *DUSP2* may make a contribution. However, two other studies raise the possibility of an oncogenic role for DUSP2 in malignant neoplasia by showing a positive correlation of DUSP2 and association of DUSP2 expression with poor outcome of ovarian carcinoma (Le et al. 2002; Givant-Horwitz et al. 2004).

4.1.3 Dab2 (Disabled-2)

Dab2 is an adaptor molecule involved in signalling cascades such as the TGF- β pathway and the Wnt pathway (Hocevar et al. 2001; Hocevar et al. 2003). Loss of Dab2 protein expression was first identified in ovarian cancer cells and cancerous ovary tissues (Mok et al. 1998). Dab2 was subsequently shown to be down-regulated in a variety of human tumours, including breast cancer, bladder cancer, head and neck squamous cell carcinoma (HNSCC), oesophageal cancer, and colorectal cancer (Fazili et al. 1999; Kleeff et al. 2002; Anupam et al. 2006; Bagadi et al. 2007; Karam et al. 2007; Hannigan et al. 2011). Identification of absent or reduced expression of Dab2 in human cancers suggests Dab2 is a tumour suppressor. Several reports show that DNA methylation of *Dab2* may contribute to this tumour suppression (Bagadi et al. 2007; Tong et al. 2010; Hannigan et al. 2011). Dab2 exerts its tumour suppressor role by regulating cancerous behaviours of cell death, growth arrest, and cell adhesion in a MAPK pathway-dependent manner (Sheng et al. 2000; He et al. 2001; Tseng et al. 2003). The Wnt pathway is also negatively regulated by Dab2 and this pathway may contribute to the tumour suppressive effect of Dab2 (Jiang et al. 2009). The prognosis of lung and prostate cancer is poor when Dab2 expression is absent, suggesting Dab2 as a candidate biomarker for tumour progression (Zhou et al. 2005; Xu et al. 2011). Another interesting function of Dab2, found in HNSCC, is that when *Dab2* is silenced due to DNA methylation this acts as a 'switch' for TGF- β to change from a tumour suppressing to an oncogenic cytokine (Hannigan et al. 2011).

4.2 Results

4.2.1 *NT5E* methylation in melanoma

4.2.1.1 *NT5E* methylation in less aggressive metastatic melanoma line C81-61 and more aggressive melanoma line C8161

Dr Tim Crook has provided the *NT5E* methylation investigation data as shown in Figure 4-1. Five melanoma cell lines were used in this investigation. In this panel one melanoma line, C81-61, with low metastatic potential is compared to its more aggressive derivative line C8161 (derived from the same patient). Normal human melanocytes, NHEM, were also included in the initial detection of *NT5E* methylation and mRNA expression (Figure 4-1 A). *NT5E* methylation was detected in cell line C81-61 by MSP, and was associated with absent *NT5E* mRNA expression by qPCR. No *NT5E* methylation was detected in the other melanoma cell lines or in melanocytes. Bisulfite sequencing was also performed on cell lines C8161 and C81-61 (Figure 4-1 B) to quantitatively determine the methylation level of *NT5E* at individual CpG sites through the whole CpG Island. *NT5E* was heavily methylated at all CpG sites in cell line C81-61, including the sites in which *NT5E* methylation was indicated by MSP. In contrast, the *NT5E* CpG island was entirely unmethylated in C8161 cells. The presence of *NT5E* methylation and absence of gene expression suggests that DNA methylation of *NT5E* transcriptionally silences gene expression. Methylation reversal treatment was then performed on cell lines C8161 and C81-61 to further confirm the effect

of aberrant *NT5E* methylation on gene expression. As shown in Figure 4-1 C, *NT5E* gene expression was strongly induced by the methylation reversal agent 5'AZA in C81-61 cells (*NT5E* methylated), but was much less affected in C8161 cells (*NT5E* unmethylated).

4.2.1.2 *NT5E* CpG island methylation in melanoma cell line panel

Based on the observation of *NT5E* CpG island methylation in melanoma cell line C81-61 by Dr Tim Crook, I analysed *NT5E* methylation in an expanded collection of melanoma cell lines by pyrosequencing. *NT5E* methylation was detected in 5 of 15 (33%) melanoma cell lines (Figure 4-2 A), which are SKMEL2, SKMEL23, MEL501, MEL505 and WM35. In this panel of 15 melanoma cell lines I also showed that *NT5E* mRNA expression is low or absent in those 5 lines where the CpG island is methylated (Figure 4-2 B). Of particular interest is cell line MEL501 which has the highest methylation level (mean methylation 89%) and undetectable *NT5E* expression.

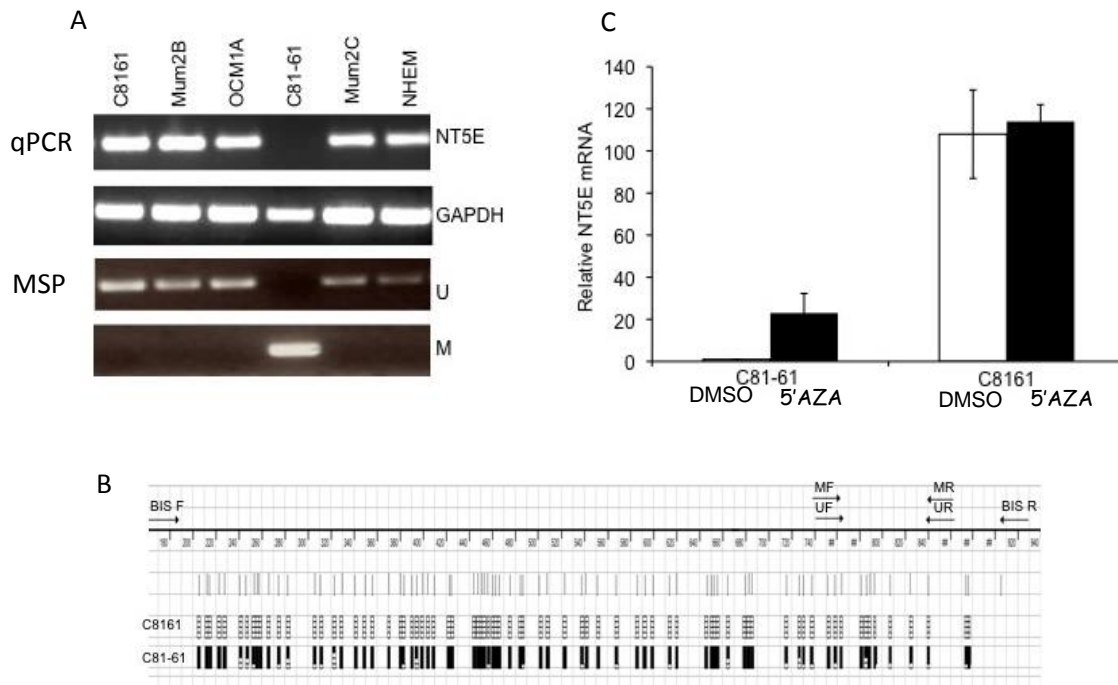


Figure 4-1: *NT5E* was methylated in the less aggressive melanoma cell line C81-61 but not in the more aggressive derivative, C8161.

(A): Expression of *NT5E* correlated inversely with CpG methylation in C81-61 and its highly metastatic isogenic C8161. *NT5E* expression and methylation was measured by qPCR and MSP, respectively. GAPDH was used as a control for qPCR. (B): Bisulfite sequencing showing the methylation status of *NT5E* at each CpG dinucleotide in the CpG island in C81-61 and C8161 cell lines. CpG sites are shown as vertical lines. Methylated CpG sites are shown as black blocks, unmethylated CpGs as open blocks. (C): Expression of *NT5E* mRNA was reactivated by demethylation in C81-61 but not in C8161.

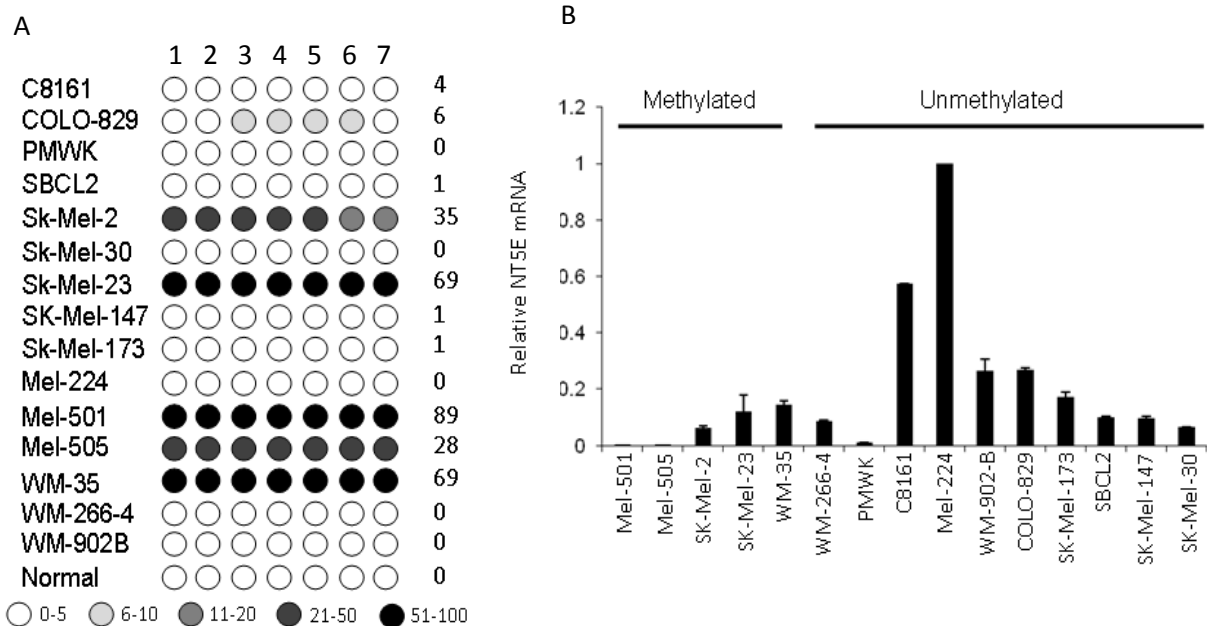


Figure 4-2: Analysis of *NT5E* expression and methylation in melanoma cell line panel.

(A): *NT5E* was frequently methylated in melanoma cell lines. Methylation was quantified by the intensity of shading in the circles, each of which represents an individual CpG dinucleotide. 5 levels of shading were used as indicated in the figure. (B): Expression of *NT5E* correlated inversely with CpG methylation in majority of melanoma cell lines. *NT5E* mRNA expression was measured by qPCR against reference gene B2M.

4.2.1.3 *NT5E* methylation in melanoma clinical samples

4.2.1.3.1 *NT5E* CpG island methylation in primary melanomas and derivative metastases

Identification of methylation-dependent transcriptional silencing of *NT5E* in the less aggressive metastatic melanoma cell line C81-61 revealed a possible association between *NT5E* methylation and less aggressive phenotype of melanomas. I therefore decided to analyse methylation of *NT5E* in two sets of paired melanomas with both primary melanoma and lymph node metastasis available. As shown in figure 4-3, *NT5E* was methylated at higher level at each CpG site in the primary tumour (red) than the metastasis (blue) in one patient, and methylated only in the primary melanoma in the other patient. The decrease in *NT5E* methylation in each metastasis compared to that in the primary melanoma supports a potential role of *NT5E* methylation in predicting good prognosis.

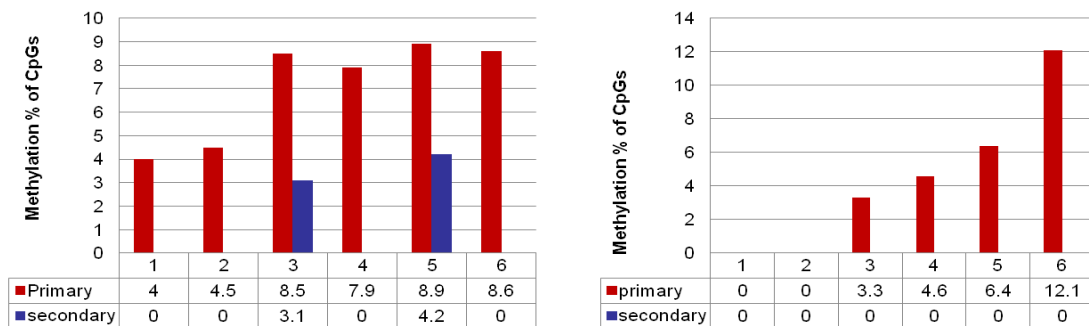


Figure 4-3: *NT5E* methylation in two sets of paired melanoma with both primary melanoma and lymph node metastasis were both available.

Pyrosequencing analysis showing methylation percentage of 6 CpG sites in two paired primary melanomas and metastasis. ■ Primaries ■ Metastasis

4.2.1.3.2 *NT5E* methylation in primary melanomas

Identification of *NT5E* CpG island methylation in melanoma cell lines encouraged me to extend the study to melanoma clinical cases and I determined *NT5E* methylation status in 27 well-characterised primary melanomas, these comprising 17 non-relapsing primary melanomas and 10 cases which subsequently relapsed with recurrent disease. 12 out of 27 (44%) cases showed *NT5E* methylation using a mean methylation level of 5% as cut-off. These cases were 10 examples of primary melanomas which did not relapse and 2 primary melanomas from patients who subsequently developed lymph node metastasis, suggesting that *NT5E* methylation may be a feature of non-relapsing cases. It is important to emphasise that *NT5E* methylation in the 10 relapsed primary melanomas was detected only in cases which relapsed as lymph node metastases (2/5 lymph node) and not in visceral metastases (0/4) or cutaneous metastases (0/1), indicating a lymph node site methylation specificity of *NT5E* methylation. Melanomas with visceral metastasis invariably have a worse prognosis than lymph node metastasis. The higher frequency of *NT5E* methylation in non-relapsing primary melanomas and the presence of *NT5E* methylation in primary tumours with lymph node only metastasis suggests that *NT5E* methylation may be a good prognostic biomarker for melanoma patient outcome.

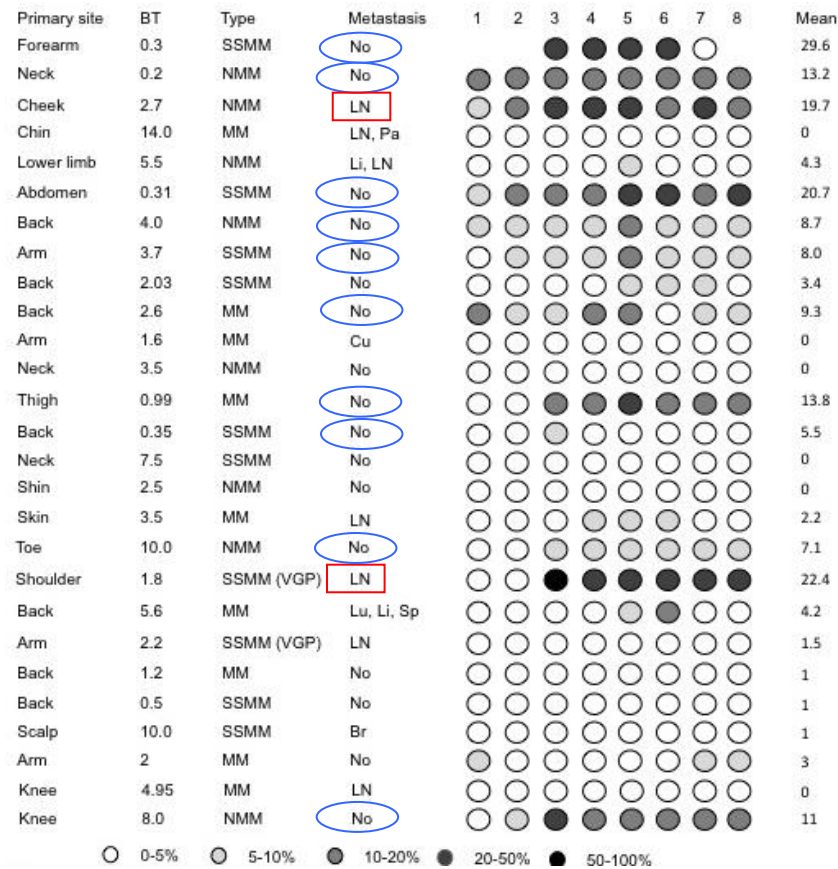


Figure 4-4: *NT5E* methylation in 27 well characterised primary melanomas.

Clinical information including primary site, Breslow thickness (BT), tumour subtype (superficial spreading malignant melanoma (SSMM), nodular malignant melanoma (NMM), malignant melanoma with unknown subtype (MM)), growth phase (vertical growth phase, VGP), site of metastasis (lymph node (LN), parotid gland (PA), liver (Li), cutaneous (Cu), lung (Lu), spleen (Sp), and brain (Br)) are all shown in the figure. *NT5E* methylation level at 8 CpG sites was shown by the intensity of shading in the circles. 5 levels of shading were used to represent differing extents of methylation. The average methylation level of *NT5E* (%) was also listed next to the quintile circles. Metastasis status of primary melanomas with greater than 5% of *NT5E* methylation was highlighted in either blue circle (no relapse) or red square (lymph node metastasis).

4.2.1.3.3 *NT5E* methylation in metastasis

Finally, I analysed *NT5E* CpG island methylation in a subset of 23 melanoma metastasis specimens, comprising 15 lymph node (LN) metastases, 3 cutaneous (Cu) metastases, 4 soft tissue (ST) metastases and 1 bladder (Bl) metastasis. By using the previously designated mean methylation level of 5% as cut off, I detected *NT5E* methylation at similar frequency (9/23, 39%) in these metastasis cases as in primary melanomas (44%). Interestingly, 7 of 9 cases with *NT5E* methylation were in lymph node metastasis from patients who did not develop other metastasis. Moreover, *NT5E* methylation was not detected in 8 of 9 cases from melanoma patients who developed visceral metastasis (liver, lung, bone, brain and bladder). The high frequency of *NT5E* methylation in lymph node metastasis from patients free of distant metastasis and the absence of *NT5E* methylation in patients with visceral metastasis further imply that *NT5E* methylation is a potential biomarker of good prognosis melanoma.

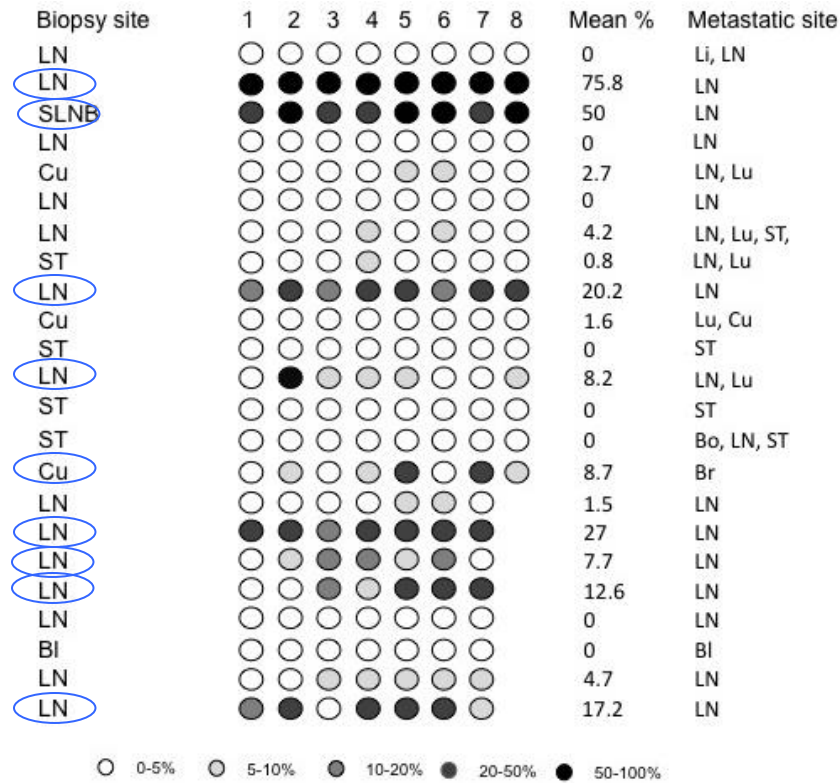


Figure 4-5: Detection of *NT5E* methylation in 23 melanoma metastasis.

The level of methylation is indicated by the intensity of shading in the circles as shown in the key, each of which represented an individual CpG site. Information including the site of biopsies for examination, the mean % methylation, and the sites of all metastasis that melanoma patients ultimately developed: BI, Bo (bone), Br, Cu, Li, LN, Lu, and ST are also shown. Sites of metastatic disease which showed higher than 5% of *NT5E* methylation are highlighted in blue circles.

4.2.2 *DUSP2* methylation in melanoma

4.2.2.1 *DUSP2* methylation in melanoma cell lines

DUSP2 methylation was quantitatively measured by pyrosequencing in 15 melanoma cell lines. 10 melanoma cell lines showed over 10% mean methylation, including 5 cell lines SKMEL147, MEL224, SBCL2, MEL501 and PMWK with a particularly high level of *DUSP2* methylation (mean methylation > 60%) (Figure 4-6 A). qPCR analysis performed on the same batch of melanoma cell lines revealed a generally low level of *DUSP2* expression in cell lines with *DUSP2* methylation (Figure 4-6 B). *DUSP2* expression was particularly low or absent in cell lines (SKMEL147, MEL224, SBCL2, MEL501 and PMWK) which have a high level of *DUSP2* methylation. Cell lines positive for *DUSP2* methylation showed significantly reduced *DUSP2* mRNA expression compared to cell lines with no *DUSP2* methylation (unpaired t test, $p < 0.01$, figure 4-6 C), suggesting that promoter methylation silences *DUSP2* gene expression at the transcriptional level. I next performed methylation reversal assay on the SKMEL2 cell line which had a mean methylation level of 32% and low gene expression, to assess if increased *DUSP2* expression in this cell line is induced by demethylation. Figure 4-6 D shows that 5'AZA alone significantly increased *DUSP2* gene expression ($p < 0.001$), and the combination of 5'AZA and TSA also significantly increased *DUSP2* expression ($p < 0.01$). Methylation reversal analysis indicated that *DUSP2* gene expression was inducible by demethylation and further confirms that DNA methylation of *DUSP2* negatively regulates gene expression.

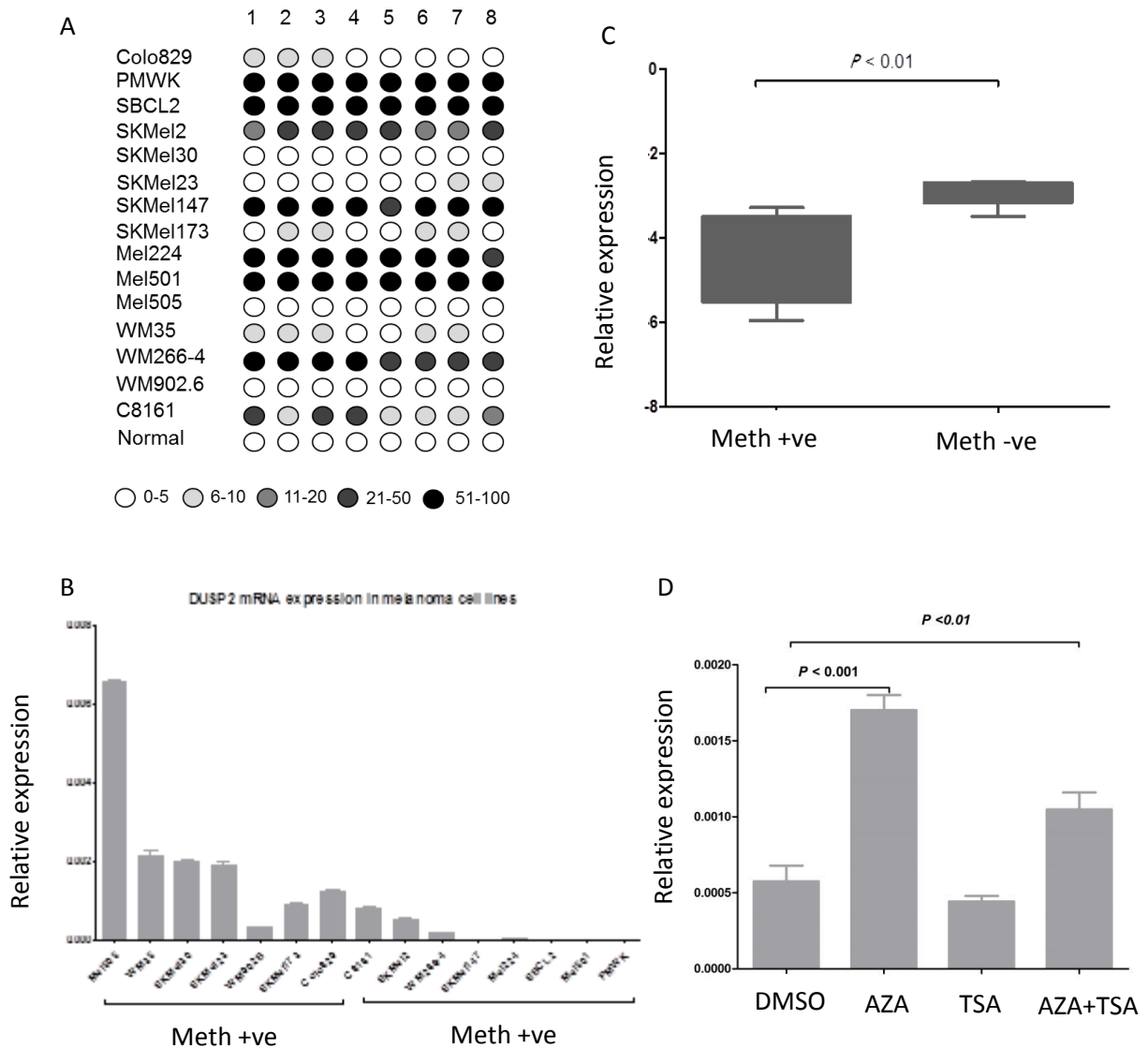


Figure 4-6: Identification of *DUSP2* methylation and mRNA expression in melanoma cell lines.

(A): *DUSP2* methylation in melanoma cell lines and normal melanocytes. The level of methylation is indicated by the intensity of shading in the circles as indicated in the key, each of which represents an individual CpG site. (B): Bar chart showing *DUSP2* relative expression in melanoma cell lines divided to methylation positive and methylation negative groups. (C): Unpaired t test showing significant inverse correlation between *DUSP2* expression and DNA methylation ($p < 0.01$). (D): Relative expression of *DUSP2* in melanoma cell line SKMEL2 with methylation reversal treatments under different conditions: DMSO, 5' AZA, TSA, and 5' AZA+TSA.

4.2.2.2 Overexpression of *DUSP2* in the metastasis of paired melanoma cell lines

Three sets of paired melanomas comprising a primary line and metastatic daughter derivative lines were then analysed for *DUSP2* gene expression and DNA methylation. Figure 4-7 A shows significant over-expression of *DUSP2* in metastatic lines WM239A, LM9 and WM983B when compared with their parental lines WM115, LM2 and WM983A, respectively. It is notable that the three metastases with significantly increased *DUSP2* expression were all derived from lymph nodes, whereas the other metastatic cell lines WM266.4 and LM29, which expressed much lower levels of *DUSP2* were both skin metastases. These results indicate that *DUSP2* may be specifically over-expressed in lymph node metastases. Cell line WM266.4 showed low level *DUSP2* expression in the whole cell line panel (Figure 4-6 C). From looking at DNA methylation and the mRNA expression level of *DUSP2* in the three sets of paired primary and metastatic daughter lines which includes WM266.4, I noticed DNA methylation levels are between 41% and 72%, and cell line WM983B which had the highest amount of *DUSP2* expression is only approximately 3 fold higher than WM266.4, suggesting an overall low level of mRNA expression across all the 8 lines. Consequently, the correlation between *DUSP2* methylation and reduced expression is not as clear as the correlation we saw in the 15 melanoma cell line panel. However, there is clearly more *DUSP2* mRNA expression in the metastasis compared to the primary tumour lines. This suggests that other mechanisms may be influencing *DUSP2* expression in metastasis but that DNA

methylation is the predominant regulatory mechanism in primary melanomas. Another possibility would be methylation of other CpG dinucleotides that have not been identified in this study may also have impact on regulating gene expression. Also, we should be bear in mind that DNA methylation does not necessarily reduce gene expression in a proportional manner.

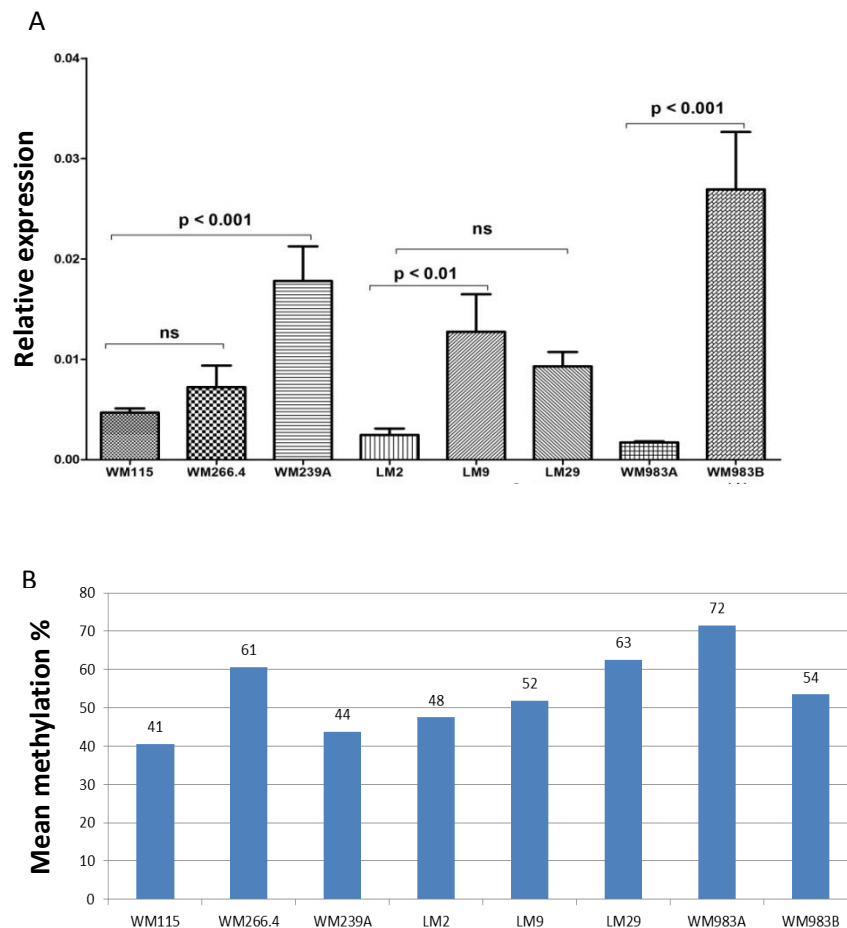


Figure 4-7: Expression and methylation of *DUSP2* in paired melanoma cell lines.

(A): *DUSP2* expression analysis by qPCR. One way ANOVA was used to compare the difference between metastatic lines and their parental primary melanomas (WM115 vs WM266.4, WM115 vs WM239A; LM2 vs LM9, LM2 vs LM29; WM983A vs WM983B) (B): Mean methylation % of *DUSP2* in paired melanoma cell lines by pyrosequencing.

4.2.2.3 *DUSP2* is methylated in melanoma clinical samples

The *DUSP2* methylation results from our melanoma cell line panel and paired cell lines prompted me to investigate *DUSP2* methylation status in melanoma clinical tissues using benign naevi as negative controls. A total of 61 clinical samples comprising 10 benign naevi, 12 primary melanomas and 39 metastases were selected for this validation investigation. Using pyrosequencing I determined that *DUSP2* methylation was at a generally low level (mean methylation less than 10%) in benign controls, with one outlier showing a higher methylation level of 15%. Comparatively, as shown in figure 4-8 A, *DUSP2* was frequently methylated at a level higher than 10% in both primary melanomas (9/12) and metastases (22/39). When comparing the differences in *DUSP2* methylation between the three groups of tissues (Figure 4-8 B), I observed that *DUSP2* was methylated at a significantly higher level in primary melanomas ($p < 0.001$) and metastases ($p < 0.01$) compared to benign naevi. Furthermore, *DUSP2* methylation in primary melanomas was also significantly higher than in metastases ($p < 0.05$). Together, these results show that *DUSP2* is frequently methylated in melanomas. The significantly higher level and frequency of *DUSP2* methylation in primary melanomas than in metastases and benign naevi supports a role for *DUSP2* methylation in initiation of melanoma, but also implies that reactivation of expression, associated with loss of methylation, may occur in disease progression.

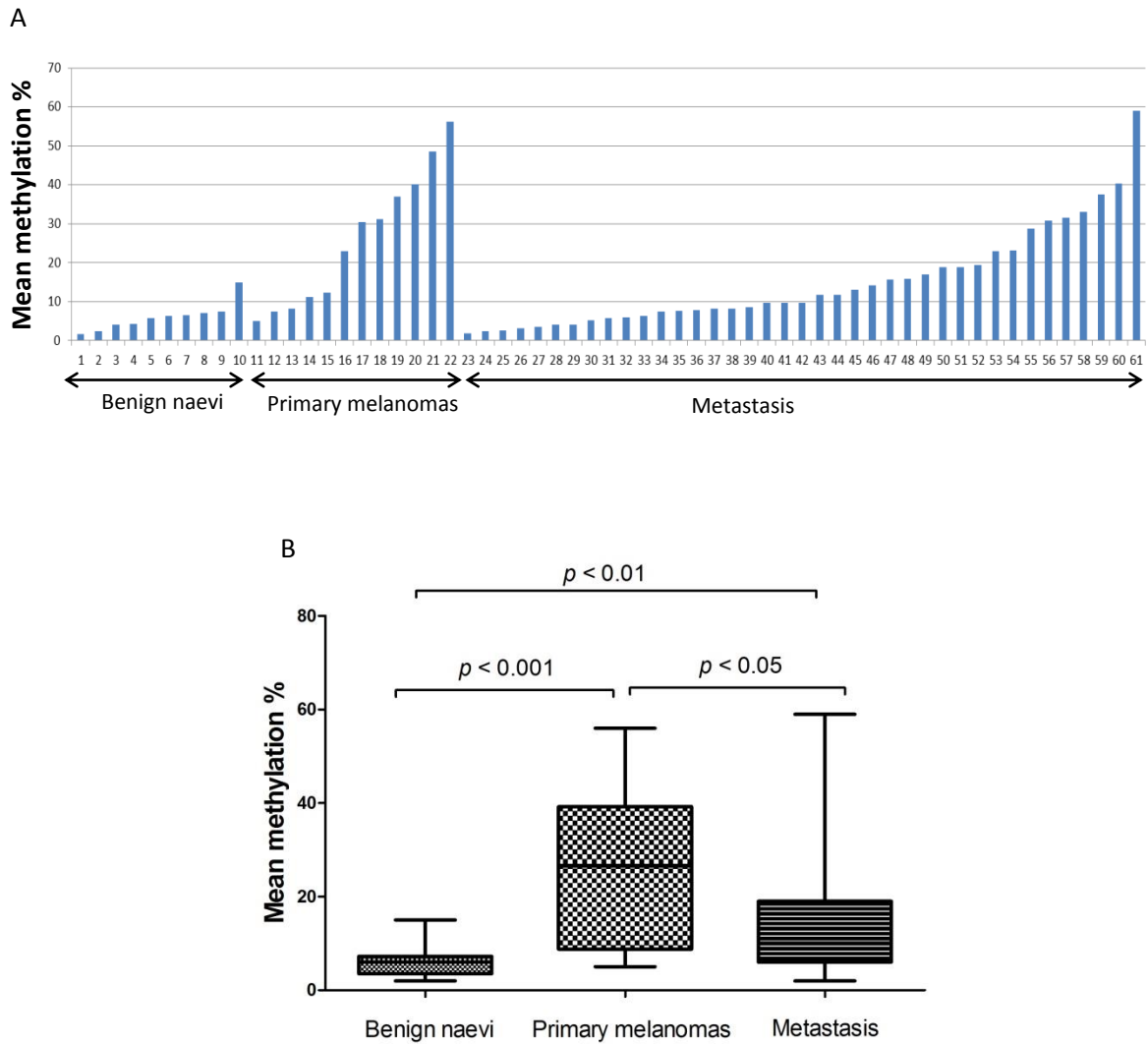


Figure 4-8: *DUSP2* methylation in melanoma tissues.

(A): Bar chart representing mean methylation of *DUSP2* in 10 benign naevi, 12 primary melanomas and 29 metastases. (B): Mann-Whitney *U* test showing the significant differences in comparisons: benign naevi vs primary melanomas ($p < 0.001$), benign naevi vs metastasis ($p < 0.01$) and primary melanomas vs metastasis ($p < 0.05$).

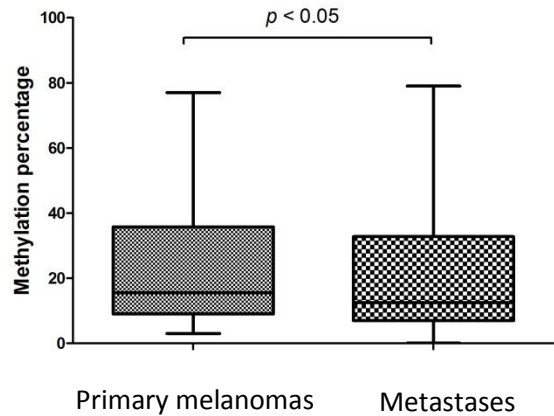
4.2.2.4 *DUSP2* methylation in paired melanoma tissues

Having observed that *DUSP2* methylation is elevated in clinical primary melanoma samples and shown decreased *DUSP2* expression in primary melanoma lines of paired cell lines, I examined 8 pairs of primary and metastatic melanoma tissue samples. These samples have also been studied for *TFPI2* methylation. As shown in figure 4-9 A and B, *DUSP2* methylation was detected at a higher average level in the primary melanomas than in the corresponding metastatic samples in 6 out of 8 pairs. The methylation level of *DUSP2* at each individual CpG site in primary melanomas was significantly higher than that in the corresponding metastasis by paired t test ($p < 0.05$). Two representative cases displayed higher *DUSP2* methylation at most of the CpGs in the primary tumour compared to the lymph node metastasis as shown in figure 4-9 C. However, the level of *DUSP2* methylation is only slightly higher in most primary tumours than metastasis, as these secondary tumours were all lymph node metastasis, which presumably still maintain similar biological properties to the primary melanomas from which they derive. I have not measured *DUSP2* mRNA expression in this set of paired primary and lymph node metastatic tissues. However, from the paired cell line data (section 4.2.2.2) I would predict that the inverse relationship between DNA methylation and mRNA expression would be stricter in primary tumour tissues than in metastatic tumour tissues, since other mechanisms may contribute to the regulation of *DUSP2* expression in the more disordered genetic and epigenetic environment of metastatic cancer.

A

Patient ID	DUSP2 methylation								
	CpG1	CpG2	CpG3	CpG4	CpG5	CpG6	CpG7	CpG8	Average
Patient 1	7	12	17	3	17	15	16	12	12
	5	9	10	0	12	10	8	7	8
Patient 2	72	75	65	55	65	77	22	18	56
	68	70	64	46	66	79	46	33	59
Patient 3	5	9	16	4	18	12	15	11	11
	4	7	11	4	13	8	10	6	8
Patient 4	9	9	10	3	11	8	9	6	8
	25	21	26	8	13	14	11	9	16
Patient 5	35	41	54	35	48	46	36	26	40
	17	10	42	26	37	42	36	36	31
Patient 6	10	33	32	25	29	26	11	17	23
	12	23	26	16	29	22	13	14	19
Patient 7	5	7	10	3	10	8	9	8	8
	2	4	4	0	5	5	0	0	3
Patient 8	45	46	43	48	39	12	13	4	31
	7	8	34	52	37	32	8	6	23

B



C

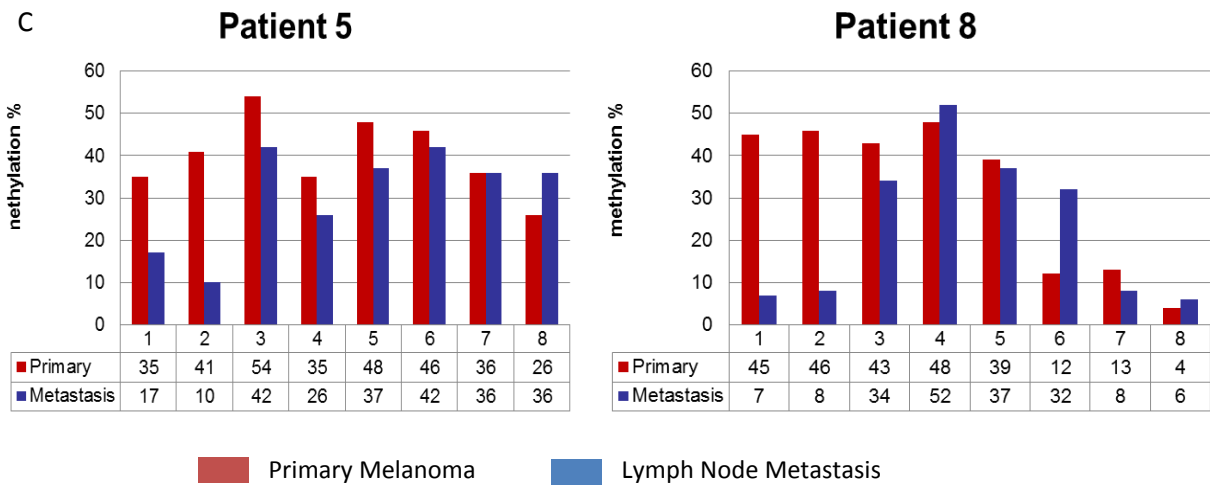


Figure 4-9: DUSP2 methylation in paired melanoma tissues.

(A): Methylation level of *DUSP2* in paired melanoma tissues. *DUSP2* methylation level at each CpG site and mean methylation value are indicated numerically and listed in a table. (B): Paired t test comparing the difference of methylation level of each CpG site of paired primaries and metastasis ($p < 0.05$). (C): Two representative cases of patients from whom we have collected both primary melanoma and lymph node metastasis showing overall decreased *DUSP2* methylation at most CpG sites.

4.2.3 *Dab2* methylation in melanoma

4.2.3.1 *Dab2* CpG island methylation is undetectable in melanoma cell lines

Using qPCR, I analysed *Dab2* mRNA expression in a panel of 17 melanoma cell lines, one normal human keratinocyte (NHK) line and two lightly pigmented human melanocyte lines, HEMA and HEMN. Cell lines under investigation showed variable levels of *Dab2* expression, suggesting that *Dab2* may be transcriptionally regulated by genetic or epigenetic mechanisms. Dysregulation of *Dab2* by aberrant DNA methylation has previously been reported in squamous carcinoma (Hannigan et al. 2011), so I asked if CpG island methylation of *Dab2* occurs in melanoma, and if methylation of *Dab2* transcriptionally regulates gene expression in our cell line panel. Unexpectedly, I did not detect *Dab2* methylation in any lines. There are a total of 53 CpG sites in the CpG island of *Dab2*. It is possible, therefore, that *Dab2* is methylated in an area of the CpG island other than the 8 CpG dinucleotides I have examined. If *Dab2* is methylated in the area outside the analysed one, methylation reversal assay may induce the gene expression in cell lines with *Dab2* methylation. However, demethylation analysis performed on three cell lines with low (MEL224), high (HEMN) and intermediate (SKMEL2) *Dab2* expression, did not show any inducible effect on *Dab2* gene expression. Therefore, I conclude that *Dab2* CpG island is not methylated in our melanoma cell lines.

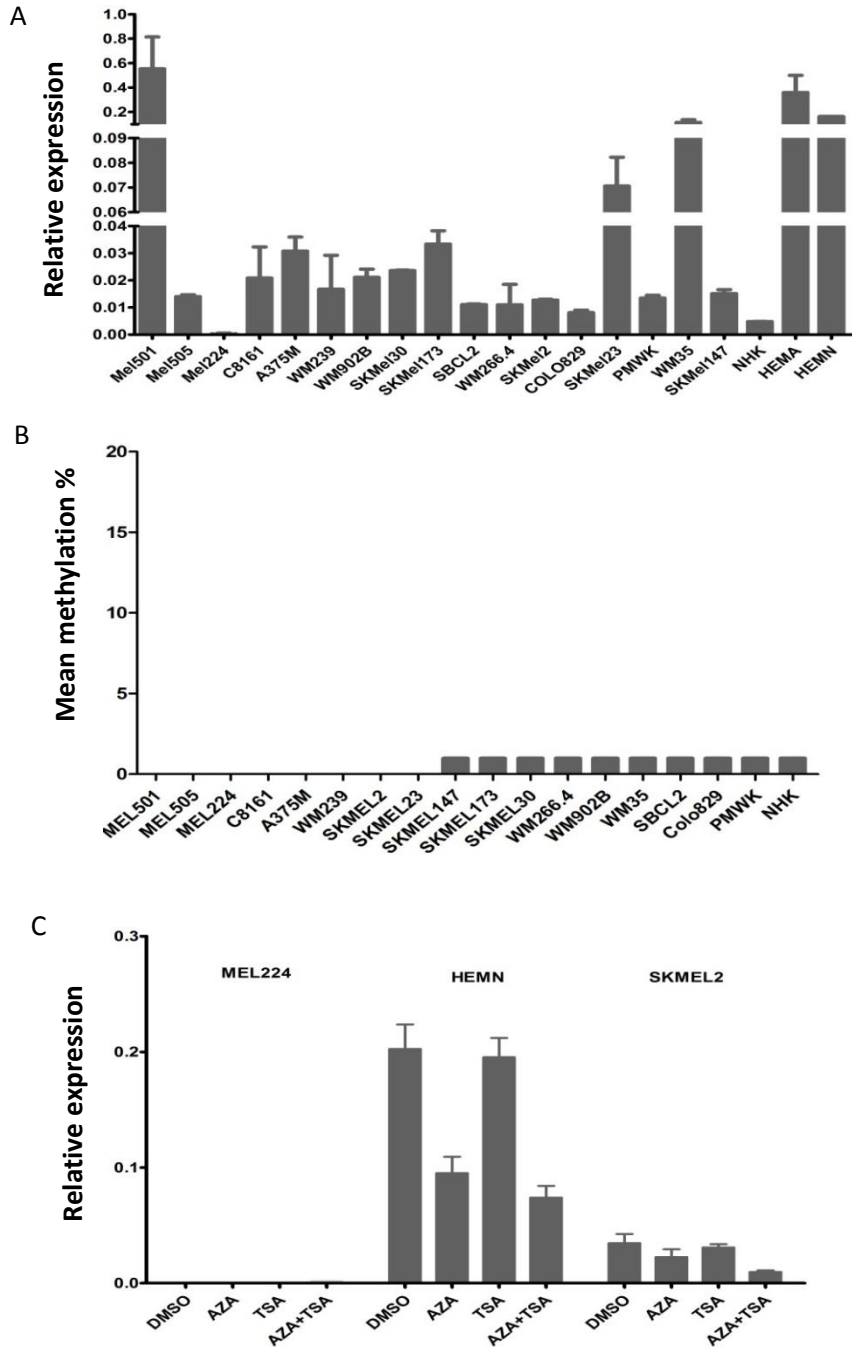


Figure 4-10: *Dab2* was not methylated in melanoma cell lines.

(A): Relative expression of *Dab2* in 17 melanoma cell lines, one keratinocyte and two melanocytes. (B): *Dab2* methylation % detection by pyrosequencing. (C): *Dab2* expression in cell lines MEL224, HEMN and SKMEL2 with demethylating treatment.

4.2.3.2 *Dab2* is frequently methylated in melanoma tissues

Despite the absence of detectable *Dab2* methylation in melanoma cell lines, I consequently identified a remarkably high level and frequency of *Dab2* methylation in a collection of 112 melanoma clinical samples including 52 primary melanomas and 60 secondary metastases by pyrosequencing. As shown in figure 4-11 A, most primary melanomas and nearly all metastases showed a greater than 10% mean methylation level of *Dab2*. A low level of *Dab2* methylation was also observed in 8 benign naevi which were used as negative controls. The *Dab2* methylation level significantly increased in primary melanomas compared with benign naevi, and was even higher in metastasis, suggesting that the methylation level of *Dab2* is elevated corresponding to the malignant transformation progress from benign naevi to primary melanoma, and ultimately to metastasis. Increased *Dab2* methylation may also be required for the adaption to the changes in microenvironments.

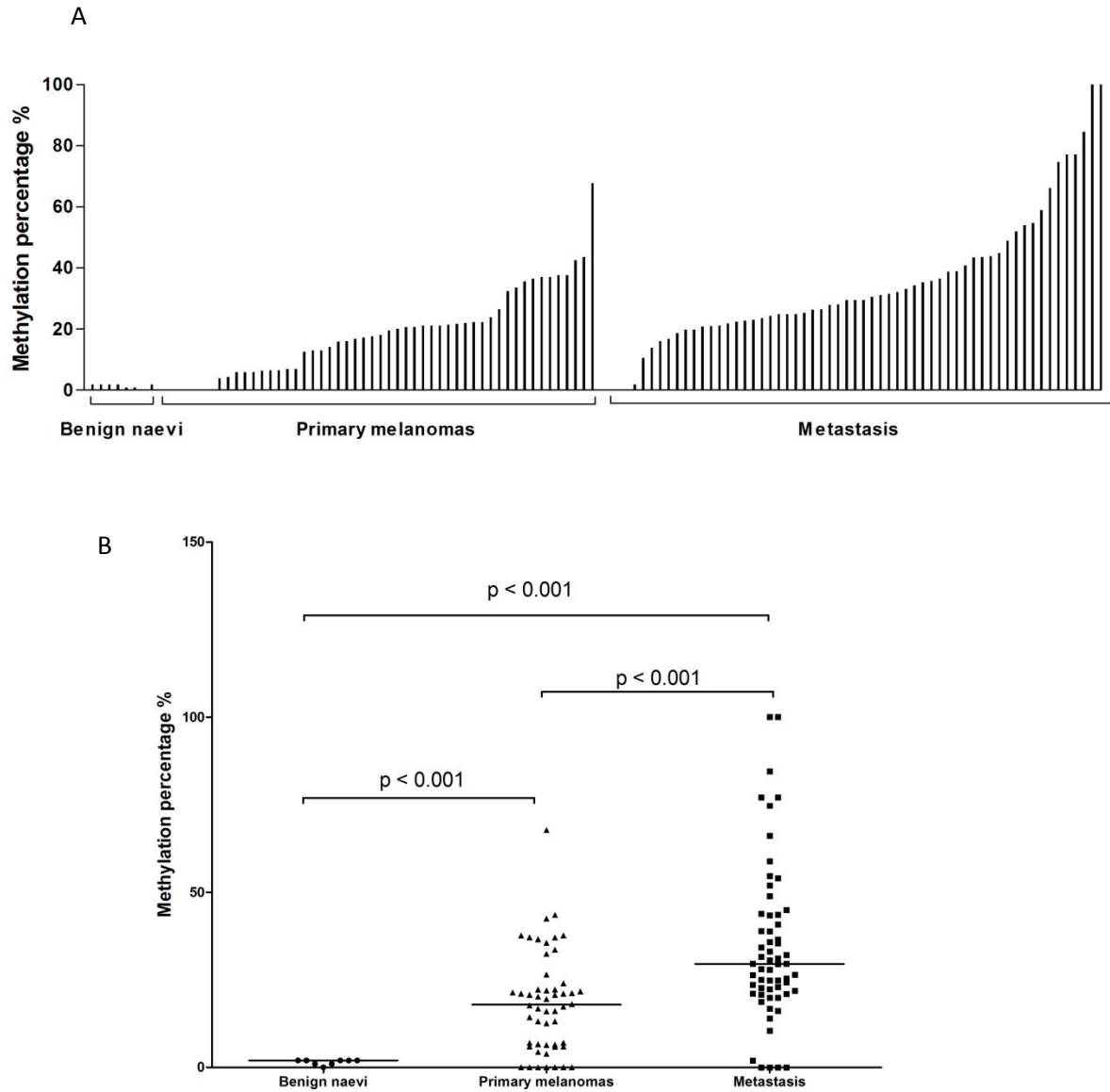


Figure 4-11: *Dab2* methylation in melanoma tissues and benign naevi.

(A): Mean methylation % of 8 benign naevi, 52 primary melanomas and 60 metastases. (B): Mann-Whitney *U* test showing methylation level of *Dab2* correlated with melanoma progression (p<0.001 for each pair-wise comparison).

4.3 Discussion

In this section I have analysed the methylation status of candidate genes that are known to be methylated in other human cancers and genes that may relate to tumour progression or tumour suppression. This is another candidate approach, in addition to the systematic approach employed in other sections of the project. Using this approach, I have assessed the methylation status of three candidates *NT5E*, *DUSP2* and *Dab2* in melanoma cell lines and clinical tissues.

Increased *NT5E* expression has been reported in highly aggressive phenotype melanoma cell lines (Sadej et al. 2006). Dr Tim Crook has observed a similar pattern of *NT5E* expression in paired metastatic melanoma cell lines such as C81-61 and C8161 which have less aggressive and highly aggressive phenotypes, respectively. *NT5E* expression was up-regulated in the highly invasive cell line C8161 but absent in its less aggressive partner C81-61, suggesting that over-expression or restoration of *NT5E* enhanced the metastatic potential of C8161. The transcriptional silencing of *NT5E* seen in less aggressive C81-61 can be attributed to promoter methylation, shown by MSP and bisulfite sequencing, and also proved by methylation reversal with 5'AZA. The dynamic alteration of *NT5E* expression from normal detectable level of expression in human melanocytes, to absent expression due to DNA methylation in the less aggressive phenotype C81-61, and ultimately to restored expression after demethylation in C8161 with greater metastatic potential suggests that epigenetic

change in *NT5E* potentially contributes to malignant progression. It also provides insight into the dynamic changes in the epigenome of the melanoma cell during evolution of individual disease. Based on these results provided by Dr Tim Crook, I have detected an intermediate frequency of *NT5E* methylation in an expanded panel of 15 melanoma cell lines (33%) and 50 melanoma clinical cases (42%) by pyrosequencing. Of the 50 clinical cases, *NT5E* was methylated at a similar frequency in 27 primary melanomas (44%) and 23 tumour metastases (39%). *NT5E* methylation in melanoma tissues appears to be a good prognosis biomarker. In 27 primary melanomas, *NT5E* methylation was only observed in primary melanomas that did not relapse with metastatic disease or relapsed with lymph node only metastasis, but was not present in cases which ultimately developed distant and/or visceral metastasis. Accordingly, cases of lymph node metastases where there was also visceral disease, were *NT5E* unmethylated. Based on these results, I conclude that *NT5E* methylation is probably important for early malignant transformation or development of lymph node metastasis and restored *NT5E* expression is required for the formation of a highly aggressive phenotype. Again, this is consistent with dynamic changes and ongoing adaptive evolution of the epigenome during the natural history of an individual melanoma.

Dynamic changes in promoter methylation of *E-cadherin* have been tracked in a breast cancer cell line (Graff et al. 2000). In this study, *E-cadherin* was hypermethylated in the cells grown in monolayer culture, but became hypomethylated when cells were grown in a three-dimensional model. Such

dynamic switching was regarded as important for cells to adapt to the different microenvironments. *NT5E* is a multifunctional protein engaged in both metabolic and molecular signalings, and tightly regulated by microenvironment, as introduced in 4.1.1. Identification of the selective pressure(s) driving the reversible *NT5E* methylation identified in this study would clearly be of interest. However, in contrast to irreversible genetic change, the reversibility of *NT5E* methylation could be exploited as a novel biomarker monitoring melanoma patients' response to chemotherapy. *NT5E* may also be a therapeutic target for a subset of melanoma patients, particularly in those with visceral metastasis.

DUSP2 methylation was initially assessed in 15 melanoma cell lines including 10 lines showing an average methylation level over 10%. Transcriptional silencing of *DUSP2* by promoter methylation was then confirmed by qPCR. In fact, of all the candidate genes I have studied, *DUSP2* showed the strongest correlation between DNA methylation and statistically significantly reduced gene expression. Interestingly, in the three sets of paired melanoma cell lines, a significant increase in *DUSP2* expression was seen in the lymph node metastasis compared to the parental primary melanoma cell lines, suggesting that a transcriptional increase in *DUSP2* expression may contribute to the formation of lymph node metastasis. However, this significant change in *DUSP2* expression was not reflected by a corresponding change in DNA methylation. A technical fault in our analysis has been ruled out by repeat analysis. This result suggests that promoter methylation of *DUSP2* in primary melanoma cell lines may be the

predominant mechanism regulating gene expression, whereas *DUSP2* mRNA expression is regulated by both DNA methylation and other mechanisms in metastatic disease. It is difficult to measure mRNA expression from paraffin embedded tissues due to the lack of reliable techniques for obtaining good quality RNA. Therefore, I could only assess the methylation level of *DUSP2* in melanoma tissues and not the expression level. An overall significant increase in *DUSP2* methylation was observed in primary melanomas compared to both benign naevi and metastases. In 8 primary melanoma tissues paired with 8 lymph node metastases, *DUSP2* was also methylated at a significantly higher level in the primary melanomas. These results suggest that *DUSP2* methylation may be an indicator of good prognosis in melanoma.

It is interesting to see similar changes in *NT5E* and *DUSP2* methylation in primary melanomas and metastasis, implying that the two genes may function in similar or related pathways in the early stages of melanoma progression. Both *NT5E* and *DUSP2* have been implicated in modulating the immune system (Jeffrey et al. 2006; Stagg et al. 2011). Here I hypothesize a potential underlying mechanism: *NT5E* and *DUSP2* could initially act as tumour suppressors during the early stage of melanomagenesis, where their transcriptional silencing is required for tumour cells to escape from host immunity. After the tumour cells have adapted to the host immune system, re-expression occurs by demethylation and their oncogenic function(s) contribute to the formation of a highly invasive phenotype and adaption to new tumour microenvironments.

Unlike *NT5E* and *DUSP2*, *Dab2* showed a classic methylation pattern in a collection of benign naevi, primary melanomas and metastases. The average level of *Dab2* methylation constantly increased according to tumour progression, from lowest in benign controls, to dramatically higher levels in primary melanomas and even higher levels in metastasis, revealing a potential role of *Dab2* methylation in predicting tumour progression. Despite being at a high level and high frequency in melanoma tissues, *Dab2* methylation was undetectable in any melanoma cell lines. The reason we see this paradoxical result in melanoma tissue and cell lines is unclear, but has been seen in other genes for examples 14-3-3 σ in breast cancer (Ferguson et al., PNAS, 2000). Therefore, *Dab2* may be a reflector, but not a functional regulator of tumour progression.

In conclusion, I have identified *NT5E* and *DUSP2* as potential epigenetic biomarkers predictive of good prognosis in melanoma, and *Dab2* in which methylation potentially correlated with tumour progression. Validation of these candidates as clinically useful biomarkers is now required in large, prospective studies.

Chapter 5 CpG island
methylation dependent
transcriptional silencing of prolyl
hydroxylases in melanoma

5.1 Introduction

The prolyl hydroxylases belong to a family of iron- and 2-oxoglutamate-dependent dioxygenase enzymes (Myllyharju 2003). At least two distinct groups of prolyl hydroxylases have been characterised: collagen prolyl hydroxylases and hypoxia-inducible factor (HIF) prolyl hydroxylases. These hydroxylases catalyse the post-translational formation of hydroxyproline residues in essential proteins such as collagens and HIFs.

5.1.1 Collagen prolyl hydroxylases (C-PHs)

Collagen prolyl 4 hydroxylases (C-P4Hs) and collagen prolyl 3 hydroxylases (C-P3Hs) catalyse the formation of hydroxyproline in collagens by binding to a proline residue in the Y position of the (X-Y-Gly) and X position of (X-Hyp-Gly) amino acid sequence, respectively (Hutton et al. 1967; Vranka et al. 2004). This biological process is critical for the biosynthesis, folding, assembly, and stabilization of collagens (Helaakoski et al. 1990; Myllyharju 2003; Shoulders and Raines 2009). Both C-P3H and C-P4H can hydroxylate a broad spectrum of collagens including collagen I, the most abundant collagen in the human body (Di Lullo et al. 2002), and collagen IV, the major constituent of the basement membrane. Human C-P4Hs are $\alpha_2\beta_2$ tetramers containing 3 variants of the catalytic α subunit, encoded by *P4HA1*, *P4HA2* and *P4HA3* and a constant β subunit encoded by *P4HB*. Isoform 1 (*P4HA1*) and isoform 2 (*P4HA2*) are expressed more abundantly in human tissues than isoform 3 (*P4HA3*) (Kukkola et al. 2003). The human genome encodes other C-P3Hs.

These are leucine proline-enriched proteoglycan 1 (leprecan, *LEPRE1*), leprecan-like 1 (*LEPREL1*), leprecan-like 2 (*LEPREL2*), cartilage-related protein (*CRTAP*) and leprecan-like 4 (*LEPREL4*) (Hatzimichael et al. 2012).

Collagen is a fundamental structural protein and constituent of basement membrane and extracellular matrix, both of which are critical components of the tumour microenvironment (TME) and thus involved in tumour invasion, metastasis and angiogenesis. Alterations of collagens in the TME by aberrant post-translational modification could impact upon tumour invasion and tumour aggressiveness (Egeblad et al. 2010). Collagen IV in the basement membranes has been well studied in human cancers. The basement membrane is a thin structural layer that provides support for epithelium, creating structural anchorage between epidermis and dermis in skin and surrounding the lumen of blood vessels (Timpl and Aumailley 1989; Paulsson 1992). In melanoma, the basement membrane at the dermo-epidermal junction (DEJ) functions as a barrier limiting the invasion of melanoma cells from epidermis to dermis. (Figure 5-1) Penetration of melanoma cells through the DEJ is the initial step in the metastatic cascade and aggressive melanoma cells are more able to break through this barrier than low grade melanomas (Meier et al. 2000).

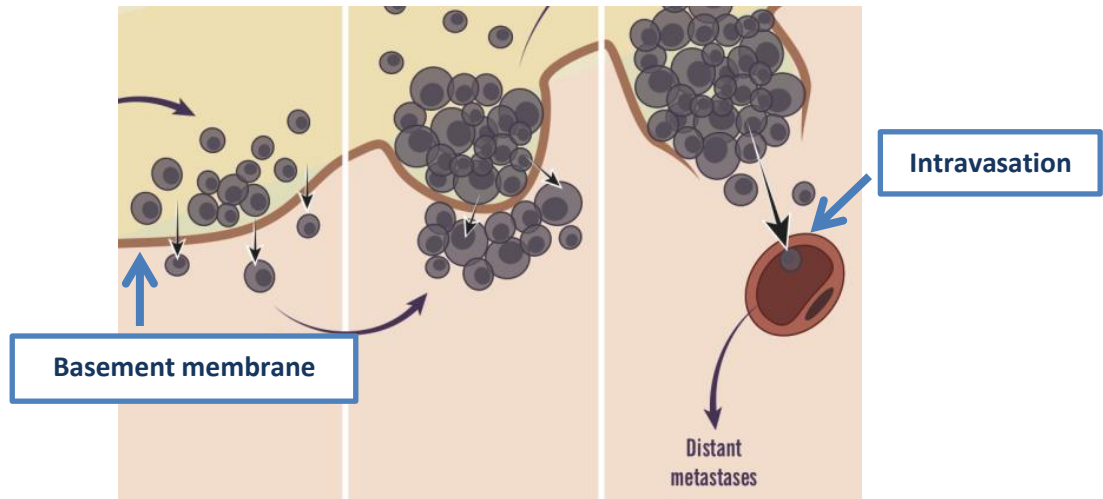


Figure 5-1: Invasion and intravasation of melanoma cells.

Accumulation of invasive melanoma cells forms a sphere which breaks through the skin basement membrane. Wandering melanoma cells in the dermis intravasate into the blood circulation through the blood vessel which contains basement membrane (Miller and Mihm 2006).

Subsequent tumour metastasis involves the formation of local and/or distant tumour growth. To establish distant metastases, melanoma cells must undertake 'intravasation', a phenomenon which entails transit of tumour cells through the blood vessel wall into the blood circulation and subsequent dissemination to distant organs to form metastases (Figure 5-1). Although unproven, it is likely that destabilization or alterations of the basement membranes consequent to dehydroxylation may allow more efficient penetration of melanoma cells. There is evidence indicating that absence of P4HA1 protein results in less assembled collagen IV and a defect in the basement membrane in mice (Holster et al. 2007). Such association between inactivated C-PHs and disrupted basement membrane is a plausible mechanism for promoting invasion and metastasis in human cancers. Collagen IV in the basement membrane contains a tumour suppressor-like domain, noncollagenous 1 (NC1), which has anti-proliferation, anti-invasion and anti-angiogenesis properties in

melanoma (Han et al. 1997; Maeshima et al. 2000; Pasco et al. 2005). Elastin is rich in proline residues and is another substrate for C-P4H. It provides elastic support for connective tissues, which are particularly important in tissues such as blood vessels and lung (Gorres and Raines 2010). Correlation between the absence of elastic tissues at invasive tumour edge and poor prognosis has been reported in melanoma, suggesting its potential as a prognostic biomarker of melanoma (Feinmesser et al. 2002). C-P3H members, *Leprel1* and *Leprel2* have previously been reported to be transcriptionally silenced by DNA methylation in breast cancer and *Leprel1* and *Leprel2* together with *P4HA2* and *P4HA3* in non-Hodgkin's lymphoma (Shah et al. 2009; Hatzimichael et al. 2012). Silenced C-P3Hs and C-P4Hs may destabilize collagen IV and elastin to disrupt their tumour suppressor functions. Identification of C-PH methylation in other cancers and their probable tumour suppressor function prompted analysis of their expression and methylation status in melanoma.

5.1.2 HIF prolyl hydroxylases (HIF-PHs)

HIF-PH is another important family of prolyl 4 hydroxylase enzymes comprising prolyl hydroxylase domain-containing protein 1 (PHD1, EGLN2), PHD2 (EGLN1) and PHD3 (EGLN 3). HIF1- α expression is induced by low oxygen, by production of reactive oxygen species (ROS) and by certain growth factors. When HIF1- α binds to HIF1- β (ARNT), the resulting HIF1- α transcription factor upregulates expression of many proteins that assist the cell, organ and organism to adapt to low oxygen (Greer et al. 2012). Whilst expression of ARNT is constitutive and levels are generally stable, those of HIF1- α can rapidly fluctuate (Huang et al. 1998). This tells us that HIF1- α is tightly regulated. The expression of HIF1- α in keratinocytes and melanocytes is a

reflection of the mildly hypoxic microenvironment in the skin (Evans et al. 2006; Rosenberger et al. 2007). Regulation of HIF1- α levels occurs by multiple post translational mechanisms (Dimova and Kietzmann 2010) and by differential regulation of specific isoforms of HIF1- α by oxygen (Weir et al. 2011). In an oxygen rich environment, EGLNs catalyse the addition of hydroxyl groups to HIF1- α in positions 402 and 564. As a result, HIF1- α is recognised by proteosomal enzymes as a target for degradation (Semenza 2001; Semenza 2004). Collagen P4Hs on the other hand do not hydroxylate HIF1- α (Jaakkola et al. 2001). However PHD/EGLN activity is tissue specific and the patterns of PHD/EGLN expression in melanocytes have not been studied to date.

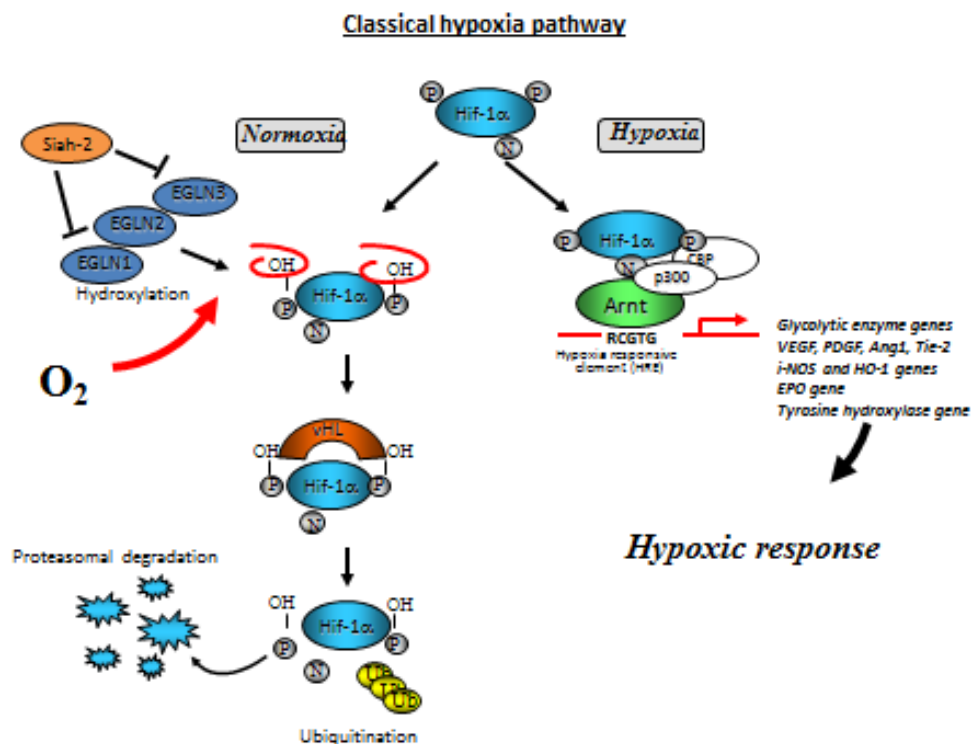


Figure 5-2: Scheme representing the classical hypoxia pathway.

In the normoxic condition, HIF1- α is tightly regulated by an EGLN-dependent proteasomal degradation pathway. Siah-2 negatively regulates EGLN1 and EGLN3. In the hypoxic condition, prolyl hydroxylase activity is limited and this leads to stabilisation of HIF1- α and subsequent activation of a number of downstream targets. This figure was generated by Dr Lynda Weir.

There is increasing interest in the role of HIF1 and hypoxia in the field of melanoma. In 2008, Zbytek et al. reported that HIF1- α expression was higher in melanoma samples compared to HIF1- α expression in benign naevi (Zbytek et al. 2008). Soon afterwards Valencak et al. detected HIF1- α by immunohistochemical staining of melanoma tissue sections in 87.6% of melanoma samples (Valencak et al. 2009). Also, in 2009, Mills et al. used melanoma cell lines to show that increasing expression of HIF1- α mRNA and protein correlated with increasing tumour severity and demonstrated that expression of HIF1- α was barely detectable in normal human melanocytes (Mills et al. 2009). Of note, HIF1- α was higher in a radial growth phase melanoma cell line, increased further in a vertical growth phase melanoma cell line and was highest of all in a metastatic melanoma cell line (Mills et al. 2009). More recently, Trevino-Villareal et al. have suggested that increased HIF1- α is not only a feature of melanoma cells but also is associated with co-localised tumour-associated stromal cells in a model where B16 melanoma cells were injected into mice (Trevino-Villarreal et al. 2011). These observations have been repeated and, by using tissue sections and HIF1- α immunostaining, the area of increased HIF1- α expression has been seen to extend into regions of keratinocytes where melanoma cells have infiltrated (Zbytek 2013).

Not only is melanoma associated with increased expression of HIF1- α protein, but hypoxia has also been shown to affect the tumourigenic behaviour of melanoma cells. Preconditioning melanoma cells with an 18hr treatment of 1% oxygen increased the invasiveness and tumourigenicity of these cells when injected into mice as judged by the number and size of lung metastases (Cheli et al. 2012). Furthermore, when B16 melanoma cells were injected into mice, those mice treated

with hypoxia for 6hrs out of every 24hrs (intermittent hypoxia treatment) developed significantly more lung metastasis than those kept throughout in a normoxic environment (Almendros et al. 2013). These experiments suggest that a hypoxic tumour environment may have detrimental effects upon tumour outcome for melanoma patients and that additional studies are warranted (Nakayama et al. 2009).

Another avenue worthy of study is the effect of methylation of *EGLN* genes on melanomas. Aberrant methylation of *ELGN* genes could result in gene silencing and reduction or cessation of *EGLN* activity. This would be predicted to impact upon HIF1- α activity and upon hypoxia signalling. Methylation of *ELNG3* has previously been reported in some human cancers (Shah et al. 2009; Hatzimichael et al. 2010; Huang et al. 2010), however this methylation is not universally applicable to all cancers (Place et al. 2011). Taken together, these observations prompted me to explore the role of *EGLN3* methylation in melanoma.

5.2 Results

5.2.1 Analysis of the biomarker utility for *C-P3H* and *C-P4H* CpG island methylation in melanoma

5.2.1.1 Identification of CpG island methylation of *C-P3H* and *C-P4H* in melanoma cell lines

Using pyrosequencing I initially investigated CpG island methylation in the *C-P3H* and *C-P4H* gene families in our melanoma cell line panel. *LEPRE1* was not included in this methylation screen, because unlike the other two *C-P3H* members, no

LEPRE1 methylation was detected in breast cancer or lymphoma (Shah et al. 2009). None of the *C-P3H* or *C-P4H* genes were found to be methylated in normal melanocytes. Similarly, no *P4HA1* methylation was detected in any melanoma cell line (Figure 5-3 A), but all other genes were methylated at varying frequencies. The most common methylated gene was *P4HA3*, with 8/13 cell lines, including cell lines derived from both primary and metastatic melanomas, being positive for methylation. In five of the primary melanoma cell lines, only *LEPREL2* and *P4HA3* were methylated, suggesting that *de novo* methylation of these two genes may occur in the early stages of melanoma.

Gene expression of *LEPREL1*, *LEPREL2*, *P4HA2* and *P4HA3* was evaluated in the same panel of cell lines by qPCR (Figure 5-3 B). Expression of *LEPREL1* and *LEPREL2* was variable, but there was a generally good correlation between CpG island methylation and down-regulated gene expression. For example, SKMEL23 and MEL501 were *LEPREL1* methylation positive and did not express *LEPREL1*, whereas *LEPREL2* expression was low or undetectable in SBCL2, PMWK and MEL501 all of which showed *LEPREL2* methylation. There was also a good inverse correlation between *P4HA3* methylation and gene expression: 7/8 cell lines with high levels of methylation had absent gene expression. Similarly, there was abundant gene expression and no *P4HA3* methylation in PMWK and COLO829. No correlation between *P4HA2* methylation and gene expression was evident.

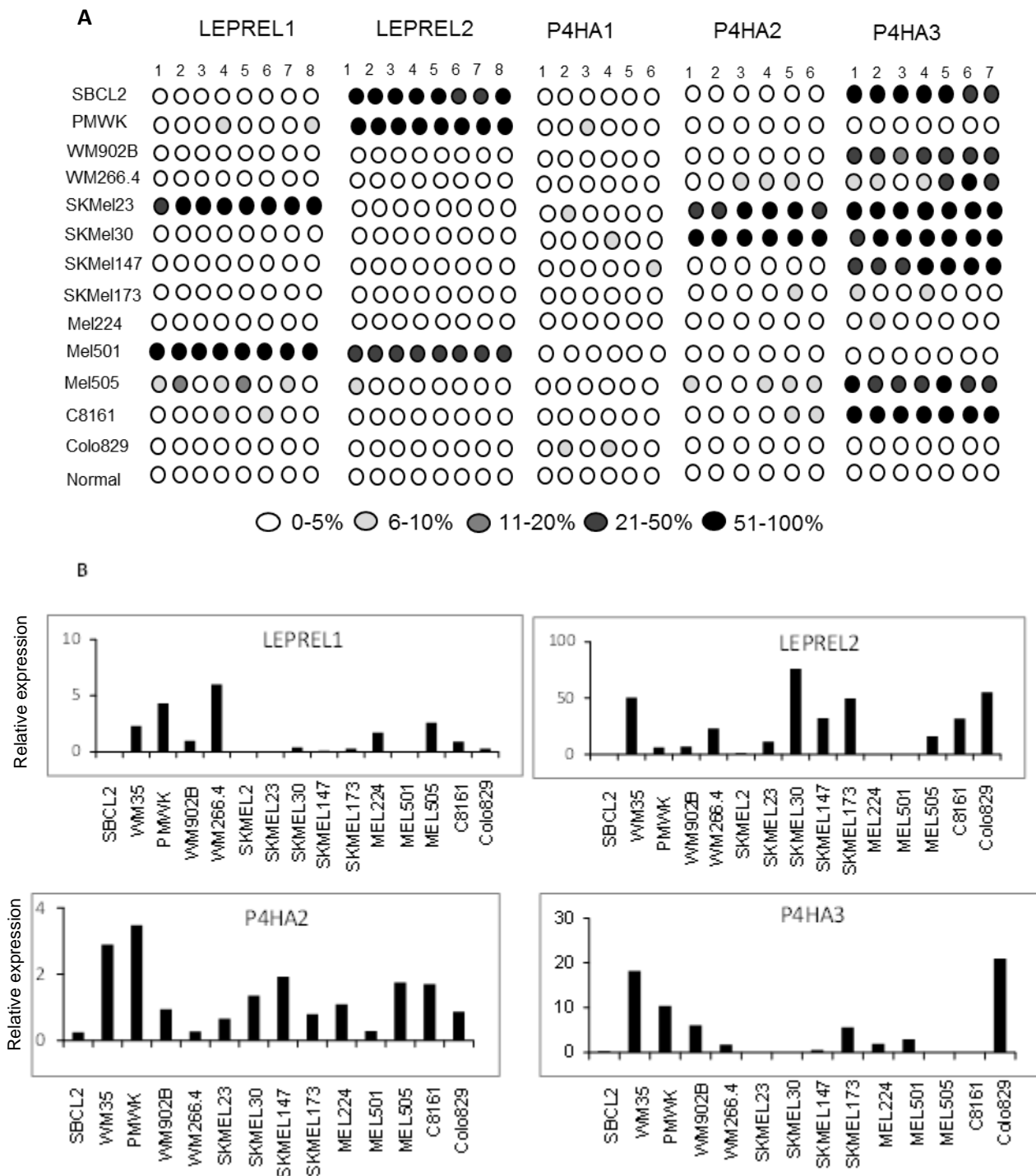


Figure 5-3: CpG island methylation and expression of *C-P3H* and *C-P4H* in melanoma cell line panel.

(A): Pyrosequencing profiles of *C-P3H* and *C-P4H* CpG island methylation in our melanocytes (normal), primary and metastatic melanoma cell lines. Methylation is quantified by the intensity of shading in the circles, each of which represents an individual CpG dinucleotide. 5 levels of shading are used as indicated in the figure. (B): qPCR analysis of *LEPREL1*, *LEPREL2*, *P4HA2* and *P4HA3* mRNA expression in melanoma cell lines.

5.2.1.2 Methylation status of *C-P3H* and *C-P4H* in paired melanoma cell lines

C-P3H and C-P4H processing of collagen IV in the basement membrane implies a potential for their involvement in tumour invasion and metastasis and this prompted me to explore correlations between *C-PH* methylation and metastatic melanoma. Again using pyrosequencing, the methylation status of *C-P3H* and *C-P4H* families was analysed in 3 sets of paired parental primary melanoma and their derivative daughter metastasis cell lines (Figure 5-4 and Table 5-1). Consistent with the high frequency of methylation already observed in the initial cell line panel analysis, *P4HA3* was also frequently and heavily methylated in these 8 cell lines. In the first set of paired cell lines (WM115/WM266.4/WM239A), *P4HA3* was moderately methylated in the primary cell line WM115 (% mean methylation 16%), and its methylation level increased in both skin metastasis WM266.4 (% mean methylation 33%) and lymph node metastasis WM239A (% mean methylation 28%). In the second set (LM2/ LM9/ LM29), there was again increased *P4HA3* methylation in the lymph node metastasis LM9 (% mean methylation 19%), compared to lower level of methylation in the primary line LM2 (% mean methylation 10%). However, in the third set (WM983A/WM983B), a lower level of *P4HA3* methylation (% mean methylation 2%) was demonstrated in the lymph node metastasis WM983B, compared to its parental line WM983A (% mean methylation *P4HA3* 19%). In these same cell lines *P4HA1*, *P4HA2* and *LEPREL2* were barely methylated, with only a small increase of *P4HA1* and *P4HA2* methylation in the skin metastasis LM29. *LEPREL1* was heavily methylated in the LM set, with increased methylation in LM29. Like *P4HA3*, *LEPREL1* was also methylated at a lower level in the metastatic WM983B cell line, suggesting this set of paired cell lines are in some way distinct from the other two

sets. Taken together however, increased methylation in the *P4HA3* CpG island was observed in the metastases of 2 out of 3 paired melanoma cell lines implying an association between its methylation and progression to advanced disease.

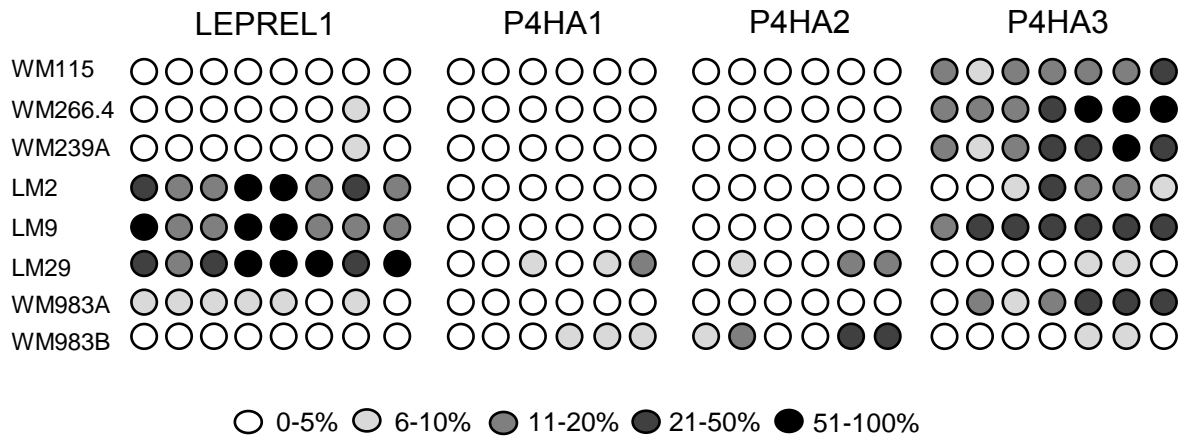


Figure 5-4: Pyrosequencing analysis of *LEPREL1*, *P4HA1*, *P4HA2* and *P4HA3* in 3 sets of paired primary melanoma and metastatic cell lines.

Methylation is quantified by the intensity of shading in the circles, each of which represents an individual CpG dinucleotide. 5 levels of shading are used as indicated in the figure. In all cases, methylation increases in the highly metastatic cell lines relative to the respective parental cell line.

Table 5-1: Mean % methylation level of *C-PHs* in paired melanoma cell lines

	LEPREL1	LEPREL2	P4HA1	P4HA2	P4HA3
WM115	2	1	1	2	16
WM266.4	3	3	3	2	33
WM239A	4	2	2	3	28
LM2	37	2	2	1	10
LM9	30	1	4	2	23
LM29	51	3	7	8	2
WM983A	6	1	1	3	19
WM983B	3	2	6	15	3

5.2.1.3 Methylation status of *C-P3H* and *C-P4H* CpG islands in melanoma tissues

5.2.1.3.1 *P4HA3* is frequently methylated in melanoma tissues

These studies reveal high level and frequent methylation in the *P4HA3* CpG island in melanoma cell lines. I next analysed, again using pyrosequencing, the methylation status of *P4HA3* in a series of clinical cases, these comprising 50 melanomas and 10 benign pigmented naevi controls, to evaluate the potential utility of *P4HA3* methylation as a melanoma biomarker (Figure 5-5). There was a significantly higher level of methylation in melanomas compared to the benign naevi controls (Mann-Whitney u test, $p < 0.01$). The mean methylation level of *P4HA3* in all 10 benign naevi was 5%, suggesting the application of 5% as an appropriate cut-off for *P4HA3* methylation. Using this cut off, *P4HA3* was hypermethylated in 37/50 (74%) of melanoma clinical samples. Only a limited number of cases in this melanoma series were primary melanomas, so it was not possible to examine any difference in *P4HA3* methylation between primary and metastatic melanomas in this cohort. We will need to expand our sample size and include a broad range of melanomas to further validate the potential of *P4HA3* for metastatic disease.

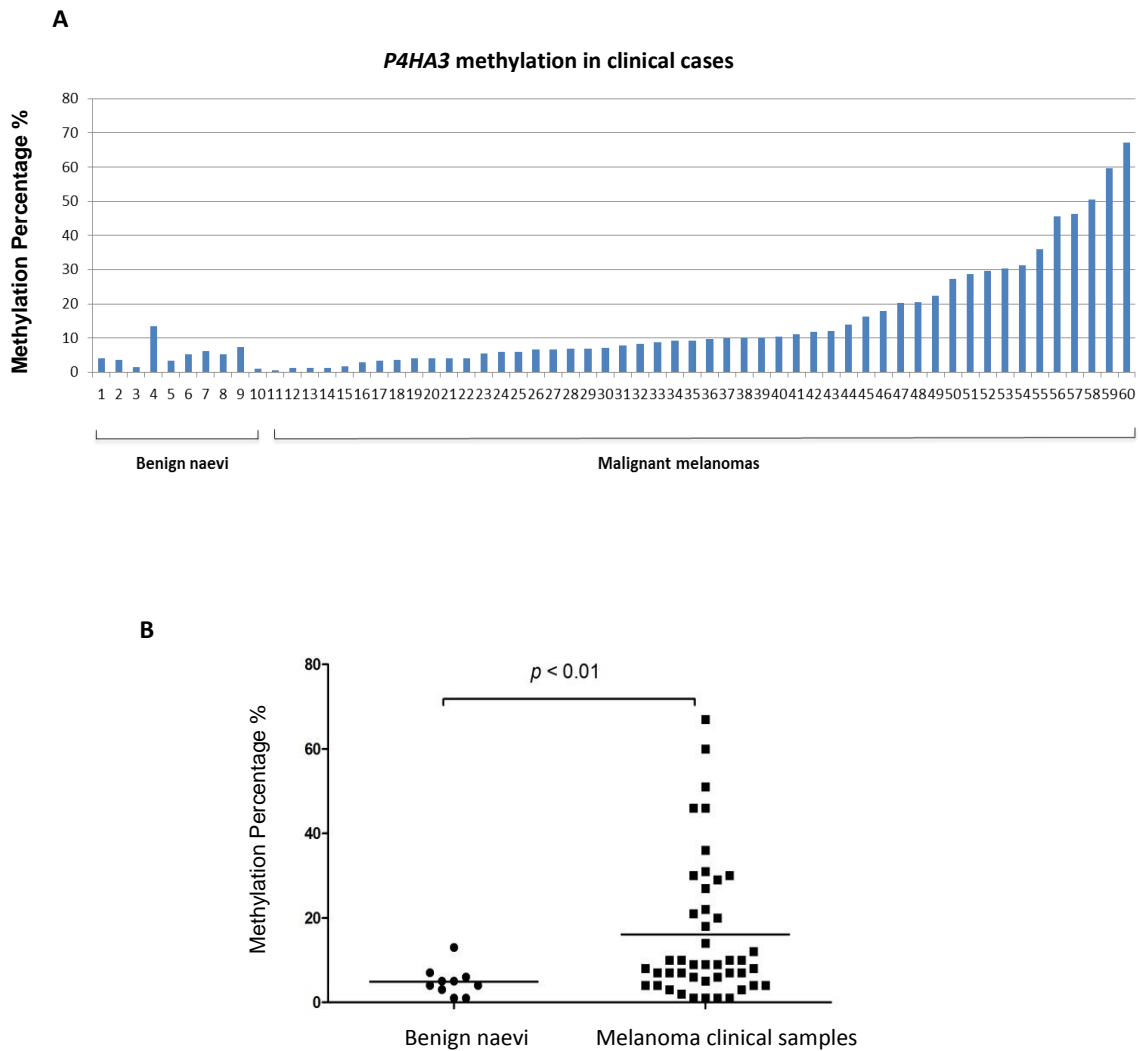
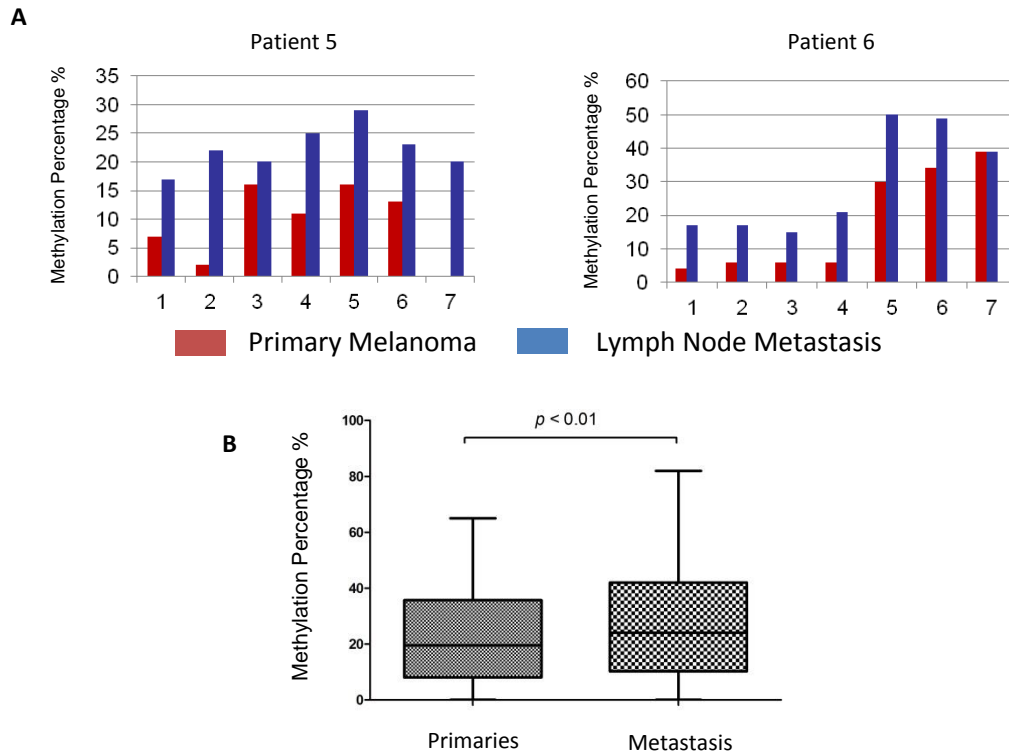


Figure 5-5: Methylation of *P4HA3* in melanoma clinical samples and benign naevi. (A): Methylation percentage of 10 cases of benign naevi and 50 cases of melanoma. (B): Mann-Whitney *U* test of methylation level between benign naevi and melanomas. ($p < 0.01$)

5.2.1.3.2 Methylation status of *P4HA3* CpG island in paired melanoma tissues

Previous analyses identified a correlation between *P4HA3* CpG island methylation and metastatic disease in paired melanoma cell lines as discussed in 5.2.1.2, consistent with a role for *P4HA3* CpG island methylation in progression of primary melanoma to metastatic disease. To further substantiate this hypothesis, I next examined the methylation status of the *P4HA3* CpG island in 8 paired melanoma tissues, each comprising a primary melanoma and nodal metastasis from the same patient. Each tissue section was subjected to micro-dissection prior to isolation of genomic DNA to maximise melanoma representation. In 5 pairs of cases there was an increased mean level of *P4HA3* CpG island methylation in the lymph node metastasis compared to the matched primary melanoma. Figure 5-6 A shows two representative cases with increased level of *P4HA3* methylation in the metastasis at the individual CpG sites within the examined sequence. I used a one-tailed paired t test (Figure 5-6 B) to compare the methylation level between all metastatic and primary melanomas at each CpG sites. This revealed a statistically significantly higher level of *P4HA3* methylation in the metastases, thus supporting a role for methylation in the *P4HA3* CpG island in melanoma progression. It will be noted, however, from the panel of results in Figure 5-6 B that two of the cases (numbers 2 and 7) showed reduced methylation level in the metastasis compared with the primary melanoma.



	P4H A3 methylation							Average
	CpG1	CpG2	CpG3	CpG4	CpG5	CpG6	CpG7	
P1	35	28	44	41	65	56	50	46
M1	33	30	58	58	60	64	51	51
P2	22	19	41	11	16	21	14	21
M2	8	0	9	21	25	7	1	10
P3	34	17	47	30	35	24	32	31
M3	18	14	35	38	32	43	33	30
P4	0	0	1	7	7	47	36	14
M4	9	15	19	36	42	40	40	29
P5	7	2	16	11	16	13	0	9
M5	17	22	20	25	29	23	20	22
P6	4	6	6	6	30	34	39	18
M6	17	17	15	21	50	49	39	30
P7	15	0	18	12	20	11	7	12
M7	7	3	5	5	8	5	5	5
P8	14	42	45	44	35	32	39	36
M8	7	49	44	51	82	49	42	46

Figure 5-6: *P4HA3* CpG island methylation in 8 pairs of clinical samples comprising primary melanomas and their matched lymph node metastasis derived from the same patient.

(A): Comparison of *P4HA3* CpG island methylation between primary melanoma and lymph node metastasis at the individual CpG sites in two representative cases. (B): Paired t test (one tailed) showed significantly higher average methylation level of *P4HA3* in lymph node metastasis compared to primary melanomas ($p < 0.01$).

5.2.1.3.3 Methylation status of *LEPREL1* CpG island in melanoma tissue and serum samples

My results showed a moderate methylation frequency of *LEPREL1* in melanoma cell line panels, so I next assessed the methylation status of the CpG island in the same series of melanoma tissues and control benign naevi previously tested for *P4HA3*. In the 10 benign naevi, *LEPREL1* methylation was invariably low. Significantly increased *LEPREL1* CpG island methylation was demonstrated in the majority of the melanoma cases ($p < 0.001$). However, compared to the high methylation level of *P4HA3* in the same cases, *LEPREL1* was methylated at a much lower level (up to 10%) in most melanoma samples. When analysing *C-P3H* methylation in the paired cell lines, I observed increased *LEPREL1* methylation in the metastasis of one set (LM2/29). I therefore attempted to determine whether *LEPREL1* methylation increased in the metastasis of the paired tissues compared to their matched primary melanomas. However, inconsistent changes in *LEPREL1* methylation were identified in the 8 pairs of matched melanoma tissue samples. Four of eight pairs (patients 1, 2, 6 and 7) showed similar (low levels) of *LEPREL1* CpG island methylation, whereas patients 4 and 5 exhibited increased *LEPREL1* methylation in the metastasis, and patients 3 and 8 showed the inverse. Therefore, no robust correlation between *LEPREL1* and metastatic disease was present in these 8 pairs, implying that *LEPREL1* is unlikely to be a useful biomarker of melanoma progression. This hypothesis was further strengthened by analysis of sera in which a generally low level of *LEPREL1* methylation was detected (Figure 5-7 B).

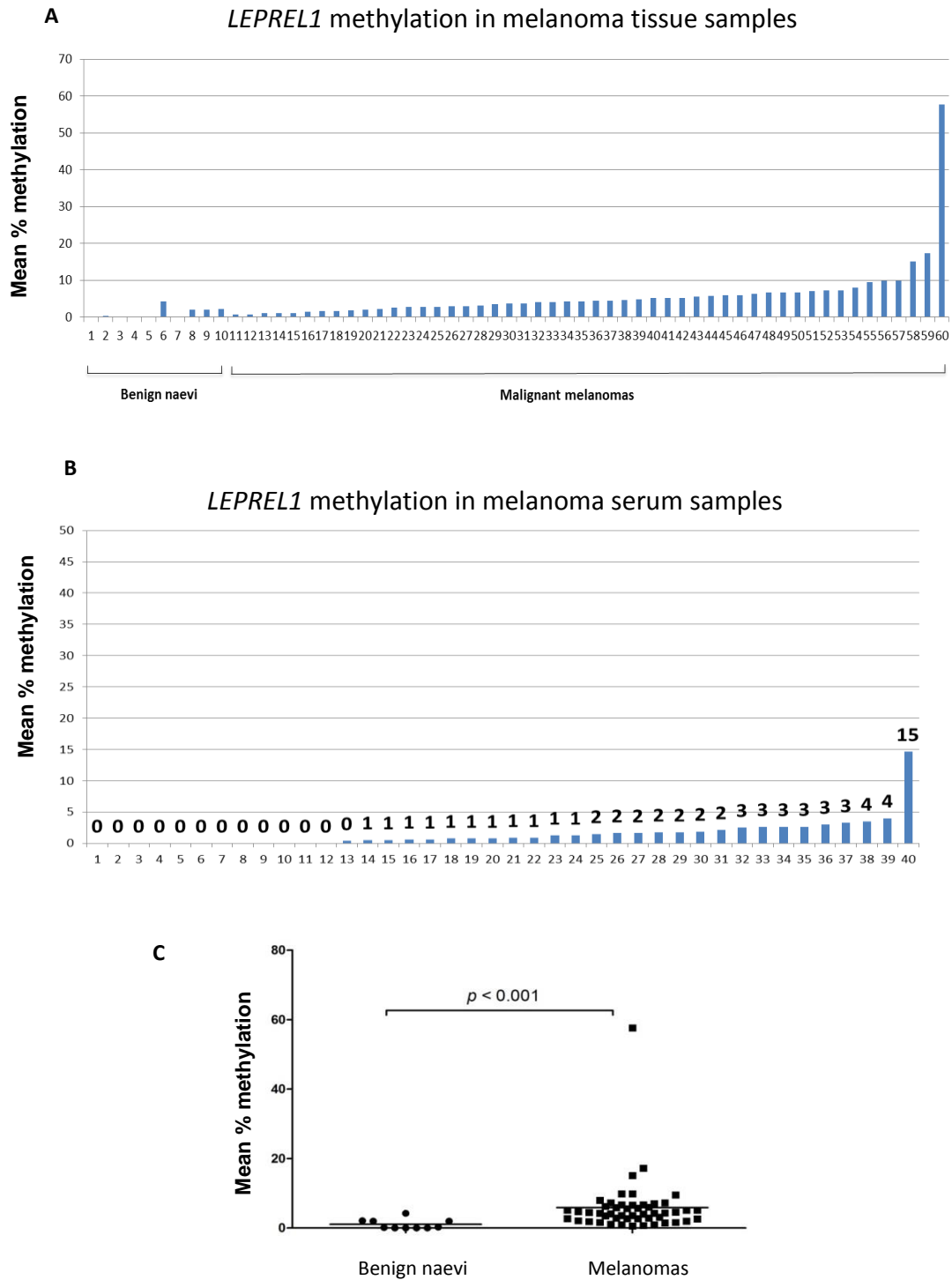


Figure 5-7: Quantitative *LEPREL1* CpG island methylation profiles in melanoma clinical samples (tissue and serum) and benign naevi.

(A): Methylation level of *LEPREL1* in 10 cases of benign naevi and 50 cases of melanoma (B): Methylation level of *LEPREL1* in 40 melanoma serum samples. (C): Mann-Whitney *U* test of methylation level between benign naevi and melanomas. ($p < 0.001$)

Table 5-2: *LEPREL1* methylation level in paired melanomas

	CpG1	CpG2	CpG3	CpG4	CpG5	CpG6	CpG7	CpG8	Average
P1	2	4	3	11	8	0	8	0	5
M1	6	7	10	12	9	3	11	0	7
P2	0	0	3	3	7	0	2	0	2
M2	0	0	0	4	0	0	1	0	1
P3	4	0	2	32	28	21	27	24	17
M3	4	5	6	19	13	5	16	8	10
P4	0	0	0	4	4	0	4	0	2
M4	6	11	9	11	12	0	9	0	7
P5	0	0	5	10	3	0	5	0	3
M5	29	22	1	11	23	0	9	26	15
P6	0	0	1	2	0	0	3	0	1
M6	0	0	0	5	5	0	3	0	2
P7	7	8	9	11	9	0	9	3	7
M7	7	7	9	9	9	0	9	0	6
P8	53	72	60	71	62	14	60	69	58
M8	10	13	5	10	11	8	10	12	10

The table shows % methylation at each CG dinucleotide in the amplified fragment of *LEPREL1* in eight matched pairs of clinical cases of primary (P): metastatic melanoma (M).

5.2.1.4 *P4HA3* is a serum biomarker for metastatic melanoma

Based on these results in paired melanoma cell lines and tissue samples, my data suggested that *P4HA3* might be potentially predictive of melanoma metastasis. Examination of the biomarker potential of methylated *P4HA3* was subsequently undertaken in a collection of serum samples from 44 patients with lymph node or visceral metastases and from 23 patients who were clinically metastasis-free at the time of blood harvesting. ROC analysis using GraphPad Prism software showed a sensitivity of 56% and a specificity of 71% for *P4HA3* methylation in detecting metastatic disease using a methylation cut-off of 5% (Figure 5-8 B). This cut-off level generated by GraphPad Prism was consistent with the level we have used to determine *P4HA3* methylation frequency in melanoma tissue samples. The area under the curve (AUC) indicated a diagnostic accuracy of 71% (95% CI, 0.59-0.83, $p < 0.01$). Risk analysis performed by Dr Mathieu Boniol (International Prevention Research Institute, Lyon, France) also showed a statistically significant association

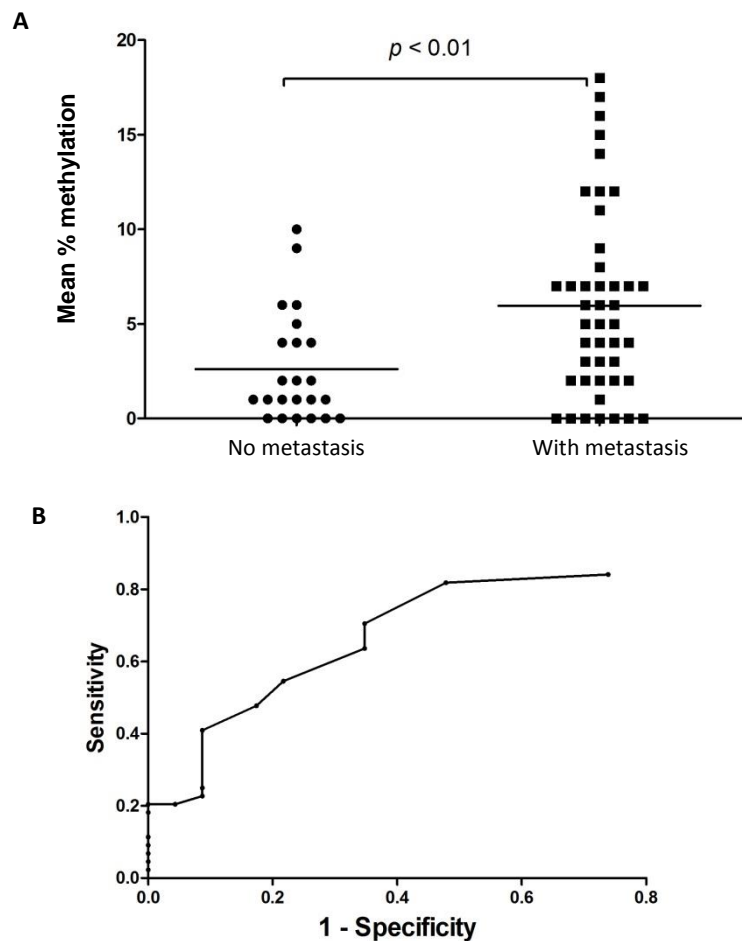
between *P4HA3* methylation and metastatic disease when using 5% as the methylation cut-off (adjusted odds ratio (OR) 6.2, 95% CI 1.7-21.8, Table 5-3).

Table 5-3: Risk analysis of association between *P4HA3* methylation and melanoma metastasis

P4HA3	Control (No metastasis)	Case (with metastasis)	OR adjusted (95% CI)
Less than 5%	19	21	1.00 Ref
5% or more	4	23	6.2 (1.7-21.8)
Adjusted on Breslow thickness			

OR: odds ratio indicating the association between *P4HA3* methylation and melanoma metastasis. CI: confidence interval.

Mann-Whitney analysis showed the level (mean %) of *P4HA3* methylation in patients with metastasis was significantly higher than in patients without metastatic disease ($p < 0.01$) (Figure 5-8 A), suggesting a correlation between *P4HA3* methylation and increased risk of metastasis. Dr Mathieu Boniol also confirmed such a correlation with his statistical analysis (OR=1.18, 95%CI 1.00-1.38). These data have demonstrated that methylated *P4HA3* genomic DNA may have utility as a serum biomarker in the detection of metastatic melanoma. In the 23 serum samples from patients free of metastatic disease, *P4HA3* was methylated in 22% (5/23). Of the 5 non-metastatic cases with methylation, only 1 was from 15 low risk melanoma patients (Breslow thickness < 2 mm). The other 4 non-metastatic cases with methylated *P4HA3* were from high risk melanoma patients (Breslow thickness > 3mm). This observation raises the interesting possibility that *P4HA3* methylation could be a serum prognostic biomarker predictive of poor patient outcome even in patients with, as yet, no clinical evidence of metastatic disease. To confirm and extend these findings, an independent prospective study involving a larger sample set needs to be similarly investigated.



	Metastasis	No metastasis
Test positive	29	5
Test negative	15	18
Statistics: Sensitivity and Specificity		
Sensitivity	56%	
Specificity	78%	
Area	0.71	
<i>p</i> - value	< 0.01	

Figure 5-8: *P4HA3* CpG island methylation in melanoma serum samples.

(A): Mann Whitney test of average methylation level of *P4HA3* in serum samples from melanoma patients with no metastasis and with metastasis. (B): Receiver Operator Characteristic curve showing predictive utility of detection of *P4HA3* CpG island methylated DNA in serum of patients with melanoma in the diagnosis of metastatic disease. The ROC curve was constructed as described in Materials and Methods

5.2.2 Identification of *EGLN3* methylation and mechanistic study of *EGLN3* in melanoma

5.2.2.1 *EGLN3* CpG island methylation in melanoma cell lines

Our paired cell line panel was used in this investigation. Using MSP, I detected partial *EGLN3* methylation in the melanoma cell line WM266.4 (Figure 5-9 A). In the same cell line, I have observed reduced *EGLN3* mRNA expression by qPCR (Figure 5-9 B), suggesting *EGLN3* methylation transcriptionally silences *EGLN3* gene expression at the RNA level. For the cell line panel as a whole there was a general correlation between *EGLN3* mRNA and protein expression (Figure 5-8 B and C). For example, cell lines LM9 and LM29 which had the highest *EGLN3* RNA expression also showed the highest level of protein expression. In the other cell lines, *EGLN3* protein expression was generally low, this correlating with low mRNA expression including cell line WM266.4 in which the *EGLN3* CpG island was partially methylated. Thus, low protein expression of *EGLN3* in this cell line may be the consequence of methylation-dependent transcriptional silencing of *EGLN3*.

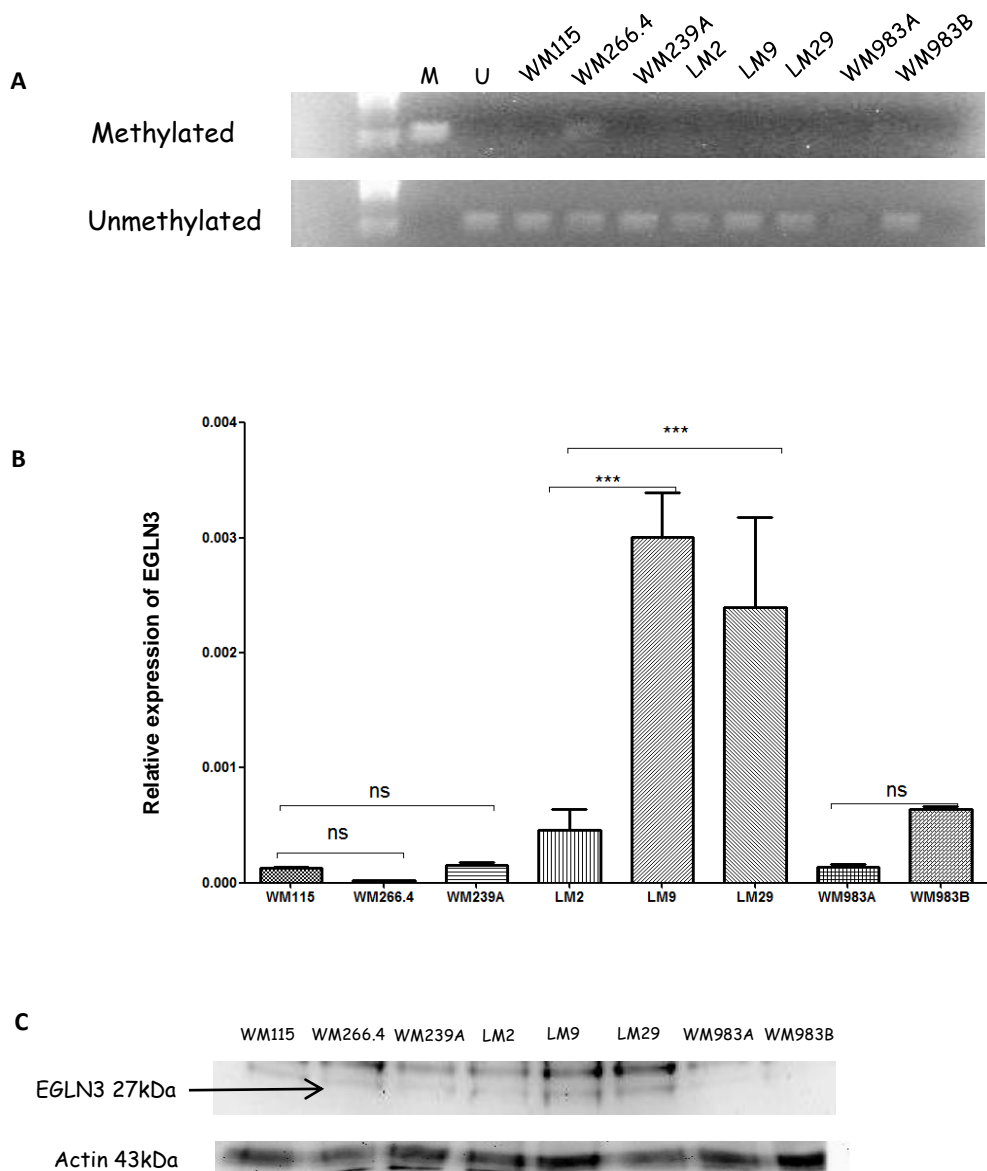


Figure 5-9: *EGLN3* methylation in melanoma cell lines.

(A): Identification of *EGLN3* methylation in 8 melanoma cell lines by MSP. (B): qPCR analysis of *EGLN3* mRNA expression in the same panel of cell lines. *** is $p < 0.001$; ns: no significance. (C): Western blots of *EGLN3* protein expression. *EGLN3* is the bottom band of the indicated double bands. Actin was used as the loading control. The *EGLN3* antibody gave 2 to 3 bands in the region of 27kDa, however later studies identified that the lower band was likely to be that of *EGLN3*.

5.2.2.2 EGLN3 protein does not inversely correlate with HIF1- α protein expression

EGLNs predominantly and negatively regulate HIF1- α activity in normoxia where oxygen is abundant. I performed western blots in 8 melanoma cell lines cultured in normoxia to test the correlation between EGLN3 and HIF1- α protein under these conditions (Figure 5-10). However, there was not a reciprocal expression pattern between EGLN3 and HIF1- α as had been expected. For examples, cell lines LM9 and LM29 which had the highest expression level for EGLN3 also showed the highest levels of HIF1- α . Moderate co-expression of EGLN3 and HIF1- α protein was also observed in the other lines. Although across these 8 lines I did not see any correlation between EGLN3 and HIF1- α level, this does not automatically imply that within a particular line alteration of EGLN3 protein level will not impact upon HIF1- α level.

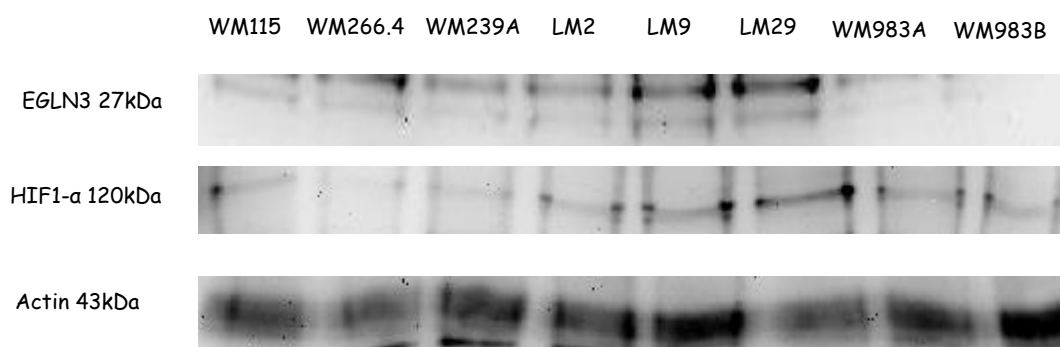


Figure 5-10: Western blots of EGLN3 and HIF1- α protein in 8 melanoma cell lines.

30 μ g protein from each cell line was loaded for detection of EGLN3 and HIF1- α proteins. HRP-labelled secondary antibodies were used before the result was visualised by VersaDoc system. Actin was used as the protein loading control.

5.2.2.3 Localization of EGLN3 and HIF1- α

Sub-cellular localisation by immunofluorescent staining of fixed cells was performed on the WM266.4 cell line cultured in normoxic conditions (21% oxygen) (Figure 5-11). Any HIF1- α located in the nucleus suggests that dimerization with ARNT has occurred and that HIF1 transcriptional machinery has been triggered in these cells. From the results presented here I show that some HIF1- α protein was located in the cytoplasm of WM266.4 cells (the cytoplasm is where HIF1- α is synthesised in cells), but most of the HIF1- α is concentrated in the nucleus. EGLN3 protein is predominantly cytoplasmic, surrounding the nucleus in a peri-nuclear location, suggesting that perhaps EGLN3 may control the amount of HIF1- α protein that enters the nucleus.

I showed that EGLN2 protein has a predominantly nuclear location in normoxia-cultured WM266.4 cells. This tells us that EGLN2 may perhaps be controlling the amount of HIF1- α in the nucleus that is available to bind to ARNT. EGLN1 staining is not as specific as that of the other EGLNs in WM266.4 cells. The reason for this is not clear but is unlikely to be due to poor antibody performance as this antibody has proven very specific when staining keratinocytes and other epithelial cell types cultured in this laboratory. In WM266.4 cells EGLN1 staining is located throughout the entire cell so I cannot surmise a specific subcellular location for the action of EGLN1 in these cells. My results highlight how EGLN expression is tissue and cell type specific.

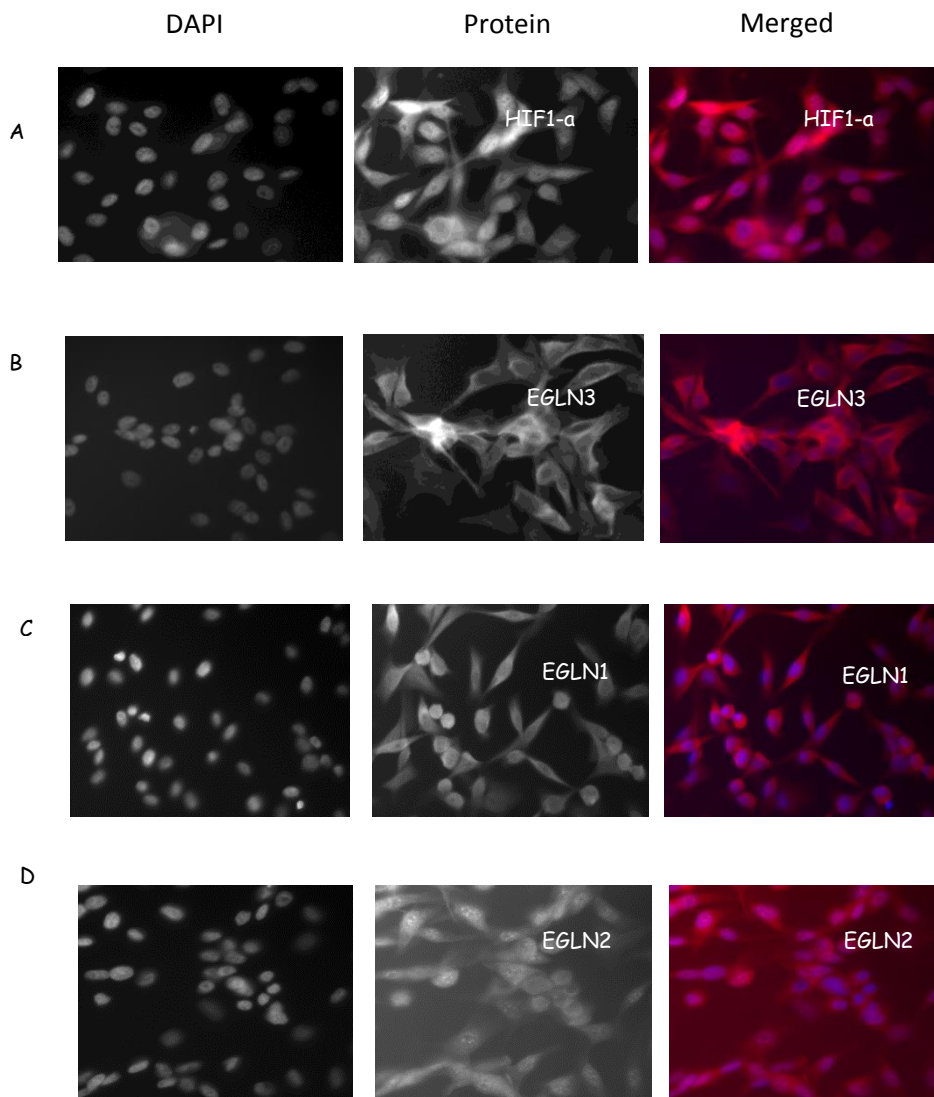


Figure 5-11: Subcellular localisation of HIF1- α , EGLN1, EGLN2 and EGLN3.

Immunofluorescence staining showing the subcellular localisation of HIF1- α (A), EGLN3 (B), EGLN1 (C), and EGLN2 (D) in melanoma cell line WM266.4. DAPI staining showed the localisation of the nuclei of the cell populations. Negative control, in which the cell line was incubated with Alexa Fluor 594 dye antibody diluent without the primary antibody, was used to rule out the non-specific staining.

5.2.2.4 Exploring the hypoxic pathway in WM266.4 cells

To determine the extent, if any, of the impact of partially methylated EGLN3 in the hypoxic response of WM266.4 cells, they were cultured in hypoxia and various parameters of the hypoxia pathway were assessed. According to the literature, EGLN1 and EGLN3 are hypoxia responsive at the mRNA level (Pescador et al. 2005). I observed a 2.7 fold increase in *EGLN1* mRNA expression after 18 hours treatment with 1% oxygen and a corresponding and impressive 25.5 fold increase in *EGLN3* mRNA expression by qPCR (Figure 5-12 A and C). *EGLN2* mRNA levels do not alter in most systems in hypoxia and the 0.4 fold decrease we see in *EGLN2* mRNA expression is consistent with these previous studies (Figure 5-12 B). *EGLN* mRNA patterns are not entirely reflected by changes at the protein level suggesting that post translational events are a feature of EGLN protein expression (Figure 5-12 E). At the protein level there was a sustained increase in EGLN1 and a transient increase, peaking after 8 hours of 1% oxygen treatment, for both EGLN2 and EGLN3 protein. An increase in EGLN protein expression in hypoxia may appear somewhat counter intuitive since oxygen is required for EGLN hydroxylation activity. However it has been suggested that EGLN protein levels and activity may increase in chronic hypoxic conditions as intracellular oxygen is released due to inhibition of mitochondria activity to decrease levels of HIF1- α to ensure cell survival (Ginouves et al. 2008).

I also measured levels of VEGF protein by ELISA. VEGF is a classical downstream target of HIF1- α transcription, and I showed a steady increase in VEGF protein

throughout the hypoxic period suggesting that the HIF pathway is intact and functioning appropriately in this cell type (Figure 5-12 D).

The overall increase in levels of *EGLN* mRNA and protein detected when WM266.4 cells are cultured in hypoxic conditions suggests that partial methylation of *EGLN3* in these cells does not block up-regulation in hypoxia. As such, partial methylation may affect a HIF1- α independent function of *EGLN3*, if it has any effect at all.

5.2.2.5 EGLN3 knock down by siRNA

We cannot rule out the possibility that *EGLN3* may be involved in a HIF1- α independent pathway in melanoma cell lines. To address this function of *EGLN3*, I used siRNA to knock down *EGLN3* expression in WM266.4 and LM2 lines (Figure 5-13). *EGLN3* was successfully silenced at both mRNA (100%) and protein levels at 72 hour and 96 hour time points in cell line WM266.4. In cell line LM2, despite a dramatic reduction in reduced *EGLN3* RNA (80%), *EGLN3* protein levels did not change at these time points, suggesting non transcriptional mechanisms may stabilise *EGLN3* protein levels in this cell line.

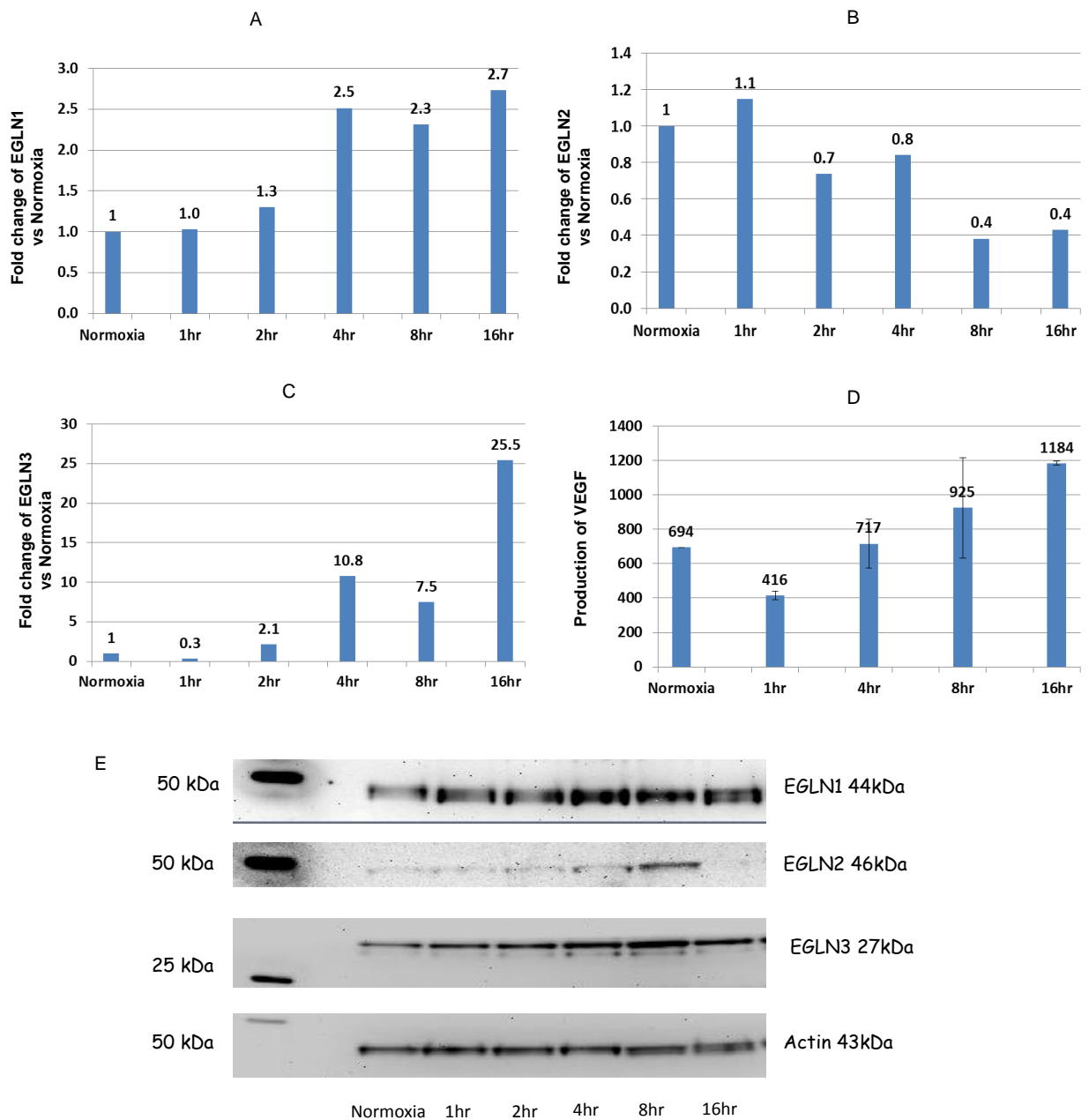


Figure 5-12: Measurement of hypoxic response of WM266.4 cells.

(A, B, C): mRNA expression of *EGLN1*, *EGLN2* and *EGLN3* in WM266.4 cell line under hypoxic time course. (D): Production of VEGF in WM266.4 cell line in hypoxia time course. (E): Protein expression of EGLN1, EGLN2, and EGLN3 by western blots, actin was also loaded as internal control.

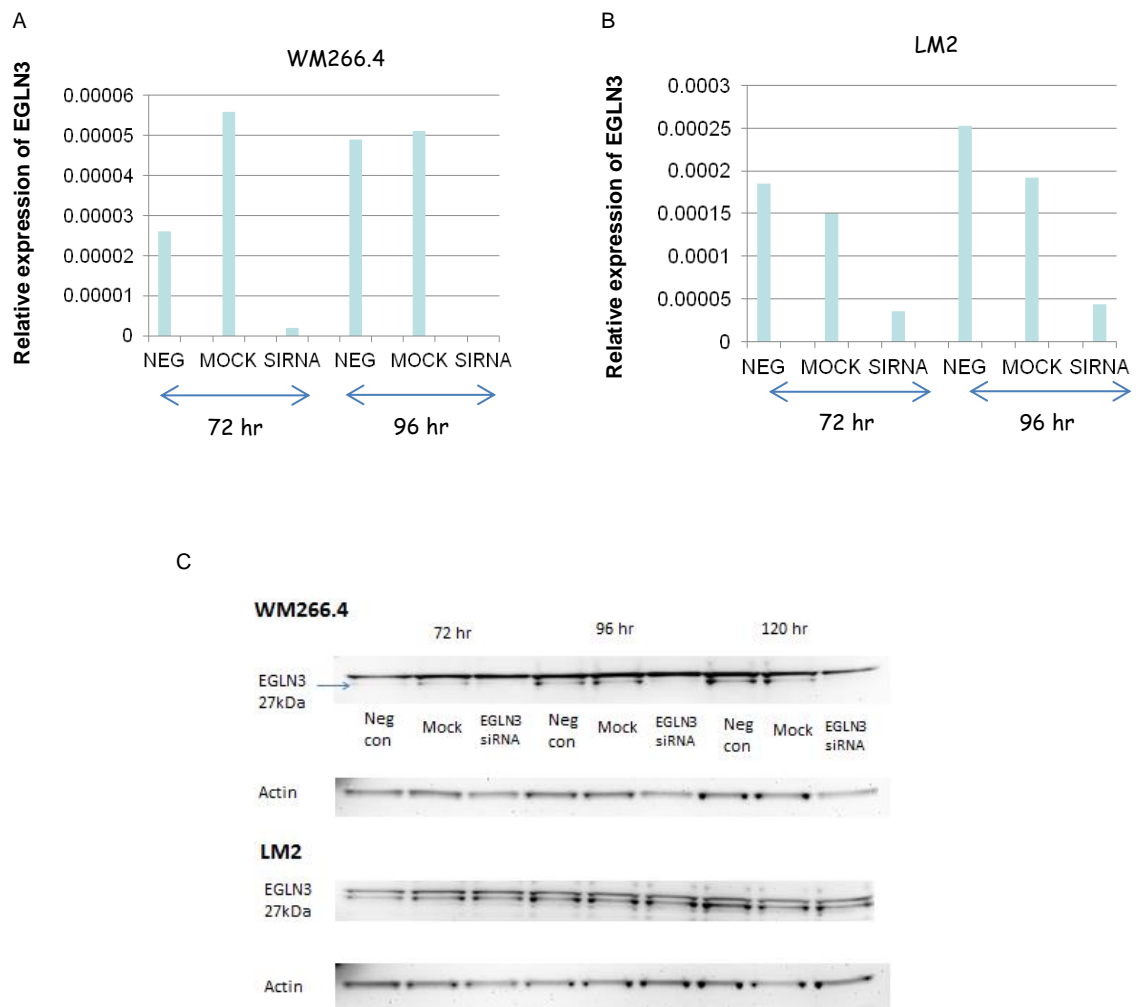


Figure 5-13: EGLN3 knock down in WM266.4 and LM2 by siRNA.

(A, B): qPCR analysis detecting *EGLN3* gene expression after *EGLN3* siRNA treatment. Untreated cells were used as negative control. Transfection reagent treated cells were also used as mock control to rule out the false effect caused by the transfection reagents. Expression of *EGLN3* was relative to endogenous control B2M. (C): Protein expression of *EGLN3* in negative control, mock control and *EGLN3* siRNA treated cells.

5.2.2.6 EGLN3 knock down does not affect the HIF1- α pathway

EGLN1 and EGLN2 protein expression was measured in WM266.4 cells in normoxia after EGLN3 knock down, in order to determine if silencing EGLN3 leads to a compensatory increase in other proteins (Figure 5-14). However, there were no compensatory increase in other proteins (Figure 5-14). However, there were no compensatory increase of EGLN1 or EGLN2 after knock down of EGLN3. I further confirmed the lack of impact of silencing EGLN3 on HIF signaling by showing sustained production of VEGF, which is a classical HIF1- α responsive target. Together, these data suggest that silencing of EGLN3 protein does not impact upon the activity of the whole pathway, and that EGLN3 may have functions other than determination of response to hypoxia in WM266.4.

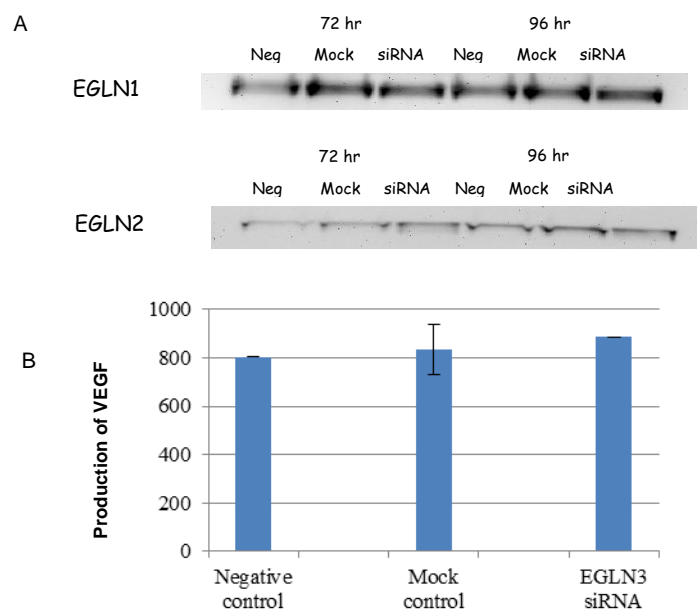


Figure 5 -14: EGLN3 knock down does not interfere the HIF1- α pathway.

(A): Western blots detecting EGLN1 and EGLN2 expression with or without EGLN3 siRNA transfection after 72 hours and 96 hours of culture. (B): Measurement of production of VEGF by VEGF ELISA in WM266.4 with or without EGLN3 siRNA transfection after 96 hours of culture.

5.2.2.7 EGLN3 knock down causes reduction in WM266.4 cell number

To further investigate the possibility of a HIF1- α independent function of EGLN3, I assessed the effect of knock down on proliferation. siRNA transfected cell lines WM266.4 (Figure 5-15 A) and LM2 (Figure 5-15 B) were seeded at the same density and the cell number counted 96 hours post transfection. In cell line WM266.4, with silenced EGLN3, there was a 0.4 fold decrease in cell number, compared to the negative control and mock control. DMOG, an inhibitor of hydroxylase activity of EGLNs failed to alter the cell number, thus suggesting a hydroxylase-independent response of EGLN3 in this cell line. There was no alteration of cell number in LM2 with stabilised EGLN3 protein after siRNA knock down. Identical results were observed in multiple repeats of these experiments. These data indicate that EGLN3 in WM266.4 cell line may promote proliferation in a HIF1- α independent way.

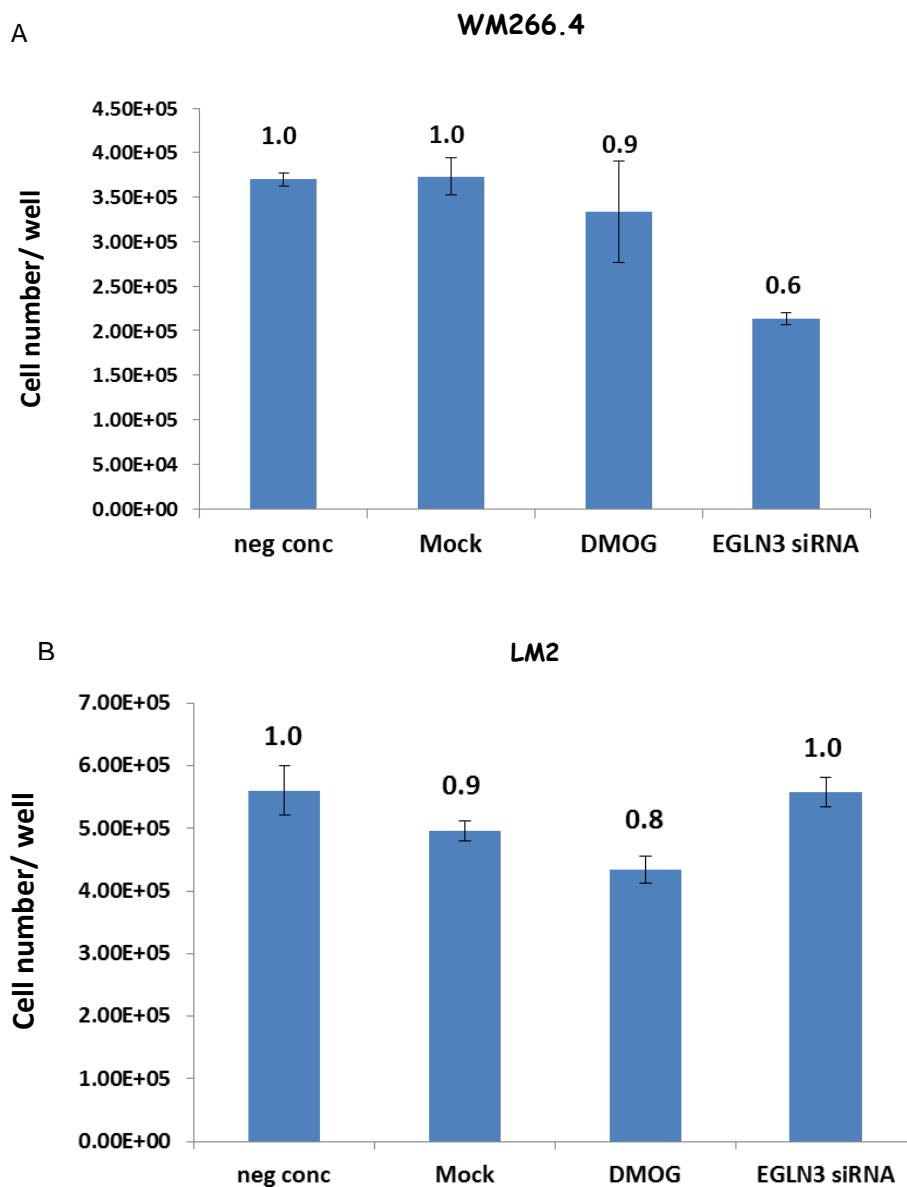


Figure 5-15: Cell counting in WM266.4 and LM2 cell lines.

(A, B): WM266.4 and LM2 cell lines were grown in different groups at the same starting density, including negative control (without treatment), mock control (transfection reagent treatment), DMOG treatment (inhibitor of hydroxylase activity of EGLNs), and EGLN3 siRNA treatment. Cell number of each group under different conditions was counted after 48 hours.

5.3 Discussion

5.3.1 Specific C-PHs are transcriptionally silenced by methylation in melanoma

Prolyl hydroxylases are fundamental components of molecular and metabolic signalling that regulate the biological activity of many essential proteins. Collagen and HIF are well known substrates of the collagen prolyl hydroxylases and HIF prolyl hydroxylases, respectively. Here I demonstrate methylation-dependent transcriptional silencing of both collagen and HIF prolyl hydroxylase members in melanoma, implying that these enzymes may be important melanoma suppressors.

In this chapter I present data showing that *P4HA3* is a potential novel epigenetic biomarker of melanoma progression and metastasis. *P4HA3* satisfies all the eligibility criteria for biomarkers that I have already discussed in Chapter 3. To briefly summarise:

(i) I have shown a good correlation between *P4HA3* methylation and melanoma by demonstrating that *P4HA3* CpG island methylation occurs at a high frequency and density in melanoma cell lines and melanoma clinical samples, compared to a generally low level of *P4HA3* methylation in melanocytes and benign naevi.

(ii) A correlation of methylation with disease progression was strongly implied by the demonstration that *P4HA3* methylation quantitatively increased in the metastases of paired melanoma cell lines and paired melanoma tissues. Specifically, I have shown increased *P4HA3* methylation in 2/3 metastatic lines in the paired melanoma cell

lines, and a significantly higher level of *P4HA3* CpG island methylation in clinical metastases relative to paired primary melanomas from which they derived.

(iii) Finally, I demonstrated a significant inverse correlation between *P4HA3* methylation and gene expression, suggesting that *P4HA3* expression is subject to transcriptional regulation by DNA methylation and may be mechanistically relevant to tumour progression and development of metastasis. These data support the candidacy of *P4HA3* methylation as a predictor of melanoma progression, implying that *P4HA3* has significant potential as a prognostic melanoma biomarker.

I went on to examine *P4HA3* methylation in melanoma patients' serum and observed significantly higher levels of detectable *P4HA3* methylated DNA in sera from melanoma patients with metastasis (n=44) than from those with no evidence of metastatic disease (n=23) (Figure 5-7 A). Importantly, with a methylation cut-off of 5%, *P4HA3* methylation showed a relatively high sensitivity (56%) and specificity (71%) for detection of metastatic disease. Risk analysis also confirmed a statistically significant association between *P4HA3* methylation and melanoma metastasis. It is also noteworthy that detection of *P4HA3* methylated DNA in serum may correlate with the classic diagnostic parameter of Breslow thickness from non-metastatic melanomas, as methylation was detected in only 1/15 samples from low risk melanoma (with a Breslow thickness less than 2 mm) and the other 3 methylated positive cases were from patients with higher risk melanomas (Breslow thickness > 3mm). Taken together, these data support methylated *P4HA3* DNA as a novel epigenetic serum biomarker for melanoma. To test whether detection of *P4HA3* methylation in non-metastatic melanoma patients' serum is predictive for poor

outcome, it will be necessary to undertake prospective studies in large patient cohorts involving the full clinical range of melanomas and these studies are now commencing.

The methylation status of other *C-PHs* in melanoma cell lines and patient materials was also analysed. *LEPREL1*, *LEPREL2* and *P4HA2* were all methylated in a smaller number of melanoma cell lines compared to *P4HA3* and methylation of *LEPREL1* and *LEPREL2* correlated well with reduced gene expression. *P4HA1* methylation was undetectable in any melanoma cell line tested. *P4HA1* and *P4HA2* have been recently proposed as oncogenes in breast cancer by Gilkes et al. and both genes were shown to have prognostic utility in breast cancer (Gilkes et al. 2013). In our melanoma study, interestingly, *P4HA2* was still expressed at a reasonable level in cell lines SKMEL23 and SKMEL30 in which CpG island methylation is detectable suggesting that CpG island methylation was not a transcriptional regulatory mechanism for *P4HA2*. Likewise, undetectable methylation of *P4HA1* raises the question of the utility of *P4HA1* and *P4HA2* as epigenetic biomarker in melanoma.

In the subsequent investigation of *LEPREL1* CpG island methylation in a panel of melanoma tissues, I observed only moderate levels of methylation in the *LEPREL1* CpG island but with significantly increased *LEPREL1* methylation in melanomas relative to control benign pigmented naevi. However despite detection in melanoma tissue, methylated *LEPREL1* genomic DNA was only rarely detectable in serum from melanoma patients. One possible reason that contributes to the lack of detectable methylated *LEPREL1* DNA but readily detectable methylated *P4HA3* DNA in

melanoma patients' serum is the different levels of *LEPREL1* and *P4HA3* CpG island methylation in melanoma tissues. DNA from melanoma released into the circulating blood is diluted by normal tissue DNA. DNA with *LEPREL1* methylation at a general low level in melanomas (mean methylation < 10%) may become undetectable after being released into the blood. In contrast, the higher level of *P4HA3* methylation seen in melanoma tissue may remain detectable in serum by pyrosequencing. Another potential explanation is the distinct functions of the two genes. The metastasis cascade is a complicated and dynamic progress. Methylated *P4HA3* but not methylated *LEPREL1* may be more functionally relevant for metastasis.

In conclusion, I have identified methylation-dependent transcriptional silencing of C-PHs in melanoma cell lines and melanoma tissues, including a particular highlighted epigenetic biomarker *P4HA3* whose methylation correlates with melanoma progression and metastasis. Importantly, *P4HA3* is a robust serum biomarker for detection of metastatic melanoma. In future work, the candidacy of *P4HA3* methylated DNA will be rigorously tested in large, prospectively collected serum samples from melanoma patients in multiple independent centres.

5.3.2 *EGLN3* methylation and involvement of *EGLN3* in HIF1- α independent pathway in melanoma

Cancer cells are frequently starved of oxygen during tumour development and progression (Harris 2002). This is because tumour cell demand for oxygen often outstrips the amount of oxygen that can be supplied from normal tissue vasculature, due to the rapid growth and cell division rates of many tumour cells. This problem is

frequently exacerbated in larger tumours that are supported by their own vasculature. Tumour vasculature is often unable to deliver appropriate amounts of oxygen owing to the faulty and abnormal nature of the vascular structures that develop during tumorigenesis (Nagy et al. 2009; Fukumura et al. 2010). The result of tumour growth in low oxygen conditions is stabilisation of HIF1- α protein and subsequent activation of many HIF1 target genes including those involved in regulation of tumour behaviour, for example senescence, apoptosis or angiogenesis. In melanoma, a role for increased HIF1- α expression has been established in both transformation of melanocytes and in the progression or metastasis of melanoma (Bedogni et al. 2005; Mills et al. 2009), as has a role for various downstream effectors of HIF1- α such as VEGF (Rofstad and Danielsen 1999). It is, however, important to appreciate that a hypoxic microenvironment will result in heterogeneous changes within the population of melanoma cells (Widmer et al. 2013) and we clearly see this from looking at HIF1- α expression in our paired primary and metastatic melanoma lines (Figure 5-9). Increased HIF1- α may drive tumour progression in some melanomas, but changes in other genes may be responsible for metastatic progression in others. It must also be borne in mind that some genetic and epigenetic changes in our melanoma cell lines may result from the techniques used to isolate and culture these cells.

EGLN proteins catalyse the addition of hydroxyl groups to specific proline residues in the HIF1- α protein. This reaction ensures recognition of the hydroxylated HIF1- α by proteosomal enzymes such that HIF1- α is degraded and is non-functional. The level of HIF1- α is tightly regulated and, as mentioned previously HIF1- α levels are regulated through multiple mechanisms. In addition to regulation of the hypoxia pathway at the level of HIF1- α , we also see control at the level of the EGLN proteins.

Several pathways are known to control the level of EGLN proteins. EGLNs 1 and 3 are regulated by a closely related protein, Siah2 (Qi et al. 2008; Nakayama et al. 2009). Siah2 proteins target both EGLN1 and EGLN3 proteins for ubiquitination and degradation by the proteosomal route. In melanoma, regulation of EGLN3 by Siah-2 was reported previously and shown to occur through both HIF1- α dependent and HIF1- α independent pathways (Qi et al. 2008). Additionally, EGLN proteins can be regulated by metabolic processes. Cancer cells frequently alter metabolism to favour anaerobic metabolic pathways. Increased glycolysis via the Krebs cycle produces succinate and fumarate, both of which inhibit EGLN activity (Selak et al. 2005). It is also appreciated that EGLN gene expression can be silenced by methylation. In this study, I have detected partial *EGLN3* methylation in one of eight melanoma cell lines and this methylation correlates with a low level of mRNA and protein expression.

In this investigation, I have obtained some preliminary evidence for a HIF1- α independent role of EGLN3, as evidenced from cell counts obtained after knockdown of EGLN3. Several HIF1- α independent roles for EGLN3 have been described. These include a description of EGLN3 as a tumour suppressor by the inhibition of tumour progression and induction of angiogenesis in glioma and pancreatic cancer (Su et al. 2010; Sciorra et al. 2012), and reports of EGLN3 functioning as an anti-apoptotic protein in non-small cell lung cancer (Chen et al. 2011). Additionally, EGLN3 has also been shown to be responsible for promoting cell cycle transition in head and neck squamous cell carcinoma (Hogel et al. 2011). However, we can only speculate as to the function of the HIF1- α - independent EGLN3 signalling in our melanoma cells as further investigation was beyond the scope of this thesis.

The use of siRNA enabled silencing of *EGLN3* mRNA and protein in the WM266.4 cell line. In the LM2 cell line, knock down of *EGLN3* mRNA levels did not cause commensurate reduction in *EGLN3* protein expression. The reason for this difference is unclear since the level of *EGLN3* protein expression was similarly low in both of these lines. Perhaps HIF1- α signalling is impaired in one of these lines, however we showed that WM266.4 underwent a normal hypoxic response by displaying a classical induction of EGLNs and VEGF in response to hypoxia. Alternatively it may be that *EGLN3* protein is differentially regulated between the two cell lines resulting in a protein with a longer half-life in LM2 cells.

There was more efficient knockdown of *EGLN3* mRNA in WM266.4 than LM2, and this could have been significant for protein expression. In WM266.4 with *EGLN3* silenced at both mRNA and protein level by siRNA, I showed that the response to hypoxia was not impaired, as there was no compensatory increase in either *EGLN1* or *EGLN2* proteins and no alteration in the amount of VEGF produced as a result of hypoxic challenge. However, the selective pressure(s) favouring *EGLN3* methylation in WM266.4 is still not clear. I had hypothesized that *EGLN3* may be important for inducing apoptosis and had assumed that in reducing *EGLN3* expression I would see a reduction in apoptotic activity accompanied perhaps by an increase in cell viability and that this may be the consequence of methylation of *EGLN3* in WM266.4 cells. However, unexpectedly the opposite was observed when *EGLN3* was knocked out in WM266.4 cells. A link between *EGLN3* and the Krebs cycle is established (Selak et al. 2005); it is known that *EGLN3* catalyses the conversion of α -ketoglutarate to succinate. When *EGLN3* is totally silenced this reaction may not occur and α -ketoglutarate levels may build up in the cells. Accumulation of α -

ketoglutarate has been shown to inhibit G1 to S phase transition in the cell cycle (Hogel et al. 2011) and is a possible explanation as to why we see a decreased cell number after silencing EGLN3 in WM266.4 cells. This hypothesis assumes that the low level of EGLN3 protein in our partially methylated WM266.4 cells was sufficient to allow some conversion of α -ketoglutarate to succinate to ensure faster progression through the cell cycle.

In future studies I would wish to examine the effects of EGLN3 overexpression and to investigate the effects of EGLN3 expression on cell viability in melanoma cells. It may be that levels of EGLN3 are critical within a specific range above which we see induction of apoptosis and below which we see slower progression through the cell cycle.

Chapter 6 Conclusions and Future Perspectives

6.1 Conclusions

Melanoma is a highly aggressive and lethal skin cancer with an increasing incidence in Caucasian populations. Genetic and epigenetic alterations collaboratively facilitate the malignant transformation from benign naevus to melanoma, and subsequently to development of local or distal metastasis. As a hallmark of cancer, metastasis is a major determinant of cancer patient outcome (Hanahan and Weinberg 2011). Although the majority of patients with low risk melanomas are cured by surgical excision of the primary lesions, the outcome for melanoma patients with metastatic disease (particularly at visceral and/or central nervous system sites) remains very poor (Balch et al. 2009). New agents including vemurafenib and ipilimumab have significantly benefited patients with advanced melanoma (Flaherty et al. 2010; Hodi et al. 2010; Chapman et al. 2011; Robert et al. 2011). However, the two treatments are least effective when they are used at late stage, large volume disease when tumour load is high and patient performance status typically poor. Indeed, there is clear evidence that ipilimumab is far more effective in stage M1a and M1b disease than in M1c (disseminated melanoma) (Hodi et al. 2010). New strategies for the early detection of sub-clinical relapsed and/or metastatic disease, such as sensitive and specific serum biomarkers would allow the introduction of these treatments when tumour load is low thereby creating a therapeutic window in which there is sufficient time for the patient to mount an effective anti-melanoma response.

Recently, methylation-dependent silencing of tumour-related genes has emerged as a frequent molecular genetic feature of cancer with specific signatures associating with defined clinico-pathological disease states (Sandoval and Esteller 2012). This highlights the potential clinical utility of assessing DNA methylation to measure tumour progression or to predict treatment response and patient outcome. Increased amounts of methylated DNA present in the circulating blood of cancer patients has made it a very attractive target for the detection of metastatic disease by a simple blood test. In this work, I have used different gene finding strategies with the goal of assembling a panel of serum epigenetic biomarkers with clinical potential for detecting metastatic melanoma. These gene finding strategies included both a systematic approach and a candidate gene approach and they have allowed me to identify a number of novel epigenetically dysregulated genes in melanoma. The systematic approach used unbiased, microarray-based methodology to screen selected melanoma cell lines, including:

(i) A pharmacological methylation reversal screen of 5 random melanoma cell lines (preliminary data provided by Dr Tim Crook) to identify a number of genes that are potentially methylated in melanomas, including some candidates that are involved in cancer-related signalling such as the TGF- β pathway and the WNT pathway (section 3.2.1). In the validation of selected candidates, a role for *TFPI2* as an epigenetic biomarker was identified and *TFPI2* was shown to have potential clinical utility in predicting melanoma progression and detection of metastasis.

(ii) An integrative analysis of genome-wide methylation profiling and expression profiling to identify additional candidate genes that are differentially regulated by DNA methylation between primary melanoma cell lines and their metastatic derivatives. Rigorous data mining analysis ultimately selected 7 candidate genes for further validation, including immunity-related gene *HLA-DP1* (Pryds et al. 1987), RAS inhibitor *RASAL1* (Bernards and Settleman 2009) and *MT1E* that are known to be methylated in human cancers (Faller et al. 2010; Noetzel et al. 2010), tumour related gene *EFNB2* (Vogt et al. 1998; Liu et al. 2004; Tachibana et al. 2007), and *LIMCH1*, *TCEA3* and *FAM134B* which are entirely novel. The potential of these genes as melanoma biomarkers is needed to be further investigated.

The candidate gene approach identified additional genes of interest. Specifically, I have shown that *NT5E* and *DUSP2* are biomarkers prognostic of good outcome when they are methylated in melanoma. Conversely, *P4HA3* has been shown to be a biomarker of poor prognosis and advanced melanoma when methylated in melanoma tissues or serum.

Taken together, my work has identified several promising epigenetic biomarkers whose methylation positively (*TFPI2* and *P4HA3*) or negatively (*NT5E* and *DUSP2*) correlates with melanoma progression. A high frequency and high level of *TFPI2* and *P4HA3* methylation in melanoma cell lines and clinical tissues

compared to an absent or low level in normal melanocytes or benign naevi suggests that methylation of these two genes forms a specific signature of malignant melanoma. My data suggests also that these two genes may be mechanistically relevant not only to melanomagenesis but also to progression from primary to metastatic disease. The significantly increased level of *TFPI2* and *P4HA3* CpG island methylation in aggressive metastatic disease suggests a role for *TFPI2* and *P4HA3* as epigenetic biomarkers that can potentially predict poor prognosis of melanoma. Furthermore, in my work a highly sensitive and specific correlation between methylation of *TFPI2/P4HA3* in melanoma patients' sera and metastatic disease has been established, implying potential clinical utility for *TFPI2* and *P4HA3* as serum biomarkers for the detection of metastatic melanoma. Validation of these two biomarkers in a larger collection of melanoma patient blood samples would establish the clinical significance of *TFPI2*, or *P4HA3*, or the combination of *TFPI2* and *P4HA3* as serum biomarkers for metastatic melanoma. Such validation in large, multi centre studies would strongly encourage the routine use of these two genes, together with additional markers identified in parallel studies, as part of the routine clinical follow up of melanoma patients. The use of protein tumour markers in oncology follow up clinics is well-established, for example CEA in colorectal cancer (Banaszkiewicz et al. 2011) and CA125 in epithelial ovarian cancer (Song et al. 2013), but no methylation marker has yet entered routine clinical use as a diagnostic or predictive tumour marker.

Methylation investigations in this study have also detected aberrant methylation of *NT5E* and *DUSP2* in melanoma cell lines and melanoma tissue materials. Despite being methylated in both primary and metastatic melanomas, methylation of *NT5E* appears to be a good prognostic biomarker of melanoma because *NT5E* methylation was associated with early stage of melanoma and became undetectable when melanoma metastasis progressed to visceral sites. Similarly, the significantly higher methylation level of *DUSP2* in primary melanomas than in metastasis implies that *DUSP2* methylation may also be a biomarker for good prognostic in melanoma. However, the sample number used in the *DUSP2* investigation is small and would need to be confirmed in a larger study. The stage specificity in distribution of methylation in *NT5E* and *DUSP2* suggests that these two genes may be involved in initiation of melanomagenesis. These genes may then exploit the dynamic reversibility of DNA methylation to switch on gene expression to promote the metastatic progression of melanoma. Such bimodal methylation may be common in the natural history of an individual cancer and illustrates how epigenetics allows changes in expression of genes as cancers evolve phenotypically.

In summary, my study proposes that epigenetic dysregulation by CpG island methylation of tumour-related genes *TFPI2*, *P4HA3*, *NT5E* and *DUSP2* is important in melanoma development and progression and that detection of methylated DNA from these genes may provide novel biomarkers for assessing tumour progression and patient outcome. Molecular functions of these

biomarkers in melanoma should be investigated in future work for the purpose of better understanding the biology of this highly aggressive tumour. Such studies may also lead to new therapeutic strategies for advanced melanoma. Moreover, detection of circulating methylated *TFPI2* and *P4HA3* from patient's sera may be useful for predicting prognosis and in the early diagnosis of metastatic disease. Given the emerging clinical evidence that new melanoma therapeutics, particularly ipilimumab, are most effective when deployed in low volume metastatic disease, such epigenetic biomarkers are likely to be of value in informing the initiation of such agents.

6.2 Future perspectives

6.2.1 Serum epigenetic biomarkers for detection of metastatic disease

The primary aim of this study is to build up a portfolio of epigenetic serum biomarkers for the early detection of metastatic disease. My preliminary work has shown that *TFPI2* and *P4HA3* are potential serum epigenetic biomarkers and methylation of *TFPI2* or *P4HA3* in melanoma patients' sera significantly correlates with metastatic disease. Prospective validation in large clinical cohorts of these two biomarkers and the new biomarkers I have identified in preliminary form by genome-wide methylation screen, is now a priority. Such studies are already underway on Tayside. Prospective study is a more appropriate for

rigorous validation because melanoma patients enrolled in any prospective study can be closely monitored for their outcome and sera are collected, processed and stored according to pre-defined protocols and at regular intervals at clinical review. There is also less potential for bias in sample selection in prospective studies.

Circulating methylated DNA levels will increase in metastasis because increased number of tumour cells intravasated into blood vessels undergo necrosis or apoptosis and release their DNA into the circulation (Weinberg 2006). Any analytical technique with high sensitivity and accuracy such as pyrosequencing is applicable for the measurement of these biomarkers in sera, and pyrosequencing has provided promising results in this study by revealing methylation of *TFPI2* and *P4HA3* in melanoma patients' sera that correlates with metastatic melanoma. All potential diagnostic tests must satisfy criteria of cost-effectiveness in addition to sensitivity and specificity. One great advantage of using methylated DNA is that its detection is amenable to automation and pyrosequencing, as evidenced by the data I present in this thesis, is clearly both sensitive and specific. Automation of the assays would undoubtedly improve cost effectiveness. I suspect that the definitive serum test for routine clinical use will require a panel of biomarkers because a combination of biomarkers is more likely to reach sufficient sensitivity and specificity to minimize false negative and false positive results. Regarding the optimal application of these biomarkers in routine clinical practice, at least two further issues need to be addressed:

- (i) Is crossing of a threshold level or an increasing level of DNA methylation in biomarker genes (or both) required to provide sufficient evidence of recurrent/ metastatic disease? To answer this question, it will be necessary to rigorously determine either a threshold level of methylation or an increased level of DNA methylation for clinical surveillance of high-risk patients. Use of such parameters enables stratification of melanoma patients into a low risk group, an intermediate risk group, and a high risk group. An increase in DNA methylation adds risk to tumour progression, therefore, high risk melanoma patients defined by such a biomarker test should be considered for treatment applicable to metastatic disease. The low concentration of DNA present in patients' sera makes it a challenging task to determine the appropriate threshold level/increase level. Using a higher DNA methylation threshold level/increase level will improve the specificity and reduce the sensitivity, whilst use of lower value will improve the sensitivity and reduce the specificity of any employed test. Therefore, adjustment of two parameters should be undertaken by rigorous statistical analysis in a prospective study. It may also be helpful to take multiple blood samples from each patient for the purpose of ruling out inconsistencies of DNA methylation from given blood samples. A further consideration is whether increasing levels of DNA methylation on serial examination of blood samples from the same individual is more important for prognosis/outcome than the

absolute level of DNA methylation achieved. Only large prospective investigation will be able to resolve this question.

- (ii) Combination of biomarkers for batch examination. As argued above, a panel of biomarkers will be required in order to optimise the clinical sensitivity and specificity. Metastatic melanoma is a heterogeneous disease and so it is very unlikely that DNA methylation will be present in all chosen biomarkers. Whether the final biomarker assay requires methylation in certain key biomarkers or if methylation in any proportion of the biomarkers is an acceptable indicator of recurrence / metastasis can only be answered by prospective validation of candidate panels of genes.

Though such rigorous testing may be time consuming, successful establishment of a portfolio of serum epigenetic biomarkers will significantly benefit melanoma patients by allowing early detection of sub-clinical metastatic disease and informing both the initiation and possibly the form (targeted therapy or immunomodulatory therapy) of therapeutic intervention.

6.2.2 Epigenetic biomarkers in melanoma tissues

Detection of the aberrant methylation of informative biomarkers not only offers the opportunity for early detection of relapsed disease in biofluids but may also

afford prognostic value in biopsy specimens. Methylated genes in cancer tissues may show better sensitivity as biomarkers due to the high concentration of tumour DNA present in the tumour tissue. Furthermore, use of methylated DNA as a biomarker may enhance the sensitivity and clinical utility of existing modalities, such as sentinel lymph node biopsy (SLNB). One of the major limitations of current SLNB protocols is that there is no way to predict from an individual positive SLNB the risk of future visceral metastatic disease (and death). A subset of patients with positive SLNB are cured by this procedure whereas a further subset will ultimately relapse and die from visceral and/or central nervous system metastasis. The ability to predict from epigenetic analysis of positive sentinel nodes the probability of such life-threatening events would be enormously valuable in informing the use of adjuvant therapies post SLNB and in identifying the group of patients in whom there is a high risk of metastatic relapse. Such patients could then be managed by close clinical follow up (potentially including the use of validated serum epigenetic biomarkers) in order to detect relapse as early as possible. This subset of patients would also be considered for appropriate adjuvant therapy. Conversely, patients whose SLNB epigenetic profile indicates a low risk of future visceral/ CNS disease can continue to be monitored with low intensity follow-up, reassured about the low risk of recurrence and spared the likely side effects of adjuvant therapies (for example the autoimmune toxicities of ipilimumab).

6.2.3 Epigenetic candidates as new therapeutic targets

Data presented within this thesis demonstrate that promoter methylation of *TFPI2* and *P4HA3* correlates with poor prognosis, while promoter methylation of *NT5E* and *DUSP2* correlates with a good prognosis of melanoma. These results have implications for therapeutic strategies aimed at reactivation of transcriptionally silenced genes. Global demethylating agents such as 5'-azacytidine and 5'-aza-2-deoxycytidine show remarkable efficacy in the treatment of haematopoietic malignancies (Kantarjian et al. 2007), but may not be suitable for melanoma due to the epigenetic heterogeneity of melanoma and, as illustrated by my work, dynamic changes in methylation even within a single gene during the natural history of an individual patient's disease. However, it is not unreasonable to hypothesise that metastatic melanoma with specific combinations of transcriptionally silenced genes such as *TFPI2* or *P4HA3* might be amenable to demethylating agents. In other solid tumours such as non-small cell lung cancer, disappointment at initial clinical results with 5' azacytidine has been replaced with optimism that appropriately dosed demethylating agents can show meaningful efficacy and acceptable toxicity in some patients, even with large volume metastatic disease. The key will be to identify the profile(s) of methylated genes which confer individual cancer sensitivity to demethylation. Such studies would be of immense interest in melanoma. Inhibitors of NT5E are available and my work in this thesis implies that these could be of value in metastatic melanoma in which there is over-expression of NT5E. Studies of therapeutic antibodies to

NT5E have shown promise in mouse models of cancer (Stagg et al. 2010; Stagg et al. 2012) and my data suggests that these merit detailed study as potential melanoma therapeutics, particularly given the apparent importance of this protein in metastatic disease.

6.2.4 Summary

The epigenetic biomarkers identified and investigated in this study offer potential utility in the early diagnosis of metastatic melanoma via detection of methylated DNA in patient serum. The biomarkers may also have prognostic utility in both primary and SLNB tissues. Validation of these first generation candidates in large, well-annotated patient cohorts is now beginning. Confirmation of my initial data in these large scale studies and similar development of the additional candidate genes identified in my later work in this thesis will support their introduction into the routine clinical management of melanoma and encourage yet further studies to determine their utility in informing the adjuvant use of current and emerging therapeutics in melanoma.

7 References

- Acevedo, L. G., et al. (2011). "Novel DNA binding domain-based assays for detection of methylated and nonmethylated DNA." *Epigenomics* **3**(1): 93-101.
- administration, U. S. F. a. D. (2013). "FDA approves two drugs, companion diagnostic test for advanced skin cancer." from <http://www.fda.gov/NewsEvents/Newsroom/PressAnnouncements/ucm354199.htm>.
- Agarwala, S. S., et al. (2009). "LDH correlation with survival in advanced melanoma from two large, randomised trials (Oblimersen GM301 and EORTC 18951)." *Eur J Cancer* **45**(10): 1807-1814.
- Aguissa-Toure, A. H. and G. Li (2012). "Genetic alterations of PTEN in human melanoma." *Cell Mol Life Sci* **69**(9): 1475-1491.
- Albino, A. P., et al. (1989). "Analysis of ras oncogenes in malignant melanoma and precursor lesions: correlation of point mutations with differentiation phenotype." *Oncogene* **4**(11): 1363-1374.
- Albino, A. P., et al. (1994). "Mutation and expression of the p53 gene in human malignant melanoma." *Melanoma Res* **4**(1): 35-45.
- Almendros, I., et al. (2013). "Intermittent hypoxia increases melanoma metastasis to the lung in a mouse model of sleep apnea." *Respir Physiol Neurobiol* **186**(3): 303-307.
- Arab, K., et al. (2011). "Epigenetic deregulation of TCF21 inhibits metastasis suppressor KISS1 in metastatic melanoma." *Carcinogenesis* **32**(10): 1467-1473.
- Arai, M., et al. (2006). "Sequential gene expression changes in cancer cell lines after treatment with the demethylation agent 5-Aza-2'-deoxycytidine." *Cancer* **106**(11): 2514-2525.
- Arya, M., et al. (2005). "Basic principles of real-time quantitative PCR." *Expert Rev Mol Diagn* **5**(2): 209-219.
- Avery-Kiejda, K. A., et al. (2011). "P53 in human melanoma fails to regulate target genes associated with apoptosis and the cell cycle and may contribute to proliferation." *BMC Cancer* **11**: 203.
- Avery-Kiejda, K. A., et al. (2008). "Small molecular weight variants of p53 are expressed in human melanoma cells and are induced by the DNA-damaging agent cisplatin." *Clin Cancer Res* **14**(6): 1659-1668.
- Azzola, M. F., et al. (2003). "Tumor mitotic rate is a more powerful prognostic indicator than ulceration in patients with primary cutaneous melanoma: an analysis of 3661 patients from a single center." *Cancer* **97**(6): 1488-1498.
- Balch, C. M., et al. (2009). "Final version of 2009 AJCC melanoma staging and classification." *J Clin Oncol* **27**(36): 6199-6206.
- Balch, C. M., et al. (2004). "An evidence-based staging system for cutaneous melanoma." *CA Cancer J Clin* **54**(3): 131-149; quiz 182-134.
- Ballantyne, A. D. and K. P. Garnock-Jones (2013). "Dabrafenib: First Global Approval." *Drugs*.

- Banaszkiewicz, Z., et al. (2011). "Usefulness of CEA concentration measurement and classic colonoscopy in follow-up after radical treatment of colorectal cancer." Pol Przegl Chir **83**(6): 310-318.
- Bardeesy, N., et al. (2001). "Dual inactivation of RB and p53 pathways in RAS-induced melanomas." Mol Cell Biol **21**(6): 2144-2153.
- Barlow, D. P. (1993). "Methylation and imprinting: from host defense to gene regulation?" Science **260**(5106): 309-310.
- Bartek, J., et al. (1991). "Aberrant expression of the p53 oncoprotein is a common feature of a wide spectrum of human malignancies." Oncogene **6**(9): 1699-1703.
- Baylin, S. B. and P. A. Jones (2011). "A decade of exploring the cancer epigenome - biological and translational implications." Nat Rev Cancer **11**(10): 726-734.
- Bedogni, B., et al. (2005). "The hypoxic microenvironment of the skin contributes to Akt-mediated melanocyte transformation." Cancer Cell **8**(6): 443-454.
- Bennett, D. C. (2008). "How to make a melanoma: what do we know of the primary clonal events?" Pigment Cell Melanoma Res **21**(1): 27-38.
- Bennett, D. C. (2008). "Ultraviolet wavebands and melanoma initiation." Pigment Cell Melanoma Res **21**(5): 520-524.
- Berdasco, M. and M. Esteller (2010). "Aberrant epigenetic landscape in cancer: how cellular identity goes awry." Dev Cell **19**(5): 698-711.
- Bernards, A. and J. Settleman (2009). "Loss of the Ras regulator RASAL1: another route to Ras activation in colorectal cancer." Gastroenterology **136**(1): 46-48.
- Bertolotto, C., et al. (2011). "A SUMOylation-defective MITF germline mutation predisposes to melanoma and renal carcinoma." Nature **480**(7375): 94-98.
- Besaratinia, A. and G. P. Pfeifer (2008). "Sunlight ultraviolet irradiation and BRAF V600 mutagenesis in human melanoma." Hum Mutat **29**(8): 983-991.
- Bibikova, M., et al. (2011). "High density DNA methylation array with single CpG site resolution." Genomics **98**(4): 288-295.
- Bird, A. P. (1986). "CpG-rich islands and the function of DNA methylation." Nature **321**(6067): 209-213.
- Bliss, J. M., et al. (1995). "Risk of cutaneous melanoma associated with pigmentation characteristics and freckling: systematic overview of 10 case-control studies. The International Melanoma Analysis Group (IMAGE)." Int J Cancer **62**(4): 367-376.
- Board, R. E., et al. (2008). "DNA methylation in circulating tumour DNA as a biomarker for cancer." Biomark Insights **2**: 307-319.
- Brenner, M. and V. J. Hearing (2008). "The protective role of melanin against UV damage in human skin." Photochem Photobiol **84**(3): 539-549.
- Breslow, A. (1979). "Prognostic factors in the treatment of cutaneous melanoma." J Cutan Pathol **6**(3): 208-212.
- Britten, C. D. (2013). "PI3K and MEK inhibitor combinations: examining the evidence in selected tumor types." Cancer Chemother Pharmacol **71**(6): 1395-1409.
- Browser, U. G. from <http://genome.ucsc.edu/>.
- Bustin, S. A. (2000). "Absolute quantification of mRNA using real-time reverse transcription polymerase chain reaction assays." J Mol Endocrinol **25**(2): 169-193.
- Byron, S. A., et al. (2012). "Sensitivity to the MEK inhibitor E6201 in melanoma cells is associated with mutant BRAF and wildtype PTEN status." Mol Cancer **11**: 75.
- Campos, A. C., et al. (2007). "Oxidative stress modulates DNA methylation during melanocyte anchorage blockade associated with malignant transformation." Neoplasia **9**(12): 1111-1121.

- Carreira, S., et al. (2005). "Mitf cooperates with Rb1 and activates p21Cip1 expression to regulate cell cycle progression." *Nature* **433**(7027): 764-769.
- Celebi, J. T., et al. (2000). "Identification of PTEN mutations in metastatic melanoma specimens." *J Med Genet* **37**(9): 653-657.
- Chand, H. S., et al. (2004). "The effect of human tissue factor pathway inhibitor-2 on the growth and metastasis of fibrosarcoma tumors in athymic mice." *Blood* **103**(3): 1069-1077.
- Chand, H. S., et al. (2005). "Structure, function and biology of tissue factor pathway inhibitor-2." *Thromb Haemost* **94**(6): 1122-1130.
- Chapman, P. B., et al. (2011). "Improved survival with vemurafenib in melanoma with BRAF V600E mutation." *N Engl J Med* **364**(26): 2507-2516.
- Cheli, Y., et al. (2012). "Hypoxia and MITF control metastatic behaviour in mouse and human melanoma cells." *Oncogene* **31**(19): 2461-2470.
- Chen, S., et al. (2011). "The expression of prolyl hydroxylase domain enzymes are up-regulated and negatively correlated with Bcl-2 in non-small cell lung cancer." *Mol Cell Biochem* **358**(1-2): 257-263.
- Christmann, M., et al. (2011). "O(6)-Methylguanine-DNA methyltransferase (MGMT) in normal tissues and tumors: enzyme activity, promoter methylation and immunohistochemistry." *Biochim Biophys Acta* **1816**(2): 179-190.
- Conway, K., et al. (2011). "DNA-methylation profiling distinguishes malignant melanomas from benign nevi." *Pigment Cell Melanoma Res* **24**(2): 352-360.
- Cooper, S., Ed. (1840). *First lines of theory and practice of surgery*. London, Longman, Orme, Brown, Green and Longman.
- Costin, G. E. and V. J. Hearing (2007). "Human skin pigmentation: melanocytes modulate skin color in response to stress." *FASEB J* **21**(4): 976-994.
- CRUK. (2013). "Skin cancer statistics." from <http://www.cancerresearchuk.org/cancer-info/cancerstats/types/skin/>.
- Curtin, J. A., et al. (2005). "Distinct sets of genetic alterations in melanoma." *N Engl J Med* **353**(20): 2135-2147.
- Dahl, C. and P. Guldberg (2007). "The genome and epigenome of malignant melanoma." *APMIS* **115**(10): 1161-1176.
- Dai, D. L., et al. (2005). "Prognostic significance of activated Akt expression in melanoma: a clinicopathologic study of 292 cases." *J Clin Oncol* **23**(7): 1473-1482.
- Dankort, D., et al. (2007). "A new mouse model to explore the initiation, progression, and therapy of BRAFV600E-induced lung tumors." *Genes Dev* **21**(4): 379-384.
- Database, T. G. H. G. from <http://www.genecards.org/>.
- Davies, H., et al. (2002). "Mutations of the BRAF gene in human cancer." *Nature* **417**(6892): 949-954.
- Dedeurwaerder, S., et al. (2011). "Evaluation of the Infinium Methylation 450K technology." *Epigenomics* **3**(6): 771-784.
- Dermatology information system, D. "Nodular Melanoma (NM)." Dermatology information system, D. "Superficial Spreading Melanoma (SSM)." from <http://www.dermis.net/dermisroot/en/51725/image.htm>.
- Derynck, R., et al. (2001). "TGF-beta signaling in tumor suppression and cancer progression." *Nat Genet* **29**(2): 117-129.
- Devaney, J. M., et al. (2013). "Identification of novel DNA-methylated genes that correlate with human prostate cancer and high-grade prostatic intraepithelial neoplasia." *Prostate Cancer Prostatic Dis*.

- Dhawan, P., et al. (2002). "Constitutive activation of Akt/protein kinase B in melanoma leads to up-regulation of nuclear factor-kappaB and tumor progression." Cancer Res **62**(24): 7335-7342.
- Di Lullo, G. A., et al. (2002). "Mapping the ligand-binding sites and disease-associated mutations on the most abundant protein in the human, type I collagen." J Biol Chem **277**(6): 4223-4231.
- Dickson, P. V. and J. E. Gershenwald (2011). "Staging and prognosis of cutaneous melanoma." Surg Oncol Clin N Am **20**(1): 1-17.
- Diffey, B. L. (2004). "The future incidence of cutaneous melanoma within the UK." Br J Dermatol **151**(4): 868-872.
- Dillon, R. L., et al. (2007). "An EGR2/CITED1 transcription factor complex and the 14-3-3sigma tumor suppressor are involved in regulating ErbB2 expression in a transgenic-mouse model of human breast cancer." Mol Cell Biol **27**(24): 8648-8657.
- Dimova, E. Y. and T. Kietzmann (2010). "Hypoxia-inducible factors: post-translational crosstalk of signaling pathways." Methods Mol Biol **647**: 215-236.
- Dominguez, G., et al. (2002). "p14ARF promoter hypermethylation in plasma DNA as an indicator of disease recurrence in bladder cancer patients." Clin Cancer Res **8**(4): 980-985.
- Dovey, M., et al. (2009). "Oncogenic NRAS cooperates with p53 loss to generate melanoma in zebrafish." Zebrafish **6**(4): 397-404.
- Du, J., et al. (2004). "Critical role of CDK2 for melanoma growth linked to its melanocyte-specific transcriptional regulation by MITF." Cancer Cell **6**(6): 565-576.
- Dupont, J. M., et al. (2004). "De novo quantitative bisulfite sequencing using the pyrosequencing technology." Anal Biochem **333**(1): 119-127.
- Eckhardt, F., et al. (2006). "DNA methylation profiling of human chromosomes 6, 20 and 22." Nat Genet **38**(12): 1378-1385.
- Egeblad, M., et al. (2010). "Dynamic interplay between the collagen scaffold and tumor evolution." Curr Opin Cell Biol **22**(5): 697-706.
- Elder, D. E., Ed. (1992). Melanocytic Tumors of the Skin (Atlas of Tumor Pathology), Armed Forces Institute of Pathology Washington, D.C.
- Elder, D. E., et al. (2005). "Cutaneous melanoma: estimating survival and recurrence risk based on histopathologic features." Dermatol Ther **18**(5): 369-385.
- Erratum (2007). "The association of use of sunbeds with cutaneous malignant melanoma and other skin cancers: A systematic review." Int J Cancer **120**(5): 1116-1122.
- Esteller, M. (2006). "The necessity of a human epigenome project." Carcinogenesis **27**(6): 1121-1125.
- Esteller, M. (2007). "Cancer epigenomics: DNA methylomes and histone-modification maps." Nat Rev Genet **8**(4): 286-298.
- Esteller, M. (2008). "Epigenetics in cancer." N Engl J Med **358**(11): 1148-1159.
- Esteller, M., et al. (2001). "A gene hypermethylation profile of human cancer." Cancer Res **61**(8): 3225-3229.
- Evans, S. M., et al. (2006). "Oxygen levels in normal and previously irradiated human skin as assessed by EF5 binding." J Invest Dermatol **126**(12): 2596-2606.
- Faller, W. J., et al. (2010). "Metallothionein 1E is methylated in malignant melanoma and increases sensitivity to cisplatin-induced apoptosis." Melanoma Res **20**(5): 392-400.
- Fargnoli, M. C., et al. (2008). "MC1R variants increase risk of melanomas harboring BRAF mutations." J Invest Dermatol **128**(10): 2485-2490.

- Feinmesser, M., et al. (2002). "Relationship of tumorigenic malignant melanomas to dermal elastin: an expression of tumor/stromal interaction that may be related to prognosis." Am J Dermatopathol **24**(2): 108-117.
- Feng, X. H. and R. Derynck (2005). "Specificity and versatility in tgf-beta signaling through Smads." Annu Rev Cell Dev Biol **21**: 659-693.
- Fernandez, A. F., et al. (2012). "A DNA methylation fingerprint of 1628 human samples." Genome Res **22**(2): 407-419.
- Fiol, D. F., et al. (2007). "Specific TSC22 domain transcripts are hypertonicity induced and alternatively spliced to protect mouse kidney cells during osmotic stress." FEBS J **274**(1): 109-124.
- Flaherty, K. T., et al. (2012). "Combined BRAF and MEK inhibition in melanoma with BRAF V600 mutations." N Engl J Med **367**(18): 1694-1703.
- Flaherty, K. T., et al. (2010). "Inhibition of mutated, activated BRAF in metastatic melanoma." N Engl J Med **363**(9): 809-819.
- Foulks, J. M., et al. (2012). "Epigenetic drug discovery: targeting DNA methyltransferases." J Biomol Screen **17**(1): 2-17.
- Franco, R., et al. (2008). "Oxidative stress, DNA methylation and carcinogenesis." Cancer Lett **266**(1): 6-11.
- Freedberg, D. E., et al. (2008). "Frequent p16-independent inactivation of p14ARF in human melanoma." J Natl Cancer Inst **100**(11): 784-795.
- Fuchshofer, R., et al. (2009). "Gene expression profiling of TGFbeta2- and/or BMP7-treated trabecular meshwork cells: Identification of Smad7 as a critical inhibitor of TGF-beta2 signaling." Exp Eye Res **88**(6): 1020-1032.
- Fukumura, D., et al. (2010). "Tumor microvasculature and microenvironment: novel insights through intravital imaging in pre-clinical models." Microcirculation **17**(3): 206-225.
- Fukushige, S. and A. Horii (2013). "DNA methylation in cancer: a gene silencing mechanism and the clinical potential of its biomarkers." Tohoku J Exp Med **229**(3): 173-185.
- Fung, C., et al. (2013). "p16(INK) (4a) deficiency promotes DNA hyper-replication and genetic instability in melanocytes." Pigment Cell Melanoma Res **26**(2): 236-246.
- Gal-Yam, E. N., et al. (2008). "Cancer epigenetics: modifications, screening, and therapy." Annu Rev Med **59**: 267-280.
- Garbe, C. and U. Leiter (2009). "Melanoma epidemiology and trends." Clin Dermatol **27**(1): 3-9.
- Garland, C. F., et al. (2003). "Epidemiologic evidence for different roles of ultraviolet A and B radiation in melanoma mortality rates." Ann Epidemiol **13**(6): 395-404.
- Garraway, L. A., et al. (2005). "Integrative genomic analyses identify MITF as a lineage survival oncogene amplified in malignant melanoma." Nature **436**(7047): 117-122.
- Gembarska, A., et al. (2012). "MDM4 is a key therapeutic target in cutaneous melanoma." Nat Med.
- George, J., et al. (2007). "Restoration of tissue factor pathway inhibitor-2 in a human glioblastoma cell line triggers caspase-mediated pathway and apoptosis." Clin Cancer Res **13**(12): 3507-3517.
- Gessler, F., et al. (2011). "Knockdown of TFPI-2 promotes migration and invasion of glioma cells." Neurosci Lett **497**(1): 49-54.
- Gilkes, D. M., et al. (2013). "Collagen prolyl hydroxylases are essential for breast cancer metastasis." Cancer Res **73**(11): 3285-3296.
- Ginouves, A., et al. (2008). "PHDs overactivation during chronic hypoxia "desensitizes" HIFalpha and protects cells from necrosis." Proc Natl Acad Sci U S A **105**(12): 4745-4750.

- Glockner, S. C., et al. (2009). "Methylation of TFPI2 in stool DNA: a potential novel biomarker for the detection of colorectal cancer." *Cancer Res* **69**(11): 4691-4699.
- Gloster, H. M., Jr. and K. Neal (2006). "Skin cancer in skin of color." *J Am Acad Dermatol* **55**(5): 741-760; quiz 761-744.
- Goel, V. K., et al. (2009). "Melanocytic nevus-like hyperplasia and melanoma in transgenic BRAFV600E mice." *Oncogene* **28**(23): 2289-2298.
- Goel, V. K., et al. (2006). "Examination of mutations in BRAF, NRAS, and PTEN in primary cutaneous melanoma." *J Invest Dermatol* **126**(1): 154-160.
- Goldstein, A. M., et al. (2006). "High-risk melanoma susceptibility genes and pancreatic cancer, neural system tumors, and uveal melanoma across GenoMEL." *Cancer Res* **66**(20): 9818-9828.
- Goldstein, A. M. and M. A. Tucker, Eds. (2001). *familial melanoma and its management*
genetic predisposition to cancer. London, UK, Edward Arnold Publishers Ltd.
- Gorres, K. L. and R. T. Raines (2010). "Prolyl 4-hydroxylase." *Crit Rev Biochem Mol Biol* **45**(2): 106-124.
- Graff, J. R., et al. (2000). "Methylation patterns of the E-cadherin 5' CpG island are unstable and reflect the dynamic, heterogeneous loss of E-cadherin expression during metastatic progression." *J Biol Chem* **275**(4): 2727-2732.
- Greer, S. N., et al. (2012). "The updated biology of hypoxia-inducible factor." *EMBO J* **31**(11): 2448-2460.
- Gudbjartsson, D. F., et al. (2008). "ASIP and TYR pigmentation variants associate with cutaneous melanoma and basal cell carcinoma." *Nat Genet* **40**(7): 886-891.
- Gupta, R., et al. (2010). "Advances in genome-wide DNA methylation analysis." *Biotechniques* **49**(4): iii-xi.
- Gwosdz, C., et al. (2006). "Comprehensive analysis of the p53 status in mucosal and cutaneous melanomas." *Int J Cancer* **118**(3): 577-582.
- Haffner, M. C., et al. (2011). "Global 5-hydroxymethylcytosine content is significantly reduced in tissue stem/progenitor cell compartments and in human cancers." *Oncotarget* **2**(8): 627-637.
- Hamilton, J. P. (2011). "Epigenetics: principles and practice." *Dig Dis* **29**(2): 130-135.
- Han, J., et al. (1997). "A cell binding domain from the alpha3 chain of type IV collagen inhibits proliferation of melanoma cells." *J Biol Chem* **272**(33): 20395-20401.
- Hanahan, D. and R. A. Weinberg (2011). "Hallmarks of cancer: the next generation." *Cell* **144**(5): 646-674.
- Hannigan, A., et al. (2011). "Epigenetic downregulation of human disabled homolog 2 switches TGF-beta from a tumor suppressor to a tumor promoter." *J Clin Invest* **120**(8): 2842-2857.
- Hansen, K. D., et al. (2011). "Increased methylation variation in epigenetic domains across cancer types." *Nat Genet* **43**(8): 768-775.
- Harris, A. L. (2002). "Hypoxia--a key regulatory factor in tumour growth." *Nat Rev Cancer* **2**(1): 38-47.
- Hatzimichael, E., et al. (2010). "The prolyl-hydroxylase EGLN3 and not EGLN1 is inactivated by methylation in plasma cell neoplasia." *Eur J Haematol* **84**(1): 47-51.
- Hatzimichael, E., et al. (2012). "The collagen prolyl hydroxylases are novel transcriptionally silenced genes in lymphoma." *Br J Cancer* **107**(8): 1423-1432.

- Haugen, B. R., et al. (2004). "Retinoic acid and retinoid X receptors are differentially expressed in thyroid cancer and thyroid carcinoma cell lines and predict response to treatment with retinoids." *J Clin Endocrinol Metab* **89**(1): 272-280.
- Hauschild, A., et al. (2012). "Dabrafenib in BRAF-mutated metastatic melanoma: a multicentre, open-label, phase 3 randomised controlled trial." *Lancet* **380**(9839): 358-365.
- Hayward, N. K. (2003). "Genetics of melanoma predisposition." *Oncogene* **22**(20): 3053-3062.
- He, Y., et al. (2011). "Identification of GPX3 epigenetically silenced by CpG methylation in human esophageal squamous cell carcinoma." *Dig Dis Sci* **56**(3): 681-688.
- Hearing, V. J. (1999). "Biochemical control of melanogenesis and melanosomal organization." *J Invest Dermatol Symp Proc* **4**(1): 24-28.
- Hegi, M. E., et al. (2005). "MGMT gene silencing and benefit from temozolomide in glioblastoma." *N Engl J Med* **352**(10): 997-1003.
- Helaakoski, T., et al. (1990). "Increases in mRNA concentrations of the alpha and beta subunits of prolyl 4-hydroxylase accompany increased gene expression of type IV collagen during differentiation of mouse F9 cells." *J Biol Chem* **265**(20): 11413-11416.
- Hemesath, T. J., et al. (1994). "microphthalmia, a critical factor in melanocyte development, defines a discrete transcription factor family." *Genes Dev* **8**(22): 2770-2780.
- Herman, J. G. and S. B. Baylin (2003). "Gene silencing in cancer in association with promoter hypermethylation." *N Engl J Med* **349**(21): 2042-2054.
- Hermeking, H. (2007). "p53 enters the microRNA world." *Cancer Cell* **12**(5): 414-418.
- Heyn, H., et al. (2013). "DNA methylation profiling in breast cancer discordant identical twins identifies DOK7 as novel epigenetic biomarker." *Carcinogenesis* **34**(1): 102-108.
- Heyn, H. and M. Esteller (2012). "DNA methylation profiling in the clinic: applications and challenges." *Nat Rev Genet* **13**(10): 679-692.
- Hibi, K., et al. (2011). "Detection of TFPI2 methylation in the serum of gastric cancer patients." *Anticancer Res* **31**(11): 3835-3838.
- Hibi, K., et al. (2012). "Methylation of TFPI2 no longer detected in the serum DNA of colorectal cancer patients after curative surgery." *Anticancer Res* **32**(3): 787-790.
- Hill, H. Z. and G. J. Hill (2000). "UVA, pheomelanin and the carcinogenesis of melanoma." *Pigment Cell Res* **13 Suppl 8**: 140-144.
- Hino, S., et al. (2000). "Nuclear translocation of TSC-22 (TGF-beta-stimulated clone-22) concomitant with apoptosis: TSC-22 as a putative transcriptional regulator." *Biochem Biophys Res Commun* **278**(3): 659-664.
- Hockberger, P. E. (2002). "A history of ultraviolet photobiology for humans, animals and microorganisms." *Photochem Photobiol* **76**(6): 561-579.
- Hodi, F. S., et al. (2010). "Improved survival with ipilimumab in patients with metastatic melanoma." *N Engl J Med* **363**(8): 711-723.
- Hodis, E., et al. (2012). "A landscape of driver mutations in melanoma." *Cell* **150**(2): 251-263.
- Hoffmann, K., et al. (2000). "UV transmission measurements of small skin specimens with special quartz cuvettes." *Dermatology* **201**(4): 307-311.
- Hogel, H., et al. (2011). "Prolyl hydroxylase PHD3 enhances the hypoxic survival and G1 to S transition of carcinoma cells." *PLoS One* **6**(11): e27112.
- Holliday, R. (1987). "The inheritance of epigenetic defects." *Science* **238**(4824): 163-170.
- Holster, T., et al. (2007). "Loss of assembly of the main basement membrane collagen, type IV, but not fibril-forming collagens and embryonic death in collagen prolyl 4-hydroxylase I null mice." *J Biol Chem* **282**(4): 2512-2519.
- Homig-Holzel, C., et al. (2011). "Antagonistic TSC22D1 variants control BRAF(E600)-induced senescence." *EMBO J* **30**(9): 1753-1765.

- Howell, P. M., Jr., et al. (2009). "Epigenetics in human melanoma." Cancer Control **16**(3): 200-218.
- Huang, K. T., et al. (2010). "DNA methylation analysis of the HIF-1alpha prolyl hydroxylase domain genes PHD1, PHD2, PHD3 and the factor inhibiting HIF gene FIH in invasive breast carcinomas." Histopathology **57**(3): 451-460.
- Huang, L. E., et al. (1998). "Regulation of hypoxia-inducible factor 1alpha is mediated by an O2-dependent degradation domain via the ubiquitin-proteasome pathway." Proc Natl Acad Sci U S A **95**(14): 7987-7992.
- Hutton, J. J., Jr., et al. (1967). "Conversion of the amino acid sequence gly-pro-pro in protein to gly-pro-hyp by collagen proline hydroxylase." Arch Biochem Biophys **121**(2): 384-391.
- Ikushima, H. and K. Miyazono (2010). "TGFbeta signalling: a complex web in cancer progression." Nat Rev Cancer **10**(6): 415-424.
- ISD. (2011). "Cancer Statistics, skin cancer, Scotland." from <http://www.isdscotland.org/Health-Topics/Cancer/Cancer-Statistics/Skin/#melanoma>.
- Izumi, H., et al. (2000). "Tissue factor pathway inhibitor-2 suppresses the production of active matrix metalloproteinase-2 and is down-regulated in cells harboring activated ras oncogenes." FEBS Lett **481**(1): 31-36.
- Jaakkola, P., et al. (2001). "Targeting of HIF-alpha to the von Hippel-Lindau ubiquitylation complex by O2-regulated prolyl hydroxylation." Science **292**(5516): 468-472.
- JANCIN, B. (2009). National Study: Acral Lentiginous Melanoma Incidence Remains Steady. CUTANEOUS ONCOLOGY.
- Jang, S. and M. B. Atkins (2013). "Which drug, and when, for patients with BRAF-mutant melanoma?" Lancet Oncol **14**(2): e60-69.
- Jee, C. D., et al. (2009). "Identification of genes epigenetically silenced by CpG methylation in human gastric carcinoma." Eur J Cancer **45**(7): 1282-1293.
- Jeffrey, K. L., et al. (2006). "Positive regulation of immune cell function and inflammatory responses by phosphatase PAC-1." Nat Immunol **7**(3): 274-283.
- Jenkins, N. C., et al. (2011). "The p16(INK4A) tumor suppressor regulates cellular oxidative stress." Oncogene **30**(3): 265-274.
- Jhappan, C., et al. (2003). "Ultraviolet radiation and cutaneous malignant melanoma." Oncogene **22**(20): 3099-3112.
- Jones, P. A. (2012). "Functions of DNA methylation: islands, start sites, gene bodies and beyond." Nat Rev Genet **13**(7): 484-492.
- Jonsson, A., et al. (2010). "High frequency of p16(INK4A) promoter methylation in NRAS-mutated cutaneous melanoma." J Invest Dermatol **130**(12): 2809-2817.
- Joseph, L. J., et al. (1988). "Molecular cloning, sequencing, and mapping of EGR2, a human early growth response gene encoding a protein with "zinc-binding finger" structure." Proc Natl Acad Sci U S A **85**(19): 7164-7168.
- Kaidbey, K. H., et al. (1979). "Photoprotection by melanin--a comparison of black and Caucasian skin." J Am Acad Dermatol **1**(3): 249-260.
- Kaminskas, E., et al. (2005). "FDA drug approval summary: azacitidine (5-azacytidine, Vidaza) for injectable suspension." Oncologist **10**(3): 176-182.
- Kanavy, H. E. and M. R. Gerstenblith (2011). "Ultraviolet radiation and melanoma." Semin Cutan Med Surg **30**(4): 222-228.
- Kantarjian, H., et al. (2007). "Results of a randomized study of 3 schedules of low-dose decitabine in higher-risk myelodysplastic syndrome and chronic myelomonocytic leukemia." Blood **109**(1): 52-57.

- Karst, A. M., et al. (2005). "PUMA expression is significantly reduced in human cutaneous melanomas." *Oncogene* **24**(6): 1111-1116.
- Kasparian, N. A., et al. (2007). "Anticipated uptake of genetic testing for familial melanoma in an Australian sample: An exploratory study." *Psychooncology* **16**(1): 69-78.
- Keshet, I., et al. (2006). "Evidence for an instructive mechanism of de novo methylation in cancer cells." *Nat Genet* **38**(2): 149-153.
- Kilaru, V., et al. (2012). "MethLAB: a graphical user interface package for the analysis of array-based DNA methylation data." *Epigenetics* **7**(3): 225-229.
- Kim, J. K., et al. (2009). "Epigenetic mechanisms in mammals." *Cell Mol Life Sci* **66**(4): 596-612.
- Kisiel, W., et al. (1994). "Evidence that a second human tissue factor pathway inhibitor (TFPI-2) and human placental protein 5 are equivalent." *Blood* **84**(12): 4384-4385.
- Klose, R. J. and A. P. Bird (2006). "Genomic DNA methylation: the mark and its mediators." *Trends Biochem Sci* **31**(2): 89-97.
- Kocemba, K. A., et al. (2012). "Transcriptional silencing of the Wnt-antagonist DKK1 by promoter methylation is associated with enhanced Wnt signaling in advanced multiple myeloma." *PLoS One* **7**(2): e30359.
- Konduri, S. D., et al. (2001). "Overexpression of tissue factor pathway inhibitor-2 (TFPI-2), decreases the invasiveness of prostate cancer cells in vitro." *Int J Oncol* **18**(1): 127-131.
- Korshunova, Y., et al. (2008). "Massively parallel bisulphite pyrosequencing reveals the molecular complexity of breast cancer-associated cytosine-methylation patterns obtained from tissue and serum DNA." *Genome Res* **18**(1): 19-29.
- Korytowski, W., et al. (1987). "Photoinduced generation of hydrogen peroxide and hydroxyl radicals in melanins." *Photochem Photobiol* **45**(2): 185-190.
- Kriaucionis, S. and N. Heintz (2009). "The nuclear DNA base 5-hydroxymethylcytosine is present in Purkinje neurons and the brain." *Science* **324**(5929): 929-930.
- Kukkola, L., et al. (2003). "Identification and characterization of a third human, rat, and mouse collagen prolyl 4-hydroxylase isoenzyme." *J Biol Chem* **278**(48): 47685-47693.
- Kuphal, S., et al. (2006). "Expression of Dickkopf genes is strongly reduced in malignant melanoma." *Oncogene* **25**(36): 5027-5036.
- Lahtz, C., et al. (2010). "Methylation of PTEN as a prognostic factor in malignant melanoma of the skin." *J Invest Dermatol* **130**(2): 620-622.
- Laird, P. W. (2010). "Principles and challenges of genomewide DNA methylation analysis." *Nat Rev Genet* **11**(3): 191-203.
- Landi, M. T., et al. (2006). "MC1R germline variants confer risk for BRAF-mutant melanoma." *Science* **313**(5786): 521-522.
- Lecomte, T., et al. (2002). "Detection of free-circulating tumor-associated DNA in plasma of colorectal cancer patients and its association with prognosis." *Int J Cancer* **100**(5): 542-548.
- Lens, M. (2008). "Current clinical overview of cutaneous melanoma." *Br J Nurs* **17**(5): 300-305.
- Lens, M. B. and M. Dawes (2004). "Global perspectives of contemporary epidemiological trends of cutaneous malignant melanoma." *Br J Dermatol* **150**(2): 179-185.
- Ley, R. D. (1997). "Ultraviolet radiation A-induced precursors of cutaneous melanoma in *Monodelphis domestica*." *Cancer Res* **57**(17): 3682-3684.
- Li, G., et al. (2003). "Reciprocal regulation of MelCAM and AKT in human melanoma." *Oncogene* **22**(44): 6891-6899.
- Li, L., et al. (2012). "DNA methylation in peripheral blood: a potential biomarker for cancer molecular epidemiology." *J Epidemiol* **22**(5): 384-394.

- Lian, C. G., et al. (2012). "Loss of 5-hydroxymethylcytosine is an epigenetic hallmark of melanoma." *Cell* **150**(6): 1135-1146.
- Liu, S., et al. (2009). "The 14-3-3sigma gene promoter is methylated in both human melanocytes and melanoma." *BMC Cancer* **9**: 162.
- Liu, S., et al. (2008). "Identification of novel epigenetically modified genes in human melanoma via promoter methylation gene profiling." *Pigment Cell Melanoma Res* **21**(5): 545-558.
- Liu, W., et al. (2004). "Effects of overexpression of ephrin-B2 on tumour growth in human colorectal cancer." *Br J Cancer* **90**(8): 1620-1626.
- Loercher, A. E., et al. (2005). "MITF links differentiation with cell cycle arrest in melanocytes by transcriptional activation of INK4A." *J Cell Biol* **168**(1): 35-40.
- Long, G. V., et al. (2012). "Dabrafenib in patients with Val600Glu or Val600Lys BRAF-mutant melanoma metastatic to the brain (BREAK-MB): a multicentre, open-label, phase 2 trial." *Lancet Oncol* **13**(11): 1087-1095.
- Lopez-Serra, L. and M. Esteller (2008). "Proteins that bind methylated DNA and human cancer: reading the wrong words." *Br J Cancer* **98**(12): 1881-1885.
- Lopez, J., et al. (2009). "The context and potential of epigenetics in oncology." *Br J Cancer* **100**(4): 571-577.
- Lujambio, A., et al. (2008). "A microRNA DNA methylation signature for human cancer metastasis." *Proc Natl Acad Sci U S A* **105**(36): 13556-13561.
- Mackie, R. M. (2000). "Malignant melanoma: clinical variants and prognostic indicators." *Clin Exp Dermatol* **25**(6): 471-475.
- Mackie, R. M., et al. (2009). "Epidemiology of invasive cutaneous melanoma." *Ann Oncol* **20 Suppl 6**: vi1-7.
- Madhunapantula, S. V. and G. P. Robertson (2009). "The PTEN-AKT3 signaling cascade as a therapeutic target in melanoma." *Pigment Cell Melanoma Res* **22**(4): 400-419.
- Maeshima, Y., et al. (2000). "Distinct antitumor properties of a type IV collagen domain derived from basement membrane." *J Biol Chem* **275**(28): 21340-21348.
- Maldonado, J. L., et al. (2003). "Determinants of BRAF mutations in primary melanomas." *J Natl Cancer Inst* **95**(24): 1878-1890.
- Maunakea, A. K., et al. (2010). "Conserved role of intragenic DNA methylation in regulating alternative promoters." *Nature* **466**(7303): 253-257.
- Mbulaitaye, S. M., et al. (2006). "High levels of Epstein-Barr virus DNA in saliva and peripheral blood from Ugandan mother-child pairs." *J Infect Dis* **193**(3): 422-426.
- McAlhany, S. J., et al. (2003). "Promotion of angiogenesis by ps20 in the differential reactive stroma prostate cancer xenograft model." *Cancer Res* **63**(18): 5859-5865.
- McGill, G. G., et al. (2002). "Bcl2 regulation by the melanocyte master regulator Mitf modulates lineage survival and melanoma cell viability." *Cell* **109**(6): 707-718.
- Meier, F., et al. (2000). "Human melanoma progression in skin reconstructs : biological significance of bFGF." *Am J Pathol* **156**(1): 193-200.
- Menezes, M. E., et al. (2012). "Dickkopf1: a tumor suppressor or metastasis promoter?" *Int J Cancer* **130**(7): 1477-1483.
- Mervic, L. (2012). "Prognostic factors in patients with localized primary cutaneous melanoma." *Acta Dermatovenerol Alp Panonica Adriat* **21**(2): 27-31.
- MethPrimer. from <http://www.urogene.org/methprimer/index1.html>.
- Mikata, R., et al. (2006). "Analysis of genes upregulated by the demethylating agent 5-aza-2'-deoxycytidine in gastric cancer cell lines." *Int J Cancer* **119**(7): 1616-1622.
- Miller, A. J. and M. C. Mihm, Jr. (2006). "Melanoma." *N Engl J Med* **355**(1): 51-65.

- Millet, C. and Y. E. Zhang (2007). "Roles of Smad3 in TGF-beta signaling during carcinogenesis." Crit Rev Eukaryot Gene Expr **17**(4): 281-293.
- Mills, C. N., et al. (2009). "Expression and function of hypoxia inducible factor-1 alpha in human melanoma under non-hypoxic conditions." Mol Cancer **8**: 104.
- Mirmohammadsadegh, A., et al. (2006). "Epigenetic silencing of the PTEN gene in melanoma." Cancer Res **66**(13): 6546-6552.
- Mitra, D., et al. (2012). "An ultraviolet-radiation-independent pathway to melanoma carcinogenesis in the red hair/fair skin background." Nature **491**(7424): 449-453.
- Mori, T., et al. (2006). "Estrogen receptor-alpha methylation predicts melanoma progression." Cancer Res **66**(13): 6692-6698.
- Muthusamy, V., et al. (2006). "Amplification of CDK4 and MDM2 in malignant melanoma." Genes Chromosomes Cancer **45**(5): 447-454.
- Myllyharju, J. (2003). "Prolyl 4-hydroxylases, the key enzymes of collagen biosynthesis." Matrix Biol **22**(1): 15-24.
- Na, Y., et al. (2012). "Promoter methylation of Wnt antagonist DKK1 gene and prognostic value in Korean patients with non-small cell lung cancers." Cancer Biomark **12**(2): 73-79.
- Nading, M. A., et al. (2010). "Implications of the 2009 American Joint Committee on Cancer Melanoma Staging and Classification on dermatologists and their patients." Semin Cutan Med Surg **29**(3): 142-147.
- Nagy, J. A., et al. (2009). "Why are tumour blood vessels abnormal and why is it important to know?" Br J Cancer **100**(6): 865-869.
- Nakashiro, K., et al. (1998). "Down-regulation of TSC-22 (transforming growth factor beta-stimulated clone 22) markedly enhances the growth of a human salivary gland cancer cell line in vitro and in vivo." Cancer Res **58**(3): 549-555.
- Nakayama, K., et al. (2009). "The ubiquitin ligase Siah2 and the hypoxia response." Mol Cancer Res **7**(4): 443-451.
- Nathanson, K. L., et al. (2013). "Tumor genetic analyses of patients with metastatic melanoma treated with the BRAF inhibitor Dabrafenib (GSK2118436)." Clin Cancer Res.
- National Institute of Allergy and Infectious Diseases (NIAID), N. DAVID Bioinformatics Resources 6.7.
- Ndlovu, M. N., et al. (2011). "Exposing the DNA methylome iceberg." Trends Biochem Sci **36**(7): 381-387.
- Neuman, H. B., et al. (2008). "A single-institution validation of the AJCC staging system for stage IV melanoma." Ann Surg Oncol **15**(7): 2034-2041.
- Nobeyama, Y., et al. (2007). "Silencing of tissue factor pathway inhibitor-2 gene in malignant melanomas." Int J Cancer **121**(2): 301-307.
- Noetzel, E., et al. (2010). "Intermediate filament dynamics and breast cancer: aberrant promoter methylation of the Synemin gene is associated with early tumor relapse." Oncogene **29**(34): 4814-4825.
- Nogueira, C., et al. (2010). "Cooperative interactions of PTEN deficiency and RAS activation in melanoma metastasis." Oncogene **29**(47): 6222-6232.
- Nojima, M., et al. (2009). "Genomic screening for genes silenced by DNA methylation revealed an association between RASD1 inactivation and dexamethasone resistance in multiple myeloma." Clin Cancer Res **15**(13): 4356-4364.
- North West Cancer Intelligence Service, N. (2011). "Age specific mortality rates in England among 15 - 24 year olds by SHA, 2008-2010." from <http://www.nwcis.nhs.uk/tya/tya-mortality/mortality-by-sha.aspx>.

- NZ, D. "Lentigo maligna and lentigo maligna melanoma." from <http://dermnetnz.org/lesions/lentigo-maligna.html>.
- Pacheco, I., et al. (2011). "Towards new therapeutic approaches for malignant melanoma." *Expert Rev Mol Med* **13**: e33.
- Palmieri, G., et al. (2009). "Main roads to melanoma." *J Transl Med* **7**: 86.
- Pan, H., et al. (2012). "Measuring the methylome in clinical samples: improved processing of the Infinium Human Methylation450 BeadChip Array." *Epigenetics* **7**(10): 1173-1187.
- Pardoll, D. M. (2012). "The blockade of immune checkpoints in cancer immunotherapy." *Nat Rev Cancer* **12**(4): 252-264.
- Parisi, F., et al. (2012). "Integrated analysis of tumor samples sheds light on tumor heterogeneity." *Yale J Biol Med* **85**(3): 347-361.
- Pasco, S., et al. (2005). "Control of melanoma cell invasion by type IV collagen." *Cancer Detect Prev* **29**(3): 260-266.
- Pastorino, L., et al. (2008). "CDKN2A mutations and MC1R variants in Italian patients with single or multiple primary melanoma." *Pigment Cell Melanoma Res* **21**(6): 700-709.
- Patton, E. E., et al. (2005). "BRAF mutations are sufficient to promote nevi formation and cooperate with p53 in the genesis of melanoma." *Curr Biol* **15**(3): 249-254.
- Paulsson, M. (1992). "Basement membrane proteins: structure, assembly, and cellular interactions." *Crit Rev Biochem Mol Biol* **27**(1-2): 93-127.
- Pescador, N., et al. (2005). "Identification of a functional hypoxia-responsive element that regulates the expression of the egl nine homologue 3 (egln3/phd3) gene." *Biochem J* **390**(Pt 1): 189-197.
- Petersen, L. C., et al. (1996). "Inhibitory properties of a novel human Kunitz-type protease inhibitor homologous to tissue factor pathway inhibitor." *Biochemistry* **35**(1): 266-272.
- Place, T. L., et al. (2011). "Aberrant promoter CpG methylation is a mechanism for impaired PHD3 expression in a diverse set of malignant cells." *PLoS One* **6**(1): e14617.
- Pollock, P. M., et al. (2003). "High frequency of BRAF mutations in nevi." *Nat Genet* **33**(1): 19-20.
- Pryds, O., et al. (1987). "HLA-DR factors associated with postpartum hypothyroidism: an early manifestation of Hashimoto's thyroiditis?" *Tissue Antigens* **30**(1): 34-37.
- Qi, J., et al. (2008). "The ubiquitin ligase Siah2 regulates tumorigenesis and metastasis by HIF-dependent and -independent pathways." *Proc Natl Acad Sci U S A* **105**(43): 16713-16718.
- Quelle, D. E., et al. (1995). "Alternative reading frames of the INK4a tumor suppressor gene encode two unrelated proteins capable of inducing cell cycle arrest." *Cell* **83**(6): 993-1000.
- Raimondi, S., et al. (2008). "MC1R variants, melanoma and red hair color phenotype: a meta-analysis." *Int J Cancer* **122**(12): 2753-2760.
- Ramirez, R. D., et al. (1999). "Progressive increase in telomerase activity from benign melanocytic conditions to malignant melanoma." *Neoplasia* **1**(1): 42-49.
- Rao, C. N., et al. (1999). "Regulation of ProMMP-1 and ProMMP-3 activation by tissue factor pathway inhibitor-2/matrix-associated serine protease inhibitor." *Biochem Biophys Res Commun* **255**(1): 94-98.
- Ravanat, J. L., et al. (2001). "Direct and indirect effects of UV radiation on DNA and its components." *J Photochem Photobiol B* **63**(1-3): 88-102.
- Reifenberger, J., et al. (2000). "Allelic losses on chromosome arm 10q and mutation of the PTEN (MMAC1) tumour suppressor gene in primary and metastatic malignant melanomas." *Virchows Arch* **436**(5): 487-493.
- Reik, W., et al. (2001). "Epigenetic reprogramming in mammalian development." *Science* **293**(5532): 1089-1093.

- Reik, W. and J. Walter (2001). "Genomic imprinting: parental influence on the genome." Nat Rev Genet **2**(1): 21-32.
- Rentsch, C. A., et al. (2006). "Differential expression of TGFbeta-stimulated clone 22 in normal prostate and prostate cancer." Int J Cancer **118**(4): 899-906.
- Retsas, S., et al. (2002). "Prognostic factors of cutaneous melanoma and a new staging system proposed by the American Joint Committee on Cancer (AJCC): validation in a cohort of 1284 patients." Eur J Cancer **38**(4): 511-516.
- Rhodes, D. R., et al. (2004). "ONCOMINE: a cancer microarray database and integrated data-mining platform." Neoplasia **6**(1): 1-6.
- Rigel, D. S. (2005). "cancer of the skin."
- Robert, C., et al. (2011). "Ipilimumab plus dacarbazine for previously untreated metastatic melanoma." N Engl J Med **364**(26): 2517-2526.
- Rodenhiser, D. I. (2009). "Epigenetic contributions to cancer metastasis." Clin Exp Metastasis **26**(1): 5-18.
- Rofstad, E. K. and T. Danielsen (1999). "Hypoxia-induced metastasis of human melanoma cells: involvement of vascular endothelial growth factor-mediated angiogenesis." Br J Cancer **80**(11): 1697-1707.
- Rollin, J., et al. (2005). "Expression and methylation status of tissue factor pathway inhibitor-2 gene in non-small-cell lung cancer." Br J Cancer **92**(4): 775-783.
- Ronaghi, M. (2001). "Pyrosequencing sheds light on DNA sequencing." Genome Res **11**(1): 3-11.
- Rosenberger, C., et al. (2007). "Upregulation of hypoxia-inducible factors in normal and psoriatic skin." J Invest Dermatol **127**(10): 2445-2452.
- Rothhammer, T. and A. K. Bosserhoff (2007). "Epigenetic events in malignant melanoma." Pigment Cell Res **20**(2): 92-111.
- Sadej, R., et al. (2006). "Expression of ecto-5'-nucleotidase (eN, CD73) in cell lines from various stages of human melanoma." Melanoma Res **16**(3): 213-222.
- Safford, M., et al. (2005). "Egr-2 and Egr-3 are negative regulators of T cell activation." Nat Immunol **6**(5): 472-480.
- Sandoval, J. and M. Esteller (2012). "Cancer epigenomics: beyond genomics." Curr Opin Genet Dev **22**(1): 50-55.
- Sarasin, A. (1999). "The molecular pathways of ultraviolet-induced carcinogenesis." Mutat Res **428**(1-2): 5-10.
- Sato, N., et al. (2005). "Epigenetic inactivation of TFPI-2 as a common mechanism associated with growth and invasion of pancreatic ductal adenocarcinoma." Oncogene **24**(5): 850-858.
- Schwarz, T. (2008). "25 years of UV-induced immunosuppression mediated by T cells-from disregarded T suppressor cells to highly respected regulatory T cells." Photochem Photobiol **84**(1): 10-18.
- Sciorra, V. A., et al. (2012). "Suppression of glioma progression by EglN3." PLoS One **7**(8): e40053.
- Sekulic, A., et al. (2010). "Activating BRAF mutations in eruptive melanocytic naevi." Br J Dermatol **163**(5): 1095-1098.
- Selak, M. A., et al. (2005). "Succinate links TCA cycle dysfunction to oncogenesis by inhibiting HIF-alpha prolyl hydroxylase." Cancer Cell **7**(1): 77-85.
- Semenza, G. L. (2001). "HIF-1, O(2), and the 3 PHDs: how animal cells signal hypoxia to the nucleus." Cell **107**(1): 1-3.
- Semenza, G. L. (2004). "Hydroxylation of HIF-1: oxygen sensing at the molecular level." Physiology (Bethesda) **19**: 176-182.

- Serrano, M., et al. (1996). "Role of the INK4a locus in tumor suppression and cell mortality." Cell **85**(1): 27-37.
- Setlow, R. B., et al. (1993). "Wavelengths effective in induction of malignant melanoma." Proc Natl Acad Sci U S A **90**(14): 6666-6670.
- Shah, R., et al. (2009). "The prolyl 3-hydroxylases P3H2 and P3H3 are novel targets for epigenetic silencing in breast cancer." Br J Cancer **100**(10): 1687-1696.
- Shaw, R. J., et al. (2008). "The role of pyrosequencing in head and neck cancer epigenetics: correlation of quantitative methylation data with gene expression." Arch Otolaryngol Head Neck Surg **134**(3): 251-256.
- Shen, J., et al. (2013). "Exploring genome-wide DNA methylation profiles altered in hepatocellular carcinoma using Infinium HumanMethylation 450 BeadChips." Epigenetics **8**(1): 34-43.
- Shibanuma, M., et al. (1992). "Isolation of a gene encoding a putative leucine zipper structure that is induced by transforming growth factor beta 1 and other growth factors." J Biol Chem **267**(15): 10219-10224.
- Shostak, K. O., et al. (2003). "Downregulation of putative tumor suppressor gene TSC-22 in human brain tumors." J Surg Oncol **82**(1): 57-64.
- Shostak, K. O., et al. (2005). "Patterns of expression of TSC-22 protein in astrocytic gliomas." Exp Oncol **27**(4): 314-318.
- Shoulders, M. D. and R. T. Raines (2009). "Collagen structure and stability." Annu Rev Biochem **78**: 929-958.
- Silva, J. M., et al. (1999). "Presence of tumor DNA in plasma of breast cancer patients: clinicopathological correlations." Cancer Res **59**(13): 3251-3256.
- Soengas, M. S., et al. (2001). "Inactivation of the apoptosis effector Apaf-1 in malignant melanoma." Nature **409**(6817): 207-211.
- Sondak, V. K., et al. (2013). "Evidence-based clinical practice guidelines on the use of sentinel lymph node biopsy in melanoma." Am Soc Clin Oncol Educ Book **2013**: 320-325.
- Song, M. J., et al. (2013). "Diagnostic value of CA125 as a predictor of recurrence in advanced ovarian cancer." Eur J Gynaecol Oncol **34**(2): 148-151.
- Soong, S. J., et al. (2010). "Predicting survival outcome of localized melanoma: an electronic prediction tool based on the AJCC Melanoma Database." Ann Surg Oncol **17**(8): 2006-2014.
- Sova, P., et al. (2006). "Discovery of novel methylation biomarkers in cervical carcinoma by global demethylation and microarray analysis." Cancer Epidemiol Biomarkers Prev **15**(1): 114-123.
- Sparrow, L. E., et al. (1995). "p53 gene mutation and expression in naevi and melanomas." Melanoma Res **5**(2): 93-100.
- Sproul, D., et al. (2011). "Transcriptionally repressed genes become aberrantly methylated and distinguish tumors of different lineages in breast cancer." Proc Natl Acad Sci U S A **108**(11): 4364-4369.
- Stagg, J., et al. (2012). "CD73-deficient mice are resistant to carcinogenesis." Cancer Res **72**(9): 2190-2196.
- Stagg, J., et al. (2011). "CD73-deficient mice have increased antitumor immunity and are resistant to experimental metastasis." Cancer Res **71**(8): 2892-2900.
- Stagg, J., et al. (2010). "Anti-CD73 antibody therapy inhibits breast tumor growth and metastasis." Proc Natl Acad Sci U S A **107**(4): 1547-1552.

- Sturgeon, S. R., et al. (2012). "Detection of promoter methylation of tumor suppressor genes in serum DNA of breast cancer cases and benign breast disease controls." Epigenetics **7**(11): 1258-1267.
- Su, Y., et al. (2010). "PHD3 regulates differentiation, tumour growth and angiogenesis in pancreatic cancer." Br J Cancer **103**(10): 1571-1579.
- Sulaimon, S. S. and B. E. Kitchell (2003). "The biology of melanocytes." Vet Dermatol **14**(2): 57-65.
- Sun, F. K., et al. (2013). "Detection of TFPI2 Methylation in the Serum of Hepatocellular Carcinoma Patients." Dig Dis Sci **58**(4): 1010-1015.
- Swalwell, H., et al. (2012). "Investigating the role of melanin in UVA/UVB- and hydrogen peroxide-induced cellular and mitochondrial ROS production and mitochondrial DNA damage in human melanoma cells." Free Radic Biol Med **52**(3): 626-634.
- Swerdlow, A. J. and M. A. Weinstock (1998). "Do tanning lamps cause melanoma? An epidemiologic assessment." J Am Acad Dermatol **38**(1): 89-98.
- Tachibana, M., et al. (2007). "Expression and prognostic significance of EFNB2 and EphB4 genes in patients with oesophageal squamous cell carcinoma." Dig Liver Dis **39**(8): 725-732.
- Tahara, T., et al. (2013). "Examination of whole blood DNA methylation as a potential risk marker for gastric cancer." Cancer Prev Res (Phila).
- Takada, H., et al. "Tissue factor pathway inhibitor 2 (TFPI2) is frequently silenced by aberrant promoter hypermethylation in gastric cancer." Cancer Genet Cytogenet **197**(1): 16-24.
- Tandler, N., et al. (2012). "Protein and non-protein biomarkers in melanoma: a critical update." Amino Acids **43**(6): 2203-2230.
- Tanemura, A., et al. (2009). "CpG island methylator phenotype predicts progression of malignant melanoma." Clin Cancer Res **15**(5): 1801-1807.
- Thompson, J. F. and H. M. Shaw (2007). "Sentinel node mapping for melanoma: results of trials and current applications." Surg Oncol Clin N Am **16**(1): 35-54.
- Timpl, R. and M. Aumailley (1989). "Biochemistry of basement membranes." Adv Nephrol Necker Hosp **18**: 59-76.
- Tommasi, S., et al. (1997). "Sunlight induces pyrimidine dimers preferentially at 5-methylcytosine bases." Cancer Res **57**(21): 4727-4730.
- Trevino-Villarreal, J. H., et al. (2011). "Host-derived pericytes and Sca-1+ cells predominate in the MART-1- stroma fraction of experimentally induced melanoma." J Histochem Cytochem **59**(12): 1060-1075.
- Tsai, J., et al. (2008). "Discovery of a selective inhibitor of oncogenic B-Raf kinase with potent antimelanoma activity." Proc Natl Acad Sci U S A **105**(8): 3041-3046.
- Tsao, H., et al. (2004). "Genetic interaction between NRAS and BRAF mutations and PTEN/MMAC1 inactivation in melanoma." J Invest Dermatol **122**(2): 337-341.
- Tsao, H., et al. (1998). "Identification of PTEN/MMAC1 alterations in uncultured melanomas and melanoma cell lines." Oncogene **16**(26): 3397-3402.
- Ugurel, S., et al. (2009). "Tumor biomarkers in melanoma." Cancer Control **16**(3): 219-224.
- Unoki, M. and Y. Nakamura (2001). "Growth-suppressive effects of BPOZ and EGR2, two genes involved in the PTEN signaling pathway." Oncogene **20**(33): 4457-4465.
- Unoki, M. and Y. Nakamura (2003). "EGR2 induces apoptosis in various cancer cell lines by direct transactivation of BNIP3L and BAK." Oncogene **22**(14): 2172-2185.
- Unoki, M. and Y. Nakamura (2003). "Methylation at CpG islands in intron 1 of EGR2 confers enhancer-like activity." FEBS Lett **554**(1-2): 67-72.
- Urteaga, O. and G. T. Pack (1966). "On the antiquity of melanoma." Cancer **19**(5): 607-610.
- Valencak, J., et al. (2009). "Prognostic relevance of hypoxia inducible factor-1alpha expression in patients with melanoma." Clin Exp Dermatol **34**(8): e962-964.

- van Bommel, D., et al. (2012). "Correlation of LINE-1 methylation levels in patient-matched buffy coat, serum, buccal cell, and bladder tumor tissue DNA samples." Cancer Epidemiol Biomarkers Prev **21**(7): 1143-1148.
- van den Hurk, K., et al. (2012). "Genetics and epigenetics of cutaneous malignant melanoma: a concert out of tune." Biochim Biophys Acta **1826**(1): 89-102.
- van Doorn, R., et al. (2005). "Aberrant DNA methylation in cutaneous malignancies." Semin Oncol **32**(5): 479-487.
- Van Neste, L., et al. (2012). "The epigenetic promise for prostate cancer diagnosis." Prostate **72**(11): 1248-1261.
- Vogt, T., et al. (1998). "Overexpression of Lerk-5/Eplg5 messenger RNA: a novel marker for increased tumorigenicity and metastatic potential in human malignant melanomas." Clin Cancer Res **4**(3): 791-797.
- Volkovova, K., et al. (2012). "Associations between environmental factors and incidence of cutaneous melanoma. Review." Environ Health **11 Suppl 1**: S12.
- Vousden, K. H. (2006). "Outcomes of p53 activation--spoilt for choice." J Cell Sci **119**(Pt 24): 5015-5020.
- Vranka, J. A., et al. (2004). "Prolyl 3-hydroxylase 1, enzyme characterization and identification of a novel family of enzymes." J Biol Chem **279**(22): 23615-23621.
- Vredevelde, L. C., et al. (2012). "Abrogation of BRAFV600E-induced senescence by PI3K pathway activation contributes to melanomagenesis." Genes Dev **26**(10): 1055-1069.
- Wang, H., et al. (2013). "Methylation of Wnt antagonist genes: a useful prognostic marker for myelodysplastic syndrome." Ann Hematol **92**(2): 199-209.
- Warner, L. E., et al. (1998). "Mutations in the early growth response 2 (EGR2) gene are associated with hereditary myelinopathies." Nat Genet **18**(4): 382-384.
- Weinberg, R. A. (2006). Moving out: Invasion and Metastasis. The biology of cancer, Garland Science, Taylor & Francis Group, LLC: 587-654.
- Weir, L., et al. (2011). "Hypoxia-mediated control of HIF/ARNT machinery in epidermal keratinocytes." Biochim Biophys Acta **1813**(1): 60-72.
- Whiteman, D. C., et al. (2006). "Anatomic site, sun exposure, and risk of cutaneous melanoma." J Clin Oncol **24**(19): 3172-3177.
- Widmer, D. S., et al. (2013). "Hypoxia Contributes to Melanoma Heterogeneity by Triggering HIF1alpha-Dependent Phenotype Switching." J Invest Dermatol.
- Wischermann, K., et al. (2008). "UVA radiation causes DNA strand breaks, chromosomal aberrations and tumorigenic transformation in HaCaT skin keratinocytes." Oncogene **27**(31): 4269-4280.
- Wong, C. M., et al. (2007). "Tissue factor pathway inhibitor-2 as a frequently silenced tumor suppressor gene in hepatocellular carcinoma." Hepatology **45**(5): 1129-1138.
- Wong, D. J., et al. (1999). "Progressive region-specific de novo methylation of the p16 CpG island in primary human mammary epithelial cell strains during escape from M(0) growth arrest." Mol Cell Biol **19**(8): 5642-5651.
- Yanamandra, N., et al. (2005). "Recombinant adeno-associated virus (rAAV) expressing TFPI-2 inhibits invasion, angiogenesis and tumor growth in a human glioblastoma cell line." Int J Cancer **115**(6): 998-1005.
- Yang, G., et al. (2006). "Expression profiling of UVB response in melanocytes identifies a set of p53-target genes." J Invest Dermatol **126**(11): 2490-2506.
- Yang, H., et al. (2013). "Tumor development is associated with decrease of TET gene expression and 5-methylcytosine hydroxylation." Oncogene **32**(5): 663-669.

- Yokota, I., et al. (2010). "Identification and characterization of early growth response 2, a zinc-finger transcription factor, as a p53-regulated proapoptotic gene." Int J Oncol **37**(6): 1407-1416.
- Yokoyama, S., et al. (2011). "A novel recurrent mutation in MITF predisposes to familial and sporadic melanoma." Nature **480**(7375): 99-103.
- Yoon, C. H., et al. (2012). "Crucial role of TSC-22 in preventing the proteasomal degradation of p53 in cervical cancer." PLoS One **7**(8): e42006.
- Yoon, H. Y., et al. (2012). "Combined hypermethylation of APC and GSTP1 as a molecular marker for prostate cancer: quantitative pyrosequencing analysis." J Biomol Screen **17**(7): 987-992.
- Yu, J., et al. (2009). "TSC-22 contributes to hematopoietic precursor cell proliferation and repopulation and is epigenetically silenced in large granular lymphocyte leukemia." Blood **113**(22): 5558-5567.
- Zbytek, B., et al. (2008). "Current concepts of metastasis in melanoma." Expert Rev Dermatol **3**(5): 569-585.
- Zbytek, B. e. a. (2013). "Putative role of HIF transcriptional activity in melanocytes and melanoma biology." Dermato-Endocrinology **5**(1): 1-13.
- Ziech, D., et al. (2011). "Reactive oxygen species (ROS)--induced genetic and epigenetic alterations in human carcinogenesis." Mutat Res **711**(1-2): 167-173.
- Zmetakova, I., et al. (2013). "Evaluation of protein expression and DNA methylation profiles detected by pyrosequencing in invasive breast cancer." Neoplasma.